



저작자표시-비영리-변경금지 2.0 대한민국

이용자는 아래의 조건을 따르는 경우에 한하여 자유롭게

- 이 저작물을 복제, 배포, 전송, 전시, 공연 및 방송할 수 있습니다.

다음과 같은 조건을 따라야 합니다:



저작자표시. 귀하는 원저작자를 표시하여야 합니다.



비영리. 귀하는 이 저작물을 영리 목적으로 이용할 수 없습니다.



변경금지. 귀하는 이 저작물을 개작, 변형 또는 가공할 수 없습니다.

- 귀하는, 이 저작물의 재이용이나 배포의 경우, 이 저작물에 적용된 이용허락조건을 명확하게 나타내어야 합니다.
- 저작권자로부터 별도의 허가를 받으면 이러한 조건들은 적용되지 않습니다.

저작권법에 따른 이용자의 권리는 위의 내용에 의하여 영향을 받지 않습니다.

이것은 [이용허락규약\(Legal Code\)](#)을 이해하기 쉽게 요약한 것입니다.

[Disclaimer](#)

이학박사 학위논문

Development of Pyrimidine-based
Natural Product-like Small Molecules
with High Molecular Diversity

피리미딘 기반의 분자 다양성이 확보된
천연물 유사 저분자 물질의 개발

2019 년 2 월

서울대학교 대학원

생물물리 및 화학생물학과

구 재 영

Abstract

Development of Pyrimidine-based Natural Product-like Small Molecules with High Molecular Diversity

Jaeyoung Koo

Department of Biophysics and Chemical Biology

College of Natural Sciences

Seoul National University

The important research goals in chemical biology are to discover small-molecule modulators that can disrupt the biological system and to identify the protein-protein interactions in which these small molecules modulate the biological system. Therefore, in order to discover new small-molecule modulators that can selectively regulate protein-protein interactions, development of drug-like small molecules is required, which have high molecular diversity and biological relevance. In this study, we proposed molecules possessing the characteristics of natural products to be suitable for constitution of compounds meeting the aforementioned requirements. For high biological relevance, we used compounds containing a pyrimidine unit as a privileged structure and explored various derivatives of three-dimensional structural diversity in order to discover compounds different from the conventionally synthesized flat molecules.

Chapter 1 introduces the different attempts made to obtain compounds with various molecular structures having high biological relevance to increase the possibility of discovering modulators of physiological activities.

Chapter 2 describes the development of pDOS (privileged substructure-based diversity-oriented synthesis) pathways involving pyrimidine. This chapter

describes the pathways for the synthesis of compounds with unique three-dimensional structures, in which pyrimidine and a 7-membered ring are fused, by using pyrimidodiazepine as a starting material. It has been demonstrated that the compounds obtained from the pathways can modulate the actual protein-protein interaction.

Chapter 3 describes the newly discovered reactivity of pyrimidodiazepine derivatives under gold catalysis. Using this reactivity, the skeletal transformation of molecular structures can be efficiently achieved in a single-step reaction. In addition, this method provides an effective way to access the pyrimidine-containing macrocycle through skeletal diversification.

Finally, Chapter 4 deals with the construction of a small-molecule library using the aforementioned gold-catalyzed reaction. We proposed construction of a small molecule library with high structural diversity by using pyrimidine-containing medium-sized ring compounds. The medium-sized rings can be converted to macrocyclic structures or other types of medium-sized rings through a gold catalyzed single-step reaction.

Through our research described in Chapters 2–4, we have obtained a large number of small molecules with three-dimensional structural diversity and discovered small-molecule modulators that can regulate the actual protein-protein interaction, thereby proving the usefulness of the pDOS libraries. The pyrimidine-based natural-product-like small molecules described in this dissertation should have high potential for deriving new physiologically active molecules in the future.

Keywords : molecular diversity, pyrimidine, privileged-substructure-based diversity-oriented synthesis (pDOS), gold catalysis, medium-sized ring, macrocycle, library construction.

Student Number : 2013-30757

Table of Contents

Chapter 1. Introduction

1.1 Purpose of Research	2
1.2 References	5

Chapter 2. Diversity-oriented synthetic strategy for developing a chemical modulator of protein–protein interaction

2.1 Introduction	8
2.2 Result and Discussion.....	12
2.3 Conclusion	25
2.4 References	26
2.5 Experimental Section.....	29

Chapter 3. Gold-catalyzed unexpected ring transformation of pyrimido-diazepine derivatives

3.1 Introduction	72
3.2 Result and Discussion.....	76
3.3 Conclusion	84
3.4 References	85
3.5 Experimental Section.....	87

Chapter 4. Construction of structurally diverse pyrimidine embedded medium/ macro and bridged small molecules via library-to-library strategy

4.1 Introduction	117
4.2 Result and Discussion.....	120
4.3 Conclusion	123
4.4 References	124

Abstract (Korean)	125
--------------------------------	-----

Appendix : Copies of ^1H and ^{13}C NMR Spectra of Representative Compounds

I . Chapter 2	128
II. Chapter 3	160

Chapter 1. Introduction

1.1 Purpose of Research

Currently, the most notable method in drug discovery, especially in the development of first-in-class drugs, is phenotype-based screening.¹ The method involves the observation of phenotypic changes in a cell or organism to identify the substance that expresses a desired phenotype. The development of high-throughput screening (HTS) and high-content screening (HCS) has enabled rapid and efficient investigation of biological activities, which require a large number of compound libraries.² The important aspect here is not the size of the library, but the skeletal and stereochemical diversity of compound structures. Most libraries constructed from a limited number of core skeletons have not been very successful in populating the multi-dimensional chemical descriptor space.³ Moreover, although the total chemical space is estimated to cover more than 10^{63} distinct organic molecules, some of them are synthetically inaccessible and only a small portion of this huge chemical space is applicable to biomedical fields.⁴ Therefore, there is a demand for efficient construction of small molecule libraries with a wide range of molecular diversity.

Natural products are known to exhibit excellent molecular diversity and their analogs have been widely used as therapeutic agents or functional modulators of specific biological processes.⁵ However, there are drawbacks associated with the use of natural products as small molecule modulators, which are difficult to structurally modify and subsequently scale-up. Therefore, it is advantageous to synthesize a natural product-like compound containing the characteristics of a natural product. The characteristic of natural products is complexity, including rich saturated bonds, and stereo centers.⁶ The more complex molecules have the ability

to access larger chemical spaces. Hence, there is greater potential to identify compounds with better specificity to the target biopolymer.⁷ Importantly, the saturated compound might also result in greater selectivity, resulting in fewer off-target effects.⁸ As small molecules are discovered during the initial drug discovery stage and converted into drugs through clinical trials, more saturated small molecules are more likely to succeed in this drug discovery process.⁹ Another descriptor of complexity, the presence of a stereo center, is also often observed in drugs that have been successfully discovered through clinical trials.¹⁰ Therefore, effective synthetic strategy needs to be developed for a new collection of natural product-like small molecules.

To address these demands, Schreiber et al. developed the diversity-oriented synthesis (DOS) strategy,¹¹ which efficiently populates the chemical space with skeletally and stereochemically diverse small molecules synthesized from simple building blocks via complexity-generating reactions. The resulting collection of organic molecules has been successfully utilized for the efficient discovery of bioactive small-molecule modulators and therapeutic agents.¹² As a result, the DOS-derived libraries have been of great value in the discovery of drug candidates, and thus DOS has emerged as an essential tool in chemical biology and drug discovery.¹³

However, an important challenge is to introduce improved biological relevance with maximize molecular diversity. Privileged structures are important for the discovery of bioactive small molecules.¹⁴ Therefore, incorporating a privileged structure into the core skeleton can improve specific interactions between small molecule and various biopolymers.¹⁵ To address these needs in order to maximize

molecular diversity with high biological relevancy, our group presented a privileged-substructure-based DOS (pDOS) strategy and attempted to emphasize the importance of skeletal diversity through creative reconstruction of privileged substructures embedded in polyheterocyclic molecular frame-works.¹⁶ This is because privileged substructures with three-dimensionally diverse skeleton are expected to exhibit high affinity toward various biopolymers owing to the natural selection process and the evolutionary similarity between gene products. The importance of privileged substructure such as benzopyran,¹⁷ oxopiperazine,¹⁸ and pyrimidine¹⁹ in pDOS library compounds has been clearly demonstrated in our laboratory by screening of bioactive small molecules and the subsequent identification of appropriate target biomolecules.^{20,19c} Bioactive compounds with particular specificities derived from pDOS, show that a privileged structure could serve as a chemical “navigator” toward biologically relevant chemical spaces.²¹

1.2 References

- [01] Swinney, D. C. *J. Biomol. Screen.* **2013**, *18*, 1186.
- [02] Dandapani, S.; Rosse, G.; Southall, N.; Salvino, J.; Thomas, C. *Curr. Protoc. Chem. Biol.* **2012**, *4*, 177.
- [03] Dobson, C. M. *Nature*, **2004**, *432*, 824.
- [04] Bohacek, R. S.; McMartin C.; Guida, W. C. *Med. Res. Rev.*, **1996**, *16*, 3.
- [05] Newman, D. J.; Cragg, G. M.; Snader, K. M. *J. Nat. Prod.* **2003**, *66*, 1022.
- [06] (a) Arya, P.; Joseph, R.; Gan, Z.; Rakic, B. *Chem. Biol.* **2005**, *12*, 163.;
(b) Feher, M.; Schmidt, J. M. *J. Chem. Inf. Comp. Sci.* **2003**, *43*, 218.
- [07] Selzer, P.; Roth, H.-J.; Ertl, P.; Schuffenhauer, A. *Curr. Opin. Chem. Biol.* **2005**, *9*, 310.
- [08] (a) McGaughey, G. B.; Gagne, M.; Rappe, A. K. *J. Biol. Chem.* **1998**, *273*, 15458.; (b) Dougherty, D. A. *Science* **1996**, *271*, 163.
- [09] Wenlock, M. C.; Austin, R. P.; Barton, P.; Davis, A. M.; Leeson, P. D. *J. Med. Chem.* **2003**, *46*, 1250.
- [10] Lovering, F.; Bikker, J.; Humblet, C. *J. Med. Chem.*, **2009**, *52*, 6752.
- [11] (a) Schreiber, S. L. *Science*, **2000**, *287*, 1964.; (b) Burke M. D.; Schreiber, S. L. *Angew. Chem., Int. Ed.*, **2004**, *43*, 46.; (c) Schreiber, S. L. *Nature* **2009**, *457*, 153.
- [12] (a) Spring, D. R. *Org. Biomol. Chem.*, **2003**, *1*, 3867.; (b) Tan, D. S. *Nat. Chem. Biol.*, **2005**, *1*, 74.; (c) Peuchmaur, M.; Wong, Y.-S. *Comb. Chem. High Throughput Screening* **2008**, *11*, 587.
- [13] (a) Galloway, W. R. J. D.; Isidro-Llobet, A.; Spring, D. R. *Nat. Commun.* **2010**, *1*, 80.; (b) Oguri, H.; Hiruma, T.; Yamagishi, Y.; Oikawa, H.; Ishiyama, A.; Otoguro, K.; Yamada, H.; Omura, S. *J. Am. Chem. Soc.* **2011**, *133*, 7096.; (c) Kopp, F.; Stratton, C. F.; Akella, L. B.; Tan, D. S. *Nat. Chem. Biol.* **2012**, *8*, 358.
- [14] Evans, B. E.; Rittle, K. E.; Bock, M. G.; DiPardo, R. M.; Freidinger, R.

- M.; Whitter, W. L.; Lundell, G. F.; Veber, D. F.; Anderson, P. S. *J. Med. Chem.* **1988**, *31*, 2235.
- [15] Mason, J. S.; Morize, I.; Menard, P. R.; Cheney, D. L.; Hulme, C.; Labaudiniere, R. F. *J. Med. Chem.* **1999**, *42*, 3251 (b) Newman, D. J. *J. Med. Chem.* **2008**, *51*, 2589.
- [16] Oh, S.; Park, S. B. *Chem. Commun.* **2011**, *47*, 12754.
- [17] (a) Ko, S. K.; Jang, H. J.; Kim, E.; Park, S. B. *Chem. Commun.* **2006**, *28*, 2962.; (b) Oh, S.; Jang, H. J.; Ko, S. K.; Ko, Y.; Park, S. B. *J. Comb. Chem.* **2010**, *12*, 548.; (c) Zhu, M.; Lim, B. J.; Koh, M.; Park, S. B. *ACS Comb. Sci.* **2012**, *14*, 124.
- [18] (a) Lee, S.-C.; Park, S. B. *J. Comb. Chem.* **2007**, *9*, 828.; (b) Kim, J.; Lee, W. S.; Koo, J.; Lee, J.; Park, S. B. *ACS Comb. Sci.* **2014**, *16*, 24.
- [19] (a) Kim, H.; Tung, T. T.; Park, S. B. *Org. Lett.* **2013**, *15*, 5814.; (b) Choi, Y.; Kim, H.; Shin, Y.; Park, S. B. *Chem. Commun.* **2015**, *51*, 13040.; (c) Kim, J.; Jung, J.; Koo, J.; Cho, W.; Lee, W.; Kim, C.; Park, W.; Park, S. B. *Nat. Commun.*, **2016**, *7*, 13196.
- [20] (a) Park, J.; Oh, S.; Park, S. B. *Angew. Chem., Int. Ed.* **2012**, *51*, 5447.; (b) Koh, M.; Park, J.; Koo, J. Y.; Lim, D.; Cha, M. Y.; Jo, A.; Choi, J. H.; Park, S. B. *Angew. Chem., Int. Ed.* **2014**, *53*, 5102.; (c) Lee, S.; Nam, Y.; Koo, J. Y.; Lim, D.; Park, J.; Ock, J.; Suk, K.; Park, S. B. *Nat. Chem. Biol.* **2014**, *10*, 1055. (d) Cho, T.-J.; Kim, J.; Kwon, S.-K.; Oh, K.; Lee, J.-a.; Lee, D.-S.; Cho, J.; Park, S. B. *Chem. Sci.* **2012**, *3*, 3071.
- [21] Kim, J.; Kim, H.; Park, S. B. *J. Am. Chem. Soc.*, **2014**, *136*, 14629.

Chapter 2. Diversity-oriented synthetic strategy for developing a chemical modulator of protein–protein interaction

Nat. Commun., **2016**, 7, 13196–13205.

Reproduced by permission of Springer Nature.

2.1 Introduction

The molecular diversity and complexity in a screening collection of drug-like small molecules is a paramount breakthrough in the discovery of novel small-molecule modulators for currently “undruggable” targets, including protein–protein interactions (PPIs) and protein–nucleic acid interactions.^{1–3} Toward this end, a strategy termed diversity-oriented synthesis (DOS) was devised, which seeks to populate the vast area of new chemical space made up of diverse and three-dimensional (3D) complex drug-like compounds.^{4–6} Although DOS has emerged as an indispensable tool to promote the unbiased screening of compounds and their interactions with diverse biological targets, one of the key challenges in this field is the identification of appropriate chemical structures that will exhibit improved biological relevance and high molecular diversity. To address this issue, synthetic community has been developing many DOS-based approaches for the generation of compound libraries embodying core scaffolds of natural products or its mimetics.^{7–11} Natural products have inherent bioactivity and high bioavailability; thus, the natural product-inspired DOS libraries with biological relevance could be of great value for the identification of bioactive compounds.^{12–14}

With the goal of targeting unexplored biologically relevant chemical space, we postulated that privileged structures could also serve as “chemical navigators” and therefore reported a privileged substructure-based DOS (pDOS) strategy, which targets the synthesis of diverse polyheterocyclic skeletons containing privileged substructures through complexity-generating reactions in order to maximize the unbiased coverage of bioactive space.^{15–17} By incorporating privileged substructures into a rigid core skeleton, we envisioned that the resulting

compounds would exhibit enhanced interactions with various bio macromolecules including proteins and DNA/RNA. Consequently, we demonstrated the importance of pDOS strategy through the discovery of new bioactive small molecules that interact with a wide range of biological targets.^{18–19}

As a continuation of our previous work, we identified pyrimidine as a new privileged substructure that could be used to navigate through bioactive chemical space. The pyrimidine moiety is commonly present in various bioactive small molecules, and it plays a critical role as a nucleoside analog in various kinase inhibitors or adenosine receptor modulators due to its hydrogen bonding ability (Fig. 2-1a).^{20–22} Therefore, many synthetic efforts toward pyrimidine-containing species have been focused on aromatic monocyclic or bicyclic skeletons, which limits the structural diversity of the pyrimidine-containing core skeletons. In addition, the 3D structural complexity of the core skeletons becomes important because planar frameworks less frequently comprise FDA-approved chemical entities, especially in regard to ‘undruggable’ targets.^{23–25}

In order to expand the molecular diversity beyond monocyclic and bicyclic pyrimidine skeletons, we develop a new pDOS strategy towards the divergent synthesis of natural product-like polyheterocycles containing pyrimidodiazepine or pyrimidine. Diazepine is also often found in complex natural products that exhibit a wide range of biological activities, and is known to be a prominent privileged structure that can improve the bioavailability and bioactivity of compounds.^{26,27} In addition, 7-membered rings that are fused to aromatic rings generally have higher conformational flexibility and a greater number of reactive sites than 6- or 5-membered fused ring systems, as confirmed by the direct comparison of

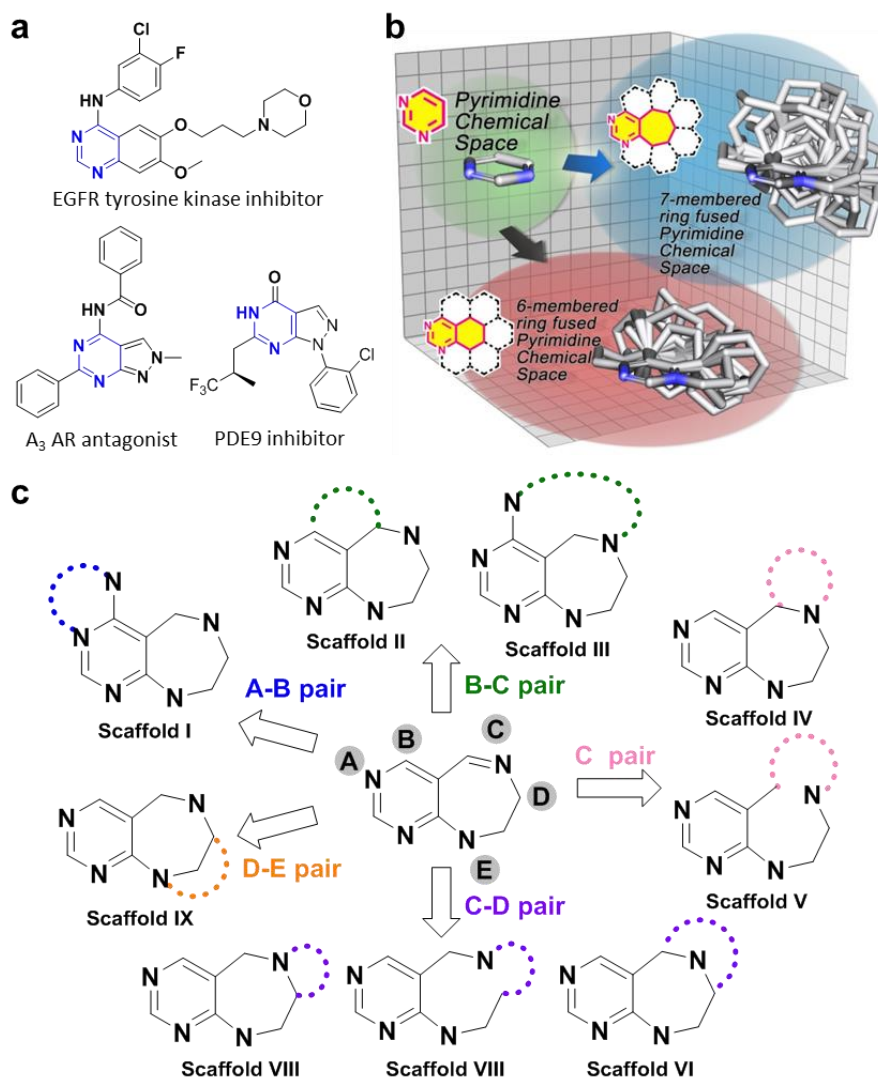


Figure 2-1. Diversity-oriented synthetic strategy with pyrimidine as a privileged structure. a) Pyrimidine-containing bioactive compounds. b) 3D chemical space of pyrimidine and the comparison between pyrimidine-containing tricyclic 6/6/6 and 6/7/6 systems in terms of 3D diversity and complexity by overlaying energy-minimized conformers aligned along the pyrimidine substructure. c) Synthetic strategy for diversity-oriented synthesis of pyrimidodiazepine- or pyrimidine-containing polyhetero-cycles through divergent pairing pathways.

pyrimidine-embedded tricyclic 6/6/6 and 6/7/6 systems by overlaying the energy-minimized conformers aligned along the pyrimidine substructure (Fig. 2-1b). Thus, pyrimidodiazepine can serve as a versatile intermediate to access highly diverse and complex polyheterocycles through the incorporation of additional ring systems, which forms the basis of a new pyrimidodiazepine-based pDOS pathway. To establish the pDOS pathway, we first design and synthesize highly functionalized pyrimidodiazepine intermediates **1** containing 5 reactive sites (A–E). In our pDOS strategy, intermediates **1** can be transformed into 9 distinct pyrimidodiazepine- or pyrimidine-containing scaffolds (**I–IX**) via pairing different functional groups at each reactive site (Fig. 2-1c). Then, we conduct ELISA-based high-throughput screening (HTS) of leucyl-tRNA synthetase (LRS)-Ras-related GTP-binding protein D (RagD) interaction²⁸ to validate whether our distinct scaffolds can target unexplored biologically relevant chemical space. This screening exercise lead to the identification of an effective hit compound, **21f**, which regulates the amino acid-dependent activation of mechanistic target of rapamycin complex 1 (mTORC1) activity via specific inhibition of LRS-RagD interaction. **21f** can serve as a research tool with a novel mode of action for specific modulation of mTORC1 signaling pathway. Collectively, we confirm that pDOS is an appropriate strategy to target challenging biological targets.

2.2 Result and Discussion

Pairing strategies for scaffolds I–III

For the synthesis of scaffolds **I–III** through A-B or B-C pairs, suitable functional groups at the B position were imperative as they participated in the pairing reaction (Fig. 2-2). First, substrates **1a–e** were readily synthesized through a series of transformations (Supplementary Fig. 1-3). For the synthesis of scaffold **I**, substrates **1a–c** were treated with sodium borohydride (NaBH_4) to afford secondary amines; the resulting secondary amines were protected with Boc and aniline was N-alkylated, which allowed for the formation of intermediates **A**. Scaffold **I** was efficiently generated via A-B pairing through an intramolecular substitution reaction, when intermediates **A** were subjected to debenzylation and the resultant alcohols were subsequently activated with methanesulfonyl chloride (MsCl). Consequently, we obtained stereochemically enriched tetracycles **2a**, **3b**, and **4c** (scaffold **I**), containing a pyrimidinium moiety, in moderate yields.

Next, we employed ring-closing metathesis (RCM) for the synthesis of scaffolds **II** and **III** via B-C pairing; in this case, a vinyl group was introduced at the C reactive site of the key substrate. Accordingly, **1d** and **1e** were subjected to N-alkylation with benzyl bromide to afford iminium ions. Diastereoselective nucleophilic addition of allyl or homoallyl Grignard reagents to the resultant iminium ions generated intermediates **B** and **C**; RCM with Grubbs' 2nd generation catalyst provided **5d**, **6d**, and **7e** (scaffold **II**), fused with 6-, 7-, and 10-membered rings, with good to excellent diastereoselectivity. Notably, this diastereoselectivity without chiral auxiliaries or catalysts could be rationalized by the preferential

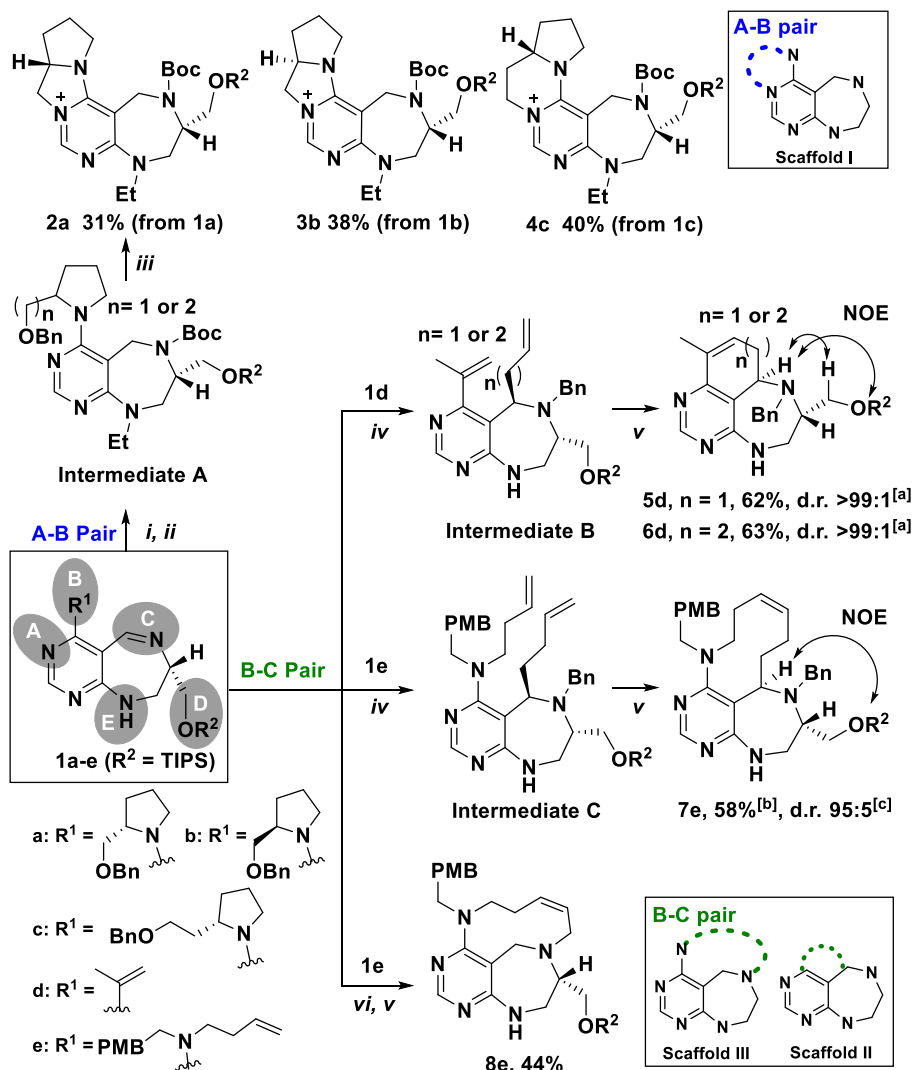


Figure 2-2. A-B and B-C pairing pathways for synthesis of scaffolds **I-III**. Reagents and conditions: i) NaBH_4 , MeOH, $0\text{ }^\circ\text{C} \rightarrow \text{r.t.}$ then Boc_2O , TEA, DCM, $0\text{ }^\circ\text{C} \rightarrow \text{r.t.}$; ii) EtI, NaH, DMF, $0\text{ }^\circ\text{C} \rightarrow \text{r.t.}$; iii) $\text{Pd}(\text{OH})_2/\text{C}$, H_2 , MeOH, then MsCl , TEA, DCM, $0\text{ }^\circ\text{C} \rightarrow \text{r.t.}$; iv) BnBr , ACN, $80\text{ }^\circ\text{C}$, then RMgBr , THF, $-78\text{ }^\circ\text{C} \rightarrow \text{r.t.}$; v) Grubbs' 2nd generation catalyst (20 mol%), toluene, reflux; vi) NaBH_4 , MeOH, $0\text{ }^\circ\text{C} \rightarrow \text{r.t.}$, then allyl bromide, TEA, DMF, $0\text{ }^\circ\text{C} \rightarrow \text{r.t.}$. TIPS, triisopropylsilyl; TEA, triethylamine; MsCl , methanesulfonyl chloride; BnBr , benzylbromide; ACN, acetonitrile. ^[a]Determined by LC-MS analysis of crude reaction mixture and by ^1H NMR analysis of samples purified by short silica-gel column. ^[b]Yield of the isolated major diastereomer. ^[c]Determined by LC-MS analysis of crude reaction mixture.

approach of Grignard reagents toward the less hindered re-face of the imine in **1d** and **1e**. The stereochemistry of each product was confirmed by nuclear Overhauser effect (NOE) spectroscopy. To generate scaffold **III**, **1e** was treated with NaBH₄. Allylation of the resulting secondary amine and subsequent RCM with Grubbs' 2nd generation catalyst yielded **8e** (scaffold **III**), fused with 10-membered rings, in 44% overall yield.

Pairing strategies for scaffolds IV-IX

As shown in Fig. 2-3, the reactive site B did not participate in the pairing reactions for the synthesis of scaffolds **IV-IX**. Therefore, we synthesized **1f** as a key substrate containing an *N*-benzyl-*N*-methyl amine moiety at the B position (Supplementary Fig. 2). For the preparation of scaffolds **IV** and **V**, the imine moiety of **1f** was the major synthetic functionality. Unlike in other pairing pathways, the imine moiety acts as both a nucleophile and electrophile concurrently, and thus, other cyclic structures could be introduced at the C position. First, we employed the rhodium-catalyzed oxygenative [2+2] cycloaddition of the alkyne and imine to generate a β -lactam ring.²⁹ The imine moiety of **1f** reacted with rhodium-complexed ketene species generated by the catalytic oxidation of the metal vinylidene complex to form zwitterionic intermediate **D**, which could be subjected to a conrotatory electrocyclic ring-closure reaction. After reaction condition screening, *trans* isomers **9f** and **10f** (scaffold **IV**) were obtained in 61% and 46% yields, respectively, with good to excellent diastereoselectivity. We performed NOE analysis and gradient-selected COSY experiment to confirm the relative stereochemistry of **9f** and **10f**. To construct another ring system, **1f** was

reacted with *N*-benzyl-2-chloroacetamide to afford the iminium ion; intramolecular nucleophilic attack of the amide on the iminium ion provided imidazolidinone-containing **11f** (scaffold **IV**) as a diastereomeric mixture (d.r = 6:1) in 61% overall yield. Moreover, without the incorporation of an additional ring structure, we obtained stereochemically enriched and highly functionalized pyrimidodiazepine **12f** (major, scaffold **IV**) and **12f'** (minor, scaffold **IV**) in 70% and 8.3% yields, respectively, via the reaction of **1f** with benzyl bromide, followed by *re-face* selective nucleophilic addition of an ethynyl Grignard reagent on the iminium ion. To generate scaffold **V**, **1f** was subjected to *N*-alkylation with methyl iodide, followed by nucleophilic addition of vinylmagnesium bromide to the resultant iminium ion afforded **SI-7** (Supplementary Fig. 4). Oxidation of **SI-7** with 3-chloroperbenzoic acid (*m*-CPBA) and conversion of 7-membered ring into 10-membered ring via in situ [2,3]-sigmatropic ring expansion of the resultant *N*-oxide provided **13f** (scaffold **V**) with excellent (*E*)-selectivity (Supplementary Fig. 4).³⁰

For the synthesis of scaffolds **VI-VIII**, the C-D pairing pathways were investigated. Deprotection of the triisopropylsilyl (TIPS) group from **1f** provided an alcohol product, that was readily converted to the desired bridged oxazolidines **14f**, **15f**, and **16f** (scaffold **VI**) in good to excellent yields upon treatment with various *N*-modifying agents such as Boc anhydride (Boc₂O), benzyl isocyanate, and 3-nitrobenzene sulfonyl chloride (*m*-NsCl) through iminium formation and subsequent intramolecular nucleophilic addition of the hydroxyl moiety.³¹ The structure of bridged oxazolidine **16f** was confirmed by X-ray crystallographic analysis (Supplementary Fig. 5, CCDC number 1500586). To generate scaffold **VII**, **1f** was subjected to *N*-alkylation with methyl iodide, followed by nucleophilic

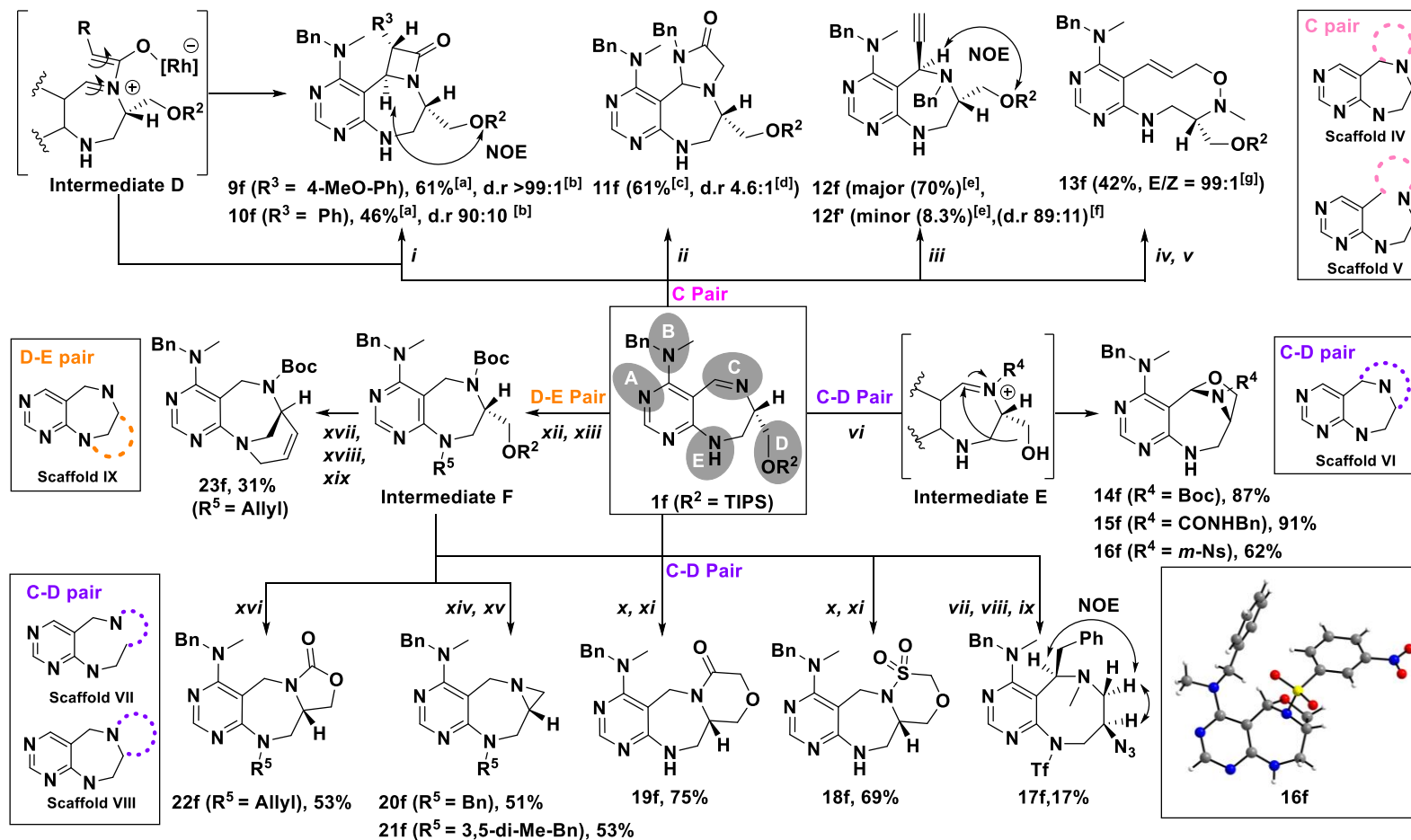


Figure 2-3. C, C-D and D-E pairing pathways for synthesis of scaffolds **IV-VII**. Reagents and conditions: i) Rh(PPh₃)₃Cl (10 mol%), 4-picoline *N*-oxide, 4-ethynylanisole or phenylacetylene, ACN, μ -wave, 90 °C, 35 min; ii) *N*-benzyl-2-chloroacetamide, NaBr, DMF, μ -wave, 110 °C, 30 min, then DBU, DMF; iii) BnBr, ACN, 80 °C, then ethynylmagnesium bromide, THF, -78 °C→r.t.; iv) MeI, ACN, 40 °C, then vinylmagnesium bromide, THF, -78 °C→r.t.; v) *m*-CPBA, DCM, then 3-chlorobenzoic acid; vi) HF/pyridine/THF, then electrophiles (Boc₂O, benzyl isocyanate or *m*-NsCl), DCM; vii) MeI, ACN, 40 °C, then benzylmagnesium bromide, THF, -78 °C →r.t.; viii) TBAF, THF; ix) Tf₂O, toluene, -40 °C, then NaN₃, -78 °C→r.t.; x) NaBH₄, MeOH, 0 °C →r.t., then chloromethanesulfonyl chloride or chloroacetic anhydride, TEA, DCM, 0 °C→r.t.; xi) TBAF, THF, then Cs₂CO₃, DMF, 90 °C; xii) NaBH₄, MeOH, 0 °C→r.t., then Boc₂O, TEA, DCM, 0 °C →r.t.; xiii) BnBr, 3,5-dimethylbenzyl bromide or Allyl bromide, NaH, DMF, 0 °C→r.t.; xiv) TBAF, THF, then TFA, DCM; xv) PS-PPh₃, DEAD, THF; xvi) TBAF, THF, then NaH, THF, 0 °C→r.t.; xvii) TBAF, THF, then Dess-Martin periodinane, DCM; xviii) Ph₃P+CH₃Br⁻, MeLi, THF, 0 °C→r.t.; xix) Grubbs' 2nd generation catalyst (20 mol%), toluene, reflux. DBU, 1,8-diazabicyclo[5.4.0]undec-7-ene; *m*-CPBA, 3-chloroper-benzoic acid; *m*-NsCl, 3-nitrobenzenesulfonyl chloride; TBAF, *tetra*-n-butylammonium fluoride; Tf₂O, trifluoromethanesulfonic anhydride; PS-PPh₃, polystyrene triphenylphosphine; DEAD, diethyl azodicarboxylate. ^[a]Yield of isolated major diastereomer. ^[b]Determined by LC-MS analysis of crude reaction mixture. ^[c]Yield of the mixture of diastereomers. ^[d]Determined by ¹H NMR spectroscopy. ^[e]Yield of isolated diastereomer. ^[f]Determined from purified yield of each diastereomer. ^[g]Determined by LC-MS analysis of crude reaction mixture after treatment of 3-chlorobenzoic acid.

addition of benzylmagnesium bromide to the resultant iminium ion and subsequent removal of the TIPS group afforded **SI-8** (Supplementary Fig. 6). Then, the hydroxyl moiety of **SI-8** was activated with trifluoromethanesulfonic anhydride to provide an aziridium intermediate and the subsequent nucleophilic ring expansion with azide anion afforded **17f** (scaffold **VII**) containing an eight-membered diazocane ring. In fact, benzodiazocine is known as an important pharmacophore, but the synthesis of diazocane has not been extensively studied due to the unfavorable transannular strain in medium-sized rings.³² The stereochemistry of **17f** was confirmed by nuclear Overhauser effect (NOE) spectroscopy. For the preparation of scaffold **VIII**, **1f** was treated with NaBH₄ to afford a secondary

amine, which underwent sulfonamide or amide formation upon treatment with chloromethane sulfonyl chloride or chloroacetic anhydride. The subsequent removal of the TIPS group and intramolecular nucleophilic attack of the resultant alcohols with electrophiles afforded **18f** or **19f** (scaffold **VIII**), fused with 6-membered sultam or lactam rings. Furthermore, to generate **20f** and **21f** (scaffold **VIII**) containing an aziridine ring, **1f** was treated with NaBH₄, and the resulting secondary amine was protected with Boc and aniline was *N*-alkylated to provide intermediates **F** (R⁵ = Benzyl or 3,5-dimethylbenzyl). The removal of the TIPS and Boc group of intermediate **F**, followed by subsequent cyclization, produced **20f** or **21f** (scaffold **VIII**) in 51% and 53% overall yields, respectively. Finally, oxazolidinone-containing **22f** (scaffold **VIII**) was obtained through the TIPS deprotection of intermediate **F** (R⁵ = allyl) and subsequent cyclization. For the synthesis of scaffold **IX** via D-E pairing, the removal of the TIPS group of intermediate **F** (R⁵ = allyl) followed by Dess-Martin periodinane oxidation provided an aldehyde. The resulting unstable aldehyde was immediately subjected to Wittig olefination, followed by RCM with Grubbs' 2nd generation catalyst to afford **23f** (scaffold **IX**) containing bridgehead [4,3,1] ring systems.

Cheminformatics analysis

Through this pDOS strategy, we synthesized 16 distinct pyrimidodiazepine- or pyrimidine-containing polyheterocycles with high 3D complexity, skeletal diversity, and biological relevancy (Fig. 2-4a). Notably, unique architectures of bioactive natural products such as medium-sized rings³³ (**E**, **F**, **I**, and **K**), bridge-head bicyclic structures³⁴ (**J** and **P**), and β -lactam rings^{35,36} (**G**), were successfully incorporated into the pyrimidine-containing core skeletons. When we overlaid the energy-minimized conformers of each scaffold in 3D space by aligning the pyrimidine substructure, we clearly demonstrated the skeletal diversity and structural complexity of the resulting polyheterocycles (Fig. 2-4b). To quantitatively analyze the molecular diversity of this pDOS pathway, we performed principal moment of inertia (PMI) analysis to compare the degree of shape diversity of the representative polyheterocycles (Supplementary Fig. 8) of this study with the collection of 15 FDA-approved drugs containing pyrimidine moiety³⁷ (Supplementary Fig. 9) and 71 bioactive natural products.³⁸ The reference set of drugs containing pyrimidine moiety were narrowly dispersed in the region of rod-and disc-like shapes. On the other hand, our compounds were widely dispersed in the PMI plot, similar to natural products, and possessed more spherical characteristics than the FDA-approved drug set, which indicates the excellent shape diversity of newly synthesized core skeletons in this study (Fig. 2-4C, Supplementary Fig. 7).

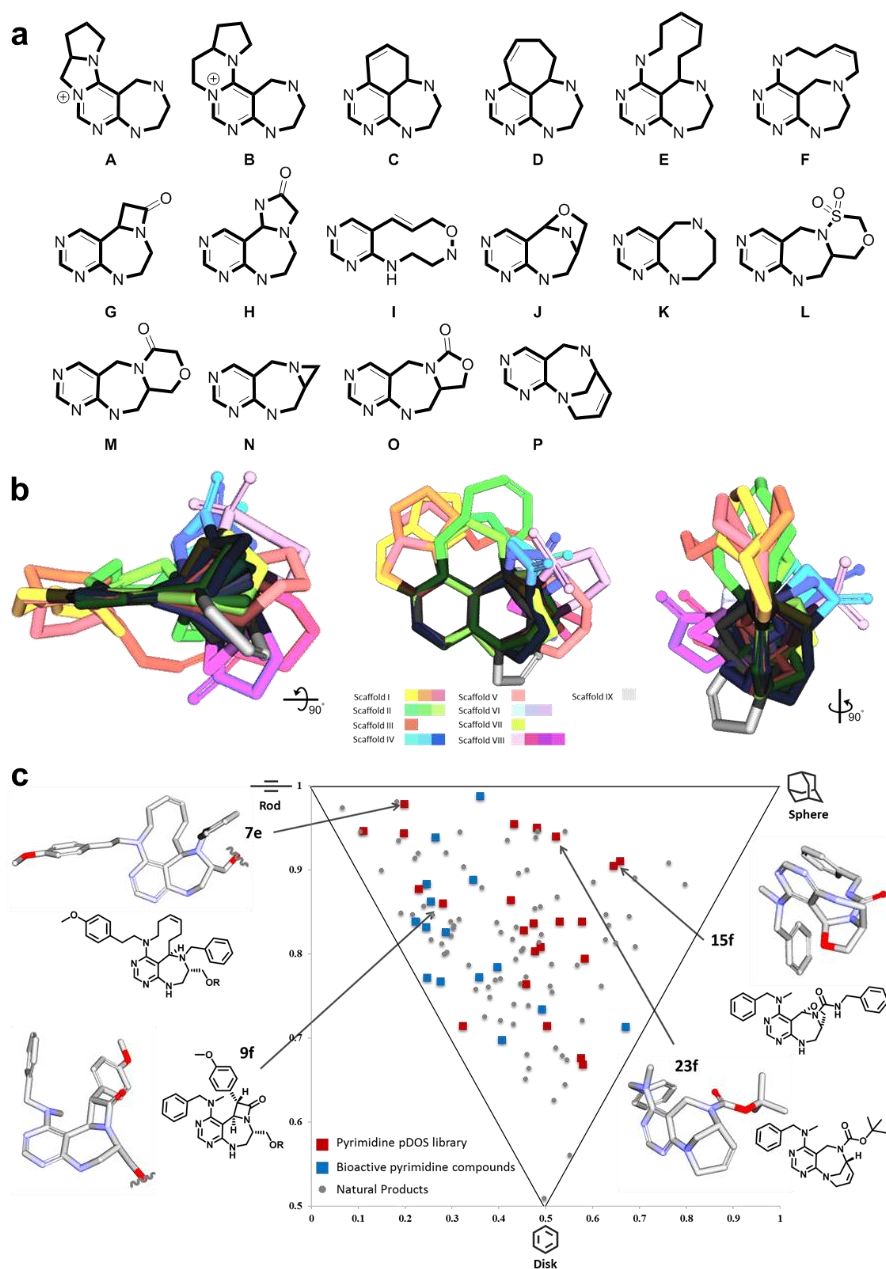


Figure 2-4. Chemoinformatic analysis for structural diversity and 3D complexity of pDOS library. a) Core skeletons of 16 natural product-like pyrimidodiazepine- or pyrimidine-containing polyheterocycles. b) Overlay of energy-minimized conformers of 16 core skeletons aligned by the pyrimidine substructure. c) Principal moment of inertia (PMI) plot. The 3D molecular shape of pDOS library (red squares) was quantitatively compared with that of 15 FDA-approved drugs embedded with pyrimidine moiety (blue squares) and 71 bioactive natural products (grey dots).

Biological evaluation

Diversification of the 3D molecular shapes of drug-like core skeletons may lead to various interactions with diverse biopolymers and allow for the identification of specific modulators of challenging targets such as PPIs and protein-nucleic acid interactions. To investigate this possibility, we have attempted to identify novel chemical inhibitors of the LRS-RagD interaction²⁸ for the modulation of mTORC1—a dominant effector that regulates cellular growth, proliferation, and autophagy.³⁹ Upon activation of mTORC1 by multiple upstream inputs such as growth factors, energy status, and amino acids, particularly the branched-chain amino acid leucine (Leu), mTORC1 plays a crucial role in triggering eukaryotic cell growth and proliferation through stimulating protein biosynthesis and other anabolic processes while suppressing a catabolic process, namely autophagy.⁴⁰ Consequently, the dysregulation of mTORC1 activation could lead to malfunction in central biological pathways that could lead to cancer cell growth, survival, and proliferation.⁴¹

LRS catalyzes the conjugation of Leu to its cognate tRNA to form an aminoacyl-tRNA, which serves as a precursor for protein synthesis.⁴² In addition to its canonical role in protein biosynthesis, a recent study suggested a noncanonical role of LRS in amino acid-dependent mTORC1 activation by sensing intracellular Leu concentration.²⁸ According to this study, LRS can mediate Leu signaling to mTORC1 via direct binding to RagD-GTP protein and form a LRS-RagD protein complex in a Leu-dependent manner, which leads to the translocation of mTORC1 to the lysosome membrane and subsequent activation of mTORC1 (Fig. 2-5a). Thus, LRS-RagD interactions could serve as a Leu sensing mechanism in the

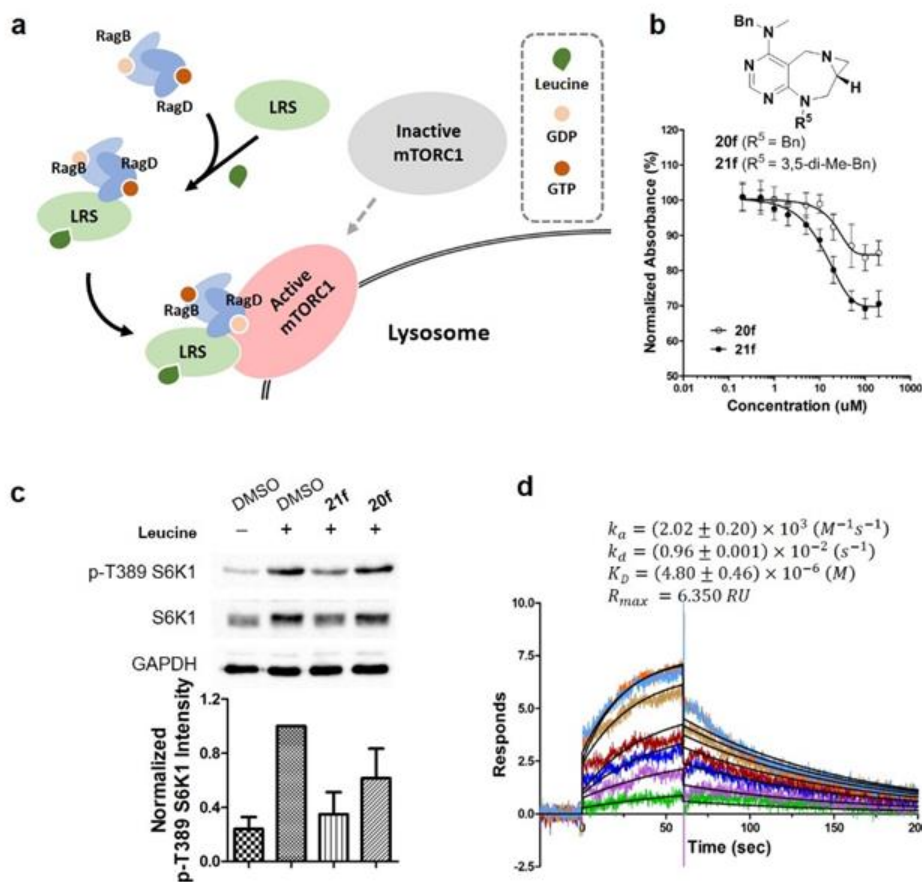


Figure 2-5. Discovery of chemical modulator for LRS-RagD interaction. a) Noncanonical role of LRS. Leucine-loaded LRS binds to RagD, which promotes the translocation of mTORC1 to lysosomal surface and subsequent activation. b) Dose-response curves in ELISA of **20f** and **21f**. The results represent the mean of three biological replicates; error bars represent the s.e.m. c) Effects of **20f** and **21f** on mTORC1 signaling pathway. HEK293T cells were treated with 20 μM of **20f** and **21f** for 3 h. As a negative control, cells were deprived of leucine for 3 h. Level of phospho-T389 S6K1 were quantified against a DMSO control. The bar graph represents the mean of five biological replicates; error bars represent the s.e.m. d) Sensorgrams of surface plasmon resonance (SPR) spectroscopy of **21f** showed its concentration-dependent binding to purified LRS. The concentration plotted are 1, 2.5, 5, 10, 12.5, 15, 17.5 and 20 μM , in order of increasing **21f**. The curve fittings are shown in black. The sensorgrams represent the mean of two biological replicates.

amino acid-dependent activation of mTORC1.^{28,41} Given that the LRS-RagD interaction and structures of human LRS and RagD have not yet been fully characterized, the discovery of novel small-molecule PPI inhibitors of LRS and RagD could shed light on the molecular mechanism of mTORC1 activation in an amino acid-dependent manner. In addition, they could serve as lead compounds for the development of potential therapeutic agents with new modes of action to treat human diseases linked to the oncogenic activation of mTORC1.^{39,41}

To identify novel small-molecule PPI modulators of the LRS-RagD interaction, our pDOS library was subjected to ELISA-based HTS using purified human LRS and GST (glutathione-S-transferase)-tagged RagD (Fig. 2-5b and Supplementary Fig. 10), where the antibody-based signal was lowered upon treatment with LRS-RagD interaction inhibitors. This screening exercise led to the identification of aziridine-containing **20f** and **21f** as dose-dependent inhibitors of the LRS-RagD interaction. Based on this initial data, we hypothesized that **20f** and **21f** might inhibit the LRS-mediated Leu signaling to mTORC1 via direct disruption of the LRS-RagD interaction. As shown in Fig. 2-5c, the level of phosphorylated p70 ribosomal protein S6 kinase 1 (S6K1),⁴³ a typical mTORC1 kinase substrate, was decreased in the absence of Leu. Similarly, **20f** and **21f** suppressed the phosphorylation of S6K1 even in the presence of Leu. Based on the reduction of LRS-RagD interaction by ELISA (**20f** 15.5%; **21f** 30.2%) and the suppression of phosphorylated S6K1 by western blotting (**20f** 16.4%; **21f** 48.9%), we selected **21f** as the candidate compound and subjected it to further analysis. The subsequent biophysical study using SPR revealed the binding affinity patterns of **21f** and other pyrimidodiazepine-containing scaffolds (**14f** and **19f**) toward purified LRS. We

clearly observed the 1:1 binding event in the SPR sensorgrams of **21f** with K_D value of $4.8 (\pm 0.46) \mu\text{M}$ and the saturation event at the high dosage (Fig. 2-5d and Supplementary Fig. 11), whereas **14f** and **19f** showed no dose-dependent responses without any specific binding events (Supplementary Fig. 11), which supported that **21f** specifically binds LRS and disrupts the interaction between LRS and RagD.

2.3 Conclusion

In this study, we developed a new pDOS strategy using pyrimidodiazepine as a privileged substructure. Highly functionalized substrate **1** allowed for the preparation of 16 distinct pyrimidodiazepine- or pyrimidine-containing polyheterocycles through different pairing reactions of 5 unique reactive sites (A-E) within an average of 2.2 steps. The newly synthesized natural product-like core skeletons with high sp^3 carbon fractions exhibited much higher skeletal diversity than existing pyrimidine-based drugs, as demonstrated by PMI analysis. Considering privileged substructures as chemical “navigators” to efficiently access unexploited regions of bioactive chemical space, the pDOS synthetic pathway using pyrimidodiazepine provides unique collections of polyheterocyclic compounds with biological relevancy. Therefore, this pDOS library could play a pivotal role in the perturbation of a wide range of challenging biological targets in a selective and specific manner. To demonstrate this, we performed ELISA-based HTS with this pDOS library and identified **21f**, a new small-molecule PPI inhibitor of the LRS-RagD interaction, which mediates Leu sensing in the mTORC1 signaling pathway. Through a series of biological experiments including western blotting, biophysical study using SPR, we confirmed that **21f** could selectively inhibit mTORC1 activity, even in the presence of Leu by disrupting the LRS-RagD interaction. Therefore, this PPI inhibitor could be a powerful tool to specifically delineate unrevealed amino acid-dependent biological processes of mTORC1. Furthermore, it could act as a lead structure in the development of novel therapeutic agents to treat diseases linked to the oncogenic activation of mTORC1, thus highlighting the great potential of the pDOS strategy to address unmet therapeutic challenges.

2.4 References

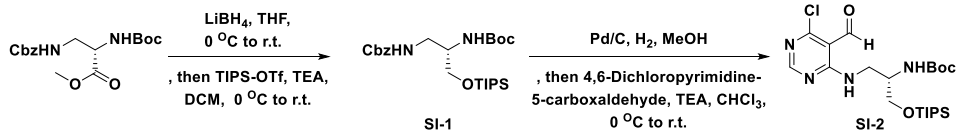
- [01] Dandapani, S.; Marcaurelle, L. A. *Nat. Chem. Biol.* **2010**, *6*, 861.
- [02] Swinney, D. C.; Anthony, J. *Nat. Rev. Drug Discov.* **2011**, *10*, 507.
- [03] O'Connor, C. J.; Laraia, L.; Spring, D. R. *Chem. Soc. Rev.* **2011**, *40*, 4332.
- [04] Schreiber, S. L. *Science*, **2000**, 287, 1964.
- [05] Schreiber, S. L. *Nature*, **2009**, 457, 153.
- [06] Galloway, W. R. J. D.; Isidro-Llobet, A.; Spring, D. R. *Nat. Commun.* **2010**, *1*, 80.
- [07] Kopp, F.; Stratton, C. F.; Akella, L. B.; Tan, D. S. *Nat. Chem. Biol.* **2012**, *8*, 358.
- [08] Beckmann, H. S. G.; Nie, F.; Hagerman, C. E.; Johansson, H.; Tan, Y. S.; Wilcke, D.; Spring, D. R. *Nat. Chem.* **2013**, *5*, 861.
- [09] Huigens III, R.; Morrison, K.; Hicklin, R.; Flood Jr, T.; Richter, M.; Hergenrother, P. *Nat. Chem.* **2013**, *5*, 195.
- [10] Mizoguchi, H.; Oikawa, H.; Oguri, H. *Nat. Chem.* **2014**, *6*, 57.
- [11] Zhang, J.; Wu, J.; Hong, B.; Ai, W.; Wang, X.; Li, H.; Lei, X. *Nat. Commun.* **2014**, *5*, 4614.
- [12] Rizzo, S.; Waldmann, H. *Chem. Rev.* **2014**, *114*, 4621.
- [13] Ibbeson, B. M.; Laraia, L.; Alza, E.; O' Connor, C. J.; Tan, Y. S.; Davies, H. M.; McKenzie, G.; Venkitaraman, A. R.; Spring, D. R. *Nat. Commun.* **2014**, *5*, 3155.
- [14] Garcia-Castro, M.; Kremer, L.; Reinkemeier, C. D.; Unkelbach, C.; Strohmman, C.; Ziegler, S.; Ostermann, C.; Kumar, K. *Nat. Commun.* **2015**, *6*, 6516.
- [15] Oh, S.; Park, S. B. *Chem. Commun.* **2011**, *47*, 12754.
- [16] Kim, H.; Tung, T. T.; Park, S. B. *Org. Lett.* **2013**, *15*, 5814.
- [17] Kim, J.; Kim, H.; Park, S. B. *J. Am. Chem. Soc.* **2014**, *136*, 14629.

- [18] Park, J.; Oh, S.; Park, S. B. *Angew. Chem. Int. Ed.* **2012**, *51*, 5447.
- [19] Lee, S.; Nam, Y.; Koo, J. Y.; Lim, D.; Park, J.; Ock, J.; Suk, K.; Park, S. B. *Nat. Chem. Biol.* **2014**, *10*, 1055.
- [20] Wakeling, A. E.; Guy, S. P.; Woodburn, J. R.; Ashton, S. E.; Curry, B. J.; Barker, A. J.; Gibson, K. H. *Cancer Res.* **2002**, *62*, 5749.
- [21] Wunder, F. *Mol. Pharmacol.* **2005**, *68*, 1775.
- [22] Yaziji, V.; Rodríguez, D.; Gutiérrez-de-Terán, H.; Coelho, A.; Caamaño, O.; García-Mera, X.; Brea, J.; Loza, M. I.; Cadavid, M. I.; Sotelo, E. *J. Med. Chem.* **2011**, *54*, 457.
- [23] Domling, A. *Curr. Opin. Chem. Biol.* **2008**, *12*, 281.
- [24] Crews, C. M. *Chem. Biol.* **2010**, *17*, 551.
- [25] Grivas, P. D.; Kiaris, H.; Papavassiliou, A. G. *Trends Mol. Med.* **2011**, *17*, 537.
- [26] Vitaku, E.; Smith, D. T.; Njardarson, J. T. *J. Med. Chem.* **2014**, *57*, 10257.
- [27] Smith, S. G.; Sanchez, R.; Zhou, M. M. *Chem. Biol.* **2014**, *21*, 573.
- [28] Han, J.; Jeong, S.; Park, M.; Kim, G.; Kwon, N.; Kim, H.; Ha, S.; Ryu, S.; Kim, S. *Cell* **2012**, *149*, 410.
- [29] Kim, I.; Roh, S. W.; Lee, D. G.; Lee, C. *Org. Lett.* **2014**, *16*, 2482.
- [30] Bailey, T. S.; Bremner, J. B.; Carver, J. A. *Tetrahedron Lett.* **1993**, *34*, 3331.
- [31] Srivastava, A. K.; Koh, M.; Park, S. B. *Chem. Eur. J.* **2011**, *17*, 4905.
- [32] Bremner J. B.; Sengpracha W. *Tetrahedron.* **2005**, *61*, 941.
- [33] Cossy, J.; Arseniyadis, S.; Meyer, C. *Metathesis in Natural Product Synthesis*; Wiley-VCH, 2011, pp 1-43.
- [34] Mak, J. Y. W.; Pouwer, R. H.; Williams, C. M. *Angew. Chem. Int. Ed.* **2014**, *53*, 13664.
- [35] Rosenblum, S. B.; Huynh, T.; Afonso, A.; Davis, H. R.; Yumibe, N.;

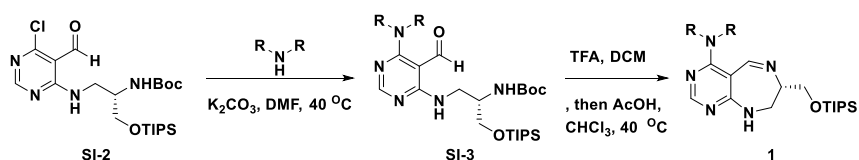
- Clader, J. W.; Burnett, D. A. *J. Med. Chem.* **1998**, *41*, 973.
- [36] Kinscherf, T. G.; Willis, D. K. *J. Antibiot.* **2005**, *58*, 817.
- [37] Baumann, M.; Baxendale, I. R. *Beilstein J. Org. Chem.* **2011**, *7*, 442.
- [38] Bauer, R. A.; Wenderski, T. A.; Tan, D. S. *Nat. Chem. Biol.* **2013**, *9*, 21.
- [39] Laplante, M.; Sabatini, D. M. *Cell* **2012**, *149*, 274.
- [40] Efeyan, A.; Comb, W. C.; Sabatini, D. M. *Nature* **2015**, *517*, 302..
- [41] Segev, N.; Hay, N. *Mol. Cell* **2012**, *46*, 4.
- [42] Cusack, S.; Yaremchuk, A.; Tukalo, M. *EMBO J.* **2000**, *19*, 2351.
- [43] Fingar, D. C.; Richardson, C. J.; Tee, A. R.; Cheatham, L.; Tsou, C.; Blenis, J. *Mol. Cell. Biol.* **2004**, *24*, 200.

2.5 Experimental Section

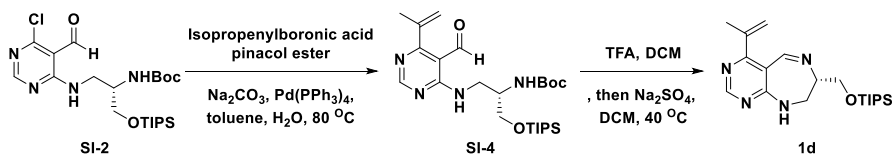
2.5.1 Supplementary Figures



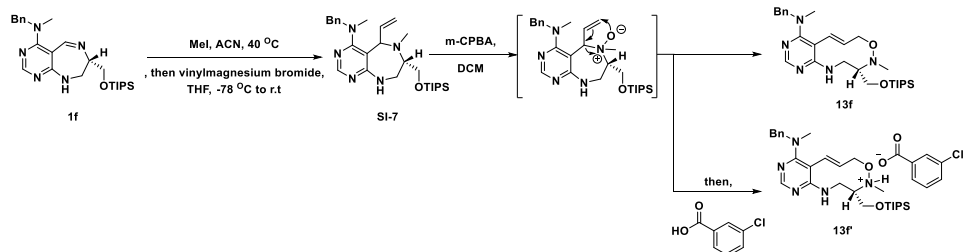
Supplementary Figure 1. Synthetic procedure for the *tert*-butyl (*S*)-(1-((6-chloro-5-formylpyrimidin-4-yl)amino)-3-(((triisopropylsilyl)oxy)propan-2-yl)carbamate (SI-2)



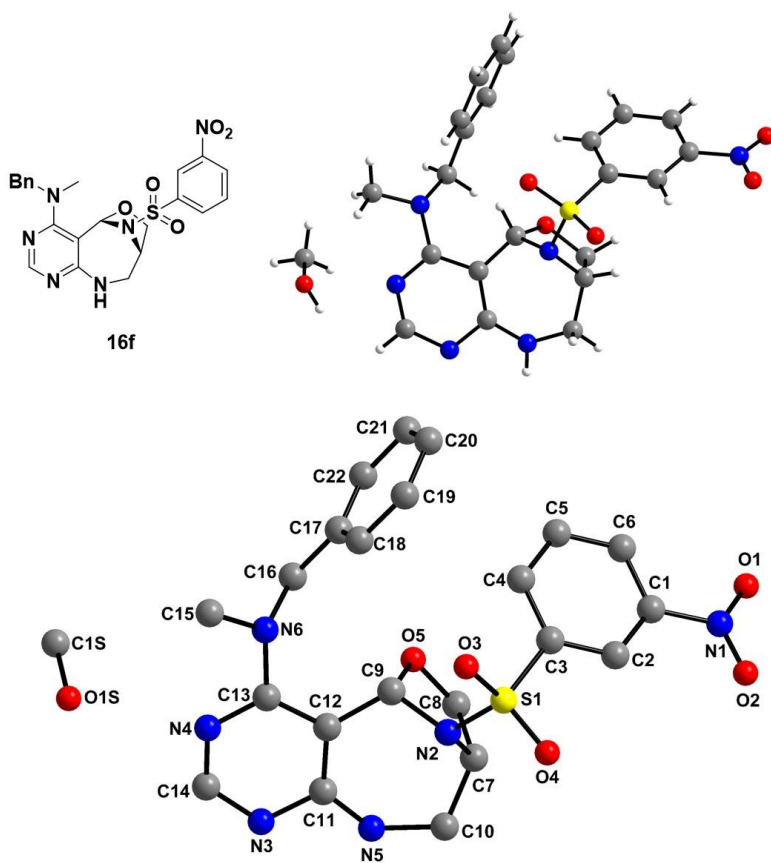
Supplementary Figure 2. General procedure for the preparation of **1a–c** and **1e–f**.



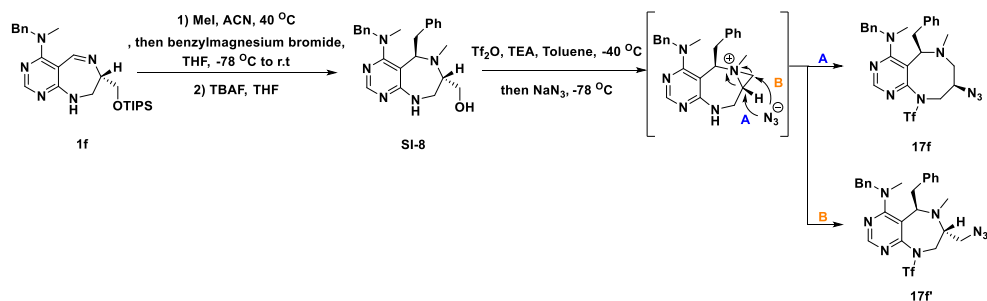
Supplementary Figure 3. Synthetic procedure for the preparation of (*S*)-4-(prop-1-en-2-yl)-7-(((triisopropylsilyl)oxy)methyl)-8,9-dihydro-7H-pyrimido[4,5-e][1,4]diazepine (**1d**).



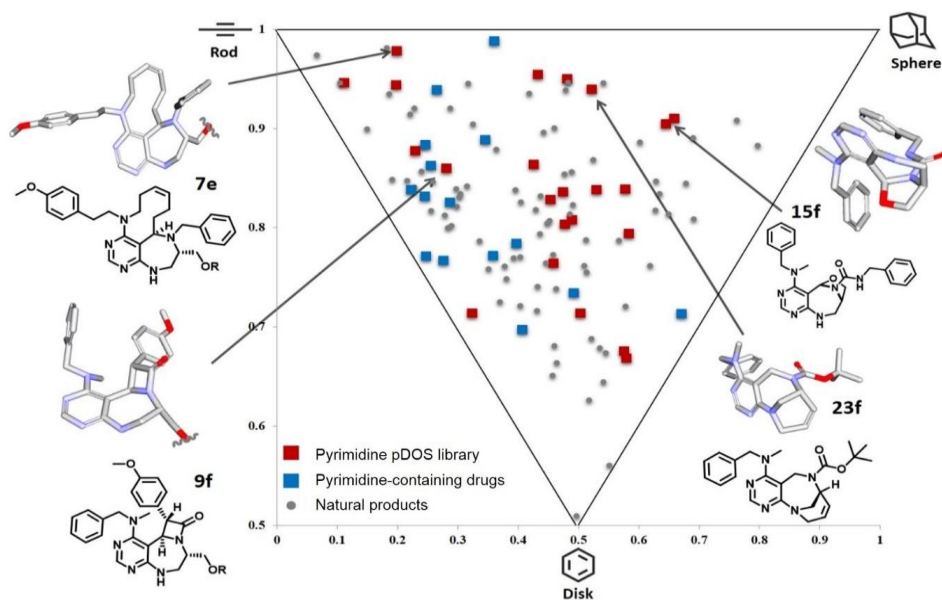
Supplementary Figure 4. Synthetic procedure for the preparation of **13f** and **13f'**.



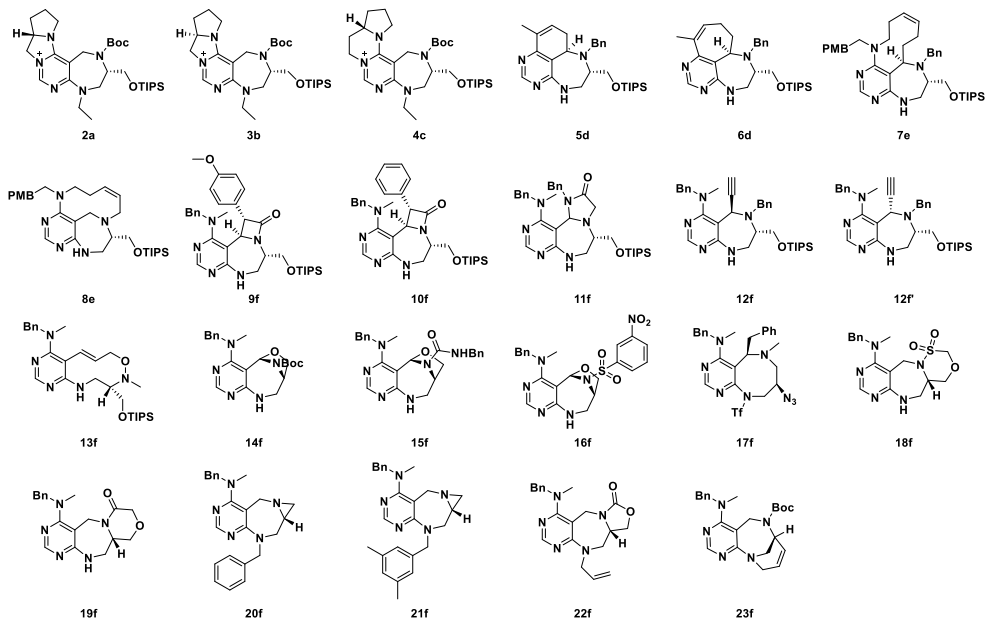
Supplementary Figure 5. X-ray structure of **16f**. Deposition number in Cambridge Structural Database: CCDC1500586.



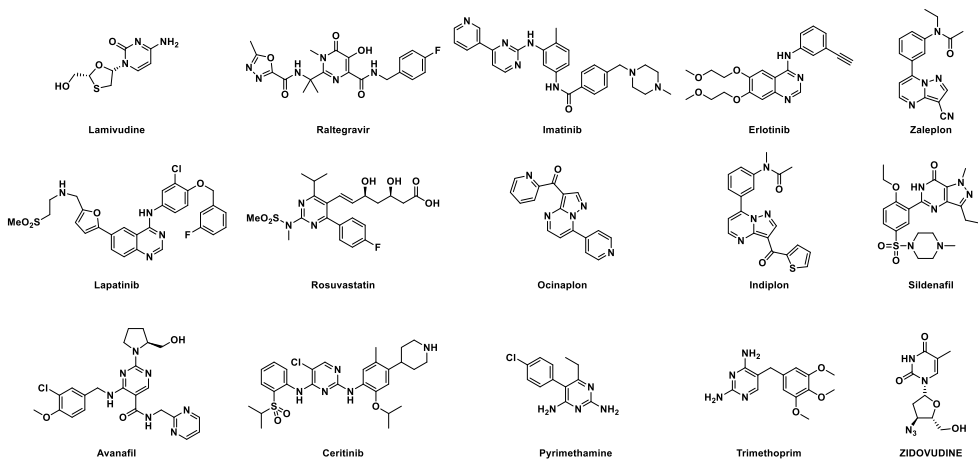
Supplementary Figure 6. Synthetic procedure for the preparation of **17f** and **17f'**.



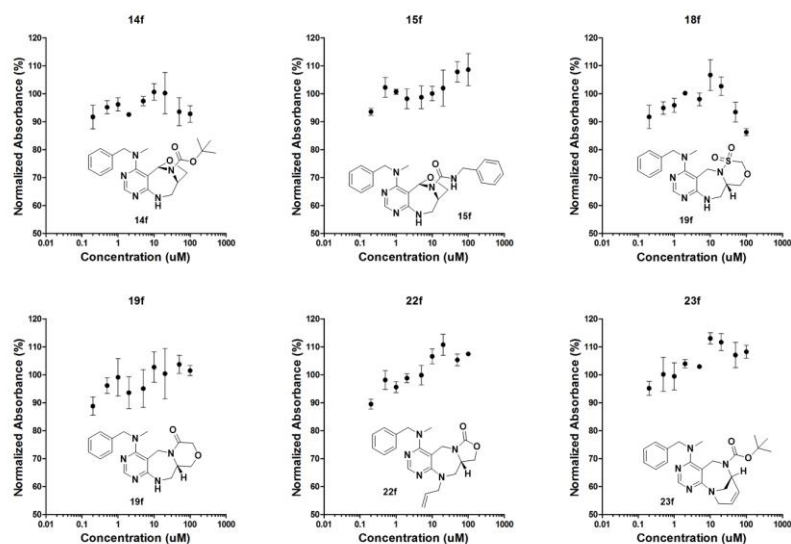
Supplementary Figure 7. Principal moment of inertia (PMI) plot.



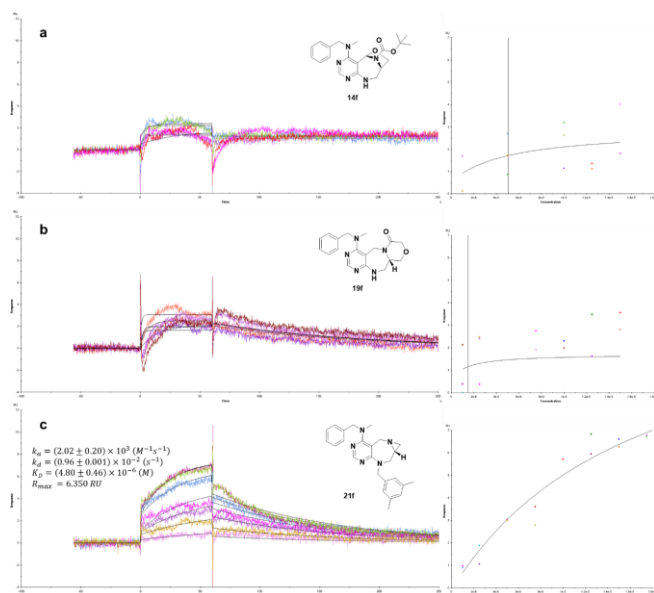
Supplementary Figure 8. Complete pDOS Library used in PMI analysis



Supplementary Figure 9. FDA-approved drugs embedded with pyrimidine moieties.¹



Supplementary Figure 10. Dose-response curves in ELISA with **14f**, **15f**, **18f**, **19f**, **22f** and **23f**.



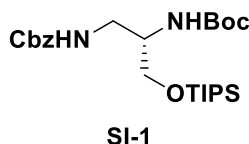
Supplementary Figure 11. SPR curves showing concentration-dependent binding to purified LRS. Normalized RUs are plotted over a time course. a) SPR curves with **14f** with 1, 5, 10, 12.5 and 15 μM concentrations. b) SPR curves with **19f** with 1, 2.5, 7.5, 10, 12.5 and 15 μM concentrations. c) SPR curves with **21f** with 1, 2.5, 5, 10, 12.5, 15, 17.5 and 20 μM concentrations.

2.5.2. General Information of Synthetic Protocols

NMR spectra were obtained on an Agilent 400-MR DD2 Magnetic Resonance System (400 MHz, Agilent, USA), JEOL JNM-LA400 with LFG [400 MHz, Jeol, Japan], Varian/Oxford As-500 [500 MHz, Varian Assoc., Palo Alto, USA] or Bruker Avance III HD 800 MHz NMR Spectrometer [800 MHz, Bruker, Germany]. Chemical shifts values were recorded as parts per million (δ), referenced to tetramethylsilane (TMS) as the internal standard or to the residual solvent peak (CDCl_3 , ^1H : 7.26, ^{13}C : 77.16, CD_3OD , ^1H : 3.31, ^{13}C : 49.00, $\text{DMSO}-d_6$, ^1H : 2.50, ^{13}C : 39.52). Multiplicities were indicated as follows: s (singlet), d (doublet), t (triplet), q (quartet); m (multiplet); dd (doublet of doublet); dt (doublet of triplet); td (triplet of doublets); br s (broad singlet) and so on. Coupling constants were reported in hertz (Hz). IR spectra were measured on a Thermo Scientific NicoletTM 6700 FT-IR spectrometer. Low resolution mass spectra were obtained on a Finnigan Surveyor MSQ Plus LC/MS [Thermo], LCQ LC/MS [Thermo] or Shimadzu LCMS-2020 using the electrospray ionization (ESI) method. High resolution mass spectra were analyzed at the Mass Spectrometry Laboratory of National Instrumentation Center for Environmental Management (NICEM) in Seoul on a LCQ LC/MS [Thermo] using the electrospray ionization (ESI) method or by Ultra High Resolution ESI Q-TOF mass spectrometer (Bruker). All commercially available reagents were used without further purification unless noted otherwise. Commercially available reagents were obtained from Sigma-Aldrich, TCI, Acros, or Alfa Aesar. All solvents were obtained by passing them through activated alumina columns of solvent purification systems from Glass Contour. Analytical thin-layer chromatography (TLC) was performed using Merck Kieselgel 60 F254 plates, and the components were visualized by observation under UV light (254 and 365 nm) or by treating the plates with ninhydrin followed by thermal visualization. Flash column chromatography was performed on Merck Kieselgel 60 (230–400 mesh). Microwave reactions were performed using the CEM Discover Benchmate and microwave reaction conditions were as indicated in the Experimental Section. HPLC purification was performed on an Agilent 1260 Infinity system with an YMC-Pack silica column (SL12S05-2520WTX, 250 mm×20 mm, 5 μm).

2.5.3. Synthesis and Characterization of Substrates

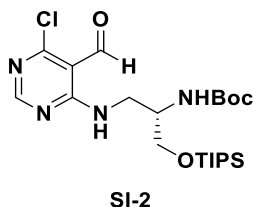
Synthetic procedure for the preparation of Benzyl *tert*-butyl (3-(((triisopropylsilyl)oxy)propane-1,2-diyl)(*S*)-dicarbamate (SI-1).



Lithium borohydride (LiBH_4) (2.0 M solution in THF, 56.8 ml, 113.5 mmol) was slowly added to a stirring solution of methyl (*S*)-3-(((benzyloxy)carbonyl)amino)-2-(((*tert*-butoxycarbonyl) amino)propanoate³ (20.00 g, 56.76 mmol) in tetrahydrofuran (THF) (570.0 ml) at 0 °C. Then, the resulting mixture was left to stir and allowed to warm to r.t. After completion of the reaction as indicated by TLC, the reaction mixture was quenched with saturated $\text{NH}_4\text{Cl}(\text{aq})$ and extracted twice with dichloromethane (DCM). The combined organic layer was dried over anhydrous $\text{Na}_2\text{SO}_4(\text{s})$ and filtered. The organic layer was condensed under reduced pressure, and the crude resultant was dissolved in dry DCM (570.0 ml) under argon atmosphere. To this solution were sequentially added triethylamine (Et_3N) (15.83 ml, 113.5 mmol) and triisopropylsilyl trifluoromethanesulfonate (TIPS-OTf) (22.88 ml, 85.14 mmol) at 0 °C. The resulting mixture was left to stir and allowed to warm to r.t. After completion of the reaction as indicated by TLC, the resultant was quenched with saturated $\text{NH}_4\text{Cl}(\text{aq})$ and extracted twice with DCM. The combined organic layer was dried over anhydrous $\text{Na}_2\text{SO}_4(\text{s})$ and filtered. The filtrate was condensed under reduced pressure, followed by silica-gel flash column chromatography to afford the desired product **SI-1** (22.37 g, 82% yield) as a colorless oil (Supplementary Fig. 1).

R_f = 0.4 (hexane/EtOAc 5:1); ^1H NMR (400 MHz, CDCl_3) δ 7.35–7.29 (m, 5H), 5.32 (br s, 1H), 5.10 (s, 2H), 5.00 (br s, 1H), 3.77–3.73 (m, 3H), 3.47–3.39 (m, 2H), 1.43 (s, 9H), 1.06 (m, 21H); ^{13}C NMR (100 MHz, CDCl_3) δ 157.0, 156.1, 136.7, 128.6, 128.11, 128.07, 79.6, 66.8, 64.3, 51.8, 43.5, 28.4, 18.0, 11.9; LRMS(ESI⁺): Calcd for $\text{C}_{25}\text{H}_{45}\text{N}_2\text{O}_5\text{Si}^+$ $[\text{M}+\text{H}]^+$ 481.31, found 481.11.

Synthetic procedure for the preparation of *tert*-butyl (*S*)-(1-((6-chloro-5-formylpyrimidin-4-yl)amino)-3-((triisopropylsilyl)oxy)propan-2-yl)carbamate (SI-2**).**



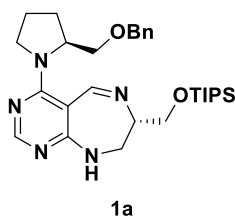
To a solution of **SI-1** (22.37 g, 46.54 mmol) in methanol (MeOH) (470.0 ml) was carefully added 10 wt. % Pd/C (11.19 g) and the mixture was vigorously stirred under H₂ atmosphere (1 atm) at r.t. After completion of the reaction as indicated by TLC, the reaction mixture was filtered through Celite® while washing with ethyl acetate. The filtrate was condensed under reduced pressure and the crude resultant was dissolved in chloroform (CHCl₃, 470.0 ml). To this solution were sequentially added Et₃N (9.737 ml, 69.81 mmol) and 4,6-dichloropyrimidine-5-carboxaldehyde (8.237 g, 46.54 mmol) at 0 °C and left to stir. After 30 min, the reaction mixture was quenched with saturated NH₄Cl(aq). The resultant was extracted twice with CHCl₃, dried over anhydrous Na₂SO₄(s), and filtered. The filtrate was condensed under reduced pressure and purified by silica-gel flash column chromatography to afford the desired product **SI-2** (15.19 g, 67% yield) as a colorless oil (Supplementary Fig. 1).

R_f = 0.5 (hexane/EtOAc 3:1); ¹H NMR (400 MHz, CDCl₃) δ 10.28 (s, 1H), 9.30 (t, J = 5.7 Hz, 1H), 8.34 (s, 1H), 4.99 (d, J = 8.6 Hz, 1H), 3.90–3.62 (m, 5H), 1.33 (s, 9H), 1.06 (m, 21H); ¹³C NMR (100 MHz, CDCl₃) δ 191.1, 165.3, 161.7, 160.7, 155.6, 108.2, 79.5, 63.7, 51.4, 42.4, 28.3, 17.9, 11.9; LRMS (ESI⁺): Calcd for C₂₂H₄₀ClN₄O₄Si⁺ [M+H]⁺ 487.25, found 487.03.

General procedure for the preparation of 1a–c and 1e–f.

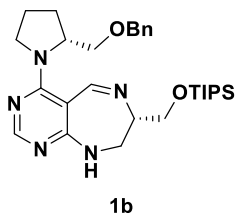
To a stirring solution of **SI-2** (500 mg, 1.026 mmol) and K₂CO₃ (283.6 mg, 2.052 mmol) in *N,N*-dimethylformamide (DMF) (10.0 ml) was added amine^{4,5} (1.539

mmol) and the resulting mixture was stirred at 40 °C. After completion of the reaction as indicated by TLC, the resultant was quenched with saturated NH₄Cl(aq) and extracted twice with ethyl acetate. The combined organic layer was dried over anhydrous Na₂SO₄(s) and filtered. The organic solvent was evaporated under vacuum to afford a crude oil, which was purified by silica-gel flash column chromatography to afford **SI-3**. To obtain the cyclic imine product **1**, **SI-3** was first treated with 10% trifluoroacetic acid (TFA) in DCM (20.0 ml) at r.t. After the starting material was consumed as indicated by TLC, any excess TFA was removed by azeotropic evaporation with toluene under reduced pressure, and the crude resultant was dissolved in 1% acetic acid (AcOH) in CHCl₃ (100.0 ml). The resulting mixture was stirred at 40 °C. After completion of the reaction as indicated by TLC, the resultant was quenched with saturated NaHCO₃(aq) and extracted twice with CHCl₃. The combined organic layer was dried over anhydrous Na₂SO₄(s) and filtered. The filtrate was condensed under reduced pressure, followed by silica-gel flash column chromatography to afford the desired product **1** (Supplementary Fig. 2).



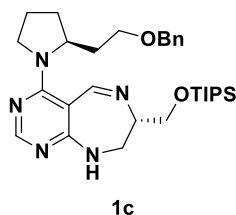
(S)-4-((S)-2-((benzyloxy)methyl)pyrrolidin-1-yl)-7-(((triisopropylsilyl)oxy)methyl)-8,9-dihydro-7H-pyrimido[4,5-e][1,4]diazepine (1a). A pale yellow oil; *R_f* = 0.2 (DCM/MeOH = 20:1); 403.1 mg, 75% overall yield; ¹H NMR (400 MHz, CDCl₃) δ 8.11 (s, 1H), 7.98 (s, 1H), 7.29

(m, 5H), 5.97 (br s, 1H), 4.74 (m, 1H), 4.54, 4.53 (ABq, *J*_{AB} = 12.1 Hz, 2H), 4.18 (dd, *J* = 9.8, 4.7 Hz, 1H), 3.90 (m, 1H), 3.80 (dd, *J* = 12.5, 5.5 Hz, 1H), 3.73 (m, 2H), 3.67 (m, 1H), 3.60 (dd, *J* = 9.4, 5.9 Hz, 1H), 3.47 (m, 1H), 3.34 (dd, *J* = 11.3, 7.0 Hz, 1H), 2.15 (m, 1H), 1.96 (m, 2H), 1.71 (m, 1H), 1.08 (m, 21H); ¹³C NMR (100 MHz, CDCl₃) δ 164.5, 160.9, 159.1, 157.4, 138.6, 128.4, 127.6, 127.5, 93.1, 73.3, 71.1, 65.1, 64.2, 58.0, 55.2, 47.8, 28.0, 26.1, 18.2, 12.0; HRMS(ESI⁺): Calcd for C₂₉H₄₆N₅O₂Si⁺ [M+H]⁺ 524.3415, found 524.3414, Δppm −0.19.



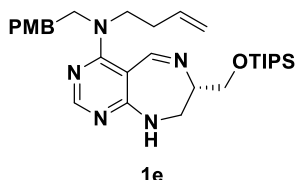
(S)-4-((R)-2-((benzyloxy)methyl)pyrrolidin-1-yl)-7-(((triisopropylsilyl)oxy)methyl)-8,9-dihydro-7H-pyrimido[4,5-e][1,4]diazepine (1b).

A pale yellow oil; R_f = 0.2 (DCM/MeOH = 20:1); 408.4 mg, 76% overall yield; ^1H NMR (400 MHz, CDCl_3) δ 8.14 (s, 1H), 7.96 (s, 1H), 7.30 (m, 5H), 6.20 (br s, 1H), 4.74 (m, 1H), 4.53 (s, 2H), 4.19 (dd, J = 9.7, 3.1 Hz, 1H), 4.02 (m, 1H), 3.84 (m, 1H), 3.74 (m, 2H), 3.63 (m, 2H), 3.46 (t, J = 9.7 Hz, 1H), 3.14 (m, 1H), 2.14 (m, 1H), 1.99 (m, 2H), 1.74 (m, 1H), 1.09 (m, 21H); ^{13}C NMR (100 MHz, CDCl_3) δ 165.0, 164.2, 156.4, 154.0, 138.4, 128.2, 127.4, 127.4, 92.0, 73.1, 70.8, 65.3, 65.0, 57.9, 55.2, 46.6, 27.8, 25.8, 18.0, 11.8; HRMS(ESI $^+$): Calcd for $\text{C}_{29}\text{H}_{46}\text{N}_5\text{O}_2\text{Si}^+$ $[\text{M}+\text{H}]^+$ 524.3415, found 524.3415.



(S)-4-((S)-2-(2-(benzyloxy)ethyl)pyrrolidin-1-yl)-7-(((triisopropylsilyl)oxy)methyl)-8,9-dihydro-7H-pyrimido[4,5-e][1,4]diazepine (1c).

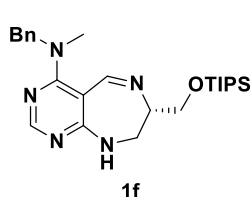
A colorless oil; R_f = 0.35 (DCM/MeOH = 20:1); 419.4 mg, 76% overall yield; ^1H NMR (400 MHz, CDCl_3) δ 8.07 (s, 1H), 7.99 (s, 1H), 7.33 (m, 4H), 7.29–7.26 (m, 1H), 6.17 (br s, 1H), 4.61 (m, 1H), 4.53, 4.26 (ABq, J_{AB} = 11.94 Hz, 2H), 4.18 (dd, J = 9.8, 4.3 Hz, 1H), 3.92 (m, 1H), 3.81–3.62 (m, 3H), 3.60–3.56 (m, 2H), 3.45 (m, 1H), 3.33 (m, 1H), 2.33–2.25 (m, 1H), 2.19–2.13 (m, 1H), 1.91–1.87 (m, 1H), 1.80–1.66 (m, 3H), 1.08 (m, 21H); ^{13}C NMR (100 MHz, CDCl_3) δ 164.8, 161.1, 159.0, 157.4, 138.6, 128.4, 127.8, 127.6, 93.2, 73.0, 67.7, 65.1, 64.3, 56.9, 55.1, 47.6, 34.1, 31.0, 26.2, 18.1, 12.0; HRMS(ESI $^+$): Calcd for $\text{C}_{30}\text{H}_{48}\text{N}_5\text{O}_2\text{Si}^+$ $[\text{M}+\text{H}]^+$ 538.3572, found 538.3571, Δppm –0.19.



(S)-N-(but-3-en-1-yl)-N-(4-methoxyphenethyl)-7-(((triisopropylsilyl)oxy)methyl)-8,9-dihydro-7H-pyrimido[4,5-e][1,4]diazepin-4-amine (1e).

A pale yellow oil; R_f = 0.4 (DCM/MeOH = 20:1); 364.2 mg, 66% overall yield; ^1H NMR (400 MHz, CDCl_3) δ 8.05 (s, 1H), 7.98 (d, J = 1.9 Hz, 1H), 7.07 (d, J = 8.6 Hz, 2H), 6.80 (d, J = 8.6 Hz, 2H), 6.42 (m, 1H), 5.72 (dddd, J = 16.8, 10.1, 6.6, 6.6 Hz, 1H), 5.02 (m, 2H), 4.18 (dd, J = 9.7, 4.3 Hz, 1H), 3.84 (m, 3H), 3.77 (s, 3H), 3.69 (m, 2H), 3.46 (m, 1H), 3.34 (m, 2H), 2.83 (t, J = 7.4 Hz,

2H), 2.33 (q, $J = 7.0$ Hz, 2H), 1.08 (m, 21H); ^{13}C NMR (100 MHz, CDCl_3) δ 167.2, 161.9, 158.2, 157.8, 157.1, 135.2, 131.0, 129.7, 117.0, 114.0, 94.3, 65.2, 64.5, 55.3, 53.5, 51.2, 47.6, 33.7, 32.6, 18.1, 12.0; HRMS(ESI $^{+}$): Calcd for $\text{C}_{30}\text{H}_{48}\text{N}_5\text{O}_2\text{Si}^{+}$ $[\text{M}+\text{H}]^{+}$ 538.3572, found 538.3572.



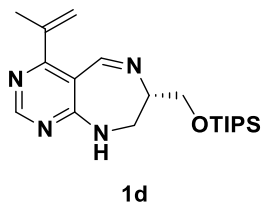
(S)-N-benzyl-N-methyl-7-

(((triisopropylsilyl)oxy)methyl)-8,9-dihydro-7H-

pyrimido[4,5-e][1,4]diazepin-4-amine (1f). A colorless oil; $R_f = 0.35$ (DCM/MeOH = 20:1); 349.1 mg, 75% overall yield; ^1H NMR (400 MHz, CDCl_3) δ 8.17 (d, $J = 1.9$ Hz,

1H), 8.06 (s, 1H), 7.35–7.25 (m, 5H), 6.99 (br s, 1H), 4.81, 4.71 (ABq, $J_{AB} = 15.2$ Hz, 2H), 4.18 (dd, $J = 9.8, 4.3$ Hz, 1H), 3.89 (m, 2H), 3.66 (t, $J = 10.0$ Hz, 1H), 3.32 (ddd, $J = 13.0, 7.1, 2.5$ Hz, 1H), 3.03 (s, 3H), 1.08 (m, 21H); ^{13}C NMR (100 MHz, CDCl_3) δ 167.4, 162.4, 157.2, 157.1, 137.3, 128.7, 127.7, 127.4, 92.7, 65.1, 64.5, 56.6, 47.3, 40.1, 18.0, 11.9; HRMS(ESI $^{+}$): Calcd for $\text{C}_{25}\text{H}_{40}\text{N}_5\text{OSi}^{+}$ $[\text{M}+\text{H}]^{+}$ 454.2997, found 454.2996, $\Delta\text{ppm} -0.22$.

(S)-4-(prop-1-en-2-yl)-7-(((triisopropylsilyl)oxy)methyl)-8,9-dihydro-7H-pyrimido[4,5-e][1,4]diazepine (1d).

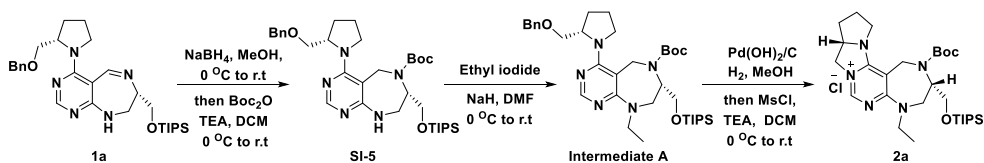


Palladium tetrakis(triphenylphosphine) $\text{Pd}(\text{PPh}_3)_4$ (119.0 mg, 0.103 mmol, 10 mol%) was added to a vigorously stirring solution of **SI-2** (500 mg, 1.026 mmol), isopropenylboronic acid pinacol ester (0.290 ml, 1.539 mmol), and Na_2CO_3 (380.6 mg, 3.591 mmol.) in toluene–water solvent mixture (25.0 ml/25.0 ml) at r.t. The resulting mixture was stirred at 80 °C. After completion of the reaction as indicated by TLC, the reaction mixture was diluted with ethyl acetate, washed with brine,

dried over anhydrous $\text{Na}_2\text{SO}_4(\text{s})$, and filtered. The filtrate was condensed under reduced pressure and the residue was purified with silica-gel flash column chromatography to provide compound **SI-4** (379.2 mg, 75% yield). To obtain the cyclic imine products **1d**, **SI-4** (379.2 mg, 0.770 mmol) was first treated with 10% TFA in DCM (100.0 ml). After the starting material was consumed as indicated by TLC, the resultant was quenched with saturated $\text{NaHCO}_3(\text{aq})$ and extracted twice with DCM. The combined organic layer was dried over anhydrous $\text{Na}_2\text{SO}_4(\text{s})$ and filtered. The filtrate was condensed under reduced pressure and the crude resultant was dissolved in DCM (100.0 ml). To this solution was added $\text{Na}_2\text{SO}_4(\text{s})$ (2.915 g, 20.52 mmol) and the resulting mixture was stirred at 40 °C. After completion of the reaction as indicated by TLC, the reaction mixture was filtered and concentrated *in vacuo*. The residue was purified with silica-gel flash column chromatography to afford the desired cyclic imine product **1d** (234.4 mg, 81% yield, 61% overall yield) as a colorless oil (Supplementary Fig. 3).

R_f = 0.2 (DCM/MeOH 20:1); ^1H NMR (400 MHz, CDCl_3) δ 8.47 (d, J = 2.3 Hz, 1H), 8.43 (s, 1H), 7.37 (br d, J = 5.0 Hz, 1H), 5.54 (s, 1H), 5.10 (s, 1H), 4.27 (dd, J = 9.7, 4.7 Hz, 1H), 3.95 (dd, J = 13.0, 7.0 Hz, 1H), 3.81 (m, 1H), 3.69 (t, J = 10.1 Hz, 1H), 3.19 (m, 1H), 2.17 (s, 3H), 1.08 (m, 21H); ^{13}C NMR (100 MHz, CDCl_3) δ 172.2, 161.0, 158.0, 157.9, 142.2, 120.9, 107.3, 65.2, 64.8, 47.4, 22.3, 18.1, 11.9; HRMS(ESI $^+$): Calcd for $\text{C}_{20}\text{H}_{35}\text{N}_4\text{OSi}^+$ $[\text{M}+\text{H}]^+$ 375.2575, found 375.2574, Δ ppm -0.27.

Synthetic procedure for the preparation of **2a**

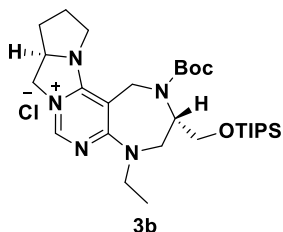


Compound 2a. To a stirring solution of **1a** (403.1 mg, 0.770 mmol) in MeOH (8.0

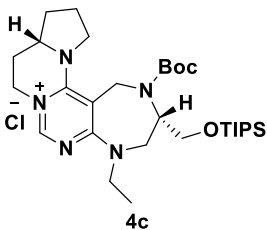
ml) was added sodium borohydride (NaBH_4) (145.6 mg, 3.850 mmol) at 0 °C. The resulting mixture was left to stir and allowed to warm to r.t. After completion of the reaction as indicated by TLC, the resultant was quenched with saturated $\text{NaHCO}_3(\text{aq})$ and extracted twice with DCM. The combined organic layer was dried over anhydrous $\text{Na}_2\text{SO}_4(\text{s})$ and filtered. The organic solvent was evaporated under reduced pressure, and the crude resultant was dissolved in DCM (8.0 ml). To this solution were sequentially added Et_3N (0.215 ml, 1.540 mmol) and di-*tert*-butyl dicarbonate (Boc_2O) (218.5 mg, 1.001 mmol) at 0 °C. The resulting mixture was left to stir and allowed to warm to r.t. After completion of the reaction as indicated by TLC, the resultant was quenched with saturated $\text{NH}_4\text{Cl}(\text{aq})$ and extracted twice with DCM. The combined organic layer was dried over anhydrous $\text{Na}_2\text{SO}_4(\text{s})$ and the filtrate was condensed under reduced pressure, followed by silica-gel flash column chromatography to afford **SI-5** (260.3 mg, 54% yield). To a solution of **SI-5** (260.3 mg, 0.416 mmol) in DMF (4.0 ml) under argon atmosphere was added NaH (60% dispersion in mineral oil, 33.28 mg, 0.832 mmol) at 0 °C and left to stir. After 30 min, ethyl iodide (0.067 ml, 0.832 mmol) was slowly added and the mixture was allowed to slowly warm to r.t. After the starting material was consumed as indicated by TLC, the reaction mixture was quenched with saturated $\text{NH}_4\text{Cl}(\text{aq})$. The resultant was extracted twice with ethyl acetate, dried with anhydrous $\text{Na}_2\text{SO}_4(\text{s})$, filtered, and concentrated *in vacuo*. The residue was purified by silica-gel flash column chromatography to obtain intermediate **A** (258.5 mg, 95% yield). To a solution of intermediate **A** (258.3 mg, 0.395 mmol) in MeOH (4.0 ml) was added 20 wt. % $\text{Pd}(\text{OH})_2/\text{C}$ (25.9 mg) and then, the mixture was vigorously stirred under H_2 atmosphere (1 atm) at r.t. After completion of the reaction as indicated by TLC, the reaction mixture was filtered through Celite® while washing with ethyl acetate. The filtrate was condensed under reduced pressure and the crude resultant was dissolved in DCM (4.0 ml). To this solution were sequentially added Et_3N (0.165 ml, 1.185 mmol) and methanesulfonyl chloride (MsCl) (0.061 ml, 0.790 mmol) at 0 °C. The resulting mixture was allowed to slowly warm up to r.t. After completion of the reaction indicated by TLC, the reaction mixture was diluted with DCM and washed twice with 1N HCl. The resultant was dried with anhydrous $\text{Na}_2\text{SO}_4(\text{s})$, filtered, condensed under reduced pressure, and purified by silica-gel flash column chromatography to afford

the desired product **2a** (280.6 mg, 61 % yield, 31% overall yield) as a white solid;

R_f = 0.1 (DCM/MeOH = 10:1); ^1H NMR (400 MHz, DMSO- d_6 , 100 °C) δ 8.50 (s, 1H), 4.64 (m, 2H), 4.48 (m, 2H), 4.33 (m, 2H), 4.13 (m, 1H), 3.82 (m, 2H), 3.76 (m, 1H), 3.69 (m, 1H), 3.62 (dd, J = 15.1, 4.6 Hz, 1H), 3.57 (m, 1H), 3.42 (m, 1H), 2.14 (m, 1H), 2.04 (m, 2H), 1.66 (m, 1H), 1.32 (br s, 9H), 1.17 (t, J = 7.1 Hz, 3H), 1.08 (m, 21H); ^{13}C NMR (100 MHz, DMSO- d_6 , 100 °C) δ 162.0, 155.8, 154.0, 146.5, 79.3, 62.8, 62.4, 50.8, 50.2, 48.9, 45.1, 29.6, 27.4, 25.7, 17.2, 12.4, 11.0; IR (neat) ν_{max} : 2940, 2866, 1698, 1638, 1523, 1174 cm^{-1} ; HRMS(ESI $^{+}$): Calcd for $\text{C}_{29}\text{H}_{52}\text{N}_5\text{O}_3\text{Si}^{+} [\text{M}]^{+}$ 546.3834, found 546.3831, Δppm –0.55; mp: 136–138 °C.



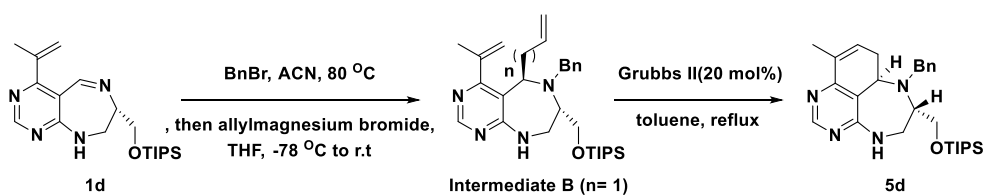
Compound 3b. A pale yellow solid; R_f = 0.1 (DCM/MeOH = 10:1); 38% overall yield; ^1H NMR (400 MHz, DMSO- d_6 , 100 °C) δ 8.42 (s, 1H), 4.88 (d, J = 16.9 Hz, 1H), 4.58 (d, J = 16.9 Hz, 1H), 4.54 (dd, J = 10.8, 9.4 Hz, 1H), 4.38 (m, 2H), 4.27 (dd, J = 10.9, 8.2 Hz, 1H), 4.16 (dd, J = 15.1, 11.9 Hz, 1H), 3.86 (m, 2H), 3.80 (m, 2H), 3.70 (m, 2H), 3.65 (m, 1H), 2.17 (m, 3H), 1.73 (m, 1H), 1.41 (s, 9H), 1.18 (t, J = 6.9 Hz, 3H), 1.09 (m, 21H); ^{13}C NMR (100 MHz, DMSO- d_6 , 100 °C) δ 162.3, 153.8, 152.8, 146.5, 93.0, 79.8, 63.2, 62.5, 56.9, 50.6, 49.0, 48.0, 46.1, 36.7, 29.2, 27.5, 26.6, 17.2, 12.3, 10.9; IR (neat) ν_{max} : 2944, 2863, 1698, 1636, 1517, 1166 cm^{-1} ; HRMS(ESI $^{+}$): Calcd for $\text{C}_{29}\text{H}_{52}\text{N}_5\text{O}_3\text{Si}^{+} [\text{M}]^{+}$ 546.3834, found 546.3833, Δppm –0.18; mp: 77–79 °C. The product was synthesized according to the synthetic procedure for the preparation of **2a** from **1b**.



Compound 4c. A pale yellow solid; R_f = 0.2 (DCM/MeOH = 10:1); 40 % overall yield; ^1H NMR (400 MHz, DMSO- d_6 , 100 °C) δ 8.34 (s, 1H), 4.48 (m, 2H), 4.23 (m, 2H), 4.05 (m, 1H), 3.85 (m, 2H), 3.79 (m, 2H), 3.71 (m, 3H), 3.61 (dd, J = 15.0, 4.6 Hz, 1H), 3.53 (m, 1H), 3.06 (br s, 1H), 3.00 (m, 1H), 2.18 (m, 1H), 1.91 (m, 3H), 1.29 (br s, 9H), 1.18 (t, J = 7.0 Hz, 2 3H), 1.09 (m, 21H); ^{13}C NMR (100 MHz, DMSO- d_6 , 100 °C) δ 161.5, 153.1, 149.2, 149.2, 71.7, 63.9, 56.3, 55.8, 49.7, 49.0, 46.8, 30.5, 28.4,

25.0, 23.6, 18.2, 13.7, 12.0; IR (neat) ν_{max} : 2946, 2867, 1694, 1625, 1529, 1457, 1116 cm^{-1} ; HRMS(ESI⁺): Calcd for $\text{C}_{30}\text{H}_{54}\text{N}_5\text{O}_3\text{Si}^+$ $[\text{M}]^+$ 560.3990, found 560.3993, Δppm -0.54 ; mp: 71–73 °C. The product was synthesized according to the synthetic procedure for the preparation of **2a** from **1c**.

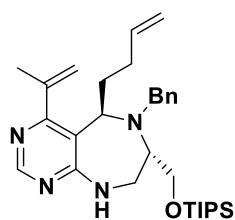
Synthetic procedure for the preparation of **5d**



Intermediate B (n=1). To a stirring solution of **1d** (100 mg, 0.267 mmol) in acetonitrile (ACN) (13.5 ml), benzyl bromide (0.048 ml, 0.401 mmol) was added and the resulting mixture was stirred at 80 °C. After completion of the reaction indicated by TLC, the organic solvent was removed under reduced pressure and the crude resultant was washed with hexane to remove any excess benzyl bromide. To a cooled solution of resultant iminium ion in dry THF (27.0 ml) was added allylmagnesium bromide (1.0 M solution in diethyl ether, 1.335 ml, 1.335 mmol) dropwise over 30 min at -78 °C. The reaction mixture was allowed to slowly warm to r.t. over an 18 h period. The resultant was quenched with saturated NH_4Cl (aq) and extracted twice with DCM. The combined organic layer was dried over anhydrous Na_2SO_4 (s) and filtered. The filtrate was condensed under reduced pressure, followed by flash column chromatography to afford intermediate **B** (n= 1, 115.0 mg, 85% yield, d.r. >99:1) as a pale yellow oil.

R_f = 0.5 (hexane/EtOAc = 1:1); ^1H NMR (400 MHz, CDCl_3) δ 8.40 (s, 1H), 7.32–7.29 (m, 3H), 7.24–7.20 (m, 2H), 5.88–5.78 (m, 2H), 5.03 (m, 2H), 4.94 (s, 1H), 4.69 (s, 1H), 4.29 (dd, J = 9.4, 5.9 Hz, 1H), 3.86 (d, J = 15.3 Hz, 1H), 3.78 (dd, J = 9.6, 3.7 Hz, 1H), 3.64–3.57 (m, 3H), 3.50–3.40 (m, 2H), 2.84 (m, 1H), 2.22 (m, 1H), 1.81 (s, 3H), 1.01 (s, 21H); ^{13}C NMR (100 MHz, CDCl_3) δ 168.4, 164.6,

155.6, 143.0, 140.1, 136.0, 128.4, 127.7, 126.9, 116.7, 116.3, 116.0, 64.4, 59.3, 57.9, 53.0, 43.3, 37.1, 23.0, 18.1, 11.9; HRMS(ESI⁺): Calcd for C₃₀H₄₇N₄OSi⁺ [M+H]⁺ 507.3514, found 507.3516, Δppm +0.39. The diastereomeric ratio was determined by LC-MS analysis of crude reaction mixture and by ¹H NMR analysis of samples purified by short silica-gel column (Supplementary Fig. 7 and 34).



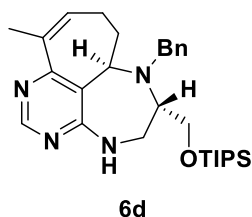
Intermediate B (n= 2)

Intermediate B (n=2). A yellow oil; R_f = 0.5 (hexane/EtOAc = 1:1); 120.8 mg, 87% yield; d.r. >99:1; ¹H NMR (400 MHz, CDCl₃) δ 8.40 (s, 1H), 7.33–7.21 (m, 5H), 5.78 (m, 1H), 5.55 (d, J = 5.1 Hz, 1H), 5.01 (dd, J = 17.2, 1.2 Hz, 1H), 4.94 (m, 2H), 4.72 (s, 1H), 4.21 (dd, J = 10.2, 5.1 Hz, 1H), 3.84 (m, 2H), 3.64–3.54 (m, 3H), 3.48–3.37 (m, 2H), 2.33–2.17 (m, 2H), 2.11–2.04 (m, 1H), 1.83 (s, 3H), 1.45–1.36 (m, 1H), 1.06 (m, 21H); ¹³C NMR (100 MHz, CDCl₃) δ 168.5, 164.7, 155.6, 143.1, 140.2, 138.2, 128.4, 127.8, 127.0, 117.7, 116.0, 114.9, 64.7, 59.2, 57.5, 52.6, 43.4, 31.7, 30.9, 23.1, 18.1, 12.0; HRMS(ESI⁺): Calcd for C₃₁H₄₉N₄OSi⁺ [M+H]⁺ 521.3670, found 521.3670. The product was synthesized according to the synthetic procedure for the preparation of **Intermediate B (n=1)** from **1d** and 3-butenylmagnesium bromide (0.2 M solution in THF). The diastereomeric ratio was determined by LC-MS analysis of crude reaction mixture and by ¹H NMR analysis of samples purified by short silica-gel column (Supplementary Fig. 8 and 35).

Compound 5d. To a solution of intermediate **B** (115.0 mg, 0.227 mmol) in toluene (11.5 ml) was added 2nd generation Grubbs' catalyst (38.20 mg, 0.045 mmol, 20 mol%) and the mixture was left to stir at reflux. After the starting material was indicated as by TLC, the organic solvent was removed under reduced pressure, and the residue was purified by silica-gel flash column chromatography to obtain the desired product **5d** (79.34 mg, 73 % yield, 62% overall yield) as a pale yellow oil.

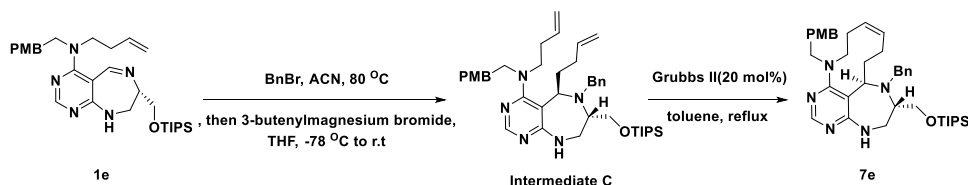
R_f = 0.4 (hexane/EtOAc = 2:1); ¹H NMR (400 MHz, CDCl₃) δ 8.43 (s, 1H), 7.34–7.18 (m, 5H), 6.08 (br s, 1H), 5.87 (d, 6.3 Hz, 1H), 5.08 (t, J = 11.0 Hz, 1H), 4.16, 3.99 (ABq, J_{AB} = 14.9 Hz, 2H), 3.87 (t, J = 13.3 Hz, 1H), 3.54–3.41 (m, 3H), 3.17 (m, 1H), 2.54 (d, J = 10.5 Hz, 2H), 2.03 (s, 3H), 0.97 (m, 21 H); ¹³C NMR (100

MHz, CDCl₃) δ 164.2, 160.4, 156.4, 141.1, 132.6, 130.4, 128.3, 128.1, 126.7, 110.9, 66.1, 61.8, 54.6, 50.5, 46.7, 29.5, 18.3, 17.9, 11.8; IR (neat) ν_{max} : 3241, 3028, 2940, 2865, 1565, 1460, 1116, 1066 cm⁻¹; HRMS(ESI⁺): Calcd for C₂₈H₄₃N₄OSi⁺ [M+H]⁺ 479.3201, found 479.3206, Δ ppm +1.04. The stereochemistry of this product was confirmed by Nuclear Overhauser Effect (NOE) spectroscopy. 1D-NOE result supported the stereochemistry as shown in Supplementary Fig. 37.



Compound 6d. A yellow oil; R_f = 0.4 (hexane/EtOAc = 2:1); 87.95 mg, 72% yield, 63% overall yield; ¹H NMR (400 MHz, CDCl₃) δ 8.42 (s, 1H), 7.22–7.12 (m, 5H), 6.10 (t, J = 6.7 Hz, 1H), 5.82 (d, J = 5.5 Hz, 1H), 3.84–3.76 (m, 5H), 3.65 (dd, J = 11.7, 7.0 Hz, 1H), 3.49 (m, 1H), 2.89 (m, 1H), 2.48 (m, 1H), 2.10 (m, 2H), 1.91 (s, 3H), 1.84 (m, 1H), 1.26 (m, 21H); ¹³C NMR (100 MHz, CDCl₃) δ 164.5, 164.1, 154.9, 140.0, 137.4, 131.8, 128.1, 127.4, 126.7, 117.1, 62.3, 61.2, 57.6, 56.3, 43.0, 35.4, 23.6, 20.1, 17.9, 11.8; IR (neat) ν_{max} : 3241, 2944, 2865, 1570, 1462, 1102, 883 cm⁻¹; HRMS(ESI⁺): Calcd for C₂₉H₄₅N₄OSi⁺ [M+H]⁺ 493.3357, found 493.3349, Δ ppm +0.41. The product was synthesized according to the synthetic procedure for the preparation of **5d** from **Intermediate B** ($n=2$). The stereochemistry of this product was confirmed by NOE spectroscopy. 1D-NOE result supported the stereochemistry as shown in Supplementary Fig. 39.

Synthetic procedure for the preparation of **7e**

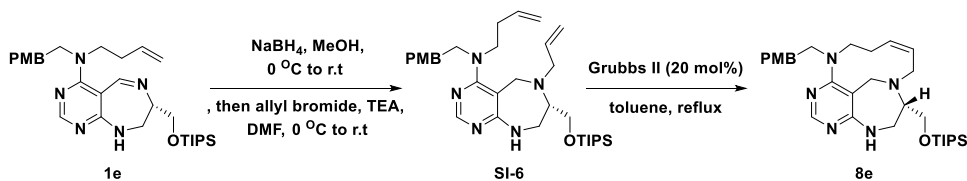


Compound 7e. To a stirring solution of **1e** (120 mg, 0.223 mmol) in acetonitrile (ACN) (11.0 ml), benzyl bromide (0.040 ml, 0.335 mmol) was added and the resulting mixture was stirred at 80 °C. After completion of the reaction indicated by

TLC, the organic solvent was removed under reduced pressure and the crude resultant was washed with hexane to remove any excess benzyl bromide. To a cooled solution of resultant iminium ion in dry THF (22.0 ml) was added 3-butenylmagnesium bromide (0.2 M solution in THF, 5.575 ml, 1.115 mmol) dropwise over 30 min at -78°C . The reaction mixture was allowed to slowly warm to r.t over an 18 h period. The resultant was quenched with saturated $\text{NH}_4\text{Cl}(\text{aq})$ and extracted twice with DCM. The combined organic layer was dried over anhydrous $\text{Na}_2\text{SO}_4(\text{s})$ and filtered. The filtrate was condensed under reduced pressure, followed by flash column chromatography to afford intermediate **C** (122.0 mg, 80% yield, d.r. 95:5). The diastereomeric ratio was determined by LC-MS analysis of crude reaction mixture (Supplementary Fig. 9). To a solution of intermediate **C** (122.0 mg, 0.178 mmol) in toluene (36.0 ml) was added 2nd generation Grubbs' catalyst (30.22 mg, 0.036 mmol, 20 mol%) and the mixture was left to stir at reflux. After the starting material was indicated as by TLC, the organic solvent was removed under reduced pressure, and the residue was purified by silica-gel flash column chromatography to obtain the desired product **7e** (85.24 mg, 73 % yield, 58% overall yield) as a pale yellow oil.

$R_f = 0.2$ (hexane/EtOAc = 3:1); ^1H NMR (400 MHz, CDCl_3) δ 8.15 (s, 1H), 7.15–7.05 (m, 5H), 6.99 (d, $J = 8.6$ Hz, 2H), 6.80 (d, $J = 8.2$ Hz, 2H), 5.47 (m, 1H), 5.37 (m, 2H), 4.30 (dd, $J = 11.9, 2.2$ Hz, 1H), 4.13 (m, 1H), 3.80 (s, 3H), 3.75 (m, 2H), 3.72 (m, 1H), 3.39 (m, 4H), 3.11 (m, 1H), 2.80 (m, 1H), 2.59 (m, 3H), 2.33 (m, 1H), 2.01 (m, 1H), 1.88 (m, 1H), 1.77 (m, 2H), 1.50 (m, 1H), 0.92 (m, 21H); ^{13}C NMR (100 MHz, CDCl_3) δ 167.4, 165.0, 158.0, 155.4, 140.2, 132.1, 131.6, 129.8, 128.8, 128.3, 128.2, 126.8, 113.9, 106.1, 64.5, 60.9, 59.2, 59.1, 57.6, 55.3, 46.9, 43.8, 34.7, 29.2, 26.3, 23.8, 18.0, 11.9; IR (neat) ν_{max} : 3245, 3000, 2942, 2865, 1572, 1512, 1247, 1113 cm^{-1} ; HRMS(ESI⁺): Calcd for $\text{C}_{39}\text{H}_{58}\text{N}_5\text{O}_2\text{Si}^+$ $[\text{M}+\text{H}]^+$ 656.4354, found 656.4345, $\Delta\text{ppm} -1.37$. The stereochemistry of **7e** was confirmed by NOE spectroscopy. 1D-NOE result supported the stereochemistry as shown in Supplementary Fig. 41.

Synthetic procedure for the preparation of **8e**



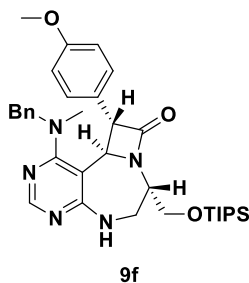
Compound 8e. To a stirring solution of **1e** (120 mg, 0.223 mmol) in MeOH (2.2 ml) was added NaBH₄ (42.18 mg, 1.115 mmol) at 0 °C and the resulting mixture was warmed to r.t. After the starting material was consumed as indicated by TLC, the resultant was quenched with saturated NaHCO₃(aq) and extracted twice with DCM. The combined organic layer was dried over anhydrous Na₂SO₄(s) and filtered. The solvent was evaporated under vacuum, and then the crude resultant was dissolved in DMF (2.2 ml). To this solution were sequentially added Et₃N (0.062 ml, 0.446 mmol) and allyl bromide (0.025 ml, 0.290 mmol) at 0 °C. The reaction was allowed to slowly warm to r.t. After completion of the reaction indicated by TLC, the resultant was quenched with saturated NH₄Cl(aq) and extracted twice with ethyl acetate. The combined organic layer was dried over anhydrous Na₂SO₄(s) and filtered. The filtrate was condensed under reduced pressure, followed by silica-gel flash column chromatography to afford **SI-6** (81.47 mg, 63% yield). To a solution of **SI-6** (81.47 mg, 0.140 mmol) in toluene (28.0 ml) was added second generation Grubbs' catalyst (23.77 mg, 0.028 mmol, 20 mol%) and the mixture was left to stir at reflux. After completion of the reaction as indicated by TLC, solvent was removed under reduced pressure and the residue was purified by silica-gel flash column chromatography to obtain the desired product **8e** (54.08 mg, 70% yield, 44% overall yield) as a yellow oil.

R_f = 0.3 (DCM/MeOH = 20:1); ¹H NMR (400 MHz, CDCl₃) δ 8.35 (s, 1H), 7.02 (d, J = 8.6 Hz, 2H), 6.79 (d, J = 8.2 Hz, 2H), 5.74 (br d, J = 5.1 Hz, 1H), 5.67 (td, J = 11.2, 4.5 Hz, 1H), 5.51 (td, J = 10.9, 4.5 Hz, 1H), 4.58 (d, J = 16.0 Hz, 1H), 4.06 (ddd, J = 14.6, 10.9, 3.1 Hz, 1H), 3.97 (d, J = 16.0 Hz, 1H), 3.76 (s, 3H), 3.59 (dd, J = 10.0, 4.1 Hz, 1H), 3.46 (m, 2H), 3.37 (m, 2H), 3.08 (m, 2H), 2.92 (m, 2H), 2.73 (m, 1H), 2.54 (m, 1H), 2.39 (ddd, J = 13.4, 10.7, 5.7, 1H), 2.18 (m, 1H), 1.76 (br d,

$J = 12.1$ Hz, 1H), 1.07 (m, 21H); ^{13}C NMR (100 MHz, CDCl_3) δ 168.2, 165.8, 157.9, 157.7, 134.3, 132.0, 129.5, 127.4, 113.7, 113.3, 69.4, 64.7, 58.1, 55.3, 52.0, 50.5, 43.9, 40.5, 33.8, 25.9, 18.0, 11.9; IR (neat) ν_{max} : 3239, 3006, 2945, 2866, 1574, 1512, 1265 cm^{-1} ; HRMS(ESI+): Calcd for $\text{C}_{31}\text{H}_{50}\text{N}_5\text{O}_2\text{Si}^+$ $[\text{M}+\text{H}]^+$ 552.3728, found 552.3722, $\Delta\text{ppm} -1.09$.

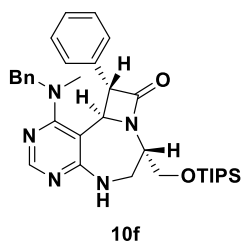
General procedure for the preparation of **9f** and **10f**

To a microwave vessel tightly sealed with a cap, were added **1f** (90.00 mg, 0.198 mmol), alkyne (0.5 mmol), 4-picoline *N*-oxide (54.57mg, 0.5 mmol) and $\text{Rh}(\text{PPh}_3)_3\text{Cl}$ (18.50 mg, 0.020 mmol, 10 mol%) in ACN (3.0 ml). The resulting mixture was heated under microwave irradiation (100 watt) at 90 °C for 35 min. The reaction mixture was diluted with DCM, washed with brine, dried over anhydrous $\text{Na}_2\text{SO}_4(\text{s})$, filtered, and concentrated *in vacuo*. The residue was purified by silica-gel flash column chromatography to obtain the desired β -lactam product.



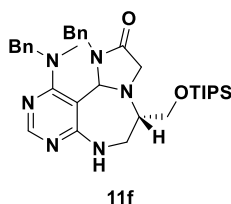
Compound 9f. A pale yellow oil; $R_f = 0.3$ (DCM/MeOH = 20:1); 72.69 mg, 61% yield; d.r. >99:1; ^1H NMR (400 MHz, CDCl_3) δ 8.10 (s, 1H), 7.25 (m, 3H), 7.11 (d, $J = 8.2$ Hz, 4H), 6.83 (d, $J = 8.2$ Hz, 2H), 6.30 (dd, $J = 6.5, 4.5$ Hz, 1H), 5.06 (s, 1H), 4.43, 4.31 (ABq, $J_{\text{AB}} = 14.9$ Hz, 2H), 4.21 (dd, $J = 10.2, 3.5$ Hz, 1H), 4.12 (m, 1H), 3.87 (m, 2H), 3.81 (s, 3H), 3.56 (s, 1H), 3.43 (ddd, $J = 14.2, 7.3, 4.3$ Hz, 1H),

2.44 (s, 3H), 1.09 (m, 21H); ^{13}C NMR (100 MHz, CDCl_3) δ 168.0, 165.3, 163.0, 159.2, 155.0, 137.5, 129.0, 128.5, 128.4, 127.3, 127.1, 114.1, 96.9, 65.2, 63.5, 59.5, 55.3, 55.2, 54.2, 42.9, 38.1, 18.0, 11.8; IR (neat) ν_{max} : 3250, 3056, 2942, 2865, 1751, 1567, 1119 cm^{-1} ; HRMS(ESI+): Calcd for $\text{C}_{34}\text{H}_{48}\text{N}_5\text{O}_3\text{Si}^+$ $[\text{M}+\text{H}]^+$ 602.3521, found 602.3528, $\Delta\text{ppm} +1.16$. The diastereomeric ratio was determined by LC-MS analysis of crude reaction mixture (Supplementary Fig. 10). The stereochemistry of this product was confirmed by NOE spectroscopy. 1D-NOE result supported the stereochemistry as shown in Supplementary Fig. 44.



Compound 10f. A yellow solid; $R_f = 0.3$ (DCM/MeOH = 20:1); 54.35 mg, 48% yield; d.r. 90:10; ^1H NMR (400 MHz, CDCl_3) δ 8.12 (s, 1H), 7.70–7.65 (m, 1H), 7.53 (m, 1H), 7.46 (m, 1H), 7.30 (m, 2H), 7.23 (m, 3H), 7.09 (m, 2H), 6.35 (dd, $J = 6.7, 4.7$ Hz, 1H), 5.11 (d, $J = 1.2$ Hz, 1H), 4.39 (m, 1H), 4.23 (m, 2H), 4.13 (m, 1H), 3.87 (m, 2H), 3.60 (d, $J = 1.5$ Hz, 1H), 3.43 (ddd, $J = 14.4, 7.3, 4.5$ Hz, 1H), 2.42 (s, 3H), 1.10 (m, 21H); ^{13}C NMR (100 MHz, CDCl_3) δ 167.6, 165.4, 163.0, 155.0, 137.4, 135.0, 132.1, 132.0, 128.7, 128.4, 127.8, 127.2, 96.9, 65.9, 63.5, 59.4, 55.2, 54.3, 42.8, 37.9, 18.0, 11.8; IR (neat) ν_{max} : 3239, 3059, 3030, 2942, 2866, 1755, 1567, 1108 cm^{-1} ; HRMS(ESI $^{+}$): Calcd for $\text{C}_{33}\text{H}_{46}\text{N}_5\text{O}_2\text{Si}^{+}$ $[\text{M}+\text{H}]^{+}$ 572.3415, found 572.3413, $\Delta\text{ppm} -0.35$; mp: 86–88 $^{\circ}\text{C}$. The diastereomeric ratio was determined by LC-MS analysis of crude reaction mixture (Supplementary Fig. 11). The stereochemistry of this product was confirmed by NOE spectroscopy. 1D-NOE result supported the stereochemistry as shown Supplementary Fig. 46.

Synthetic procedure for the preparation of 11f



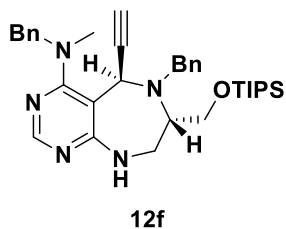
Compound 11f. To a microwave vessel tightly sealed with a cap, were added **1f** (90mg, 0.198 mmol), *N*-benzyl-2-chloroacetamide (54.54 mg, 0.297 mmol) and NaBr (30.56 mg, 0.297 mmol) in DMF (3.0 ml). The resulting mixture was heated under microwave irradiation (150 watt) at 110 $^{\circ}\text{C}$ for 30 min. The reaction mixture was cooled to r.t. 1,8-Diazabicyclo[5.4.0]undec-7-ene (DBU, 0.059 ml, 0.396 mmol) was added and left to stir at r.t. After completion of the reaction as indicated by TLC, the reaction mixture was diluted with ethyl acetate, washed with saturated $\text{NaHCO}_3(\text{aq})$, dried over anhydrous $\text{Na}_2\text{SO}_4(\text{s})$, filtered, and concentrated *in vacuo*.

The residue was purified by HPLC to obtain desired product **11f** (72.57 mg, 61%, d.r. 6:1) as a pale yellow oil. The diastereomeric ratio was determined by ^1H NMR spectroscopy (Supplementary Fig. 47).

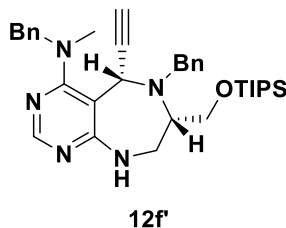
$R_f = 0.3$ (hexane/EtOAc = 1:1); ^1H NMR (400 MHz, CDCl_3) δ 8.17 (s, 0.83H, *major diastereomer*), 8.12 (s, 0.13H, *minor diastereomer*), 7.28 (br s, 3H), 7.19 (br s, 3H), 6.89 (br s, 2H), 6.73 (br s, 2H), 6.11 (br s, 0.12H, *minor diastereomer*), 5.90 (s, 0.78H, *major diastereomer*), 5.28 (s, 0.84H, *major diastereomer*), 5.08 (s, 0.13H, *minor diastereomer*), 4.98 (m, 1H), 4.44, 4.34 (ABq, $J_{AB} = 16.2$ Hz, 2H), 3.78 (m, 2H), 3.66–3.37 (m, 4H), 3.24 (m, 2H), 2.73 (m, 3H), 1.05–0.95 (m, 21H); ^{13}C NMR (100 MHz, CDCl_3) δ 173.3, 167.1, 162.9, 157.3, 137.4, 136.0, 128.6, 128.5, 127.8, 127.1, 126.9, 126.7, 88.1, 77.3, 65.0, 59.6, 57.8, 52.0, 44.1, 42.9, 37.9, 18.03, 18.02, 11.9; IR (neat) ν_{max} : 3290, 3030, 2943, 2865, 1694, 1629, 1571, 1118 cm^{-1} ; HRMS(ESI+): Calcd for $\text{C}_{34}\text{H}_{49}\text{N}_6\text{O}_2\text{Si}^+$ $[\text{M}+\text{H}]^+$ 601.3681, found 601.3693, $\Delta\text{ppm} +2.00$.

Synthetic procedure for the preparation of **12f** and **12f'**

To a stirring solution of **1f** (180.0 mg, 0.397 mmol) in ACN (20 ml), benzyl bromide (0.071 ml, 0.596 mmol) was added and the resulting mixture was stirred at 80 °C. After the starting material was consumed as indicated by TLC, the organic solvent was removed under reduced pressure to afford the crude iminium ion. After washing with hexane to remove any excess benzyl bromide, ethynylmagnesium bromide (0.5 M solution in THF, 3.970 ml, 1.985 mmol) was added dropwise to a cooled solution of resultant iminium ion in dry THF (40 ml) over 30 min at –78 °C. The reaction was allowed to slowly warm to r.t over an 18 h period. The mixture was quenched with saturated $\text{NH}_4\text{Cl}(\text{aq})$ and extracted twice with DCM. The combined organic layer was dried over anhydrous $\text{Na}_2\text{SO}_4(\text{s})$ and the filtrate was condensed under reduced pressure, followed by silica-gel flash column chromatography to afford **12f** (major) and **12f'** (minor).



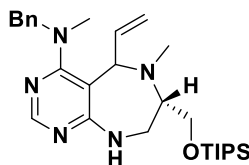
Compound 12f (major). A pale yellow oil; $R_f = 0.4$ (hexane/EtOAc = 3:1); 158.4 mg, 70% yield; ^1H NMR (400 MHz, CDCl_3) δ 8.16 (s, 1H), 7.33–7.24 (m, 5H), 7.17–7.14 (m, 3H), 6.79–6.78 (m, 2H), 6.27 (m, 1H), 4.74 (d, $J = 2.3$ Hz, 1H), 4.64 (d, $J = 14.9$ Hz, 1H), 4.31, 4.26 (ABq, $J_{AB} = 15.1$ Hz, 2H), 3.92–3.85 (m, 2H), 3.78 (d, $J = 14.5$ Hz, 1H), 3.73 (dd, $J = 10.0, 3.3$ Hz, 1H), 3.54 (ddd, $J = 14.4, 7.6, 1.4$ Hz, 1H), 2.93 (m, 1H), 2.60 (s, 3H), 2.53 (d, $J = 2.3$ Hz, 1H), 1.10–1.00 (m, 21H); ^{13}C NMR (100 MHz, CDCl_3) δ 167.4, 164.2, 155.8, 138.9, 138.3, 128.5, 128.4, 128.3, 127.6, 127.4, 126.7, 102.0, 83.9, 74.9, 65.3, 62.0, 58.5, 58.2, 48.5, 40.2, 39.6, 18.1, 12.0; IR (neat) ν_{max} : 3241, 2943, 2865, 1573, 1404, 1101, 669 cm^{-1} ; HRMS(ESI+) Calcd for $\text{C}_{34}\text{H}_{48}\text{N}_5\text{OSi}^+ [\text{M}+\text{H}]^+$ 570.3623, found 570.3614, $\Delta\text{ppm} = 1.58$. The stereochemistry of this product was confirmed by NOE spectroscopy. 1D-NOE result supported the stereochemistry as shown in Supplementary Fig. 49.



Compound 12f' (minor). A pale yellow oil; $R_f = 0.25$ (hexane/EtOAc = 3:1); 18.78 mg, 8.3% yield; ^1H NMR (400 MHz, CDCl_3) δ 8.21 (s, 1H), 7.33–7.31 (m, 3H), 7.21–7.17 (m, 5H), 6.84 (m, 2H), 6.34 (m, 1H), 4.79 (m, 1H), 4.71 (d, $J = 2.3$ Hz, 1H), 4.54, 4.20 (ABq, $J_{AB} = 15.5$ Hz, 2H), 4.07 (t, $J = 10.2$ Hz, 1H), 3.84, 3.71 (ABq, $J_{AB} = 13.7$ Hz, 2H), 3.64 (dd, $J = 9.8, 5.1$ Hz, 1H), 3.57 (ddd, $J = 15.0, 7.7, 4.7$ Hz, 1H), 3.37 (m, 1H), 2.68 (s, 3H), 2.50 (d, $J = 2.7$ Hz, 1H), 1.04 (br s, 21H); ^{13}C NMR (100 MHz, CDCl_3) δ 168.7, 164.4, 156.1, 139.0, 138.2, 129.0, 128.5, 128.4, 127.6, 127.3, 126.8, 99.9, 87.5, 74.8, 68.3, 64.7, 60.7, 58.5, 46.7, 44.0, 38.9, 18.1, 12.0; IR (neat) ν_{max} : 3239, 2940, 2865, 1571, 1404, 1102, 698 cm^{-1} ; HRMS(ESI+): Calcd for $\text{C}_{34}\text{H}_{48}\text{N}_5\text{OSi}^+ [\text{M}+\text{H}]^+$ 570.3623, found 570.3625, $\Delta\text{ppm} = +0.35$. The stereochemistry of this product was confirmed by NOE spectroscopy. 1D-NOE result supported the stereochemistry as shown in Supplementary Fig. 51.

Synthetic procedure for the preparation of 13f and 13f'.

Compound SI-7



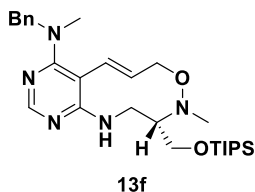
SI-7

To a stirring solution of **1f** (90 mg, 0.198 mmol) in ACN (10.0 ml), iodomethane (0.018 ml, 0.297 mmol) was added and the resulting mixture was stirred at 40 °C. After the starting material was consumed as indicated by TLC, the organic solvent and any excess iodomethane were removed under reduced pressure to afford the crude iminium ion. To a cooled solution of resultant iminium ion in dry THF (20.0 ml) was added vinylmagnesium bromide (1.0 M solution in THF, 0.990 ml, 0.990 mmol) dropwise over 30 min at –78 °C. The reaction was allowed to slowly warm to r.t over an 18 h period. The mixture was quenched with saturated NH₄Cl(aq) and extracted twice with DCM. The combined organic layer was dried over anhydrous Na₂SO₄(s) and the filtrate was condensed under reduced pressure, followed by silica-gel flash column chromatography to afford **SI-7** (70.68 mg, 72% yield, d.r. 9:1) as a yellow oil (Supplementary Fig. 4). The diastereomeric ratio was determined by ¹H NMR spectroscopy (Supplementary Fig. 52).

R_f = 0.27 (DCM/MeOH = 20:1); ¹H NMR (400 MHz, CDCl₃) δ 8.22 (s, 0.08 H, *minor diastereomer*), 8.17 (s, 0.71H, *major diastereomer*), 7.36–7.24 (m, 6H, *major diastereomer+minor diastereomer*), 6.25 (m, 1H), 5.64 (br s, 0.12H, *minor diastereomer*), 5.29 (br s, 0.97H, *major diastereomer*), 5.20 (d, J = 10.2 Hz, 1H), 4.88 (d, J = 17.2 Hz, 1H), 4.56–4.45 (m, 3H), 3.84–3.77 (m, 2H), 3.55 (t, J = 9.4 Hz, 1.11H, *major diastereomer*), 3.43 (t, J = 9.8 Hz, 0.15 H, *minor diastereomer*), 3.19 (m, 1H), 2.86–2.81 (m, 4H), 2.74 (s, 0.38H, *minor diastereomer*), 2.42 (s, 0.38H, *minor diastereomer*), 2.27 (s, 3H, *major diastereomer*), 1.10–1.02 (m, 25H, *major diastereomer+minor diastereomer*); ¹³C NMR (100 MHz, CDCl₃) δ 167.6, 165.5, 155.4, 138.7, 136.5, 128.6, 127.3, 127.1, 118.2, 102.9, 64.9, 63.6, 62.8, 58.3,

44.2, 41.4, 39.4, 18.1, 12.0; HRMS(ESI⁺): Calcd for C₂₈H₄₆N₅OSi⁺ [M+H]⁺ 496.3466, found 496.3465, Δppm −0.20.

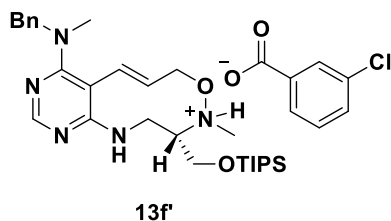
Compound 13f



To a solution of **SI-7** (70.68 mg, 0.143 mmol) in DCM (14.3 ml) was added 3-chloroperbenzoic acid (*m*-CPBA, 32.08 mg, 0.186 mmol) and the mixture was left to stir at reflux. After 1h, solvent was removed under reduced pressure and the residue was purified by silica-gel flash column chromatography to obtain the desired product **13f** (42.45 mg, 58% yield, 42% overall yield) as a colorless oil (Supplementary Fig. 4).

R_f = 0.3 (hexane/EtOAc = 3:1); ¹H NMR (500 MHz, CDCl₃) δ 8.11 (s, 1H), 7.32 (m, 2H), 7.24 (m, 1H), 7.20 (m, 2H), 6.63 (d, J = 16.1 Hz, 1H), 6.09 (m, 1H), 4.82 (br s, 3H), 4.09 (m, 3H), 3.71 (m, 2H), 3.45–3.27 (m, 1H), 3.04 (s, 3H), 2.77 (m, 1H), 2.63–2.55 (m, 3H), 1.08 (m, 21H);); IR (neat) ν_{\max} : 3395, 3254, 3060, 3028, 2926, 1946, 1713, 1567, 1493, 1452, 1266, 1105 cm^{−1}; HRMS(ESI⁺): Calcd for C₂₈H₄₆N₅O₂Si⁺ [M+H]⁺ 512.3415, found 512.3417, Δ ppm +0.39. The ¹H NMR spectrum of **13f** was too broad to analyze. As shown below, the structure of **13f** was fully confirmed only after treatment of 3-chlorobenzoic acid as a salt product, **13f'**, when broad peak of **13f** converted to sharp and well-resolved NMR signals.

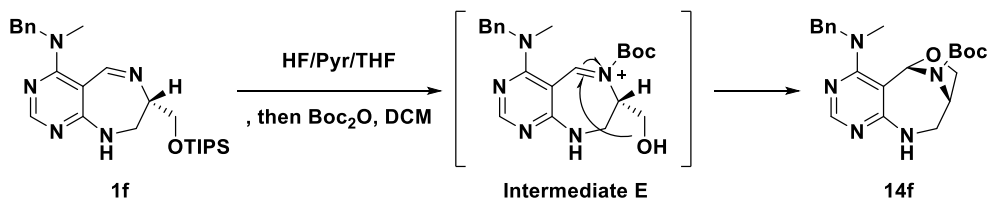
Compound 13f'



To a solution of **SI-7** (70.68 mg, 0.143 mmol) in DCM (14.3 ml) was added 3-chloroperbenzoic acid (*m*-CPBA, 32.08 mg, 0.186 mmol) and the mixture was left to stir at reflux. After 1 h, 3-chlorobenzoic acid (22.39mg, 0.143 mmol) was added and left to stir at r.t. After completion of the reaction as indicated by TLC, solvent was removed under reduced pressure and the residue was purified by silica-gel flash column chromatography to obtain the desired product **13f'** (70.72mg, 74% yield, 53% overall yield) as a pale yellow oil (Supplementary Fig. 4). The *E/Z* ratio (99:1) was determined by LC-MS analysis of the crude reaction mixtures (Supplementary Fig. 12).

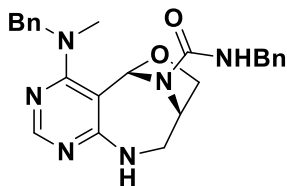
R_f = 0.3 (hexane/EtOAc 1:1); ^1H NMR (500 MHz, CDCl_3) δ 8.19 (s, 1H), 7.95 (s, 1H, 3-chlorobenzoic acid-H), 7.85 (d, J = 7.8 Hz, 1H, 3-chlorobenzoic acid-H), 7.54 (d, J = 8.3 Hz, 1H, 3-chlorobenzoic acid-H), 7.37 (t, J = 7.8 Hz, 1H, 3-chlorobenzoic acid-H), 7.29–7.26 (m, 2H), 7.22–7.19 (m, 3H), 6.49 (d, J = 16.6 Hz, 1H), 5.96 (dt, J = 16.6, 5.9 Hz, 1H), 5.51 (t, J = 6.4 Hz, 1H), 4.74 (m, 2H), 4.66, 4.62 (ABq, J_{AB} = 15.0 Hz, 2H), 3.96 (m, 2H), 3.70 (dd, J = 9.8, 8.3 Hz, 1H), 3.55 (dt, J = 14.3, 5.6 Hz, 1H), 2.90 (s, 3H), 2.76 (m, 1H), 2.67 (s, 3H), 1.06 (m, 21H), ^{13}C NMR (100 MHz, CDCl_3) δ 165.1, 162.8, 161.2, 155.4, 138.4, 134.7, 133.3, 131.7, 129.84, 129.75, 128.9, 128.6, 127.8, 127.79, 127.2, 127.1, 96.3, 70.2, 65.6, 61.0, 56.0, 45.2, 40.5, 39.1, 18.1, 11.9; IR (neat) ν_{max} : 3396, 3062, 3026, 2945, 2863, 1724, 1572, 1253, 1117 cm^{-1} ; HRMS(ESI $^{+}$): Calcd for $\text{C}_{35}\text{H}_{51}\text{ClN}_5\text{O}_4\text{Si}^{+}$ $[\text{M}+\text{H}]^{+}$ 668.3393, found 668.3387, Δppm –0.90.

Synthetic procedure for the preparation of **14f**



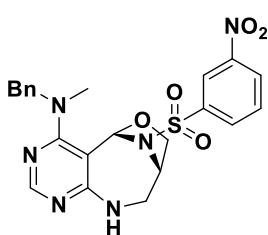
Compound 14f. **1f** (90.00 mg, 0.198 mmol) was treated with HF/pyridine/THF (5/5/90) solution (2 ml) and then, the mixture was stirred at r.t. After the starting material was consumed as indicated by TLC, ethoxytrimethylsilane (2 ml) was added and allowed to react for 1 h to quench any excess HF (HF/pyridine protocol). The reaction mixture was condensed *in vacuo* to afford the crude product. To a solution of crude product in DCM (4 ml) was added Boc_2O (56.09 mg, 0.257 mmol) and then, the mixture was stirred at r.t. After completion of the reaction as indicated by TLC, solvent was removed under reduced pressure and the residue was purified through the recrystallization in hexane to obtain desired product **14f** (68.47 mg, 87% overall yield) as a white solid.

$R_f = 0.3$ (EA); ^1H NMR (400 MHz, CDCl_3) δ 8.13 (s, 1H), 7.35–7.24 (m, 5H), 6.62 (s, 1H), 5.63 (br s, 1H), 4.76 (m, 2H), 4.55 (d, $J = 15.3$ Hz, 1H), 4.01 (d, $J = 7.0$ Hz, 1H), 3.87 (t, $J = 6.7$ Hz, 1H), 3.55 (br d, $J = 13.6$ Hz, 1H), 3.48–3.43 (m, 1H), 2.98 (s, 3H), 1.43 (s, 9H); ^{13}C NMR (100 MHz, CDCl_3) δ 166.7, 164.0, 155.8, 153.0, 138.3, 128.6, 127.9, 127.2, 103.0, 85.2, 81.6, 68.5, 57.5, 53.7, 48.0, 40.7, 28.4; IR (neat) ν_{max} : 3248, 2975, 2931, 1700, 1571, 1403, 1162, 1048, 699 cm^{-1} ; HRMS(ESI $^{+}$): Calcd for $\text{C}_{21}\text{H}_{28}\text{N}_5\text{O}_3^{+}$ $[\text{M}+\text{H}]^{+}$ 398.2187, found 398.2174, $\Delta\text{ppm} = 3.26$; mp: 50–52 $^{\circ}\text{C}$.



15f

Compound 15f. A white solid; $R_f = 0.4$ (EA); 77.57 mg, 91% yield; ^1H NMR (500 MHz, CDCl_3) δ 8.18 (s, 1H), 7.29–7.28 (m, 2H), 7.25–7.24 (m, 4H), 7.19–7.18 (m, 2H), 7.14 (d, $J = 6.4$ Hz, 2H), 6.57 (s, 1H), 5.55 (br s, 1H), 4.86 (t, $J = 5.4$ Hz, 1 H), 4.74 (m, 1H), 4.46 (br d, $J = 1.5$ Hz, 2H), 4.32 (d, $J = 5.4$ Hz, 2H), 4.02 (dd, $J = 7.3, 1.0$ Hz, 1H), 3.91 (m, 1H), 3.55 (m, 1H), 3.38 (dt, $J = 13.2, 4.2$ Hz, 1H), 2.83 (s, 3H); ^{13}C NMR (100 MHz, CDCl_3) δ 166.8, 164.1, 156.0, 154.9, 138.8, 137.8, 128.7, 128.6, 127.7, 127.5, 127.4, 127.3, 104.3, 84.0, 68.7, 58.2, 53.7, 48.0, 44.7, 40.3; IR (neat) ν_{max} : 3258, 2971, 1633, 1542, 1405, 1049, 698 cm^{-1} ; HRMS(ESI+): Calcd for $\text{C}_{24}\text{H}_{27}\text{N}_6\text{O}_2^+$ $[\text{M}+\text{H}]^+$ 431.2190, found 431.2184, $\Delta\text{ppm} -1.39$; mp: 67–69 $^\circ\text{C}$. The product was synthesized according to the synthetic procedure for the preparation of **14f** from **1f** and benzyl isocyanate (1.3 equiv.).

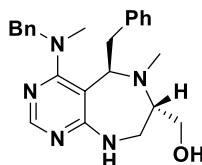


16f

Compound 16f. A white solid; $R_f = 0.3$ (EA); 59.2 mg, 62% yield; ^1H NMR (400 MHz, $\text{DMSO}-d_6$) δ 8.54–8.53 (m, 2H), 8.02 (s, 1H), 7.98 (d, $J = 7.8$ Hz, 1H), 7.83 (t, $J = 8.2$ Hz, 1H), 7.39 (m, 2H), 7.26 (m, 4H), 6.63 (s, 1H), 4.84 (br s, 1H), 4.65, 4.54 (ABq, $J_{\text{AB}} = 15.6$ Hz, 2H), 3.61 (d, $J = 7.4$ Hz, 1H), 3.51–3.45 (m, 1H), 3.28 (d, $J = 14.1$ Hz, 1H), 2.88 (m, 4H); ^{13}C NMR (400 MHz, $\text{DMSO}-d_6$) δ 165.6, 163.2, 155.8, 148.0, 138.9, 138.1, 133.3, 131.7, 128.5, 127.4, 127.1, 122.4, 122.3, 101.4, 87.3, 66.7, 57.4, 55.8, 54.9, 47.8, 40.0; IR (neat) ν_{max} : 2920, 1573, 1535, 1354, 1176, 734 cm^{-1} ; HRMS(ESI+): Calcd for $\text{C}_{22}\text{H}_{23}\text{N}_6\text{O}_5\text{S}^+$ $[\text{M}+\text{H}]^+$ 483.1445, found 483.1450, $\Delta\text{ppm} +1.03$; mp: 101–103 $^\circ\text{C}$. The product was synthesized according to the synthetic procedure for the preparation of **14f** from **1f** and 3-nitrobenzene sulfonyl chloride (*m*-NsCl) (1.3 equiv.). Purified by silica-gel flash column chromatography to afford **16f**. The structure of **16f** was confirmed by X-ray crystallographic analysis (Supplementary Fig. 5, Supplementary Table 1–5, CCDC number 1500586).

Synthetic procedure for the preparation of 17f'.

Compound SI-8.



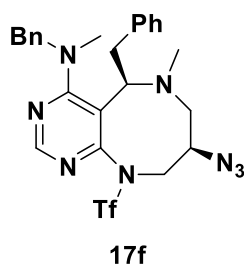
SI-8

To a stirring solution of **1f** (180 mg, 0.397 mmol) in ACN (20.0 ml), iodomethane (0.036 ml, 0.594 mmol) was added and the resulting mixture was stirred at 40 °C. After the starting material was consumed as indicated by TLC, the organic solvent and any excess iodomethane were removed under reduced pressure to afford the crude iminium ion. To a cooled solution of resultant iminium ion in dry THF (40.0 ml) was added benzylmagnesium bromide (2.0 M solution in THF, 0.99 ml, 1.98 mmol) dropwise over 30 min at –78 °C. The reaction was allowed to slowly warm to r.t over an 18 h period. The mixture was quenched with saturated NH₄Cl(aq) and extracted twice with DCM. The combined organic layer was dried over anhydrous Na₂SO₄(s) and the filtrate was condensed under reduced pressure, followed by filtration through a short pad of silica gel with hexane/EtOAc (1:1) to afford crude product. To a solution of crude product in THF (4 ml) was added TBAF (1.0 M solution in THF, 0.516 ml, 0.516 mmol). The reaction mixture was then left to stir at r.t. After completion of the reaction as indicated by TLC, the solvent was removed under reduced pressure and the residue was purified through the silica-gel flash column chromatography to obtain product **SI-8** (121.8 mg, 76% yield) as a white solid (Supplementary Fig. 6).

R_f = 0.4 (DCM/MeOH = 10:1); ¹H NMR (400 MHz, CDCl₃) δ 8.13 (s, 1H), 7.32–7.25 (m, 3H), 7.20–7.13 (m, 3H), 6.99 (d, J = 7.2 Hz, 2H), 6.73 (d, J = 6.7 Hz, 2H), 5.40 (d, J = 5.9 Hz, 1H), 4.35, 4.28 (ABq, J_{AB} = 16.0, 15.6 Hz, 2H), 4.19 (dd, J = 9.6, 4.5 Hz, 1H), 3.60 (dd, J = 10.6, 5.1 Hz, 1H), 3.46 (dd, J = 10.8, 5.7 Hz, 1H), 3.31–3.04 (m, 4H), 2.88 (dd, J = 12.9, 4.3 Hz, 1H), 2.62 (s, 3H), 2.51 (br s, 1H), 2.32 (s, 3H); ¹³C NMR (100 MHz, CDCl₃) δ 168.4, 166.1, 154.9, 139.3, 138.1,

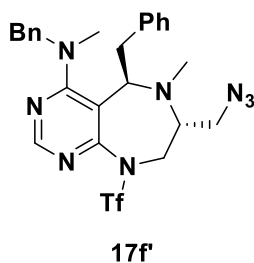
129.0, 128.6, 128.1, 127.4, 127.1, 126.2, 103.3, 65.0, 61.7, 58.5, 58.0, 46.2, 38.7, 38.6, 34.5; HRMS (ESI⁺): Calcd for C₂₄H₃₀N₅O⁺ [M+H]⁺ 404.2445, found 404.2446, Δppm +0.25; mp: 70–72 °C.

Compound 17f and 17f'. To a stirring solution of **SI-8** (121.8 mg, 0.302 mmol) in toluene (3.0 ml) under argon atmosphere were sequentially added Et₃N (0.126 ml, 0.906 mmol) and trifluoromethanesulfonic anhydride (Tf₂O) (0.112 ml, 0.664 mmol) at –40 °C and left to stir. After 1 h, the temperature of the reaction mixture was brought down to –78 °C and NaN₃ (58.9 mg, 0.906 mmol) was added. The reaction was allowed to slowly warm to r.t over an 18 h period. The resultant was quenched with saturated NaHCO₃(aq) and extracted twice with DCM. The combined organic layer was dried over anhydrous Na₂SO₄(s) and the filtrate was condensed under reduced pressure, followed by silica-gel flash column chromatography to afford the **17f** (Path A, eight-membered ring) and **17f'** (Path B, seven-membered ring) as shown in Supplementary Fig. 6.



Compound 17f (Path A, eight-membered ring, Supplementary Fig. 6). A white solid; *R*_f = 0.6 (hexane/EtOAc = 3:1); 37.2 mg, 22% yield, 17% overall yield; ¹H NMR (800 MHz, CDCl₃) δ 8.29 (s, 1H), 7.32 (m, 2H), 7.28 (m, 1H), 7.17 (m, 2H), 7.13 (m, 1H), 7.00 (d, *J* = 7.3 Hz, 2H), 6.74 (d, *J* = 7.3 Hz, 2H), 4.33, 4.27 (ABq, *J*_{AB} = 15.7 Hz, 2H), 4.23 (dd, *J* = 14.9, 6.6 Hz, 1H), 3.99 (dd, *J* = 10.3, 3.9 Hz, 1H), 3.96 (dd, *J* = 15.7, 1.5 Hz, 1H), 3.89 (m, 1H), 3.38 (dd, *J* = 14.9, 10.5 Hz, 1H), 3.07 (m, 1H), 2.98 (dd, *J* = 12.5, 3.7 Hz, 1H), 2.84 (br dd, *J* = 16.0, 1.6 Hz, 1H), 2.66 (s, 3H), 2.59 (s, 3H); ¹³C NMR (100 MHz, CDCl₃) δ 169.2, 160.3, 154.0, 138.1, 136.7, 129.1, 128.8, 128.3, 127.64, 127.57, 126.5, 120.7 (q, ¹*J*_{C,F} = 324.4 Hz), 115.0, 66.0, 59.9, 57.4, 56.0, 52.1, 49.1, 38.8, 37.5; IR (neat) ν_{max}: 3028, 2929, 2868, 2108, 1566, 1393 cm⁻¹; HRMS(ESI⁺) Calcd for C₂₅H₂₈F₃N₈O₂S⁺ [M+H]⁺

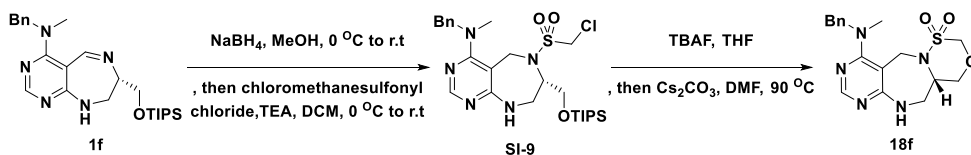
561.2003, found 561.2009, Δ ppm +1.07; mp: 103–105 °C. The stereochemistry of this product was confirmed by NOE spectroscopy. 1D-NOE result supported the stereochemistry as shown in Supplementary Fig. 60.



Compound 17f' (Path B, seven-membered ring, Supplementary Fig. 6). A white solid; R_f = 0.5 (hexane/EtOAc = 3:1); 55.9 mg, 33% yield, 25% overall yield; ¹H NMR (500 MHz, CDCl₃) δ 8.32 (s, 1H), 7.34 (m, 2H), 7.29 (m, 1H), 7.14 (m, 3H), 6.96 (d, J = 7.3 Hz, 2H), 6.73 (br d, J = 7.3 Hz, 2H), 4.56, 4.49 (ABq, J_{AB} = 16.5 Hz,

2H), 4.23 (d, J = 15.2 Hz, 1 H), 3.91 (dd, J = 11.2, 2.9 Hz, 1H), 3.67 (dd, J = 13.7, 4.4 Hz, 1H), 3.50 (dd, J = 14.9, 10.5 Hz, 1H), 3.32 (m, 1H), 3.19 (dd, J = 13.7, 2.4 Hz, 1H), 3.10 (t, J = 11.8 Hz, 1H), 2.96 (dd, J = 13.0, 3.2 Hz, 1H), 2.78 (s, 3H), 2.31 (s, 3H); ¹³C NMR (100 MHz, CDCl₃) δ 168.1, 159.7, 154.7, 138.3, 137.2, 129.1, 128.8, 128.3, 127.5, 127.0, 126.5, 120.1 (q, $^1J_{C,F}$ = 322.6 Hz), 110.1, 66.6, 59.6, 57.4, 56.3, 51.5, 42.1, 38.0, 31.5; IR (neat) ν_{max} : 3030, 2930, 2869, 2105, 1578, 1529, 1391, 1212, 1043 cm⁻¹; HRMS(ESI+) Calcd for C₂₅H₂₈F₃N₈O₂S⁺ [M+H]⁺ 561.2003, found 561.2011, Δ ppm +1.43; mp: 140–142 °C. The stereochemistry of this product was confirmed by NOE spectroscopy. 1D-NOE result supported the stereochemistry as shown in Supplementary Fig. 62.

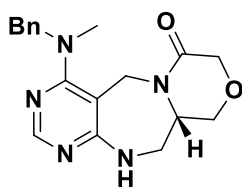
Synthetic procedure for the preparation of 18f



Compound 18f. To a stirring solution of **1f** (90mg, 0.198 mmol) in MeOH (2 ml) was added NaBH₄ (36.88 mg, 0.975 mmol) at 0 °C. The resulting mixture was left to stir and allowed to warm to r.t. After the starting material was consumed as indicated by TLC, the resultant was quenched with saturated NaHCO₃(aq) and extracted twice with DCM. The combined organic layer was dried over anhydrous Na₂SO₄(s) and filtered. The solvent was evaporated under reduced pressure, and the resulting crude secondary amine was dissolved in DMF (2 ml). To this solution were sequentially added Et₃N (0.055 ml, 0.396 mmol) and chloromethane sulfonyl chloride (0.023 ml, 0.257 mmol) at 0 °C. The resulting mixture was left to stir and allowed to warm to r.t. After completion of the reaction as indicated by TLC, the resultant was quenched with saturated NH₄Cl(aq) and extracted twice with DCM. The combined organic layer was dried over anhydrous Na₂SO₄(s) and the filtrate was condensed under reduced pressure, followed by silica-gel flash column chromatography to afford **SI-9** (97.89 mg, 87% yield). To a solution of **SI-9** (97.89 mg, 0.172 mmol) in THF (2 ml) was added TBAF (1.0 M solution in THF, 0.224 ml, 0.224 mmol). The reaction mixture was then left to stir at r.t. After completion of the reaction as indicated by TLC, the solvent was removed under reduced pressure. To a solution of the crude resultant in DMF (2 ml) was added Cs₂CO₃ (168.1 mg, 0.516 mmol). Then the resulting mixture was stirred at 90 °C. After completion of the reaction as indicated by TLC, the reaction mixture was diluted with ethyl acetate, washed with brine, dried over anhydrous Na₂SO₄(s), filtered, and concentrated *in vacuo*. The residue was purified with silica-gel flash column chromatography to obtain desired product **18f** (51.02 mg, 79% yield, 69% overall yield) as a white solid.

$R_f = 0.4$ (DCM/MeOH = 20:1); ¹H NMR (400 MHz, DMSO-*d*₆) δ 7.98 (s, 1H), 7.34–7.23 (m, 6H), 4.84 (d, $J = 11.7$ Hz, 1H), 4.71–4.59 (m, 3H), 4.47 (d, $J = 15.3$

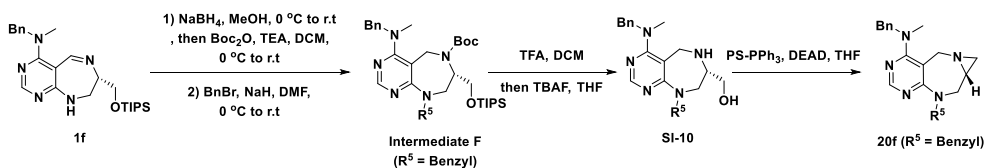
Hz, 1H), 4.33 (d, $J = 15.7$ Hz, 1H), 4.19 (br s, 1H), 3.89 (d, $J = 10.4$ Hz, 1H), 3.80 (t, $J = 11.2$ Hz, 1H), 3.54 (br s, 1H), 3.38 (br s, 1H), 2.81 (s, 3H); ^{13}C NMR (100 MHz, DMSO- d_6) δ 165.0, 163.2, 153.5, 138.1, 128.4, 127.5, 127.0, 95.6, 62.0, 55.4, 40.2, 39.4; IR (neat) ν_{max} : 3230, 2926, 1574, 1409, 1155, 736 cm^{-1} ; HRMS(ESI $^{+}$): Calcd for $\text{C}_{17}\text{H}_{22}\text{N}_5\text{O}_3\text{S}^{+}$ $[\text{M}+\text{H}]^{+}$ 376.1438, found 376.1437, Δppm -0.27 ; mp: 196–198 $^{\circ}\text{C}$.



19f

Compound 19f. A colorless oil; $R_f = 0.5$ (DCM/MeOH = 20:1); 50.40 mg, 75% overall yield; ^1H NMR (400 MHz, CDCl_3) δ 8.02 (s, 1H), 7.39–7.33 (m, 4H), 7.27–7.23 (m, 1H), 6.97 (m, 1H), 5.23 (d, $J = 15.7$ Hz, 1H), 4.78, 4.41 (ABq, $J_{\text{AB}} = 15.7$ Hz, 2H), 4.21, 4.12 (ABq, $J_{\text{AB}} = 16.4$ Hz, 2H), 4.09–4.01 (m, 2H), 3.97–3.87 (m, 2H), 3.78 (t, $J = 11.0$ Hz, 1H), 3.00 (dd, $J = 15.3, 7.4$ Hz, 1H), 2.89 (s, 3H); ^{13}C NMR (100 MHz, CDCl_3) δ 166.7, 166.5, 164.3, 154.7, 137.8, 128.5, 127.5, 127.1, 95.4, 67.7, 66.5, 57.5, 56.2, 42.2, 40.7, 39.1; IR (neat) ν_{max} : 3237, 2908, 1653, 1573, 1408, 1119, 737 cm^{-1} ; HRMS(ESI $^{+}$): Calcd for $\text{C}_{18}\text{H}_{22}\text{N}_5\text{O}_2^{+}$ $[\text{M}+\text{H}]^{+}$ 340.1768, found 340.1765, Δppm -0.88 . The product was synthesized according to the synthetic procedure for the preparation of **18f** from **1e** and chloroacetic anhydride.

Synthetic procedure for the preparation of **20f**

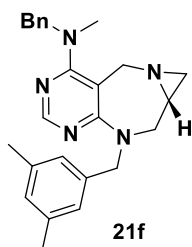


Compound 20f. To a stirring solution of **1f** (135.0 mg, 0.298 mmol) in MeOH (3.0 ml) was added NaBH_4 (56.37 mg, 1.490 mmol) at 0 $^{\circ}\text{C}$. Then the resulting mixture was left to stir and allowed to warm to r.t. After the starting material was consumed as indicated by TLC, the resultant was quenched with saturated $\text{NaHCO}_3(\text{aq})$ and extracted twice with DCM. The combined organic layer was dried over anhydrous

Na₂SO₄(s) and filtered. The solvent was evaporated under reduced pressure, and the resulting crude secondary amine was dissolved in DCM (3.0 ml). To this solution were sequentially added Et₃N (0.083 ml, 0.596 mmol) and Boc₂O (84.55 mg, 0.387 mmol) at 0 °C. The resulting mixture was left to stir and allowed to warm to r.t. After completion of the reaction as indicated by TLC, the resultant was quenched with saturated NH₄Cl(aq) and extracted twice with DCM. The combined organic layer was dried over anhydrous Na₂SO₄(s) and the filtrate was condensed under reduced pressure, followed by silica-gel flash column chromatography to afford the Boc-protected product (162.3 mg, 98% yield). To a solution of Boc-protected product (162.3 mg, 0.292 mmol) in DMF (3.0 ml) under argon atmosphere was added NaH (60% dispersion in mineral oil, 23.36 mg, 0.584 mmol) at 0 °C and left to stir. After 30 min, benzylbromide (0.052 ml, 0.438 mmol) was slowly added. The resulting mixture was left to stir and allowed to warm to r.t. After completion of the reaction as indicated by TLC, the reaction mixture was quenched with saturated NH₄Cl(aq). The resultant was extracted twice with ethyl acetate, dried with anhydrous Na₂SO₄(s), filtered, and concentrated *in vacuo*. The residue was purified by silica-gel flash column chromatography to obtain the intermediate **F** (R⁵ = benzyl, 164.1 mg, 87% yield). Intermediate **F** (164.1 mg, 0.254 mmol) was first treated with 10% trifluoroacetic acid (TFA) in DCM (12.5 ml) at r.t. After the starting material was consumed as indicated by TLC, any excess TFA was removed by azeotropic evaporation with toluene under reduced pressure. To a solution of the resulting Boc-deprotected product in THF (2.5 ml) was added TBAF (1.0 M solution in THF, 0.330 ml, 0.330 mmol) and the mixture was stirred at r.t. After completion of the reaction as indicated by TLC, the reaction mixture was quenched with saturated NaHCO₃(aq). The resultant was extracted twice with DCM, dried with anhydrous Na₂SO₄(s), filtered, and concentrated *in vacuo*, followed by silica-gel flash column chromatography to afford **SI-10** (73.21 mg, 74% yield). To a **SI-10** (73.21 mg, 0.188 mmol) in THF (20.0 ml) under argon atmosphere was added polymer-bound triphenylphosphine (587.5 mg, 0.94 mmol), purchased from Sigma-Aldrich (100-200 mesh, 1.6 mmol/g), and the mixture was stirred at r.t. After 30 min, diethyl azodicarboxylate (DEAD, 0.058 ml, 0.376 mmol) was slowly added. The mixture was stirred at r.t for 18h. The reaction mixture was filtered through Celite® while washing with DCM. The filtrate was

condensed under reduced pressure and purified by silica-gel flash column chromatography to afford the desired product **20f** (R^5 = benzyl) (56.57 mg, 81% yield, 52% overall yield) as a pale yellow oil.

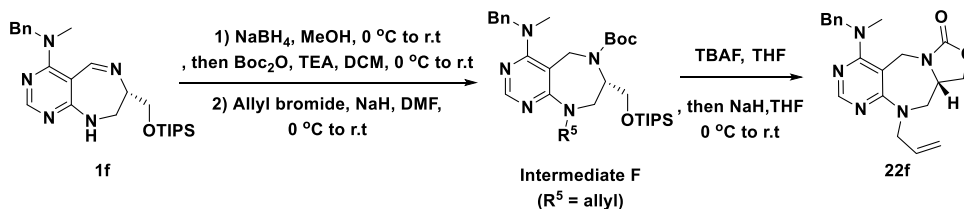
R_f = 0.4 (DCM/MeOH 20:1); ^1H NMR (400 MHz, CDCl_3) δ 8.24 (s, 1H), 7.35–7.27 (m, 10H), 5.10, 4.88 (ABq, J_{AB} = 15.3 Hz, 2H), 4.61, 4.39 (ABq, J_{AB} = 15.3 Hz, 2H), 4.26 (d, J = 13.7, 1H), 4.09 (dd, J = 15.3, 11.3 Hz, 1H), 3.58 (d, J = 13.7, 1H), 3.42 (dd, J = 15.5, 4.1 Hz, 1H), 2.82 (s, 3H), 2.43 (m, 1H), 1.78 (d, J = 5.1, 1H), 1.30 (d, J = 3.1, 1H); ^{13}C NMR (100 MHz, CDCl_3) δ 167.4, 163.8, 155.4, 138.8, 138.7, 128.7, 128.6, 127.8, 127.6, 127.3, 127.1, 100.3, 57.8, 53.9, 51.5, 48.7, 39.7, 34.4, 32.8; IR (neat) ν_{max} : 3027, 2920, 2853, 1559, 1356, 735, 700 cm^{-1} ; HRMS(ESI $^{+}$): Calcd for $\text{C}_{23}\text{H}_{26}\text{N}_5^{+}$ $[\text{M}+\text{H}]^{+}$ 372.2183, found 372.2189, Δppm +1.61.



Compound 21f (R^5 = 3,5-dimehtylbenzyl). A pale yellow oil;

R_f = 0.5 (DCM/MeOH = 20:1); 49.82 mg, 81% yield, 53% overall yield; ^1H NMR (500 MHz, CDCl_3) δ 8.25 (s, 1H), 7.34–7.25 (m, 5H), 6.91 (m, 3H), 5.04, 4.78 (ABq, J_{AB} = 15.2 Hz, 2H), 4.61, 4.38 (ABq, J_{AB} = 15.2 Hz, 2H), 4.26 (d, J = 13.7, 1H), 4.04 (dd, J = 14.2, 11.7 Hz, 1H), 3.57 (d, J = 13.7, 1H), 3.41 (dd, J = 15.4, 2.2 Hz, 1H), 2.81 (s, 3H), 2.43(m, 1H), 2.29 (s, 6H), 1.77 (d, J = 2.9, 1H), 1.28 (s, 1H); ^{13}C NMR (100 MHz, CDCl_3) δ 167.4, 163.8, 155.4, 138.8, 138.6, 138.3, 129.0, 128.6, 127.8, 127.1, 125.4, 100.3, 57.9, 53.7, 51.5, 48.4, 39.7, 34.5, 32.7, 29.8, 21.5; IR (neat) ν_{max} : 3026, 2922, 2863, 1564, 1355, 735, 700 cm^{-1} ; HRMS(ESI $^{+}$): Calcd for $\text{C}_{25}\text{H}_{30}\text{N}_5^{+}$ $[\text{M}+\text{H}]^{+}$ 400.2496, found 400.2495, Δppm – 0.25. The product was synthesized according to the synthetic procedure for the preparation of **20f** from **1f** and 3,5-dimehtylbenzyl bromide.

Synthetic procedure for the preparation of 22f

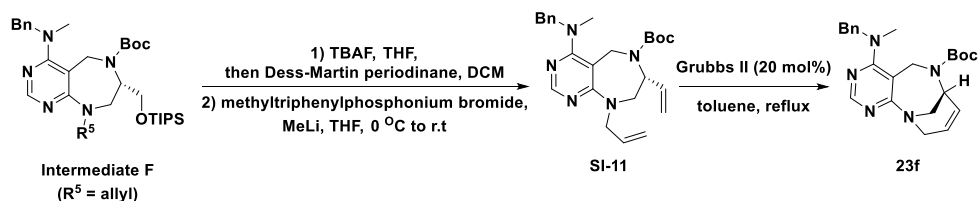


Compound 22f. To a stirring solution of **1f** (135.0 mg, 0.298 mmol) in MeOH (3.0 ml) was added NaBH_4 (56.37 mg, 1.490 mmol) at 0°C . Then the resulting mixture was left to stir and allowed to warm to r.t. After the starting material was consumed as indicated by TLC, the resultant was quenched with saturated $\text{NaHCO}_3(\text{aq})$ and extracted twice with DCM. The combined organic layer was dried over anhydrous $\text{Na}_2\text{SO}_4(\text{s})$ and filtered. The solvent was evaporated under reduced pressure, and the resulting crude secondary amine was dissolved in DCM (3.0 ml). To this solution were sequentially added Et_3N (0.083 ml, 0.596 mmol) and Boc_2O (84.55 mg, 0.387 mmol) at 0°C . The resulting mixture was left to stir and allowed to warm to r.t. After completion of the reaction as indicated by TLC, the resultant was quenched with saturated $\text{NH}_4\text{Cl}(\text{aq})$ and extracted twice with DCM. The combined organic layer was dried over anhydrous $\text{Na}_2\text{SO}_4(\text{s})$ and the filtrate was condensed under reduced pressure, followed by silica-gel flash column chromatography to afford the Boc-protected product (162.3 mg, 98% yield). To a solution of Boc-protected product (162.3 mg, 0.292 mmol) in DMF (3.0 ml) under argon atmosphere was added NaH (60% dispersion in mineral oil, 23.36 mg, 0.584 mmol) at 0°C and left to stir. After 30 min, allyl bromide (0.038 ml, 0.438 mmol) was slowly added. The resulting mixture was left to stir and allowed to warm to r.t. After completion of the reaction as indicated by TLC, the reaction mixture was quenched with saturated $\text{NH}_4\text{Cl}(\text{aq})$. The resultant was extracted twice with ethyl acetate, dried with anhydrous $\text{Na}_2\text{SO}_4(\text{s})$, filtered, and concentrated *in vacuo*. The residue was purified by silica-gel flash column chromatography to obtain the intermediate **F** ($\text{R}^5 = \text{allyl}$, 141.2 mg, 81% yield). To a solution of intermediate **F** (141.2 mg, 0.237 mmol) in THF (2.5 ml) was added TBAF (1.0 M solution in THF, 0.308 ml, 0.308 mmol) and the mixture was stirred at r.t. After completion of the reaction as indicated by TLC, the reaction mixture was quenched with saturated

NaHCO₃(aq). The resultant was extracted twice with DCM, dried with anhydrous Na₂SO₄(s), filtered, and concentrated *in vacuo*. To a solution of the crude resultant in THF (2.5 ml) under argon atmosphere was added NaH (60% dispersion in mineral oil, 14.22 mg, 0.356 mmol) at 0 °C. Then the resulting mixture was left to stir and allowed to warm to r.t. After completion of the reaction as indicated by TLC, the reaction mixture was diluted with DCM, washed with brine, dried over anhydrous Na₂SO₄(s), filtered, and concentrated *in vacuo*. The residue was purified with silica-gel flash column chromatography to obtain desired product **22f** (56.30 mg, 65% yield, 53% overall yield) as a white solid.

R_f = 0.2 (EA); ¹H NMR (400 MHz, CDCl₃) δ 8.23 (s, 1H), 7.36–7.31 (m, 4H), 7.28 (m, 1H), 5.92 (m, 1H), 5.21 (d, J = 10.2 Hz, 1H), 5.15 (dd, J = 17.2, 1.2 Hz, 1H), 4.72–4.65 (m, 2H), 4.61 (dd, J = 15.5, 4.9 Hz, 1H), 4.55–4.44 (m, 2H), 4.11–4.07 (m, 2H), 4.02 (d, J = 16.0 Hz, 1H), 3.91 (dd, J = 15.5, 6.5 Hz, 1H), 3.76 (dd, J = 14.9, 2.0 Hz, 1H), 3.25 (dd, J = 15.1, 3.3 Hz, 1H), 2.91 (s, 3H); ¹³C NMR (100 MHz, CDCl₃) δ 166.9, 164.9, 157.3, 155.0, 138.1, 134.2, 128.7, 127.9, 127.3, 117.8, 97.0, 65.1, 56.9, 56.7, 54.5, 52.4, 42.1, 39.7; IR (neat) ν_{\max} : 3049, 2976, 2917, 1758, 1561, 1410, 1266, 746 cm⁻¹; HRMS(ESI⁺): Calcd for C₂₀H₂₄N₅O₂⁺ [M+H]⁺ 366.1925, found 366.1924, Δ ppm –0.27; mp: 89–91 °C.

Synthetic procedure for the preparation of **23f**



Compound 23f. To a solution of intermediate **F** (R⁵ = allyl, 243.1 mg, 0.408 mmol) in THF (4.1 ml) was added TBAF (1.0 M solution in THF, 0.530 ml, 0.530 mmol) and the mixture was stirred at r.t. After completion of the reaction as indicated by TLC, the reaction mixture was quenched with saturated NaHCO₃(aq).

The resultant was extracted twice with DCM, dried with anhydrous Na₂SO₄(s), filtered, and concentrated *in vacuo*. To a solution of the crude resultant in DCM (8.2 ml) was added Dess-Martin periodinane (259.6 mg, 0.612 mmol) and the mixture was stirred at r.t. After completion of the reaction as indicated by TLC, the reaction mixture was quenched with saturated NaHCO₃(aq). The resultant was extracted twice with DCM, dried with anhydrous Na₂SO₄(s), filtered, and concentrated *in vacuo*. The residue was purified by silica-gel flash column chromatography to obtain the aldehyde product (148.3 mg, 83% yield). To a stirring suspension of methyltriphenylphosphonium bromide (363.3 mg, 1.017 mmol) in THF under argon atmosphere was added MeLi (1.6 M in diethyl ether, 0.530 ml, 0.848 mmol) at 0 °C. After 30min, the resulting aldehyde product (148.3 mg, 0.339 mmol) was added. Then the reaction mixture was allowed to slowly warm to r.t over a 12 h period. The reaction mixture was quenched with saturated NH₄Cl(aq). The resultant was extracted twice with ethyl acetate, dried with anhydrous Na₂SO₄(s), filtered, and concentrated *in vacuo*, followed by silica-gel flash column chromatography to afford **SI-11** (130.0 mg, 88% yield). To a solution of **SI-11** (130.0 mg, 0.298 mmol) in toluene was added second generation Grubbs' catalyst (50.94 mg, 0.060 mmol, 20 mol%) and the mixture was left to stir at reflux. After 4h, solvent was removed under reduced pressure and the residue was purified by silica-gel flash column chromatography to obtain desired product **23f** (44.83 mg, 52% recovery yield, 31% overall yield) as a yellow oil.

R_f = 0.2 (hexane/EA = 1:1); ¹H NMR (400 MHz, DMSO-*d*₆, 100 °C) δ 8.06 (s, 1H), 7.35–7.29 (m, 4H), 7.27–7.23 (m, 1H), 6.35 (ddd, J = 9.9, 5.3, 1.8 Hz, 1H), 5.78 (ddd, J = 10.1, 3.9, 1.8 Hz, 1H), 4.92 (d, J = 16.5 Hz, 1H), 4.86–4.81 (m, 1H), 4.76 (d, J = 15.3 Hz, 1H), 4.56 (d, J = 15.9 Hz, 1H), 4.42 (dd, J = 15.3, 1.2 Hz, 1H), 4.34 (d, J = 15.3 Hz, 1H), 4.00 (dd, J = 4.9, 1.8 Hz, 1H), 3.77 (dq, J = 18.3, 2.2 Hz, 1H), 3.30 (dd, J = 15.3, 2.4 Hz, 1H), 2.84 (s, 3H), 1.42 (s, 9H); ¹³C NMR (100 MHz, DMSO-*d*₆, 100 °C) δ 166.0, 163.6, 154.6, 153.5, 137.9, 128.0, 127.7, 127.3, 127.1, 126.3, 99.7, 79.0, 55.4, 49.9, 49.4, 45.7, 41.9, 38.7, 27.7; IR (neat) ν_{\max} : 3031, 2978, 2928, 1690, 1588, 1408, 1164 cm⁻¹; HRMS(ESI⁺): Calcd for C₂₃H₃₀N₅O₂⁺ [M+H]⁺ 408.2394, found 408.2382, Δppm –2.94.

2.5.4. General Information of Biological Assay

Kits, reagents and materials

Micro BCA™ protein assay kit was purchased from PIERCE and used for the measurement of protein concentration of cell lysate. Cell proliferation enzyme-linked immunosorbent assay (ELISA) and 5-bromo-2'-deoxyuridine (BrdU) colorimetric kit were purchased from Roche, Sigma-Aldrich. Ez-cytox WST-based cell viability, proliferation & cytotoxicity assay kit was purchased from Daeil Lab. Compounds used for bioassays were prepared in dimethyl sulfoxide (DMSO) solution. DMSO was purchased from Acros Organics. Tween® 20 was purchased from Sigma-Aldrich. Dulbecco modified eagle medium (DMEM), RPMI 1640, fetal bovine serum (FBS), and antibiotic-antimycotic solution were purchased from Gibco, Invitrogen. Phosphate-buffered saline (PBS) buffer and leucine-free DMEM were purchased from WELGENE. 3,3', 5,5''-tetramethylbenzidine (TMB), a substrate of horseradish peroxidase (HRP) conjugated in secondary antibody, was purchased from Invitrogen. Protein gel casters and western blot equipments including polyvinylidene difluoride (PVDF) membrane were purchased from Bio-Rad. Amersham ECL prime western blotting detection system (Amersham ECL prime solution) was purchased from GE Healthcare Life Science. 100-mm cell culture dish, transparent 96-well plate [#3598], and half-bottom 96 well clear plate [#3690] were purchased from CORNING. Lipofectamine™ 2000 reagent was purchased from Invitrogen. Human embryonic kidney (HEK)293T, DU145, Ca Ski, and HeLa cells were obtained from American Type Culture Collection [ATCC, VA, USA]. Nunc™ Lab-Tek™ II chambered cover glass was purchased from Thermo Scientific.

Antibodies, plasmids and proteins

Anti-LC3B (ab51520), anti-S6K1 (ab32359), anti-phospho-T389 S6K1 (ab2571), and HRP-labeled anti-horse IgG secondary antibodies (ab6802) were purchased from Abcam. Anti-glutathione-S-transferase (GST) antibody (sc-459) was purchased from Santa Cruz Biotechnology. Anti-p62 (CST 5114), anti-glyceraldehyde-3-phosphate dehydrogenase (GAPDH) (CST 2118), anti-phospho-

S65 4E-BP1 (CST 9451), anti-phospho-S757 ULK1 (CST 6888), anti-phospho-S473 Akt (CST 4058), anti-phospho-T172 AMPK α (CST 2531), and HRP-labeled anti-rabbit IgG secondary antibodies (CST 7074) were purchased from Cell Signaling Technology. His-tagged LRS and GST-tagged RagD were in our laboratory stocks. mCherry-GFP-LC3 plasmid (pBabe vector) was from Dr. Heesun Cheong, Division of Chemical Biology, Research Institute, National Cancer Center, Korea.

Instruments and programs

For developing of ELISA, the absorbance of 96-well plate was measured by BioTek Synergy HT Microplate reader. ChemoDoc™ MP imaging system from Bio-Rad was used for analyzing chemiluminescent signal in western blotting assay. Following signal quantification was done by ImageLab 4.0 program provided by Bio-Rad.

DeltaVision Elite imaging system from GE Healthcare was used for imaging experiment. Objective lenses were equipped with Olympus IX-71 inverted microscope with PLAN APO 60 \times /Oil (PLAPON60 \times O), 1.42 NA, WD 0.15 mm. sCMOS camera and InSightSSI fluorescence illumination module were equipped with the system. Four-color fluorescent protein (Live Cell) filter set [GE Healthcare, 52-852113-013] was used for imaging. For live cell imaging, CO₂ supporting chamber with an objective air heater were installed with the system. Images were analyzed with SoftWorks program supported by GE Healthcare. Graphs and figures provided were analyzed with GraphPad Prism 5 program.

2.5.5. Experimental Procedures of Biological Assay

Cell Culture

HEK293T cell was cultured in Dulbecco modified eagle medium (DMEM) with 10% (v/v) fetal bovine serum (FBS) and 1% (v/v) antibiotic-antimycotic solution. HeLa, DU145, and Ca Ski cell were cultured in RPMI 1640 medium with 10% (v/v) FBS and 1% antibiotic-antimycotic solution. Both cells were maintained in 100-mm cell culture dish in an incubator at 37 °C, in a humidified atmosphere with 5% CO₂.

ELISA

His-tagged human LRS were diluted in carbonate buffer (100 mM, pH 9.6) at the concentration of 0.5 ng μl^{-1} . Solution were distributed to the half-bottom 96 well clear plate from CORNING 3690. After incubation overnight at 4 °C (sealed), coating solution from each well was removed and washed for three times with phosphate buffered saline with 0.05% Tween[®] 20 (PBST). 5% bovine serum albumin (BSA) in PBS solution was treated to each well for blocking step, followed by the treatment of each compound and GST-tagged human RagD simultaneously for 3 h. GST protein itself was treated as negative control. Diluted GST antibody in PBST was added and incubated at room temperature for 1 h. After washing with PBST, the HRP-conjugated anti-horse IgG secondary antibody diluent was treated and incubated at room temperature for 1 h. TMB was added to each well for colorimetric development. Blue color should be developed in positive wells. To stop the color reaction, 1 M H₃PO₄ stopping solution was added. Finally, absorbance at 450 nm were measured.

Western Blotting

Cells were lysed with radio-immunoprecipitation assay (RIPA) buffer (50 mM Tris, pH 7.8, 150 mM NaCl, 0.5% deoxycholate, 1% IGEPAL CA-630, protease inhibitor cocktail, and phosphatase inhibitors). Protein was obtained after centrifugation at 15000 rpm for 20 min, by transferring supernatant. Protein

concentration was normalized with Micro BCATM protein assay kit. Overall protein sampling procedure was done at 4 °C. Prepared protein samples were analyzed with SDS-PAGE and following western blot procedure. Protein was transferred into nitrocellulose membrane after SDS-PAGE experiment. Membrane was blocked with 2% BSA in TBST over 1 h on r.t. Primary antibodies were treated overnight at 4 °C , followed by washing with TBST. HRP-labeled anti-rabbit IgG secondary antibody (1:5000) was treated at room temperature for 1 h. Antibodies were treated with the concentration indicated in antibody manufacturer's protocol. After washing with TBST, membrane was developed by Amersham ECL prime solution. Chemiluminescent signal was measured by ChemiDocTM MP imaging system.

Surface Plasmon Resonance (SPR) Assay

The dissociation rate constant (K_D) toward His-LRS was determined by surface plasmon resonance (SPR) technique at the national center for inter-university research facilities (NCRF) in Seoul National University using a Biacore T100 instrument from GE Healthcare. The carboxyl group on the surface of CM5 sensor chip was replaced with reactive succinimide ester using combination of 1-ethyl-3-(3-dimethylaminopropyl)-carbodiimide (EDC) and *N*-hydroxysuccinimide (NHS) in flow cells 1 and 2. Human LRS (1.5× PBS, pH 7.3) were immobilized on the flow cell 2 (aimed RU; 12000) through formation of amide bond by reacting with the resulting NHS ester. The remaining NHS ester on flow cells 1 and 2 was quenched by injection of 1 M ethanolamine-HCl (pH 8.0) solution. During the immobilization process, PBS was used as running buffer. After the immobilization of hLRS, compounds were injected for 60 s at a flow rate of 20 $\mu\text{l min}^{-1}$ in various concentration from 1 μM to 15 μM . At the same flow rate, dissociation of compounds from the sensor surface was monitored for 200s. As a running buffer, 1× PBS (pH 7.3) containing 3% DMSO and 0.005% P20 solution were used. The binding events were measured at 25 °C. Data analysis were done by using Biacore T100 Evaluation software from GE Healthcare. Final sensorgrams were obtained after the elimination of responses from flow cell 1 and buffer-only control. The dissociation constant (K_D) was calculated by fitting the sensorgrams to the 1:1 binding model.

Chapter 3. Gold-catalyzed unexpected ring transformation of pyrimidodiazepine derivatives

Org. Lett., **2017**, 19, 344–347.

Reproduced by permission of ACS publication.

3.1 Introduction

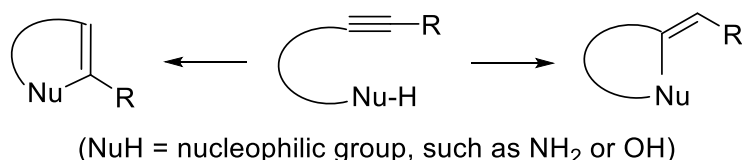
The chemical and biological properties of privileged heterocycles are of continued interest because of the existence of these moieties in many bioactive natural products and FDA-approved pharmaceutical drugs.¹ Among them, pyrimidine has been extensively utilized in pharmaceuticals as a key structural motif owing to its ability to mimic the structures and properties of nucleosides.² Pyrimidine and its derivatives exhibit diverse biological activities, including antibacterial,³ antifungal,⁴ antiviral,⁵ and anticancer⁶ properties.

Recently, we reported the synthesis of pyrimidine-containing polyheterocycles via the recombination of a pyrimidine ring with various heterocycles to expand the molecular diversity using the privileged substructure-based diversity-oriented synthesis (pDOS) strategy.^{7,8} We also showed that privileged structures serve as “chemical navigators” to efficiently access the bioactive chemical space.^{8,9,10} Indeed, skeletal diversity has evolved as a key element in the design strategy for the construction of drug-like small molecule library,¹¹ and there is a high demand in developing efficient methods to increase the skeletal diversity. Thus, we have been pursuing new intramolecular transformations of pyrimidine-embedded polyheterocycles using transition-metal catalysts. In fact, transition-metal catalysis provides an efficient way to induce remarkable changes within molecular frameworks in a single step.¹² In particular, gold-catalyzed reactions have attracted much interest in organic synthesis because of the unique ability of gold catalysts to activate unsaturated carbon–carbon bonds so that they can react with various nucleophiles.¹³ Gold catalysts have been widely used as selective alkynophiles for inter- and intramolecular nucleophilic reactions under mild conditions with

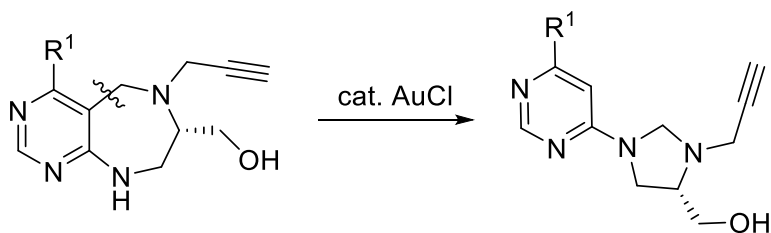
excellent functional group tolerance to afford various heterocyclic products (Scheme 3-1A).¹⁴

Scheme 3-1. Unexpected Discovery of a Novel Gold-Catalyzed Reaction

A. General reactivity of gold catalyst ; cyclization of alkynyl substrate



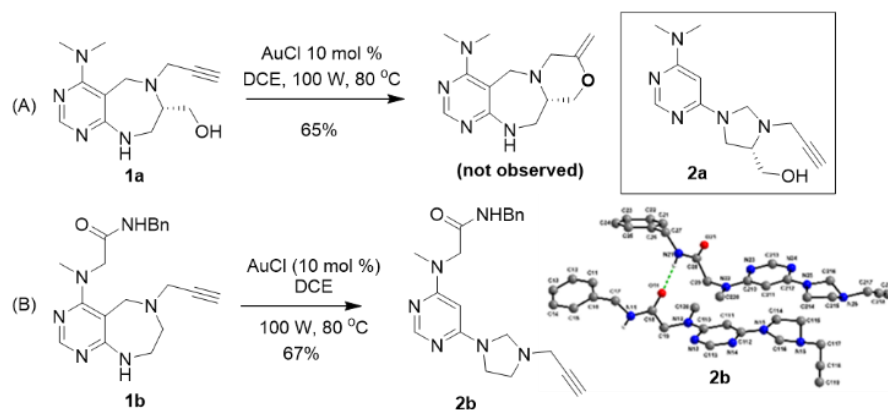
B. *This work* ; Gold catalyzed bond-cleavage and cyclization reaction



As a part of our continuing interest in the diversification of pyrimidine-embedded molecular frameworks, herein, we report a novel synthetic method using a gold catalyst; this involves a retro-Mannich-type C–C bond cleavage in pyrimidodiazepines followed by intramolecular cyclization. The unique reactivity of the gold catalyst is mainly discussed. Under the AuCl-catalyzed microwave reaction conditions, the pyrimidodiazepine moiety can be transformed into imidazolidines, oxazinanes, and oxazolidines depending on the location and type of intramolecular nucleophiles through an iminium intermediate (Scheme 3-1B). This gold-catalyzed ring transformation can be used for the skeletal diversification of one pyrimidine-containing macrocycles to another in a single step at the late stage of synthesis. Moreover, this gold-catalyzed C–C bond cleavage occurs in preference to alkynophilic activation. To the best of our knowledge, no gold-

catalyzed methodology with orthogonal reactivity of substrates in the presence of terminal acetylene moiety has been reported.

Scheme 3-2. Initial Discovery of a Novel Gold-Catalyzed Reaction

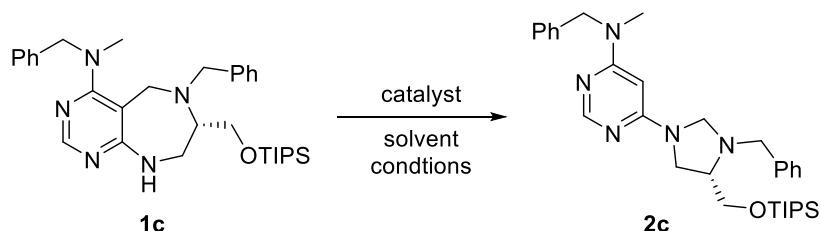


We recently focused on the diversification of pyrimidodiazepine using the pDOS strategy^{7,8} to construct various polyheterocyclic scaffolds for molecular diversity to systematically explore the protein–protein⁸ and protein–DNA/RNA interactions.⁹ During this exploration, we designed and synthesized substrate **1a** bearing a terminal acetylene group which can be activated by a gold catalyst; subsequent cyclization via the intramolecular nucleophilic attack of primary alcohol group would afford a fused morpholine moiety. However, we failed to obtain the fused morpholine moiety under typical gold-catalyzed reaction conditions using microwave irradiation (Scheme 3-2A). Instead, the terminal acetylene moiety was found to be intact by ¹H and ¹³C NMR spectroscopy. Surprisingly, this unexpected product **2a** was a ring-contracted heterocycle containing an imidazolidine moiety, formed by gold-catalyzed C–C bond cleavage and subsequent intramolecular nucleophilic cyclization of the anilinic nitrogen. To confirm this transformation, we

designed and tested **1b** containing a terminal acetylene group as substrate **1a** and no primary alcohol nucleophile. As shown in Scheme 3-2B, the imidazolidine-containing product **2b** was obtained with the terminal acetylene moiety intact, as determined by ¹H-NMR spectroscopy. The exact structure of **2b** was confirmed by X-ray crystallography (see Supporting Information).

3.2 Result and Discussion

Table 3-1. Optimization of Reaction Conditions ^a



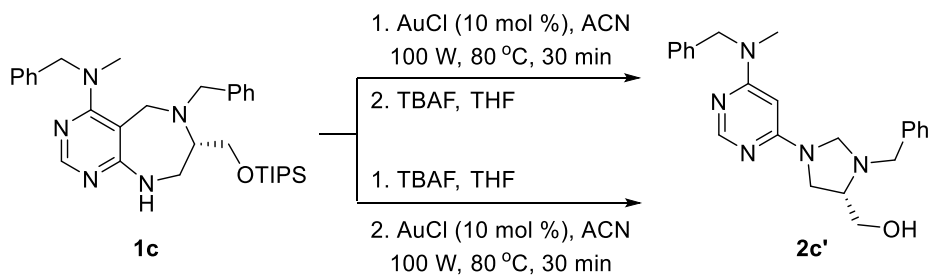
entry	catalyst	conditions ^b	s.m. (%) ^c	product (%) ^c
1	AuCl	DCE, 80 °C, 23 h	-	96
2	AuCl ₃	DCE, 80 °C, 2 h	-	83
3	Au(PPh ₃)OTf	DCE, 80 °C, 20 h	95	-
4	AgSbF ₆	DCE, 80 °C, 20 h	65	21
5	AgOTf	DCE, 80 °C, 20 h	87	-
6 ^d	AuCl	DCE, 80 °C, 100 W, 30 min	82	14
7 ^d	AuCl	CHCl ₃ , 80 °C, 100 W, 30 min	89	10
8 ^d	AuCl	DMF, 80 °C, 100 W, 30 min	55	47
9 ^d	AuCl	THF, 80 °C, 100 W, 30 min	96	-
10 ^d	AuCl	ACN, 80 °C, 100 W, 30 min	-	95

^a Reaction condition: SM, catalyst (10 mol %), solvent (0.1 M). ^b DCE: 1,2-dichloro ethane, DMF: dimethylformamide, THF: tetrahydrofuran, ACN: acetonitrile. ^c Yields determined by the ¹H-NMR analysis of crude products using an internal standard (1, 3,5-tri-MeO-C₆H₃). ^d Microwave conditions

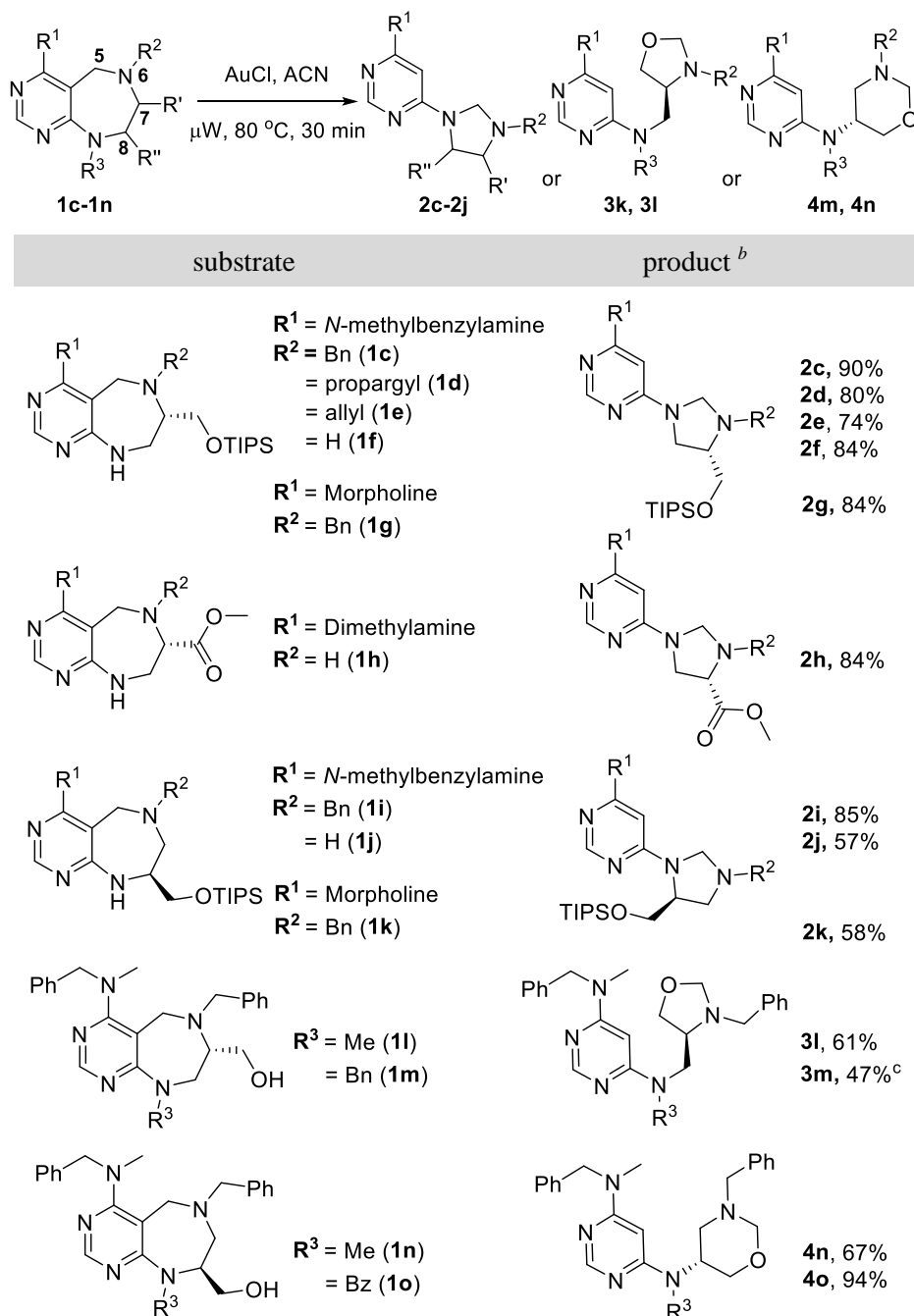
Intrigued by this unexpected result, we attempted to optimize the gold-catalyzed transformation under various conditions (Table 3-1). The feasibility of this process was investigated using substrate **1c** without the terminal acetylene moiety and various coinage metal catalysts and conditions. First, **1c** was thermally activated in the presence of various gold and silver catalysts (entries 1–5). Among the tested

coinage metal catalysts, AuCl showed the efficient transformation of **1c** to **2c**, but this thermal reaction was quite slow (23 h, entry 1). Although the reaction rate of AuCl₃ was faster than other catalysts, the reaction was not clean (entry 2). In the case of microwave-assisted activation, the reaction time was effectively reduced,¹⁵ but the yield was also significantly decreased (entry 6). To solve this problem, different solvents were screened; the desired product **2c** was obtained in an excellent yield within a short reaction time when using acetonitrile (entry 10).

Scheme 3-3. Priority of the Nucleophiles



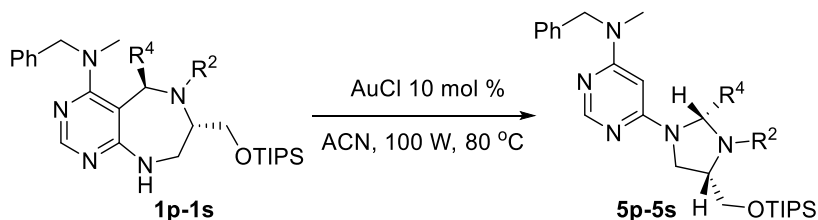
Model substrate **1c** contains two potential nucleophiles, anilinic nitrogen and TIPS-protected alcohol. For the reaction optimization, **1c** was used to simplify the outcome of this transformation. To investigate the priority of two competing nucleophiles, the following experiment were performed by changing the reaction sequence. As shown in Scheme 3, the TIPS group of **1c** was deprotected using tetrabutylammonium fluoride (TBAF) to generate **1c'** with two competing nucleophiles (aniline and primary alcohol), followed by gold-catalyzed ring transformation. The resulting product **2c'** was identical to the product prepared by the gold-catalyzed ring transformation of **1c**, followed by TIPS deprotection. These outcomes clearly confirmed that the anilinic nitrogen has a higher priority over the alcoholic nucleophile when both are available.¹⁹

Table 3-2. Substrate Scope of Gold-catalyzed Ring Transformation Reaction^a

^a Reaction conditions: SM, AuCl (10 mol %), ACN (0.1 M), Microwave, 100 W, 80 °C 30 min. ^b Yield of the isolated product. ^c Based on recovered starting material.

With the optimized conditions in hand, we performed a series of reactions to investigate the substrate scope of this gold-catalyzed ring transformation. As shown in Table 3-2, alkyl amines and cyclic amines at the R¹ position were well tolerated providing imidazolidine products in good-to-excellent yields. Diverse substituents on secondary amine at the R² position were also tolerated, including alkynyl (**1a**, **1b**, and **1d**), allyl (**1e**), benzyl (**1c**, **1g**, **1i**, and **1k–1o**) as well as unmodified secondary amines (**1f**, **1h**, and **1j**). The ester moiety (**1h**) at the C-7 position and the silyl ether moiety (**1c–1g** and **1i–1k**) at the C-7 and C-8 positions of the pyrimidodiazepine provided the corresponding products in good yields. However, tosyl or carbonyl substituents at the R² position failed to provide the desired products, probably because of the electron-withdrawing nature of the substituents at the R² position for this reaction (data not shown). Next, the ability of alcohol nucleophile to form different types of heterocycles (Table 3-2, **1l–1o**) was investigated. The primary alcohol substituents at the C-7 or C-8 position in the gold-catalyzed transformation of pyrimidodiazepine afforded either 1,3-oxazinanes (**3l** and **3m**) or oxazolidines (**4n** and **4o**), respectively. To decrease the nucleophilicity of aniline, electron-donating alkyl substituents as well as electron-withdrawing carbonyl substituents were introduced at the R³ position. Notably, different reactive nucleophiles in pyrimidodiazepine **1** result in the diverse ring transformations, generating different heterocycles from the same skeleton.

Using the synthetic method for the pyrimidodiazepine core skeleton (see Scheme S6), various R⁴ substituents were introduced at the C-5 position at the stage of the formation of iminium intermediate, generated by *N*-alkylation of **SI-4**, using Grignard reagents. The diastereomeric outcome of the alkyl substituents in **1p–1s**

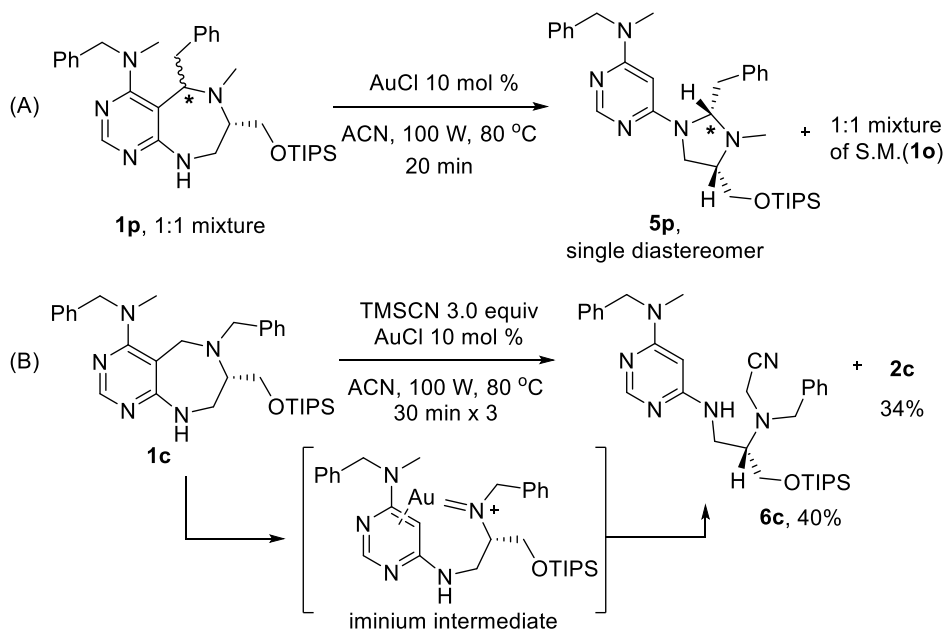
Table 3-3. Steric Effects of R² and R⁴ Substituents on Diastereomeric Ratio

entry	R ⁴	R ²	s.m. dr ratio ^b	pdt dr ratio ^b	yield (%) ^c
1	Bn	Me (1p)	4:1	≫99:1	(5p) 72
2	Bn	Bn (1q)	3.6:1	≫99:1	(5q) 81
3	Me	Bn (1r)	2.7:1	2:1	(5r) 70
4	Me	Me (1s)	3.6:1	1.21:1	(5s) 92

^a Reaction conditions: SM, AuCl (10 mol %), ACN (0.1 M), Microwave, 100 W, 80 °C. ^b Diastereomeric ratio was determined by ¹H-NMR analysis. ^c Yield of the isolated product.

varied due to the chiral environment generated by the TIPS-containing substituent at the C-7 position of iminium intermediate.⁸ As shown in Table 3, the diastereomeric ratio of the starting materials (**1p–1s**) was influenced by the size of R² substituent at the N-6 position owing to the facial selectivity of Grignard reagents. After the preparation of a full matrix of either methyl or benzyl substituent at the C-5 and N-6 positions, the gold-catalyzed ring transformation reaction was performed. Surprisingly, a single product (**5p** and **5q**) was observed from a 4:1 mixture of **1p** and 3.6:1 mixture of **1p**, respectively, in a good yield and excellent diastereoselectivity under the optimized reaction conditions. However, the corresponding diastereoselectivity decreased when the size of R⁴ substituents at the C-5 position was smaller (methyl instead of benzyl) in the case of **1r** and **1s**. To understand the mechanistic origin of this diastereoselectivity, the reactivity of gold-catalyzed ring transformation was further investigated using a 1:1 mixture of pyrimidodiazepine substrate **1p** containing benzyl and methyl moieties at the C-5

Scheme 3-4. Experimental Investigation to Elucidate the Reaction Mechanism of Gold-catalyzed Ring Transformation

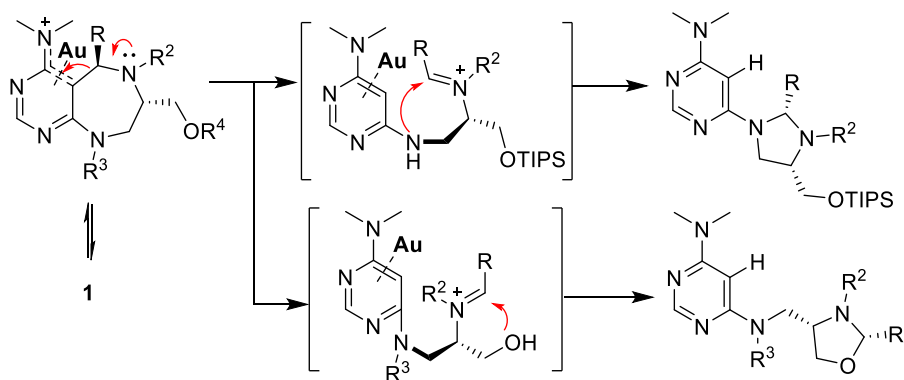


and N-6 position, respectively. When this gold-catalyzed reaction of **1p** was quenched prior to its full conversion, the desired imidazolidine **5p** was obtained as a single diastereomer, and the remaining starting material **1p** was obtained as a 1:1 mixture as confirmed by crude ^1H NMR spectroscopy (Scheme 3-4A). This observation indicates that the gold-catalyzed reaction occurred through the formation of an identical intermediate from both the diastereomeric starting materials with the same reaction rate, followed by the intramolecular nucleophilic addition of anilinic nitrogen to afford the desired product **5p** as a single diastereomer.

Based on these experimental results, a probable mechanism of this gold-catalyzed ring transformation involving an iminium intermediate is proposed (Scheme 5).¹⁶ Strongly nucleophilic trimethylsilyl cyanide (TMSCN) was added to trap the

acyclic iminium intermediate of the gold-catalyzed reaction of **1c**; the CN-trapped product **6c** was observed along with the desired imidazolidine product **2c** (Scheme 3-4B).¹⁹ Therefore, it can be concluded that this AuCl-catalyzed ring transformation of pyrimidodiazepine is mediated via the *in situ* generation of an acyclic iminium intermediate through gold-catalyzed ring opening¹⁷ and subsequent intramolecular nucleophilic cyclization. The stereochemical enrichment of this unusual gold-catalyzed reaction can be attributed to the retro-Mannich-type cleavage of C–C bond,¹⁸ followed by the face-selective trapping of iminium intermediates (Scheme 3-5).

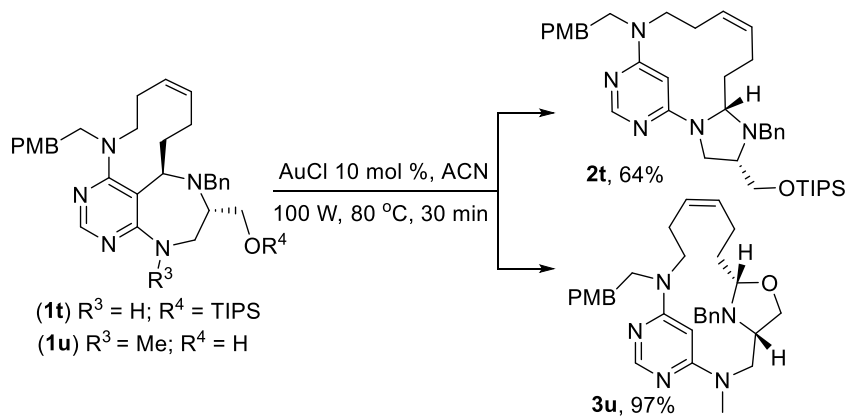
Scheme 3-5. Plausible Mechanism of Gold-Catalyzed Ring Transformation of Pyrimidodiazepine



To demonstrate the potential of this synthetic method, the gold-catalyzed reaction was used to transform medium-sized rings into larger macrocycles at the last stage of synthesis for skeletal diversification (Scheme 3-6). The starting materials (**1t** and **1u**) were prepared using our standard synthetic methods including olefin metathesis (Scheme S7).⁸ The 10-membered pyrimidodiazepines (**1t** and **1u**) were subjected to the gold-catalyzed reaction, allowing the ring enlargement to 12-membered **2s** and 15-membered **3t** via the intramolecular nucleophilic cyclization

with aniline and alcohol nucleophiles, respectively. It is noteworthy that significantly different macrocycles were obtained from the same skeleton simply by switching the reactive nucleophiles. The stereochemical configuration of **2s** and **3t** was confirmed by 2D NOESY NMR analysis.¹⁹

Scheme 3-6. Synthetic utility of this method



3.3 Conclusion

In conclusion, a novel orthogonal gold-catalyzed ring transformation method was developed for pyrimidodiazepine derivatives in the presence of an alkyne moiety. This gold-catalyzed reaction is mediated by the in situ generation of acyclic iminium intermediates via unusual C-C bond cleavage and subsequent nucleophilic cyclization. The formation of imidazolidine, oxazolidine, and oxazinane derivatives depends on the type of intramolecular nucleophiles in pyrimidodiazepines. The stereo-chemical enrichment of this gold-catalyzed reaction is probably caused by the facial selectivity of iminium intermediates. This synthetic method was successfully used to synthesize two different types of macrocycles from the same skeleton. This method provides a highly concise and effective protocol to synthesize novel drug candidates with diverse structures. Further investigations on the mechanistic details of this gold-catalyzed reaction are currently underway.

3.4 References

- [01] (a) Baumann, M.; Baxendale, I. R.; Ley, S. V.; Nikbin, N. *Beilstein J. Org. Chem.* **2011**, 7, 442. (b) Baumann, M.; Baxendale, I. R. *Beilstein J. Org. Chem.* **2013**, 9, 2265. (c) Vitaku, E.; Smith, D. T.; Njardarson, J. T. *J. Med. Chem.* **2014**, 57, 10257.
- [02] (a) Wang, S.; Folkes, A.; Chuckowree, I.; Cockcroft, X.; Sohal, S.; Miller, W.; Milton, J.; Wren, S. P.; Vicker, N.; Depledge, P.; Scott, J.; Smith, L.; Jones, H.; Mistry, P.; Faint, R.; Thompson, D.; Cocks, S. *J. Med. Chem.* **2004**, 47, 1329. (b) Bhuyan, P.; Boruah, R. C.; Sandhu, J. S. *J. Org. Chem.* **1990**, 55, 568.
- [03] Ribble, W.; Hill, W. E.; Ochsner, U. A.; Jarvis, T. C.; Guiles, J. W.; Janjic, N.; Bullard, J. M. *Antimicrob. Agents Chemother.* **2010**, 54, 4648.
- [04] Sun, L.; Wu, J.; Zhang, L.; Luo, M.; Sun, D.; *Molecules* **2011**, 16, 5618.
- [05] Holý, A.; Votruba, I.; Masojídková, M.; Andrei, G.; Snoeck, R.; Naesens, L.; De Clercq, E.; Balzarini, J. *J. Med. Chem.* **2002**, 45, 1918.
- [06] Ma, L.-Y.; Zheng, Y.-C.; Wang, S.-Q.; Wang, B.; Wang, Z.-R.; Pang, L.-P.; Zhang, M.; Wang, J.-W.; Ding, L.; Li, J.; Wang, C.; Hu, B.; Liu, Y.; Zhang, X.-D.; Wang, J.-J.; Wang, Z.-J.; Zhao, W.; Liu, H.-M. *J. Med. Chem.* **2015**, 58, 1705.
- [07] Kim, H.; Tung, T. T.; Park, S. B. *Org. Lett.* **2013**, 15, 5814.
- [08] Kim, J.; Jung, J.; Koo, J.; Cho, W.; Lee, W. S.; Kim, C.; Park, W.; Park, S. B. *Nat. Commun.* **2016**, 7, 13196.
- [09] Lim, D.; Byun, W. G.; Koo, J. Y.; Park, H.; Park, S. B. *J. Am. Chem. Soc.* **2016** 138, 13630.
- [10] (a) Choi, Y.; Kim, H.; Shin, Y.-H.; Park, S. B. *Chem. Commun.* **2015**, 51, 13040. (b) Kim, H.; Jo, A.; Ha, J.; Lee, Y.; Hwang, Y. S.; Park S. B. *Chem. Commun.* **2016**, 52, 7822.
- [11] (a) Couladouros, E. A.; Sronglios, A. T. *Angew. Chem., Int. Ed.* **2002**, 41, 3677. (b) Burke, M. D.; Berger, E. M.; Schreiber, S. L. *Science* **2003**, 302,

613. (c) Burke, M. D.; Schreiber, S. L. *Angew. Chem., Int. Ed.* **2004**, *43*, 46.
- [12] For a selected review, see: Nakamura, I.; Yamamoto, Y.; *Chem. Rev.* **2004**, *104*, 2127.
- [13] For a selected review, see: Hashmi A. S. K. *Chem. Rev.* **2007**, *107*, 3180.
- [14] (a) Taskaya, S.; Menges, N.; Balci, M. *Beilstein J. Org. Chem.* **2015**, *11*, 897. (b) Yao, L.-F.; Wang, Y.; Huang, K.-W. *Org. Chem. Front.* **2015**, *2*, 721. (c) James, T.; Simpson, I.; Grant, J. A.; Sridharan, V.; Nelson, A. *Org. Lett.* **2013**, *15*, 6094.
- [15] (a) Kappe, C. O. *Angew. Chem., Int. Ed.* **2004**, *43*, 6250. (b) Kappe, C.O.; Dallinger, D. *Mol Divers.* **2009**, *13*, 71.
- [16] A similar type of reaction mechanism and its intermediate were proposed in the visible light-induced cyclization of diamines. Xuan, J.; Cheng, Y.; An, J.; Lu, L.-Q.; Zhang, X.-X.; Xiao, W.-J. *Chem. Commun.* **2011**, *47*, 8337.
- [17] (a) Yeager, A. R.; Min, G. K.; Porco, J. A., Jr.; Schaus, S. E. *Org. Lett.* **2006**, *8*, 5065. (b) Sawama, Y.; Sawama, Y.; Krause, N. *Org. Lett.* **2009**, *11*, 5034.
- [18] (a) Cramer, N.; Juretschke, J.; Laschat, S.; Baro, A.; Frey, W. *Eur. J. Org. Chem.* **2004**, 1397. (b) White, J. D.; Li, Y.; Ihle, D. C. *J. Org. Chem.* **2010**, *75*, 3569. (c) Xia, Y.; Lin, L.; Chang, F.; Liao, Y.; Liu, X.; Feng, X. *Angew. Chem. Int. Ed.* **2016**, *55*, 12228.
- [19] See supporting information

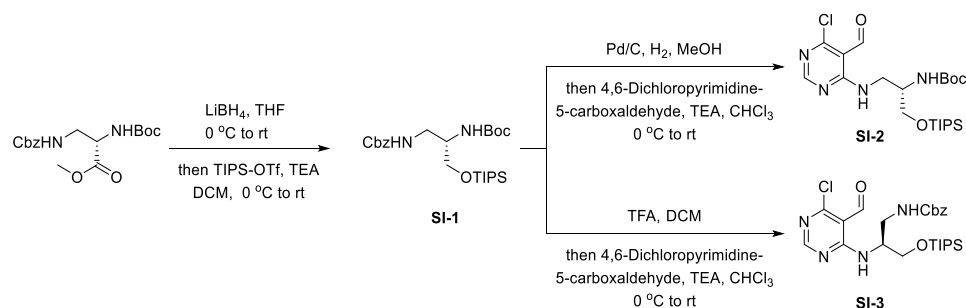
3.5 Experimental Section

3.5.1. General information

NMR spectra were obtained on an Agilent 400-MR DD2 Magnetic Resonance System [400 MHz, Agilent, USA], Varian/Oxford As-500 [500 MHz, Varian Assoc., Palo Alto, USA] or Bruker Avance 600 [600 MHz, Bruker, Germany]. Chemical shift values were recorded as parts per million (δ), referenced to tetramethylsilane (TMS) as the internal standard or to the residual solvent peak (CDCl_3 , ^1H : 7.26, ^{13}C : 77.16, $\text{DMSO}-d_6$, ^1H : 2.50, ^{13}C : 39.52). Multiplicities were indicated as follows: s (singlet), d (doublet), t (triplet), q (quartet), m (multiplet), dd (doublet of doublet), dt (doublet of triplet), td (triplet of doublets), br s (broad singlet) and so on. Coupling constants were reported in hertz (Hz). High resolution mass spectra (HRMS) were analyzed at the Organic Chemistry Research Center in Sogang University on a Ultra High Resolution ESI Q-TOF mass spectrometer [Bruker, Germany] using the electrospray ionization (ESI) method. All commercially available reagents were used without further purification unless noted otherwise. Commercially available reagents were obtained from Sigma-Aldrich, TCI, Acros, or Alfa Aesar. All solvents were obtained by passing them through activated alumina columns of solvent purification systems from Glass Contour. Analytical thin-layer chromatography (TLC) was performed using Merck Kieselgel 60 F254 plates, and the components were visualized by observation under UV light (254 and 365 nm) or by treating the plates with ninhydrin followed by thermal visualization. Flash column chromatography was performed on Merck Kieselgel 60 (230-400 mesh). Microwave reactions were performed using the CEM Discover Benchmate and microwave reaction conditions were as indicated in the Experimental Section. X-ray crystallographic analysis was performed at Ewha Womans University, Seoul.

3.5.2. Synthesis and Characterization of Substrates

Scheme S1. Preparation of SI-2 and SI-3



tert-Butyl (S)-(1-((6-chloro-5-formylpyrimidin-4-yl)amino)-3-((triisopropylsilyl)-oxy)propan-2-yl)carbamate (**SI-2**) was prepared according to the previous report.^{1, 2,3}

Synthetic procedure of SI-3

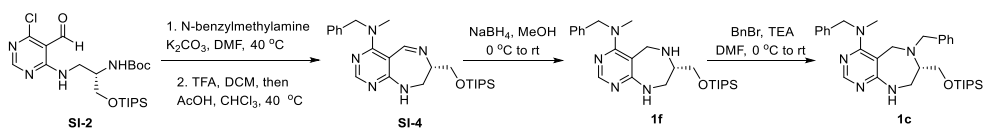
To a solution of **SI-1** (5.0 g, 10.4 mmol) in dichloromethane (DCM) (0.1 M, 90 mL) was treated with trifluoroacetic acid (TFA) (10 mL, 10 vol.%) at r.t. After the starting material was consumed as indicated by TLC, any excess TFA was removed by azeotropic evaporation with toluene under reduced pressure, and the crude resultant was dissolved in chloroform (CHCl_3 , 0.1 M). To this solution were sequentially added Et_3N (2.2 mL, 15.6 mmol) and 4,6-dichloropyrimidine-5-carboxaldehyde (1.8 g, 10.4 mmol) at 0 °C and left to stir. After 30 min, the reaction mixture was quenched with saturated $\text{NH}_4\text{Cl}(\text{aq})$. The resultant was extracted twice with CHCl_3 , dried over anhydrous $\text{Na}_2\text{SO}_4(\text{s})$, and filtered. The filtrate was condensed under reduced pressure and purified by silica-gel flash column chromatography to afford the desired product **SI-3** (3.4 g, 63% overall yield) as a colorless oil.

¹ Stojković, M. R.; Piotrowski, P.; Schmuck, C.; Piantanida I. *Org. Biomol. Chem.* **2015**, *13*, 1629.

² Kim, J.; Jung, J.; Koo, J.; Cho, W.; Lee, W. S.; Kim, C.; Park, W.; Park, S. B. *Nat. Comm.* **2016**, *7*, 13196.

³ Zheng, L.; Yang, F.; Dang, Q.; Bai, X. *Org. Lett.*, **2008**, *10*, 889.

Scheme S2. Preparation of **1f** and **1c**



To a stirring solution of **SI-2** (3.0 g, 6.2 mmol) and K_2CO_3 (1.7 g, 12.4 mmol) in *N,N*-dimethylformamide (DMF) (0.1 M) was added *N*-benzylmethylamine (1.2 mL, 12.4 mmol) and the resulting mixture was stirred at 40 °C. After completion of the reaction as indicated by TLC, the resultant was quenched with saturated $NH_4Cl(aq)$ and extracted twice with ethyl acetate. The combined organic layer was dried over anhydrous $Na_2SO_4(s)$ and filtered. The organic solvent was evaporated under reduced pressure to afford a crude oil, which was purified by silica-gel flash column chromatography. To obtain the cyclic imine product **SI-4**, the above product was first treated with 10 vol.% of trifluoroacetic acid (TFA) in DCM (100 mL) at r.t. After the starting material was consumed as indicated by TLC, any excess TFA was removed by azeotropic evaporation with toluene under reduced pressure, and the crude resultant was dissolved in 1 vol.% acetic acid (AcOH) in $CHCl_3$ (100 mL). The resulting mixture was stirred at 40 °C. After completion of the reaction as indicated by TLC, the resultant was quenched with saturated $NaHCO_3(aq)$ and extracted twice with $CHCl_3$. The combined organic layer was dried over anhydrous $Na_2SO_4(s)$ and filtered. The filtrate was condensed under reduced pressure, followed by silica-gel flash column chromatography to afford the desired product **SI-4** (2.3 g, 83%) as a off white powder.

To a stirring solution of **SI-4** (2.3 g, 5.1 mmol) in MeOH (0.1 M) was added sodium borohydride ($NaBH_4$) (973.3 mg, 25.5 mmol) at 0 °C. The resulting mixture was left to stir and allowed to warm to r.t. After completion of the reaction as indicated by TLC, the resultant was quenched with saturated $NaHCO_3(aq)$ and extracted twice with DCM. The combined organic layer was dried over anhydrous $Na_2SO_4(s)$ and filtered. The filtrate was condensed under reduced pressure, followed by silica-gel flash column chromatography to afford **1f** (2.1 g, 90% yield) as a yellow oil.

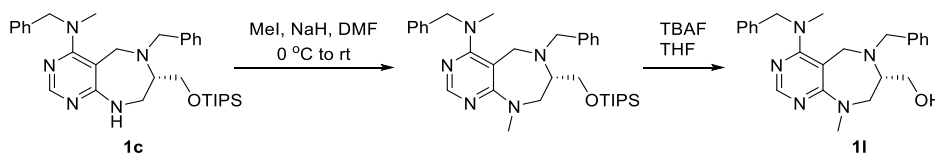
To a solution of the **1f** (2.0g, 4.4 mmol) in DMF (0.1 M) were sequentially added

Et₃N (1.2 mL, 8.8 mmol) and benzyl bromide (680.3 μ L, 5.7 mmol) at 0 °C. The resulting mixture was left to stir and allowed to warm to r.t. After completion of the reaction as indicated by TLC, the resultant was quenched with saturated NH₄Cl(aq) and extracted twice with ethyl acetate. The combined organic layer was dried over anhydrous Na₂SO₄(s) and filtered. The filtrate was condensed under reduced pressure, followed by silica-gel flash column chromatography to afford **1c** (2.1 g, 87% yield) as a pale yellow oil.

Substrates **1d**, **1e** and **1g** were prepared according to Scheme S2.

Substrate **1a** was prepared according to Scheme S2, followed by TIPS deprotection with TBAF (1.0 M in THF, 1.5 equiv.).

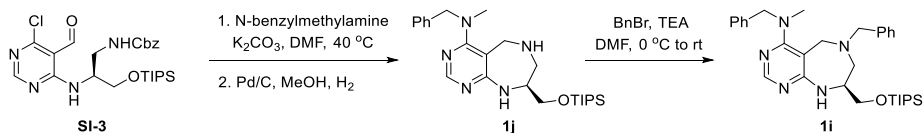
Scheme S3. Preparation of **1l**



To a solution of the **1c** (1.0 g, 1.83 mmol) in DMF (0.1 M) under argon atmosphere was added NaH (60% dispersion in mineral oil, 146.5 mg, 3.66 mmol) at 0 °C and left to stir. After 30 min, iodomethane (170.9 μ L, 2.74 mmol) was slowly added. The resulting mixture was left to stir and allowed to warm to r.t. After completion of the reaction as indicated by TLC, the reaction mixture was quenched with saturated NH₄Cl(aq). The resultant was extracted twice with ethyl acetate, dried with anhydrous Na₂SO₄(s), filtered, and concentrated. To a solution of the crude resultant in THF (0.1 M) was added TBAF (1.0 M in THF, 2.7 mL) and the mixture was stirred at r.t. After completion of the reaction as indicated by TLC, the reaction mixture was quenched with saturated NaHCO₃(aq). The resultant was extracted twice with DCM, dried with anhydrous Na₂SO₄(s), filtered, and concentrated *in vacuo*. The residue was purified with silica-gel flash column chromatography to obtain desired product **1l** (524.3 mg, 71% overall yield) as a colorless oil.

Substrates **1m**, **1n** and **1u** were prepared according to Scheme S3.

Scheme S4. Preparation of **1j** and **1i**

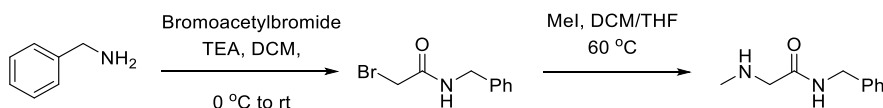


To a stirring solution of **SI-3** (3.0 g, 5.8 mmol) and K_2CO_3 (1.6 g, 11.5 mmol) in *N,N*-dimethylformamide (DMF) (0.1 M) was added *N*-benzylmethylamine (1.1 mL, 8.6 mmol) and the resulting mixture was stirred at 40 °C. After completion of the reaction as indicated by TLC, the resultant was quenched with saturated $NH_4Cl(aq)$ and extracted twice with ethyl acetate. The combined organic layer was dried over anhydrous $Na_2SO_4(s)$ and filtered. The filtrate was condensed under reduced pressure and the crude resultant was dissolved in methanol (0.1 M). To this solution (1.0 equiv.) was carefully added 10 wt.% Pd/C (1.5 g) and the mixture was vigorously stirred under H_2 atmosphere (1 atm) at r.t. After completion of the reaction as indicated by TLC, the reaction mixture was filtered through Celite® while washing with ethyl acetate. The filtrate was condensed under reduced pressure, followed by silica-gel flash column chromatography to afford **1j** (1.6 g, overall 61% yield) as a pale yellow oil.

To a solution of the **1j** (1.5 g, 3.3 mmol) in DMF (0.1 M) were sequentially added Et_3N (917.5 μL , 6.6 mmol) and benzyl bromide (508.9 μL , 4.3 mmol) at 0 °C. The resulting mixture was left to stir and allowed to warm to r.t. After completion of the reaction as indicated by TLC, the resultant was quenched with saturated $NH_4Cl(aq)$ and extracted twice with ethyl acetate. The combined organic layer was dried over anhydrous $Na_2SO_4(s)$ and filtered. The filtrate was condensed under reduced pressure, followed by silica-gel flash column chromatography to afford **1i** (1.5 g, 83% yield) as a pale yellow oil.

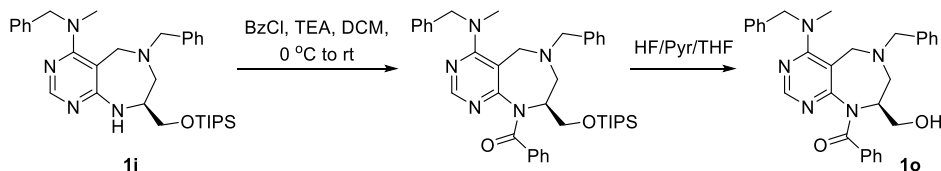
Substrates **1b**, **1h**, and **1k** were prepared according to Scheme S4.

N-benzyl-2-(methylamino)acetamide for the preparation of **1b** was prepared via acylation and alkylation sequence as follows.



To a solution of benzyl amine (1.0 g, 5.84 mmol) in dry DCM (0.1 M) under argon atmosphere was added Et₃N (896.4 μ L, 6.43 mmol) at 0 °C and left to stir. After 15 min, bromoacetyl bromide was slowly added. The resulting mixture was left to stir and allowed to warm to r.t. After completion of the reaction as indicated by TLC, the reaction mixture was condensed under reduced pressure. The crude resultant was dissolved in THF (0.1 M). To this solution was added methylamine (2.0 M in THF, 29.2 mL, 58.4 mmol) and the resulting mixture was stirred at 60 °C. After completion of the reaction as indicated by TLC, the resultant was quenched with saturated NaHCO₃(aq) and extracted twice with DCM. The combined organic layer was dried over anhydrous Na₂SO₄(s) and filtered. The organic solvent was evaporated under vacuum to afford a crude oil, which was used without further purification in the S_NAr reaction according to Scheme S4.

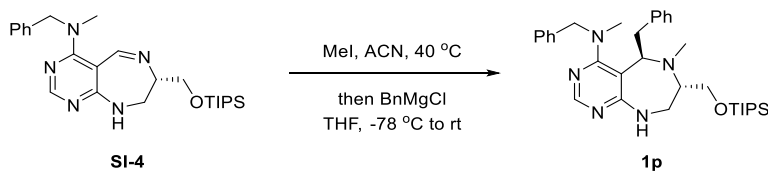
Scheme S5. Preparation of **1o**



To a solution of the **1i** (545.8 mg, 1.00 mmol) in DCM (0.1 M) were sequentially added Et₃N (278.8 μ L, 2.00 mmol) and benzoyl chloride (150.9 μ L, 1.30 mmol) at 0 °C. The resulting mixture was left to stir and allowed to warm to r.t. After completion of the reaction as indicated by TLC, the resultant was extracted twice with brine/DCM. The combined organic layer was dried over anhydrous Na₂SO₄(s),

filtered, and concentrated under reduced pressure. To a solution of the crude resultant in THF (0.1 M) was added HF/pyridine/THF (5/5/90) solution (20 mL) and the mixture was stirred at r.t. After the starting material was consumed as indicated by TLC, ethoxytrimethylsilane (20 mL) was added and allowed to react for 1 h to quench any excess HF (based on HF/pyridine protocol). The reaction mixture was condensed *in vacuo*, followed by silica-gel flash column chromatography to afford **1o** (424.5 mg, 86% yield) as a clear oil.

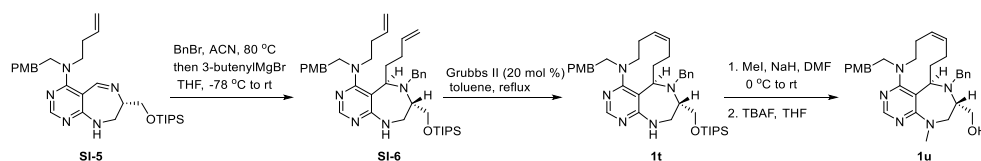
Scheme S6. Preparation of **1p**



To a stirring solution of **SI-4** (453.7 mg, 1.00 mmol) in ACN (0.1 M), iodomethane (124.5 μ L, 2.00 mmol) was added and the resulting mixture was stirred at 40 $^{\circ}$ C. After the starting material was consumed as indicated by TLC, the organic solvent was removed under reduced pressure to afford the crude iminium ion. After washing with hexane to remove any excess iodomethane, benzylmagnesium chloride (2.0 M solution in THF, 2.5 mL, 5.00 mmol) was added dropwise to a cooled solution of resultant iminium ion in dry THF (0.05 M) over 30 min at -78 ° C. The reaction was allowed to slowly warm to r.t over an 18 h period. The mixture was quenched with saturated $\text{NH}_4\text{Cl(aq)}$ and extracted twice with DCM. The combined organic layer was dried over anhydrous $\text{Na}_2\text{SO}_4\text{(s)}$ and the filtrate was condensed under reduced pressure, followed by silica-gel flash column chromatography to afford **1p** (397.5 mg, 71% yield) as a colorless oil.

Substrates **1q**, **1r**, and **1s** were prepared according to Scheme S6.

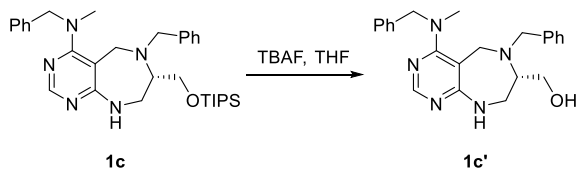
Scheme S7. Preparation of **1t**



Substrate **1t** was prepared according to the previous report.² To a stirring solution of **SI-5** (1.0 g, 1.86 mmol) in acetonitrile (ACN) (0.1 M), benzyl bromide (331.7 μL , 2.79 mmol) was added and the resulting mixture was stirred at $80\text{ }^{\circ}\text{C}$. After completion of the reaction indicated by TLC, the organic solvent was removed under reduced pressure and the crude resultant was washed with hexane to remove any excess benzyl bromide. To a cooled solution of resultant iminium ion in dry THF (0.05 M) was added 3-butenylmagnesium bromide (0.5 M solution in THF, 18.6 mL, 9.30 mmol) dropwise over 30 min at $-78\text{ }^{\circ}\text{C}$. The reaction mixture was allowed to slowly warm to r.t over an 12 h period. The resultant was quenched with saturated $\text{NH}_4\text{Cl(aq)}$ and extracted twice with DCM. The combined organic layer was dried over anhydrous $\text{Na}_2\text{SO}_4(\text{s})$ and filtered. The filtrate was condensed under reduced pressure, followed by flash column chromatography to afford **SI-6** (1.0 g, 79 %) as a clear oil. To a solution of **SI-6** in toluene (0.005 M) was added 2nd generation Grubbs' catalyst (20 mol%) and the mixture was left to stir at reflux. After the starting material was indicated as by TLC, the organic solvent was removed under reduced pressure, and the residue was purified by silica-gel flash column chromatography to obtain the desired product **1t** (607.3 mg, 63 % yield) as a brown oil.

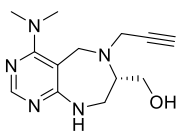
Substrate **1u** was prepared from **1t** according to the Scheme S3.

Scheme S8. Preparation of **1c'**



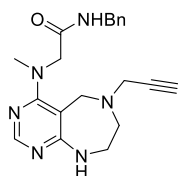
To a solution of **1c** (100.0 mg, 0.18 mmol) in THF (0.1 M) was added TBAF (1.0 M in THF, 270 μ L, 0.37 mmol) and the mixture was stirred at r.t. After completion of the reaction as indicated by TLC, the reaction mixture was quenched with saturated $\text{NaHCO}_3(\text{aq})$. The resultant was extracted twice with ethyl acetate, dried with anhydrous $\text{Na}_2\text{SO}_4(\text{s})$, filtered, and concentrated *in vacuo*. The residue was purified with silica-gel flash column chromatography to obtain desired product **1c'** (67.0 mg, 96% yield) as a white solid.

Similarly, **2c'** was prepared from **2c** according to the Scheme S8



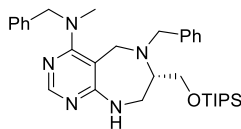
1a

(1a) Prepared according to Scheme S2; 56% overall yield, 132.4 mg; pale yellow oil; ^1H NMR (400 MHz, CDCl_3): δ 7.91 (s, 1H), 6.20 (t, $J = 5.1$ Hz, 1H), 4.07 (br s, 1H), 3.80 (m, 2H), 3.36–3.47 (m, 6H), 3.09 (m, 1H), 2.82 (s, 6H), 2.18 (m, 1H); ^{13}C NMR (100 MHz, CDCl_3): δ 167.2, 164.4, 155.0, 95.1, 80.1, 72.9, 63.2, 62.0, 47.4, 45.1, 44.2, 41.4.



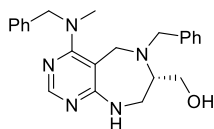
1b

(1b) Prepared according to Scheme S4; 72% overall yield, 220.1 mg; white solid; ^1H NMR (400 MHz, $\text{DMSO}-d_6$): δ 8.48 (t, $J = 6.1$ Hz, 1H), 7.85 (s, 1H), 7.30–7.24 (m, 4H), 7.19 (m, 1H), 6.57 (t, $J = 3.9$ Hz, 1H), 4.29 (d, $J = 5.9$ Hz, 2H), 3.98 (s, 2H), 3.35–3.30 (m, 7H), 2.98 (s, 3H), 2.73 (m, 2H); ^{13}C NMR (100 MHz, $\text{DMSO}-d_6$): δ 169.5, 167.7, 164.8, 154.0, 139.5, 128.2, 127.1, 126.7, 96.9, 79.4, 75.8, 55.7, 55.2, 52.7, 46.8, 43.7, 42.0, 39.9.



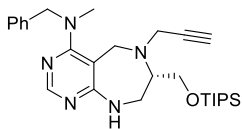
1c

(1c) Prepared according to Scheme S2; 87% yield from **1f**, 2.1 g; pale yellow oil; ^1H NMR (400 MHz, CDCl_3): δ 8.15 (s, 1H), 7.28 (m, 3H), 7.20 (m, 3H), 7.13 (m, 2H), 6.92 (m, 2H), 5.50 (m, 1H), 4.44, 4.20 (ABq, $J_{\text{AB}} = 15.7$ Hz, 2H), 4.09 (d, $J = 16.0$ Hz, 1H), 3.86 (m, 2H), 3.78 (m, 1H), 3.67 (dd, $J = 10.0, 4.5$ Hz, 1H), 3.56 (m, 3H), 3.14 (m, 1H), 2.66 (s, 3H), 1.02 (m, 21H); ^{13}C NMR (100 MHz, CDCl_3): δ 167.6, 165.1, 155.2, 139.6, 138.2, 129.1, 128.5, 128.3, 127.4, 127.1, 126.9, 96.4, 65.7, 64.8, 60.3, 57.2, 46.1, 45.3, 38.6, 18.1, 11.9.



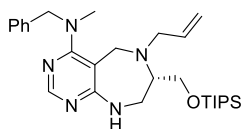
1c'

(1c') Prepared according to Scheme S8; 96% yield from **1c**, 67.0 mg; colorless oil; ^1H NMR (400 MHz, CDCl_3): δ 8.19 (s, 1H), 7.31 (m, 3H), 7.21 (m, 3H), 7.06 (m, 2H), 6.87 (m, 2H), 5.67 (m, 1H), 4.45, 4.17 (ABq, $J_{\text{AB}} = 15.7$ Hz, 2H), 3.95 (d, $J = 16.4$ Hz, 1H), 3.88 (m, 2H), 3.71–3.63 (m, 1H), 3.49–3.34 (m, 3H), 3.32–3.26 (m, 2H), 2.89 (br s, 1H), 2.65 (s, 3H); ^{13}C NMR (100 MHz, CDCl_3): δ 167.9, 164.9, 155.4, 138.8, 137.8, 129.3, 128.6, 128.5, 127.6, 127.4, 127.1, 95.0, 65.3, 61.7, 60.3, 57.0, 45.0, 43.0, 38.6.



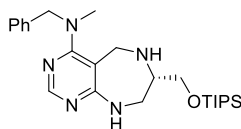
1d

(1d) Prepared according to Scheme S2; 79% yield from **1c**, 171.6 mg; colorless oil; ^1H NMR (400 MHz, CDCl_3): δ 8.16 (s, 1H), 7.38–7.25 (m, 5H), 5.38 (s, 1H), 4.72, 4.63 (ABq, $J_{\text{AB}} = 16.0$ Hz, 2H), 3.75 (dd, $J = 9.8, 5.1$ Hz, 1H), 3.65 (m, 2H), 3.51 (m, 1H), 3.23 (m, 3H), 2.97 (s, 3H), 2.83 (d, $J = 12.1$ Hz, 1H), 2.67 (m, 1H), 2.17 (m, 1H), 1.10 (m, 21H); ^{13}C NMR (100 MHz, CDCl_3): δ 166.6, 166.5, 155.3, 138.5, 128.7, 127.2, 127.2, 99.1, 78.7, 73.5, 64.4, 57.8, 57.4, 56.2, 53.3, 47.7, 38.5, 18.1, 11.9.



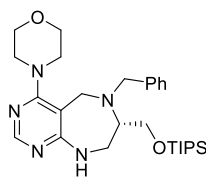
1e

(1e) Prepared according to Scheme S2; 89% yield from **1c**, 194.1 mg; colorless oil; ^1H NMR (400 MHz, CDCl_3): δ 8.09 (s, 1H), 7.34–7.24 (m, 5H), 5.76 (dddd, $J = 16.8, 10.1, 6.6, 6.6$ Hz, 1H), 5.35 (m, 1H), 5.04 (dd, $J = 18.0, 10.5$ Hz, 2H), 4.61 (d, $J = 15.3$ Hz, 1H), 4.35 (d, $J = 15.7$ Hz, 1H), 4.09 (d, $J = 16.0$ Hz, 1H), 3.80–3.67 (m, 3H), 3.57 (m, 2H), 3.33 (dd, $J = 13.7, 6.2$ Hz, 1H), 3.18 (dd, $J = 14.0, 6.6$ Hz, 1H), 3.05 (m, 1H), 2.78 (s, 3H), 1.05 (m, 21H); ^{13}C NMR (100 MHz, CDCl_3): δ 167.3, 164.9, 155.1, 138.5, 136.4, 128.5, 127.7, 127.1, 117.5, 96.8, 65.1, 63.8, 59.3, 56.8, 47.3, 44.6, 39.3, 18.1, 11.9.



1f

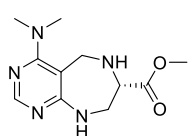
(1f) Prepared according to Scheme S2; 75% overall yield, 2.1 g, off white solid; ^1H NMR (400 MHz, CDCl_3): δ 8.09 (s, 1H), 7.35–7.24 (m, 5H), 5.22 (t, $J = 4.3$ Hz, 1H), 4.59, 4.54 (ABq, $J_{\text{AB}} = 15.6$ Hz, 2H), 3.98 (d, $J = 15.3$ Hz, 1H), 3.73–3.63 (m, 3H), 3.58 (m, 1H), 3.30 (m, 1H), 3.16 (m, 1H), 2.88 (s, 3H), 2.04 (br s, 1H), 1.06 (m, 21H); ^{13}C NMR (100 MHz, CDCl_3): δ 166.3, 166.2, 154.7, 138.3, 128.6, 127.5, 127.1, 100.8, 65.0, 60.3, 56.8, 46.1, 44.8, 39.1, 18.1, 11.9.



1g

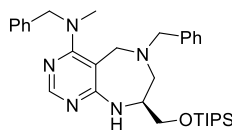
(1g) Prepared according to Scheme S2; 66% overall yield, 160.5 mg; pale yellow oil; ^1H NMR (400 MHz, CDCl_3): δ 8.14 (s, 1H), 7.24 (m, 3H), 7.13 (d, $J = 6.7$ Hz, 2H), 5.46 (m, 1H), 4.06 (d, $J = 16.0$ Hz, 1H), 3.87 (m, 2H), 3.70 (m, 2H), 3.58 (m, 4H), 3.50 (m, 3H), 3.15 (m, 1H), 3.06 (m, 4H), 1.04 (m, 21H);

^{13}C NMR (100 MHz, CDCl_3) : δ 166.7, 165.1, 155.7, 139.3, 129.1, 128.2, 127.2, 98.4, 66.8, 65.6, 64.6, 60.3, 49.9, 45.7, 45.1, 18.1, 11.9.



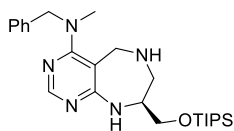
1h

(1h) Prepared according to Scheme S4; 43% overall yield, 2.3g; off white solid; ^1H NMR (400 MHz, CDCl_3): δ 8.05 (s, 1H), 5.44 (m, 1H), 3.96 (d, $J = 16.0$ Hz, 1H), 3.91 (m, 1H), 3.83 (m, 1H), 3.78 (s, 3H), 3.75 (m, 1H), 3.68 (m, 1H), 2.96 (s, 6H), 2.45 (br s, 1H); ^{13}C NMR (100 MHz, CDCl_3) : δ 172.7, 166.3, 165.3, 154.6, 99.6, 61.1, 52.4, 46.1, 43.9, 41.3.



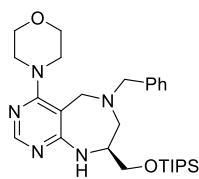
1i

(1i) Prepared according to Scheme S4; 83% yield from **1j**; 1.5 g, pale yellow oil; ^1H NMR (400 MHz, CDCl_3): δ 8.13 (s, 1H), 7.30–7.21 (m, 6H), 7.19–7.16 (m, 4H), 5.31 (s, 1H), 4.66, 4.54 (ABq, $J_{\text{AB}} = 16.0$ Hz, 2H), 3.66 (d, $J = 13.7$ Hz, 1H), 3.61 (m, 1H), 3.54 (m, 2H), 3.46 (m, 2H), 3.20 (d, $J = 13.3$ Hz, 1H), 2.81 (s, 3H), 2.72 (d, $J = 12.5$ Hz, 1H), 2.52 (m, 1H), 1.04 (m, 21H); ^{13}C NMR (100 MHz, CDCl_3) : δ 166.5, 166.3, 155.4, 138.6, 138.3, 129.3, 128.6, 128.3, 127.3, 127.2, 127.0, 98.5, 64.7, 63.0, 57.6, 57.0, 55.4, 53.9, 38.1, 18.1, 11.9.



1j

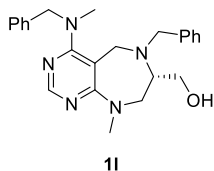
(1j) Prepared according to Scheme S4; 61% overall yield, 1.6 g, pale yellow oil; ^1H NMR (400 MHz, CDCl_3): δ 8.14 (s, 1H), 7.36–7.23 (m, 5H), 5.35 (br s, 1H), 4.68, 4.50 (ABq, $J_{\text{AB}} = 15.7$ Hz, 2H), 3.96 (d, $J = 15.3$ Hz, 1H), 3.80 (m, 1H), 3.67 (m, 2H), 3.60 (d, $J = 15.3$ Hz, 1H), 3.06 (d, $J = 12.1$ Hz, 1H), 2.90 (s, 3H), 2.86 (m, 1H), 2.17 (br s, 1H), 1.08 (m, 21H); ^{13}C NMR (100 MHz, CDCl_3) : δ 166.2, 165.8, 155.0, 138.3, 128.6, 127.5, 127.2, 100.7, 63.8, 57.6, 56.9, 51.9, 47.0, 38.9, 18.1, 11.9. ,



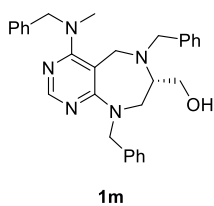
1k

(1k) Prepared according to Scheme S4; 75% overall yield, 171.3 mg; pale yellow oil; ^1H NMR (400 MHz, CDCl_3): δ 8.14 (s, 1H), 7.36–7.27 (m, 5H), 5.41 (s, 1H), 3.68 (m, 4H), 3.60 (m, 2H), 3.50 (m, 4H), 3.27 (m, 4H), 3.20 (d, $J = 13.3$ Hz, 1H), 2.84 (m,

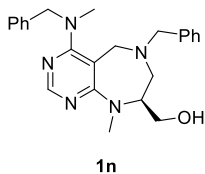
1H), 2.75 (m, 1H), 1.07 (m, 21H); ¹³C NMR (100 MHz, CDCl₃) : δ 166.2, 165.9, 155.8, 138.2, 129.4, 128.5, 127.7, 100.2, 66.8, 64.8, 63.5, 58.6, 54.6, 53.3, 49.8, 18.1, 11.9.



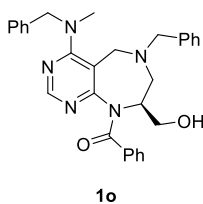
(1l) Prepared according to Scheme S3; 71% overall yield from **1c**, 524.3 mg, colorless oil; ¹H NMR (400 MHz, CDCl₃): δ 8.30 (s, 1H), 7.30 (m, 3H), 7.21 (m, 3H), 7.01 (m, 2H), 6.89 (m, 2H), 4.52 (d, *J* = 15.3 Hz, 1H), 4.14 (d, *J* = 15.3 Hz, 1H), 3.89 (m, 2H), 3.78 (dd, *J* = 12.5, 4.7 Hz, 2H), 3.45 (m, 1H), 3.42–3.32 (m, 3H), 3.29 (s, 3H), 3.28–3.20 (m, 1H), 2.89 (br s, 1H), 2.63 (s, 3H); ¹³C NMR (100 MHz, CDCl₃) : δ 167.6, 164.3, 154.9, 138.6, 138.1, 129.2, 128.6, 128.5, 127.6, 127.5, 127.0, 95.3, 62.7, 61.5, 59.9, 56.9, 53.3, 44.2, 38.9, 38.0.



(1m) Prepared according to Scheme S3; 77% overall yield from **1c**, 675.8 mg; colorless oil; ¹H NMR (400 MHz, CDCl₃): δ 8.32 (s, 1H), 7.36–7.27 (m, 8H), 7.23–7.19 (m, 3H), 7.00 (m, 2H), 6.90 (m, 2H), 5.20, 4.79 (ABq, *J*_{AB} = 15.3 Hz, 2H), 4.55, 4.17 (ABq, *J*_{AB} = 15.3 Hz, 2H), 3.91, 3.41 (ABq, *J*_{AB} = 16.4 Hz, 2H), 3.80, 3.72 (ABq, *J*_{AB} = 12.5 Hz, 2H), 3.71 (m, 1H), 3.33 (m, 1H), 3.20 (m, 3H), 2.86 (m, 1H), 2.65 (s, 3H); ¹³C NMR (100 MHz, CDCl₃) : δ 168.0, 164.2, 155.0, 138.6, 138.5, 138.0, 129.2, 128.7, 128.6, 128.5, 128.0, 127.6, 127.5, 127.4, 127.0, 94.8, 62.9, 61.5, 59.9, 56.9, 52.4, 50.0, 44.0, 39.0.

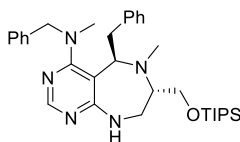


(1n) Prepared according to Scheme S3; 81% overall yield from **1i**, 598.1 mg; colorless oil; ¹H NMR (400 MHz, CDCl₃): δ 8.28 (s, 1H), 7.33–7.23 (m, 8H), 7.17 (m, 2H), 4.70, 4.58 (ABq, *J*_{AB} = 16.0 Hz, 2H), 3.85 (dd, *J* = 13.3, 1.6 Hz, 1H), 3.71 (dd, *J* = 11.2, 7.2 Hz, 1H), 3.56 (m, 1H), 3.45 (m, 1H), 3.41, 3.29 (ABq, *J*_{AB} = 12.9 Hz, 2H), 3.19 (s, 3H), 2.97 (m, 1H), 2.91 (d, *J* = 13.3 Hz, 1H), 2.86 (s, 3H), 2.34 (dd, *J* = 12.3, 2.2 Hz, 1H), 2.20 (br s, 1H); ¹³C NMR (100 MHz, CDCl₃) : δ 166.2, 165.6, 154.9, 138.5, 138.4, 129.0, 128.7, 128.5, 127.4, 127.2, 127.1, 100.8, 64.1, 63.3, 61.6, 57.2, 56.5, 56.4, 40.6, 38.2.



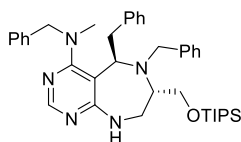
1o

(1o) Prepared according to Scheme S5; 86% overall yield from **1i**, 424.5 mg, colorless oil.; ^1H NMR (400 MHz, CDCl_3): δ 8.13 (s, 1H), 7.95 (d, $J = 8.2$ Hz, 2H), 7.54 (m, 1H), 7.40 (m, 2H), 7.30 (m, 2H), 7.24–7.17 (m, 8H), 5.37 (br s, 1H), 4.69, 4.58 (ABq, $J_{\text{AB}} = 16.0$ Hz, 2H), 4.34 (m, 1H), 4.25 (m, 1H), 3.84 (m, 1H), 3.47 (m, 4H), 2.85 (s, 3H), 2.81 (m, 1H), 2.75 (m, 1H); ^{13}C NMR (100 MHz, CDCl_3): δ 166.4, 166.3, 165.5, 155.2, 138.3, 138.2, 133.3, 129.8, 129.6, 129.1, 128.7, 128.5, 128.4, 127.4, 127.1, 98.7, 65.3, 63.0, 57.3, 57.0, 54.2, 53.1, 38.2.



1p

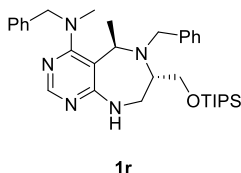
(1p) Prepared according to Scheme S6; 71% overall yield, 397.5 mg, colorless oil; ^1H NMR (500 MHz, CDCl_3 , major isomer): δ 8.11 (s, 1H), 7.31–7.20 (m, 3H), 7.19–7.09 (m, 3H), 6.93 (d, $J = 7.0$ Hz, 2H), 6.69 (d, $J = 6.7$ Hz, 2H), 5.18 (d, $J = 6.7$ Hz, 1H), 4.32 (ABq, $J = 16.0$ Hz, 2H), 3.96 (dd, $J = 10.2, 3.1$ Hz, 1H), 3.87 (dd, $J = 9.6, 2.9$ Hz, 1H), 3.73 (m, 1H), 3.46 (m, 1H), 3.12 (m, 1H), 3.02 (m, 2H), 2.88 (dd, $J = 12.5, 2.7$ Hz, 1H), 2.59 (s, 3H), 2.30 (s, 3H), 1.06 (m, 21H); ^{13}C NMR (100 MHz, CDCl_3): δ 168.0, 166.5, 154.6, 140.0, 138.3, 129.1, 128.5, 127.9, 127.3, 126.9, 125.9, 103.0, 66.5, 64.5, 60.3, 57.9, 47.9, 40.9, 38.1, 33.6, 18.1, 12.0.



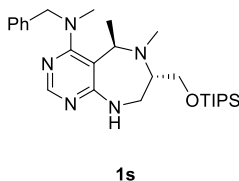
1q

(1q) Prepared according to Scheme S6; 54% overall yield, 343.4 mg; yellow oil; ^1H NMR (400 MHz, CDCl_3 , diastereomeric mixture, 3.6:1): δ 8.11 (s, 1H, minor), 8.09 (s, 1H, major), 7.37 (m, 3H, minor), 7.24–7.09 (m, 13H, major/minor), 6.80 (m, 4H, major), 6.74 (m, 2H, minor), 6.63 (m, 2H, minor), 5.33 (br s, 1H, major), 5.02 (m, 1H, minor), 4.71 (s, 1H, minor), 4.39, 4.11 (Abq, $J = 15.3$ Hz, 2H, major), 4.15 (m, 1H, minor), 4.04 (m, 3H, minor), 3.85 (m, 3H, major/minor), 3.71 (d, $J = 14.1$ Hz, 1H, major), 3.64 (m, 2H, minor), 3.44 (m, 1H, major), 3.35 (d, $J = 7.4$ Hz, 2H, major), 3.16 (m, 3H, major/minor), 2.97 (m, 1H, minor), 2.90 (m, 1H, minor), 2.73 (m, 1H, minor), 2.64 (m, 1H, minor), 2.49 (s, 3H, major), 2.26 (s, 3H, minor), 1.05 (m, 21H, minor),

0.90 (m, 21H, major); ^{13}C NMR (100 MHz, CDCl_3) : δ 167.4, 164.6, 154.9, 154.3, 139.7, 139.6, 139.3, 139.2, 138.0, 137.8, 129.0, 128.9, 128.7, 128.5, 128.3, 128.2, 128.2, 128.1, 127.9, 127.8, 127.4, 127.0, 126.9, 126.7, 125.9, 101.0, 64.3, 63.6, 60.8, 58.4, 57.2, 43.8, 38.3, 36.6, 18.0, 17.8, 11.9, 11.7.

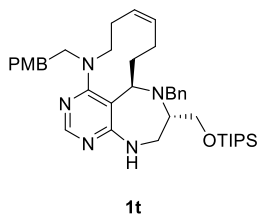


(1r) Prepared according to Scheme S6; 68% overall yield, 380.7 mg; pale yellow oil; ^1H NMR (500 MHz, CDCl_3 , diastereomeric mixture, 2.7:1): δ 8.18 (s, 1H, minor), 8.10 (s, 1H, major), 7.30–7.12 (m, 12H, major/minor), 7.08 (m, 2H, major/minor), 7.01 (m, 1H, major/minor), 5.40 (m, 1H, minor), 5.33 (m, 1H, major), 4.52 (d, $J = 15.3$ Hz, 1H, major), 4.31 (m, 1H, major/minor), 4.22 (m, 1H, major/minor), 3.88–3.63 (m, 3H, major/minor), 3.42 (m, 3H, major/minor), 3.05 (m, 1H, major/minor), 2.65 (s, 3H, major), 2.54 (s, 3H, minor), 1.39 (d, $J = 6.7$ Hz, 3H, major), 1.36 (d, $J = 7.4$ Hz, 1H, minor), 1.01 (m, 21H, minor), 0.90 (m, 21H, major); ^{13}C NMR (100 MHz, CDCl_3) : δ 166.9, 165.9, 164.6, 155.2, 155.0, 140.2, 140.1, 138.4, 138.3, 128.6, 128.5, 128.5, 128.4, 128.3, 128.3, 127.8, 127.5, 127.1, 127.0, 127.0, 126.9, 104.7, 64.7, 64.5, 63.2, 60.9, 59.7, 58.8, 58.1, 57.5, 54.3, 53.3, 46.1, 43.2, 39.6, 38.9, 18.1, 18.0, 17.2, 12.0, 11.9.

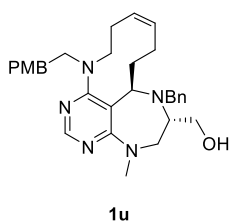


(1s) Prepared according to Scheme S6; 76% overall yield, 367.6 mg; pale yellow oil; ^1H NMR (400 MHz, CDCl_3 , diastereomeric mixture, 3.6:1): δ 8.15 (s, 1H, minor), 8.13 (s, 1H, major), 7.35–7.21 (m, 5H, major/minor), 5.22 (m, 1H, minor), 5.14 (m, 1H, major), 4.49 (ABq, $J_{\text{AB}} = 15.7$ Hz, 2H, major), 4.39 (ABq, $J_{\text{AB}} = 15.3$ Hz, 2H, minor), 4.22 (q, $J = 6.7$ Hz, 1H, major), 4.11 (q, $J = 7.0$ Hz, 1H, minor), 3.90 (m, 1H, minor), 3.81 (dd, $J = 9.8, 3.9$ Hz, 1H, major), 3.70 (m, 1H, major/minor), 3.58 (m, 1H, major), 3.49 (t, $J = 9.2$ Hz, 1H, major), 3.33 (m, 1H, minor), 3.10 (m, 1H, major/minor), 2.99 (m, 1H, major/minor), 2.84 (s, 3H, major), 2.79 (s, 3H, minor), 2.37 (s, 3H, minor), 2.23 (s, 3H, major), 1.27 (d, $J = 7.0$ Hz, 3H, minor), 1.23 (d, $J = 6.7$ Hz, 3H, major), 1.03 (m, 21H, major/minor); ^{13}C NMR (100 MHz, CDCl_3) : δ 167.8, 167.4, 165.9, 165.6, 157.3, 155.2, 154.9, 138.7, 138.6, 128.7, 128.6, 127.6, 127.4, 127.2, 127.1, 107.1, 106.5, 66.1, 64.5, 62.4, 59.5, 58.8, 58.5, 58.0, 55.9, 45.7, 45.6, 43.6, 39.9, 39.4,

18.1, 14.4, 12.0.



(**1t**) Prepared according to Scheme S7; 50% overall yield, 607.3 mg; colorless oil; ^1H NMR (400 MHz, CDCl_3) δ 8.15 (s, 1H), 7.15–7.05 (m, 5H), 6.99 (d, $J = 8.6$ Hz, 2H), 6.80 (d, $J = 8.2$ Hz, 2H), 5.47 (m, 1H), 5.37 (m, 2H), 4.30 (dd, $J = 11.9, 2.2$ Hz, 1H), 4.13 (m, 1H), 3.80 (s, 3H), 3.75 (m, 2H), 3.72 (m, 1H), 3.39 (m, 4H), 3.11 (m, 1H), 2.80 (m, 1H), 2.59 (m, 3H), 2.33 (m, 1H), 2.01 (m, 1H), 1.88 (m, 1H), 1.77 (m, 2H), 1.50 (m, 1H), 0.92 (m, 21H); ^{13}C NMR (100 MHz, CDCl_3) δ 167.4, 165.0, 158.0, 155.4, 140.2, 132.1, 131.6, 129.8, 128.8, 128.3, 128.2, 126.8, 113.9, 106.1, 64.5, 60.9, 59.2, 59.1, 57.6, 55.3, 46.9, 43.8, 34.7, 29.2, 26.3, 23.8, 18.0, 11.9. The stereochemistry of this product was previously reported².



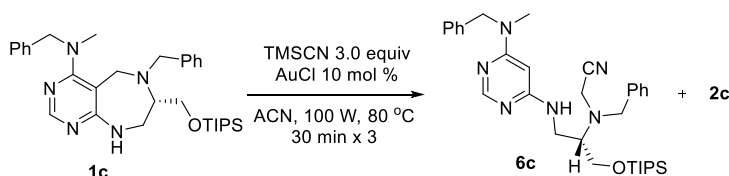
(**1u**) Prepared according to Scheme S7; 60% yield from **1t**, 140.9 mg; pale yellow oil; ^1H NMR (400 MHz, CDCl_3): δ 8.27 (s, 1H), 7.17 (m, 2H), 7.07 (m, 3H), 7.00 (d, $J = 8.2$ Hz, 2H), 6.81 (d, $J = 8.2$ Hz, 2H), 5.40 (td, $J = 10.8, 5.1$ Hz, 1H), 5.29 (m, 1H), 4.38 (d, $J = 10.2$ Hz, 1H), 4.12 (m, 1H), 3.79 (s, 3H), 3.75 (d, $J = 8.2$ Hz, 1H), 3.68 (d, $J = 15.7$ Hz, 1H), 3.43 (m, 3H), 3.30 (dd, $J = 14.5, 7.4$ Hz, 1H), 3.18 (s, 3H), 3.14 (m, 1H), 2.75 (m, 1H), 2.67–2.51 (m, 3H), 2.32 (m, 1H), 1.93 (br s, 1H), 1.79 (m, 4H), 1.31 (m, 2H); ^{13}C NMR (100 MHz, CDCl_3): δ 166.9, 164.9, 158.0, 155.1, 139.7, 131.9, 131.6, 129.9, 129.1, 128.8, 128.3, 127.2, 113.9, 107.4, 63.6, 60.5, 59.8, 59.7, 57.3, 55.5, 55.4, 47.3, 39.6, 34.8, 27.4, 26.1, 23.8.

3.5.3. Synthesis and Characterization of Products

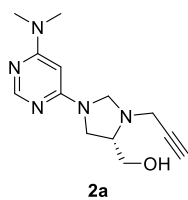
Representative Procedure for the conversion of 1c into 2c:

To a stirred solution of **1c** (27.3 mg, 0.050 mmol) in Acetonitrile (0.5 mL) was added AuCl (1.2 mg, 0.005 mmol). The resulting mixture was heated under microwave irradiation (100 watt) at 80 °C for 30 min. The solvent was removed *in vacuo* and the residual oil was purified by flash chromatography to give **2c** (24.6 mg, 90% yield) of pale yellow oil.

Intermediate trap; Procedure for the conversion of 1c into 6c:

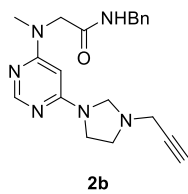


To a stirred solution of **1c** (27.3 mg, 0.050 mmol) in Acetonitrile (0.5 mL) were sequentially added TMSCN (18.8 μ L, 0.15 mmol), AuCl (1.2 mg, 0.005 mmol). The resulting mixture was heated under microwave irradiation (100 watt) at 80 °C for 30 min, 3 times. The solvent was removed *in vacuo* and the residual oil was purified by flash chromatography to give **6c** (11.5 mg, 40% yield) of clear oil with **2c** (9.2 mg, 34% yield).



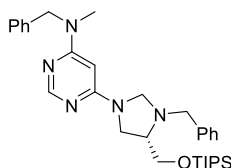
2a

(2a) 65% yield from **1a**, 16.3 mg; as a white solid; ^1H NMR (400 MHz, CDCl_3): δ 8.21 (s, 1H), 5.17 (s, 1H), 4.66 (d, $J = 5.9$ Hz, 1H), 4.29 (d, $J = 6.3$ Hz, 1H), 3.75 (m, 1H), 3.66–3.55 (m, 4H), 3.46–3.36 (m, 2H), 3.06 (s, 6H), 2.83 (br s, 1H), 2.27 (t, $J = 2.2$ Hz, 1H); ^{13}C NMR (100 MHz, CDCl_3) : δ 162.5, 159.6, 157.2, 80.3, 78.0, 73.9, 67.3, 61.3, 59.9, 46.7, 39.8, 37.4; HRMS(ESI $^+$): Calcd for $\text{C}_{13}\text{H}_{20}\text{N}_5\text{O}^+$ $[\text{M}+\text{H}]^+$ 262.1662, found 262.1662.



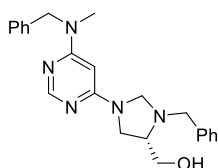
2b

(2b) 67% yield from **1b**, 12.2 mg; as a white solid; ^1H NMR (400 MHz, CDCl_3): δ 8.13 (s, 1H), 7.28–7.16 (m, 5H), 6.79 (m, 1H), 5.17 (s, 1H), 4.40 (d, $J = 5.9$ Hz, 2H), 4.23 (m, 2H), 4.18 (s, 2H), 3.48 (d, $J = 2.0$ Hz, 4H), 3.06 (m, 2H), 3.03 (s, 3H), 2.25 (t, $J = 2.3$ Hz, 1H); ^{13}C NMR (100 MHz, CDCl_3) : δ 170.0, 162.1, 159.9, 157.3, 138.2, 128.7, 127.5, 127.4, 80.8, 78.2, 73.6, 67.1, 54.3, 50.9, 44.7, 43.2, 41.4, 37.0; HRMS(ESI $^+$): Calcd for $\text{C}_{20}\text{H}_{25}\text{N}_6\text{O}^+$ $[\text{M}+\text{H}]^+$ 365.2084, found 365.2082. The exact structure of **2b** was confirmed by X-ray crystallography.



2c

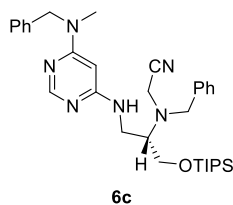
(2c) 90% yield from **1c**, 24.5 mg; as a pale yellow oil; ^1H NMR (400 MHz, CDCl_3): δ 8.21 (s, 1H), 7.38–7.17 (m, 10H), 5.16 (s, 1H), 4.78 (m, 2H), 4.48 (br s, 1H), 4.13 (d, $J = 13.3$ Hz, 1H), 3.96 (m, 1H), 3.90 (dd, $J = 10.0, 5.3$ Hz, 1H), 3.71 (dd, $J = 10.0, 6.8$ Hz, 1H), 3.65 (m, 1H), 3.59 (d, $J = 13.3$ Hz, 1H), 3.34 (m, 1H), 3.22 (m, 1H), 2.97 (s, 3H), 1.05 (m, 21H); ^{13}C NMR (100 MHz, CDCl_3) : δ 162.4, 159.9, 157.5, 138.6, 138.2, 128.6, 128.5, 127.3, 127.2, 127.1, 80.3, 69.4, 65.4, 64.4, 58.3, 52.5, 48.0, 35.6, 18.1, 12.0; HRMS(ESI $^+$): Calcd for $\text{C}_{32}\text{H}_{48}\text{N}_5\text{OSi}^+$ $[\text{M}+\text{H}]^+$ 546.3623, found 546.3621.



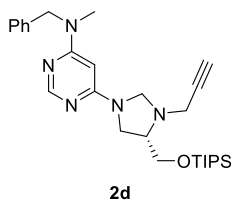
2c'

(2c') 95% yield from **1c'**, 18.5 mg; as a white solid; ^1H NMR (400 MHz, CDCl_3): δ 8.20 (s, 1H), 7.39–7.12 (m, 10H), 5.18 (s, 1H), 4.78 (s, 2H), 4.55 (m, 1H), 4.05 (d, $J = 6.7$ Hz, 1H), 4.00 (d, $J = 12.9$ Hz, 1H), 3.73 (dd, $J = 11.3, 3.9$ Hz, 1H), 3.62–3.54 (m, 3H), 3.41 (m, 1H), 3.28 (m, 1H), 2.97 (s, 3H); ^{13}C

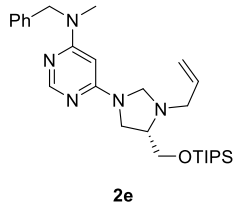
NMR (100 MHz, CDCl₃) : δ 162.4, 159.8, 157.4, 138.0, 137.8, 128.7, 128.6, 127.6, 127.2, 127.1, 80.3, 68.4, 63.7, 60.1, 57.4, 52.4, 46.5, 35.5; HRMS(ESI⁺): Calcd for C₂₃H₂₈N₅O⁺ [M+H]⁺ 390.2288, found 390.2288.



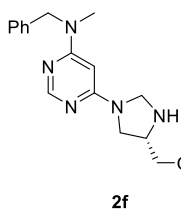
(6c) 40% yield from **1c**, 11.5 mg; as a clear oil; ¹H NMR (400 MHz, CDCl₃): δ 8.20 (s, 1H), 7.34–7.17 (m, 10H), 5.34 (s, 1H), 5.07 (m, 1H), 4.79 (s, 1H), 4.06 (m, 1H), 3.99 (m, 2H), 3.83 (d, *J* = 13.7 Hz, 1H), 3.63–3.51 (m, 3H), 3.39 (m, 1H), 3.15 (m, 1H), 3.00 (s, 3H), 1.08 (m, 21H); ¹³C NMR (100 MHz, CDCl₃) : δ 162.9, 162.8, 157.8, 138.0, 137.2, 129.0, 128.9, 128.7, 128.0, 127.2, 127.1, 117.1, 80.3, 62.4, 54.8, 52.5, 40.4, 39.0, 35.5, 18.1, 11.9; HRMS(ESI⁺): Calcd for C₃₃H₄₉N₆OSi⁺ [M+H]⁺ 573.3732, found 573.3730.



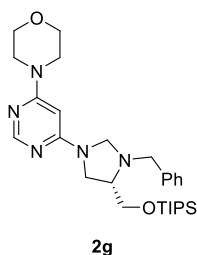
(2d) 80% yield from **1d**, 19.7 mg; as a pale yellow oil; ¹H NMR (400 MHz, CDCl₃): δ 8.20 (s, 1H), 7.32–7.22 (m, 3H), 7.18 (m, 2H), 5.30 (br s, 1H), 4.78 (m, 2H), 4.32 (m, 1H), 4.11 (m, 1H), 4.02 (m, 1H), 3.92 (d, *J* = 8.6 Hz, 1H), 3.69 (t, *J* = 9.0 Hz, 1H), 3.49 (s, 2H), 3.21 (d, *J* = 9.0 Hz, 1H), 2.95 (s, 3H), 2.94 (m, 1H), 2.22 (m, 1H), 1.03 (m, 21H); ¹³C NMR (100 MHz, CDCl₃) : δ 162.4, 160.6, 160.3, 157.4, 138.0, 128.5, 127.0, 80.2, 78.2, 73.3, 67.7, 62.3, 58.2, 53.2, 52.3, 40.9, 35.2, 17.9, 11.9; HRMS(ESI⁺): Calcd for C₂₈H₄₄N₅OSi⁺ [M+H]⁺ 494.3310, found 494.3309.



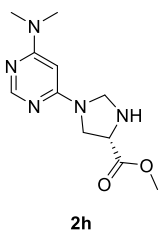
(2e) 74% yield from **1e**, 18.3 mg; as a pale yellow oil; ¹H NMR (400 MHz, CDCl₃): δ 8.24 (s, 1H), 7.33–7.17 (m, 5H), 5.90 (m, 1H), 5.26–5.13 (m, 3H), 4.79 (s, 2H), 4.58 (m, 1H), 3.99 (d, *J* = 5.9 Hz, 1H), 3.90 (dd, *J* = 10.0, 5.3 Hz, 1H), 3.67 (dd, *J* = 9.8, 7.0 Hz, 1H), 3.62–3.52 (m, 2H), 3.31 (m, 1H), 3.16 (m, 1H), 3.09 (dd, *J* = 13.7, 7.0 Hz, 1H), 3.00 (s, 3H), 1.06 (m, 21H); ¹³C NMR (100 MHz, CDCl₃) : δ 162.4, 159.9, 157.5, 138.2, 135.1, 128.6, 127.2, 127.1, 117.9, 80.3, 69.1, 65.2, 64.2, 57.1, 52.5, 47.8, 35.5, 18.1, 12.0; HRMS(ESI⁺): Calcd for C₂₈H₄₆N₅OSi⁺ [M+H]⁺ 496.3466, found 496.3467.



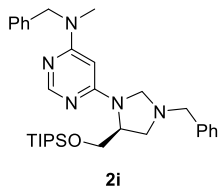
(2f) 84% yield from **1f**, 19.1 mg; as a pale clear oil; ^1H NMR (400 MHz, CDCl_3): δ 8.23 (s, 1H), 7.32–7.16 (m, 5H), 5.18 (s, 1H), 4.78 (s, 2H), 4.62 (d, $J = 7.0$ Hz, 1H), 4.30 (d, $J = 8.2$ Hz, 1H), 3.90 (m, 2H), 3.49–3.36 (m, 2H), 3.28 (t, $J = 8.2$ Hz, 1H), 2.98 (s, 3H), 1.04 (m, 21H); ^{13}C NMR (100 MHz, CDCl_3): δ 162.5, 159.8, 157.6, 138.2, 128.7, 127.2, 127.1, 80.5, 63.8, 61.9, 59.9, 52.5, 46.7, 35.5, 18.1, 12.0; HRMS(ESI $^+$): Calcd for $\text{C}_{25}\text{H}_{42}\text{N}_5\text{OSi}^+$ $[\text{M}+\text{H}]^+$ 456.3153, found 456.3154.



(2g) 84% yield from **1g**, 21.5 mg; as a yellow oil; ^1H NMR (400 MHz, CDCl_3): δ 8.19 (s, 1H), 7.39–7.25 (m, 5H), 5.22 (s, 1H), 4.47 (m, 1H), 4.15 (d, $J = 13.3$ Hz, 1H), 3.96 (m, 1H), 3.91 (dd, $J = 10.2, 5.1$ Hz, 1H), 3.79–3.65 (m, 6H), 3.59 (d, $J = 13.3$ Hz, 1H), 3.51 (t, $J = 4.7$ Hz, 4H), 3.37 (m, 1H), 3.23 (m, 1H), 1.05 (m, 21H); ^{13}C NMR (100 MHz, CDCl_3): δ 162.9, 160.1, 157.5, 138.6, 128.6, 128.5, 127.4, 81.2, 69.4, 66.7, 65.4, 64.4, 58.3, 48.1, 44.6, 18.1, 12.0; HRMS(ESI $^+$): Calcd for $\text{C}_{28}\text{H}_{46}\text{N}_5\text{O}_2\text{Si}^+$ $[\text{M}+\text{H}]^+$ 512.3415, found 512.3417.

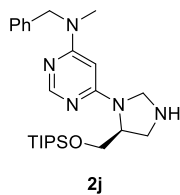


(2h) 84% yield from **1h**, 21.0 mg; as a pale yellow solid; ^1H NMR (400 MHz, CDCl_3): δ 8.21 (s, 1H), 5.16 (s, 1H), 4.66 (d, $J = 7.8$ Hz, 1H), 4.40 (d, $J = 7.8$ Hz, 1H), 4.15 (t, $J = 7.0$ Hz, 1H), 3.80 (s, 3H), 3.75 (m, 1H), 3.49 (dd, $J = 9.6, 6.8$ Hz, 1H), 3.06 (s, 6H); ^{13}C NMR (100 MHz, CDCl_3): δ 172.2, 162.6, 159.5, 157.4, 80.8, 63.2, 59.5, 52.7, 48.4, 37.4; HRMS(ESI $^+$): Calcd for $\text{C}_{11}\text{H}_{18}\text{N}_5\text{O}_2^+$ $[\text{M}+\text{H}]^+$ 252.1455, found 252.1454.

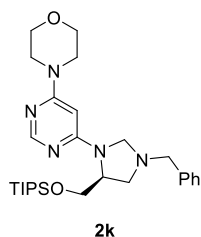


(2i) 85% yield from **1i**, 23.1 mg; as a pale yellow oil; ^1H NMR (400 MHz, CDCl_3): δ 8.21 (s, 1H), 7.38–7.15 (m, 10H), 5.28 (br s, 1H), 4.78 (q, $J = 15.7$ Hz, 2H), 4.32 (br s, 1H), 4.01 (br s, 1H), 3.92 (m, 2H), 3.77 (t, $J = 9.0$ Hz, 1H), 3.69 (m, 2H), 3.23 (d, $J = 8.2$ Hz, 1H), 2.95 (s, 3H), 2.75 (m, 1H), 1.02 (m, 21H); ^{13}C NMR (100 MHz, CDCl_3): δ 162.5, 160.4, 157.6, 138.3, 138.2, 128.7, 128.5,

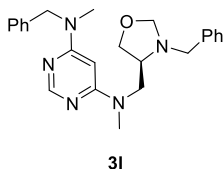
127.3, 127.2, 127.2, 80.3, 69.4, 62.5, 58.2, 58.0, 55.0, 52.4, 35.4, 18.1, 12.0;
HRMS(ESI⁺): Calcd for C₃₂H₄₈N₅OSi⁺ [M+H]⁺ 546.3623, found 546.3625.



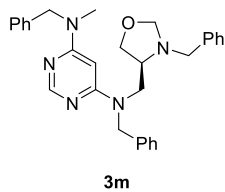
(2j) 57% yield from **1j**, 13.0 mg; as a pale yellow oil; ¹H NMR (400 MHz, CDCl₃): δ 8.21 (s, 1H), 7.30–7.16 (m, 5H), 5.21 (s, 1H), 4.76 (s, 2H), 4.42 (d, *J* = 8.2 Hz, 1H), 4.15 (d, *J* = 8.2 Hz, 1H), 3.92 (m, 2H), 3.81 (m, 1H), 3.39 (d, *J* = 12.1 Hz, 1H), 3.09 (dd, *J* = 11.9, 6.8 Hz, 1H), 2.98 (s, 3H), 1.00 (m, 21H); ¹³C NMR (100 MHz, CDCl₃) : δ 162.5, 159.9, 157.6, 138.1, 128.7, 127.2, 127.1, 80.8, 64.9, 64.0, 57.5, 52.6, 50.6, 35.6, 18.0, 11.9; HRMS(ESI⁺): Calcd for C₂₅H₄₂N₅OSi⁺ [M+H]⁺ 456.3153, found 456.3153.



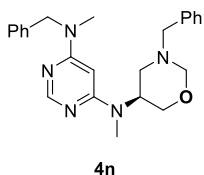
(2k) 58% yield from **1k**, 14.8 mg; as a yellow oil; ¹H NMR (400 MHz, CDCl₃): δ 8.17 (s, 1H), 7.36–7.23 (m, 5H), 5.33 (s, 1H), 4.30 (m, 1H), 4.02 (m, 1H), 3.91 (m, 2H), 3.80–3.65 (m, 7H), 3.48 (m, 4H), 3.21 (m, 1H), 2.75 (dd, *J* = 9.0, 6.7 Hz, 1H), 1.03 (m, 21H); ¹³C NMR (100 MHz, CDCl₃) : δ 163.0, 160.6, 157.6, 138.2, 128.6, 128.5, 127.4, 81.5, 69.3, 66.6, 62.7, 58.3, 58.0, 55.1, 44.6, 18.1, 12.0; HRMS(ESI⁺): Calcd for C₂₈H₄₆N₅O₂Si⁺ [M+H]⁺ 512.3415, found 512.3416.



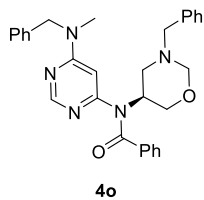
(3l) 61% yield from **1l**, 12.3 mg; as a yellow oil; ¹H NMR (400 MHz, CDCl₃): δ 8.19 (s, 1H), 7.33–7.17 (m, 10H), 5.26 (s, 1H), 4.79 (s, 2H), 4.37 (m, 2H), 4.01 (t, *J* = 7.2 Hz, 1H), 3.71 (m, 2H), 3.61 (m, 1H), 3.51–3.35 (m, 3H), 2.99 (s, 3H), 2.93 (s, 3H); ¹³C NMR (100 MHz, CDCl₃) : δ 162.7, 162.4, 157.0, 139.1, 138.3, 128.9, 128.7, 128.3, 127.3, 127.2, 86.0, 79.8, 67.0, 62.3, 59.7, 52.6, 52.0, 37.5, 35.6; HRMS(ESI⁺): Calcd for C₂₄H₃₀N₅O⁺ [M+H]⁺ 404.2445, found 404.2444.



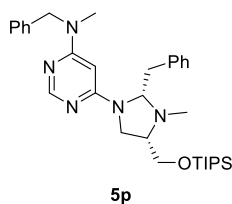
(3m) 25% yield from **1m**, 7.5 mg, (47 % brsm); as a yellow oil; ^1H NMR (400 MHz, CDCl_3): δ 8.19 (s, 1H), 7.31–7.08 (m, 15H), 5.25 (s, 1H), 4.76–4.59 (m, 4H), 4.33 (ABq, $J_{\text{AB}} = 5.8$ Hz, 2H), 3.97 (t, $J = 7.4$ Hz, 1H), 3.69 (ABq, $J_{\text{AB}} = 12.9$ Hz, 2H), 3.56 (m, 2H), 3.36 (dd, $J = 8.4, 4.1$ Hz, 1H), 3.30 (dd, $J = 13.7, 8.2$ Hz, 1H), 2.89 (s, 3H); ^{13}C NMR (100 MHz, CDCl_3): δ 162.7, 162.4, 157.3, 139.0, 138.2, 138.0, 128.9, 128.7, 128.6, 128.3, 127.3, 127.2, 127.1, 126.8, 85.9, 80.6, 67.1, 62.1, 59.8, 52.7, 52.6, 50.2, 35.6; HRMS(ESI $^{+}$): Calcd for $\text{C}_{30}\text{H}_{34}\text{N}_5\text{O}^{+}$ $[\text{M}+\text{H}]^{+}$ 480.2758, found 480.2759.



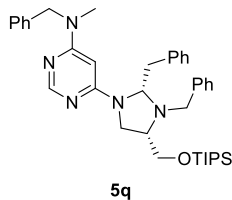
(4n) 67% yield from **1n**, 13.5 mg; as a pale yellow oil; ^1H NMR (400 MHz, CDCl_3): δ 8.25 (s, 1H), 7.35–7.16 (m, 10H), 5.36 (s, 1H), 5.08 (m, 1H), 4.78 (s, 2H), 4.31, 4.22 (ABq, $J_{\text{AB}} = 9.8$ Hz, 2H), 4.03 (dd, $J = 10.6, 4.3$ Hz, 1H), 3.92, 3.86 (ABq, $J_{\text{AB}} = 13.3$ Hz, 2H), 3.70 (t, $J = 10.2$ Hz, 1H), 3.02 (m, 1H), 2.98 (s, 3H), 2.93 (m, 1H), 2.88 (s, 3H); ^{13}C NMR (100 MHz, CDCl_3): δ 163.1, 163.0, 157.2, 138.3, 138.2, 129.0, 128.7, 128.5, 127.3, 127.2, 83.9, 80.1, 69.2, 56.4, 52.6, 52.0, 44.7, 35.6, 30.7; HRMS(ESI $^{+}$): Calcd for $\text{C}_{24}\text{H}_{30}\text{N}_5\text{O}^{+}$ $[\text{M}+\text{H}]^{+}$ 404.2445, found 404.2444.



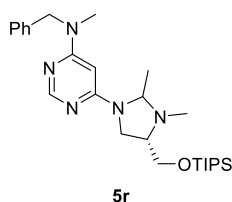
(4o) 94% yield from **1o**, 23.1 mg; as a clear oil; ^1H NMR (400 MHz, CDCl_3): δ 8.24 (s, 1H), 8.02 (m, 2H), 7.55 (m, 1H), 7.41 (m, 2H), 7.38–7.23 (m, 8H), 7.21 (m, 2H), 5.58 (br s, 1H), 4.81 (m, 2H), 4.70 (d, $J = 7.4$ Hz, 1H), 4.44 (d, $J = 4.7$ Hz, 1H), 4.34 (m, 2H), 3.87 (m, 1H), 3.77, 3.70 (ABq, $J_{\text{AB}} = 12.9$ Hz, 2H), 3.19 (d, $J = 9.0$ Hz, 1H), 3.00 (s, 3H), 2.80 (m, 1H); ^{13}C NMR (100 MHz, CDCl_3): δ 166.5, 162.6, 160.3, 157.6, 138.2, 137.9, 133.1, 130.1, 129.8, 128.6, 128.6, 128.5, 128.4, 127.4, 127.2, 127.1, 80.9, 69.2, 64.2, 57.9, 55.6, 55.3, 52.4, 35.6; HRMS(ESI $^{+}$): Calcd for $\text{C}_{30}\text{H}_{32}\text{N}_5\text{O}_2^{+}$ $[\text{M}+\text{H}]^{+}$ 494.2551, found 494.2549.



(5p) 72% yield from **1p**, 20.1 mg; as a clear oil; ^1H NMR (400 MHz, CDCl_3): δ 8.29 (s, 1H), 7.32–7.05 (m, 10H), 5.14 (s, 1H), 4.80, 4.74 (ABq, $J_{\text{AB}} = 16.0$ Hz, 2H), 4.55 (br s, 1H), 3.68 (dd, $J = 9.8, 5.1$ Hz, 1H), 3.64 (m, 1H), 3.37 (dd, $J = 9.8$ Hz, 7.0 Hz, 1H), 3.13 (m, 1H), 2.99 (s, 3H), 2.91 (m, 1H), 2.79 (m, 1H), 2.46 (t, $J = 9.6$ Hz, 1H), 2.40 (s, 3H), 1.02 (m, 21H); ^{13}C NMR (100 MHz, CDCl_3) : δ 162.5, 159.6, 157.5, 138.2, 137.6, 130.8, 128.7, 127.5, 127.2, 127.1, 126.1, 81.5, 81.1, 66.0, 65.2, 52.6, 49.4, 40.7, 38.3, 35.6, 18.1, 12.0; HRMS(ESI $^+$): Calcd for $\text{C}_{33}\text{H}_{50}\text{N}_5\text{OSi}^+$ $[\text{M}+\text{H}]^+$ 560.3779, found 560.3777. The stereochemistry of this product was confirmed by NOESY spectroscopy.

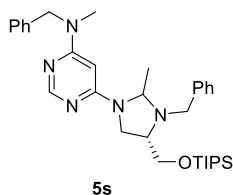


(5q) 81% yield from **1q**, 25.7 mg; as a pale yellow oil; ^1H NMR (400 MHz, CDCl_3): δ 8.30 (s, 1H), 7.35–7.04 (m, 15H), 5.14 (s, 1H), 4.95 (m, 1H), 4.77 (m, 2H), 3.82, 3.75 (ABq, $J_{\text{AB}} = 12.9$ Hz, 2H), 3.70 (m, 1H), 3.38 (m, 1H), 3.19 (m, 1H), 3.10 (m, 1H), 3.00 (s, 3H), 2.93 (m, 1H), 2.70 (m, 1H), 2.61 (m, 1H), 0.94 (m, 21H); ^{13}C NMR (100 MHz, CDCl_3) : δ 162.3, 159.3, 157.3, 139.0, 138.0, 137.7, 130.6, 129.3, 128.5, 128.2, 127.6, 127.2, 127.1, 127.0, 126.0, 81.0, 80.6, 66.7, 63.9, 60.7, 52.6, 48.7, 39.6, 35.5, 17.9, 11.7; HRMS(ESI $^+$): Calcd for $\text{C}_{39}\text{H}_{54}\text{N}_5\text{OSi}^+$ $[\text{M}+\text{H}]^+$ 636.4092, found 636.4092.

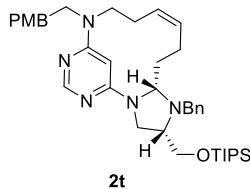


(5r) 70% yield from **1r**, 16.9 mg; as a yellow oil; ^1H NMR (400 MHz, CDCl_3 , diastereomeric mixture, 2:1): δ 8.24 (s, 1H, major), 8.20 (s, 1H, minor), 7.41–7.15 (m, 15H, major/minor), 5.23 (s, 1H, major), 5.16 (s, 1H, minor), 4.95 (m, 1H, minor), 4.84–4.71 (m, 3H, major/minor), 4.65 (m, 1H, major), 4.09 (m, 1H, minor), 3.92–3.82 (m, 4H, major/minor), 3.68 (m, 2H, major/minor), 3.60 (m, 1H, minor), 3.53 (m, 1H, major), 3.46–3.34 (m, 2H, major/minor), 3.16 (m, 1H, major), 3.00 (s, 3H, major), 2.98 (s, 3H, minor), 1.25 (d, $J = 5.1$ Hz, 3H, major), 1.22 (d, $J = 5.9$ Hz, 3H, minor), 1.00 (m, 21H, major/minor); ^{13}C NMR (100 MHz, CDCl_3) : δ 162.4, 159.8, 159.5, 157.5, 157.4, 139.5, 139.0, 138.3, 138.3, 128.9, 128.7, 128.6, 128.5, 128.4, 128.3, 127.3, 127.2,

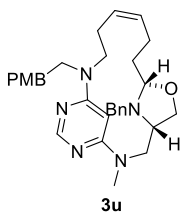
127.2, 127.1, 81.2, 80.3, 76.2, 71.9, 66.7, 65.6, 64.7, 60.3, 59.3, 52.7, 52.6, 51.9, 48.9, 48.7, 35.7, 35.6, 21.2, 18.1, 18.1, 13.8, 12.0, 11.9; HRMS(ESI⁺): Calcd for C₃₃H₅₀N₅OSi⁺ [M+H]⁺ 560.3779, found 560.3779.



(5s) 92% yield from **1s**, 25.7 mg; as a yellow oil; ¹H NMR (400 MHz, CDCl₃, diastereomeric mixture, 1.1:1): δ 8.25 (s, 1H, major), 8.24 (s, 1H, minor), 7.33–7.20 (m, 5H, major/minor), 5.24 (s, 1H, major), 5.19 (s, 1H, minor), 4.85–4.72 (m, 2H, major/minor), 4.26 (m, 1H, minor), 4.19 (q, *J* = 5.1 Hz, 1H, major), 3.92 (dd, *J* = 9.8, 4.7 Hz, 1H, major), 3.86 (m, 1H, minor), 3.81 (m, 1H, major), 3.74–3.64 (m, 1H, major/minor), 3.24 (m, 1H, major/minor), 3.01 (s, 3H, major), 3.00 (s, 3H, minor), 2.80 (m, 1H, major), 2.45 (s, 3H, major), 2.44 (s, 3H, minor), 1.40 (d, *J* = 5.1 Hz, 3H, major), 1.07 (m, 21H, major/minor); ¹³C NMR (100 MHz, CDCl₃): δ 162.5, 162.4, 160.2, 159.6, 157.4, 157.3, 138.3, 138.2, 128.7, 127.2, 127.1, 81.4, 80.3, 77.8, 74.4, 65.7, 65.5, 65.1, 61.7, 52.6, 50.2, 48.7, 39.4, 35.7, 35.6, 35.1, 19.8, 18.1, 13.8, 12.0; HRMS(ESI⁺): Calcd for C₂₇H₄₆N₅OSi⁺ [M+H]⁺ 484.3466, found 484.3465.



(2t) 64% yield from **1t**, 20.9 mg; as a pale yellow oil; ¹H NMR (400 MHz, CDCl₃): δ 8.25 (s, 1H), 7.36–7.23 (m, 5H), 7.12 (d, *J* = 8.2 Hz, 2H), 6.81 (d, *J* = 8.6 Hz, 2H), 5.34 (m, 1H), 5.01 (s, 1H), 4.96 (m, 1H), 4.63 (dd, *J* = 11.3, 7.0 Hz, 1H), 4.46 (d, *J* = 10.2 Hz, 1H), 3.95 (d, *J* = 12.9 Hz, 1H), 3.85–3.74 (m, 3H), 3.77 (s, 3H), 3.66 (dd, *J* = 9.6, 4.9 Hz, 1H), 3.56 (m, 1H), 3.34 (m, 1H), 3.23 (m, 1H), 3.03 (m, 1H), 2.86 (dd, *J* = 14.9, 6.7 Hz, 1H), 2.78 (m, 2H), 2.35 (m, 1H), 2.12 (m, 1H), 1.89 (m, 1H), 1.79 (m, 1H), 1.66 (m, 1H), 1.49 (m, 1H), 1.01 (m, 21H); ¹³C NMR (100 MHz, CDCl₃): δ 160.3, 160.1, 158.1, 157.9, 139.3, 131.8, 130.5, 130.0, 129.4, 128.6, 128.3, 127.4, 113.9, 84.2, 76.7, 66.7, 64.7, 60.4, 55.3, 51.5, 50.3, 47.8, 38.8, 34.6, 26.4, 23.4, 18.1, 11.9; HRMS(ESI⁺): Calcd for C₃₉H₅₈N₅O₂Si⁺ [M+H]⁺ 656.4354, found 656.4351. The stereochemistry of this product was confirmed by NOESY spectroscopy.



(3u) 97% yield from **1u**, 24.9 mg; ^1H NMR (400 MHz, CDCl_3): δ 8.24 (s, 1H), 7.14 (m, 7H), 6.82 (d, $J = 8.6$ Hz, 2H), 5.92 (s, 1H), 5.57 (m, 1H), 5.33 (m, 1H), 4.50 (dd, $J = 6.1, 2.9$ Hz, 1H), 4.05 (dt, $J = 13.8, 7.0$ Hz, 1H), 3.97 (dd, $J = 8.8, 7.2$ Hz, 1H), 3.78 (s, 3H), 3.72 (m, 2H), 3.66 (m, 1H), 3.51 (m, 2H), 3.39 (m, 1H), 3.09 (m, 1H), 2.96 (m, 2H), 2.87 (m, 2H), 2.73 (s, 3H), 2.43 (m, 1H), 2.19 (m, 1H), 2.08 (m, 2H), 1.56 (m, 2H); ^{13}C NMR (100 MHz, CDCl_3) : δ 163.5, 161.4, 158.1, 157.3, 138.6, 132.4, 132.1, 130.0, 129.5, 128.2, 127.5, 125.2, 113.9, 98.4, 80.7, 68.1, 61.2, 60.9, 56.2, 55.3, 50.2, 49.3, 36.4, 34.2, 34.1, 24.8, 22.1; HRMS(ESI $^+$): Calcd for $\text{C}_{31}\text{H}_{40}\text{N}_5\text{O}_2^+$ $[\text{M}+\text{H}]^+$ 514.3177, found 514.3175. The stereochemistry of this product was confirmed by NOESY spectroscopy.

3.5.4. Structural Determination of Products

The stereochemistry of these product were confirmed by NOESY spectroscopy. 2D-NOE spectra supported the geometry as shown.

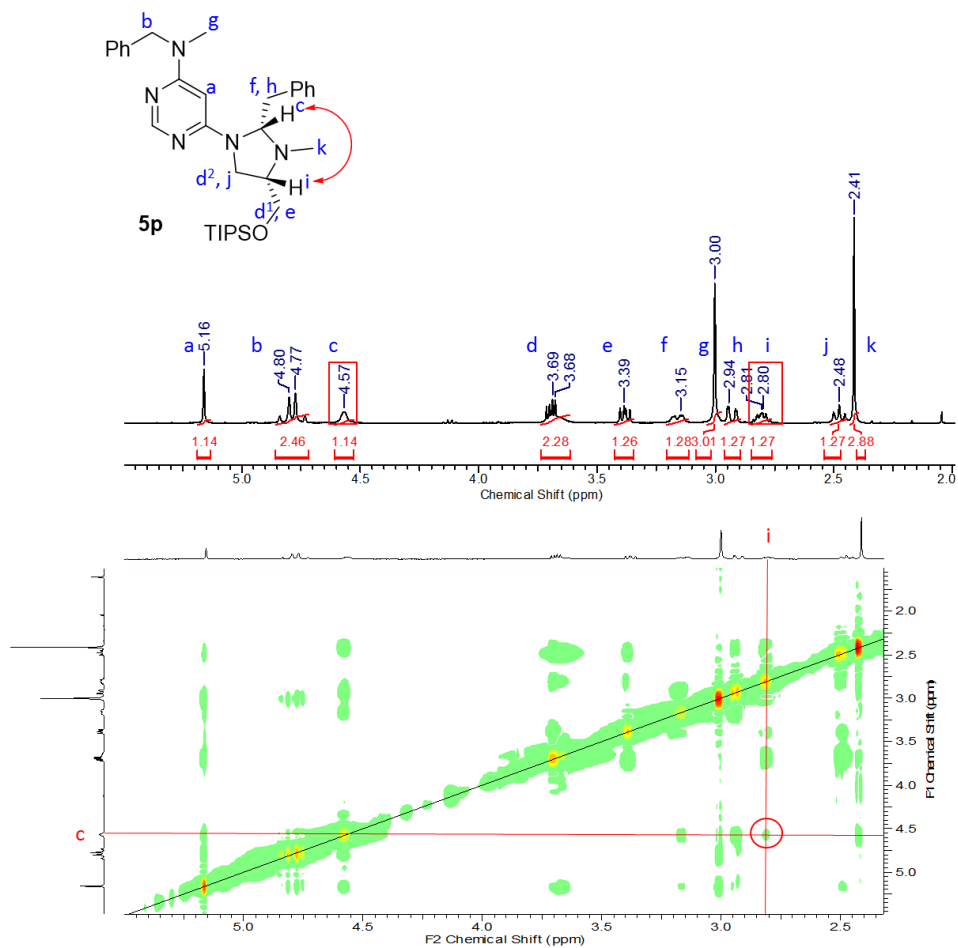


Figure S1. NOESY spectra of compound **5p**

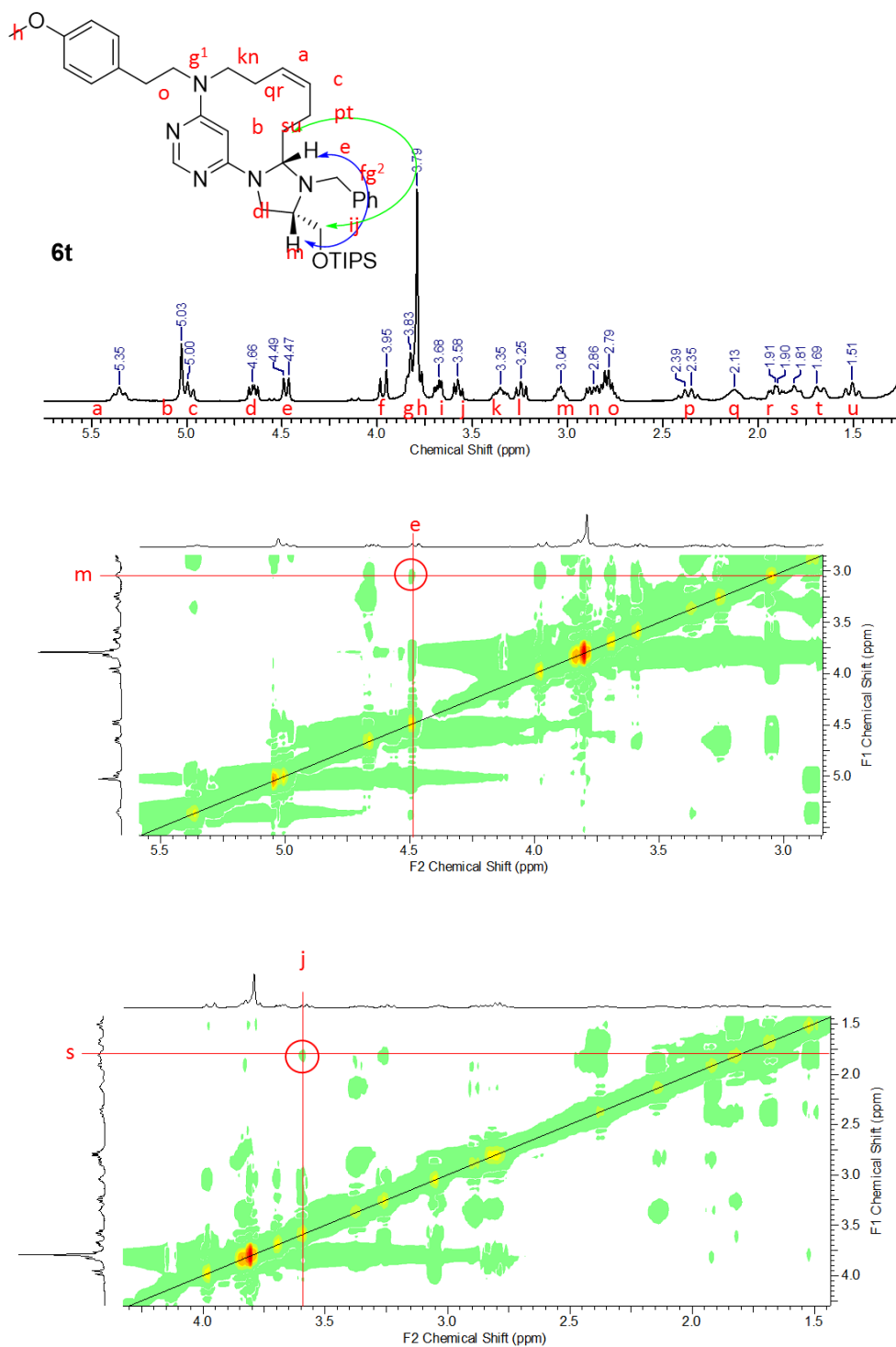


Figure S2. NOESY spectra of compound **6t**

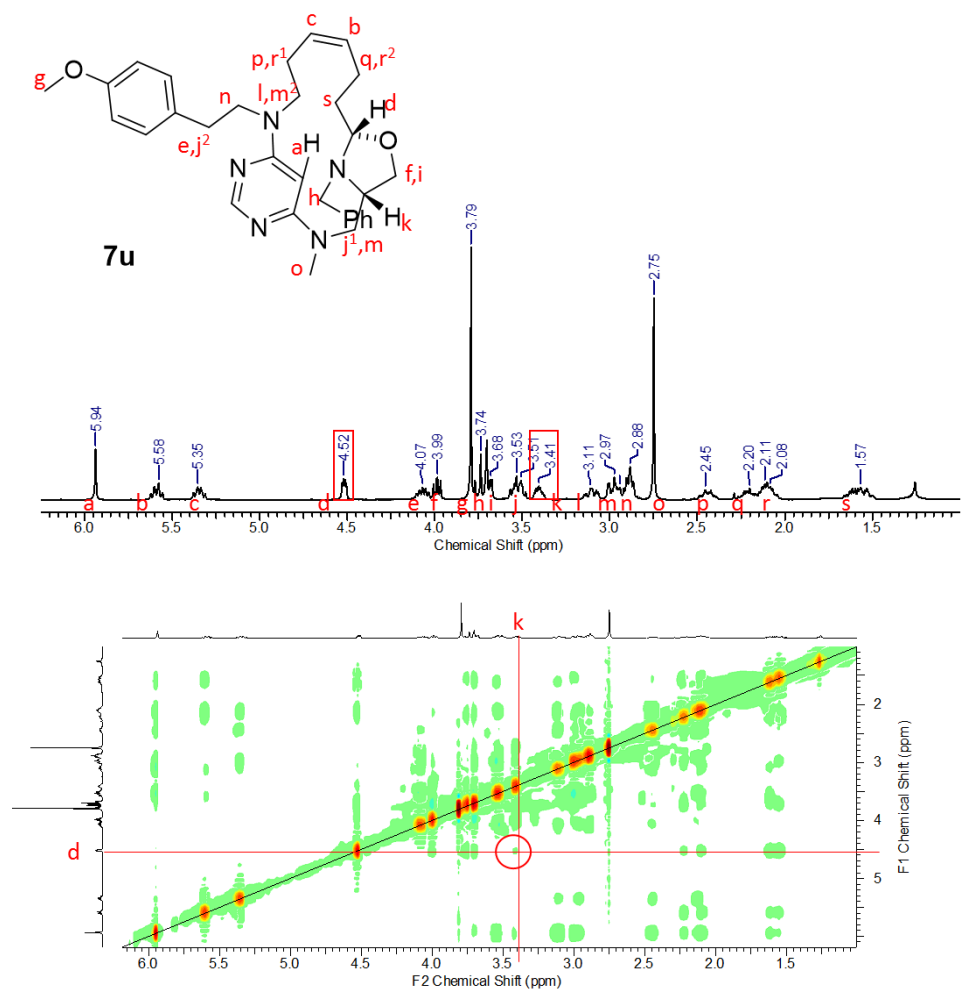


Figure S3. NOESY spectra of compound **7u**

3.5.5. X-ray crystallographic analysis data for 2b

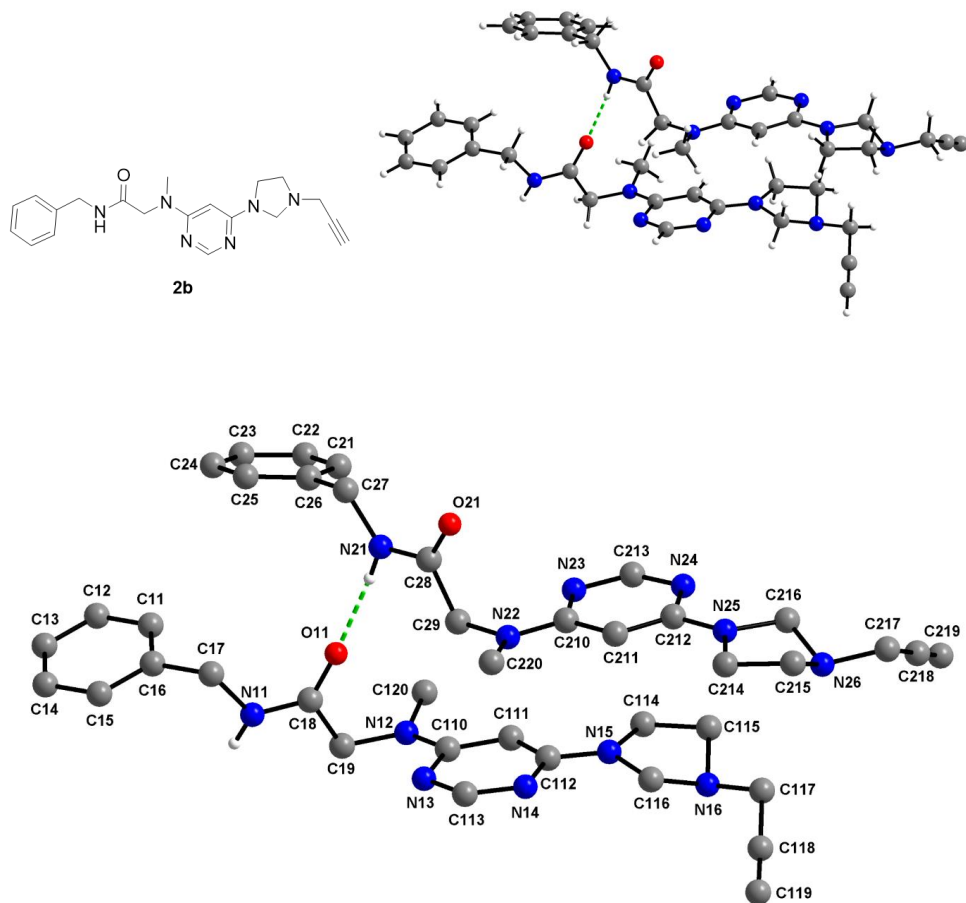


Figure S4. X-ray structure of **5p**. Deposition number in Cambridge Structural Database: CCDC 1519179.

Formula: C₂₀ H₂₄ N₆ O₁

Unit Cell Parameters: a 9.4370(19) b 11.928(2) c 34.465(7) P212121

Chapter 4. Construction of structurally diverse pyrimidine-embedded medium/macro and bridged small molecules via the library-to-library strategy

4.1 Introduction

Biopolymers in living organisms recognize molecules as three-dimensional (3D) surfaces of charges, polarities, and other specific bonding interactions.¹ Thus, when constructing compound libraries it is important to include the skeletal and stereochemical diversity of their structures.² To generate diverse molecular collections, the diversity-oriented synthesis (DOS) strategy was developed, which aims to populate new chemical space with drug-like compounds containing a high degree of molecular diversity.³ Furthermore, there is privileged substructure-based DOS (pDOS) for constructing a library of compounds with enhanced biological relevance.⁴

The capability of a privileged substructure to act as a chemical “navigator” has been demonstrated with specific examples of novel bioactive small-molecule modulators discovered using the pDOS strategy.⁵ The excellent specificity of bioactive pDOS-derived compounds is presumably due to the importance of privileged substructures as a chemical “navigator” of biologically relevant chemical space as well as the unique 3D structures of polyheterocycles.⁶

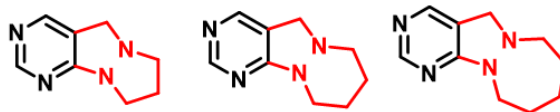
Currently, in our laboratory, the pDOS pathways have been developed using pyrimidine as a privileged substructure.⁷ From this pyrimidine-containing pDOS library, we identified novel bioactive small molecules that modulated the cellular level of lipid droplets^{7b} or inhibited the protein-protein interaction between leucyl-tRNA synthetase (LRS) and Ras-related GTP-binding protein D (RagD).^{7c}

Recently, we developed a new divergent synthetic pathway for skeletally distinct pyrimidine-containing medium-sized azacycles using the *N*-quaternized

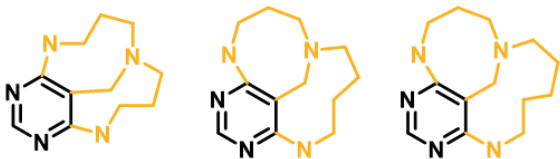
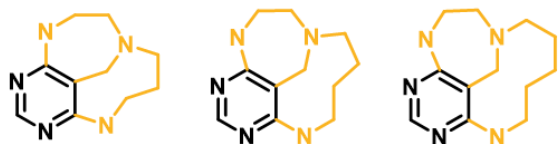
intermediates.⁸ Easily accessible intermediates can be efficiently transformed to 14 discrete scaffolds through selective bond cleavage or migration. With this strategy, we can obtain medium-sized rings in an efficient manner, which are difficult to obtain by conventional head-to-tail cyclization due to the entropy and enthalpy factors. To maximize the coverage of a chemical space with the pDOS strategy, we focused on the diversification of ring size and conformation in a 3D space. The core skeletons containing a medium- or large-cyclic framework can occupy the unexplored chemical space that the previously constructed pyrimidine libraries could not occupy.

For this purpose, a transition-metal catalyst has been used to transform the molecular structure. In fact, transition-metal catalysis provides an efficient way to induce remarkable changes in the molecular frameworks in a single step.⁹ In our laboratory, we recently found that gold catalysis proceeds through the in situ generation of an acyclic iminium intermediate and the subsequent intramolecular nucleophilic cyclization.¹⁰ This provides a highly concise and effective protocol for skeletal diversification at the late stage of synthesis. Furthermore, we propose a library-to-library strategy (Figure 4-1), in which the constructed library compounds are used as a substrate for other libraries. An advantage of this strategy is that the intermediates need not be synthesized for each library, because the compounds that constitute one library can be transformed into compounds with completely different structures, and new libraries can be built in just one step using a gold catalyst.

Library #1 ;
medium ring



Library #2 ;
C-C-N
bridged ring



Library #3 ;
Macrocycle

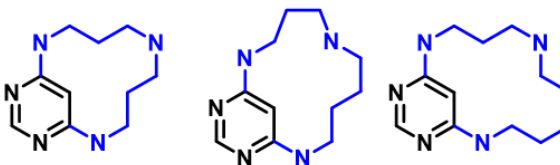
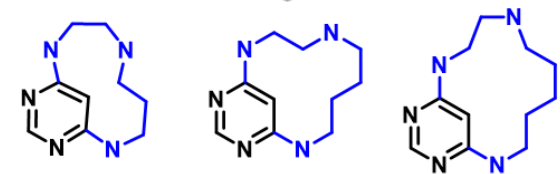
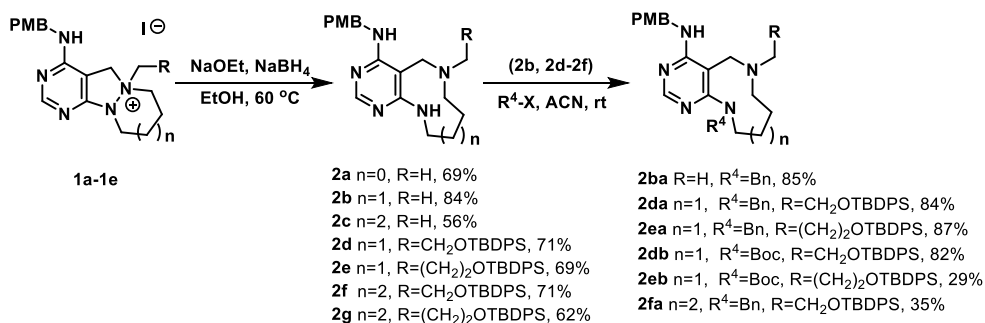


Figure 4-1. Library to library strategy

4.2 Result and Discussion

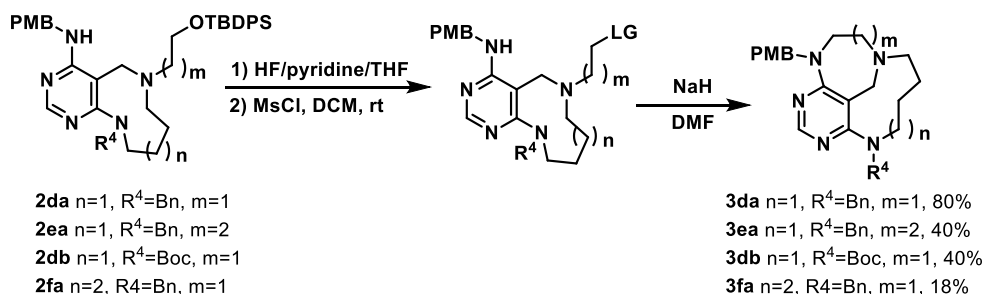
To prepare library # 2, library # 1 obtained through N-N bond selective cleavage is required. The N-N cleavage reaction robustly proceeds from *N*-quaternized azacycle in one step.⁸ Thus, using the functionalized alkyl halide in the *N*-quaternization step, additional ring fusion can be used to construct library # 2. (Scheme 4-1)

Scheme 4-1. Synthesis of the library #1



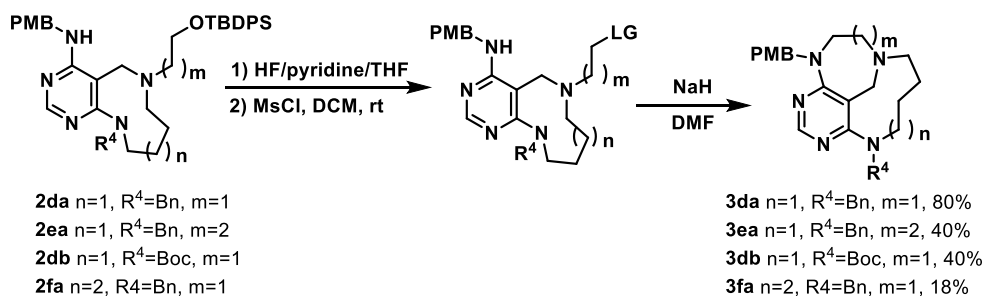
In this pathway, co-treatment with base and hydride allowed the selective cleavage of the N–N bridge, forming pyrimidine-fused medium-sized diazacycles. Regardless of the size of the rings and the length of the side chain, the reaction proceeded robustly. (**2a-2e**) Structural diversity can be introduced in library # 2 by controlling the number of fused cyclic members and chain length of the alkyl halide, and functional group diversity by changing each of the *N*-substituents. So far, it has been confirmed that the compounds **4d** and **4e** can be formed from library # 1 obtained using 5/6, and 5/7 azacyclic precursors with *O*-silyl-protected iodoethanol and iodopropanol. (Scheme 4-2)

Scheme 4-2. Synthesis of the library #2



Libraries # 3 and # 4 can be obtained by gold catalysis of a library # 2 compound. Library # 3 can be obtained from a library # 2 compound using an external nucleophile and a gold catalyst when it does not have an internal nucleophile ($R \neq H$). The iminium intermediate induced by gold-catalyzed ring opening is trapped by the external nucleophile, resulting in a large-sized ring. So far, it has been confirmed that the desired compound **5d** and **5e** can be successfully obtained from compound **4d** and **4e** of library # 2. (Scheme 4-3)

Scheme 4-3. Synthesis of the library #3



To visualize molecular diversity, *in silico* analysis was performed on the representative skeletal structure of each library. The energy minimized conformers were aligned to the pyrimidine substructure and overlaid on the 3D space (Figure 4-2a); we demonstrated the structural diversity of each skeleton with wide spatial coverage. We also performed the principal-moment of inertia (PMI) analysis¹¹ to show the shape-based distribution of molecules. As shown in Figure 4-2b, representative structure of each library was dispersed in the PMI plot, indicating diverse shapes of each library. Currently, substrate preparation is in progress and transformation will be tested.

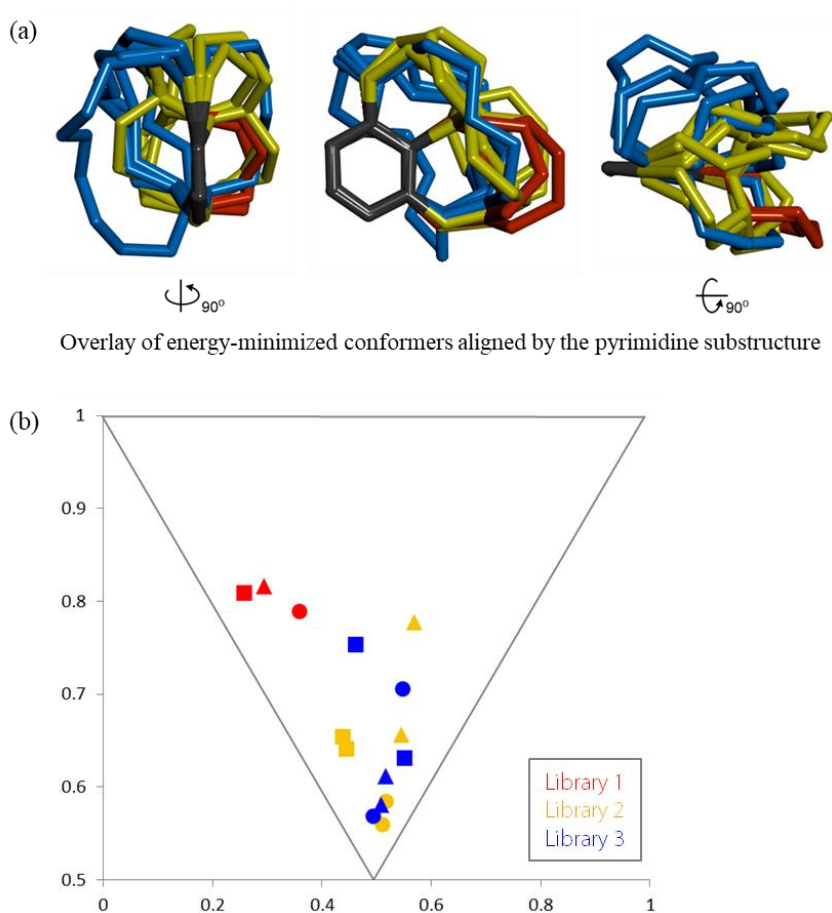


Figure 4-2. *in silico* analysis of library compounds.

4.3 Conclusion

Herein, we have proposed a new strategy for the construction of structurally diverse pyrimidine-embedded medium/macro-cyclic small molecule library using the library-to-library strategy. An advantage of the library-to-library strategy is that the constructed library compounds can be directly used as a substrate for other libraries. This strategy is possible due to the transformation of molecular frameworks in a single step by gold catalysis. The molecular diversity of each scaffold was confirmed by a series of computational studies, structural alignment of energy-minimized 3D conformers, and shape diversity studies by the PMI analysis. This strategy allows the efficient construction of a library with wide spatial occupation around pyrimidine as the privileged substructure that ensures high potential for molecular interactions with biopolymers. Further investigations on various substrates are currently underway.

4.4 References

- [01] Mander, L.; Liu, H. *Comprehensive natural products II*; Elsevier, **2010**.
- [02] C. M. Dobson, *Nature*, **2004**, 432, 824.
- [03] (a) Schreiber, S. L. *Science*, **2000**, 287, 1964. (b) Schreiber, S. L. *Nature*, **2009**, 457, 153.; (c) Galloway, W. R. J. D.; Isidro-Llobet, A.; Spring, D. R. *Nat. Commun.* **2010**, 1, 80.
- [04] Oh, S.; Park, S. B. *Chem. Commun.* **2011**, 47, 12754.
- [05] (a) Park, J.; Oh, S.; Park, S. B. *Angew. Chem., Int. Ed.* **2012**, 51, 5447.; (b) Koh, M.; Park, J.; Koo, J. Y.; Lim, D.; Cha, M. Y.; Jo, A.; Choi, J. H.; Park, S. B. *Angew. Chem., Int. Ed.* **2014**, 53, 5102.; (c) Lee, S.; Nam, Y.; Koo, J. Y.; Lim, D.; Park, J.; Ock, J.; Suk, K.; Park, S. B. *Nat. Chem. Biol.* **2014**, 10, 1055. (d) Cho, T.-J.; Kim, J.; Kwon, S.-K.; Oh, K.; Lee, J.-a.; Lee, D.-S.; Cho, J.; Park, S. B. *Chem. Sci.* **2012**, 3, 3071.
- [06] Kim, J.; Kim, H.; Park, S. B. *J. Am. Chem. Soc.*, **2014**, 136, 14629.
- [07] (a) Kim, H.; Tung, T. T.; Park, S. B. *Org. Lett.* **2013**, 15, 5814.; (b) Choi, Y.; Kim, H.; Shin, Y.; Park, S. B. *Chem. Commun.* **2015**, 51, 13040.; (c) Kim, J.; Jung, J.; Koo, J.; Cho, W.; Lee, W.; Kim, C.; Park, W.; Park, S. B. *Nat. Commun.*, **2016**, 7, 13196.
- [08] *Chem. Sci.*, **2019**, doi: 10.1039/C8SC04061C
- [09] Nakamura, I.; Yamamoto, Y. *Chem. Rev.* **2004**, 104, 2127.
- [10] Koo, J.; Kim J.; Park, S. B. *Org. Lett.* **2017**, 19, 344.
- [11] Sauer, W. H. B.; Schwarz, M. K. *J. Chem. Inf. Comp. Sci.* **2003**, 43, 987.

국 문 초 록

피리미딘 기반의 분자다양성이 확보된 천연물 유사 저분자 물질의 개발

서울대학교 대학원

생물물리 및 화학생물학과

구 재 영

화학생물학 에서의 중요한 연구 목표는 생물학적 시스템을 교란할 수 있는 저분자 화합물 조절자를 발굴하고, 이들이 작용하는 단백질간의 상호작용을 밝혀 생물학적 시스템을 이해하는 데에 있다. 따라서 단백질간의 상호작용을 선택적으로 조절할 수 있는 새로운 저분자 화합물 조절자를 발굴하기 위해서는 분자 다양성이 풍부하며 생물학적 관련성이 높은 약물 유사 저분자 화합물의 개발이 필수적이다. 본 연구에서는 위의 요구에 적합한 화합물의 확보를 위하여 천연물의 특징을 도입한 분자를 제안하였다. 높은 생물학적 관련성을 도입하기 위하여 피리미딘을 독점적 구조로 포함하는 화합물을 이용하였고, 기존에 합성되어왔던 편평한 분자들과는 차별화 된 다양한 3차원적 구조 다양성을 가지는 화합물을 발굴하고자 하였다.

1 장에서는 생리활성 조절물질의 발굴 가능성을 높이기 위한 전략으로 다양한 분자 구조를 가지며 생물학적 연관성이 높은 화합물 군을 확보하기 위한 다양한 시도에 관하여 소개하고 있다.

2 장에서는 피리미딘을 포함하는 독점적 구조 기반 다양성 추구 조합 화학 반응 경로의 개발에 관하여 서술하고 있다. 피리미딘과 7각 링이 융합된 피리미도다이하지핀 구조를 출발물질로 하여 창의적인 3차원적 구조를 점유하는 화합물들을 합성하는 경로에 대해 설명하였고, 이를 통해 얻어진 화합물이 실제 단백질간의 상호작용을 조절할 수 있음을 증명하였다.

3 장에서는 피리미도다이하지핀 구조에서 발굴된 금 촉매의 신규 반응성에 관하여 서술하고 있다. 이 반응성을 이용하여 분자 구조를 한 단계 반응으로 효율적으로 변형할 수 있으며, 합성적 접근이 어려운 거대

고리구조에 손쉽게 접근이 가능함을 보였다.

마지막으로 4 장에서는 상기에 서술된 금 촉매 반응을 이용한 저분자 화합물 라이브러리의 구축에 관하여 다루었다. 피리미딘이 포함된 중간고리 화합물을 이용하여 금 촉매의 한 단계 반응을 통해 다른 형태를 갖는 중간고리 구조 혹은 거대고리 구조로의 변형을 유도하여 풍부한 구조 다양성을 갖는 저분자 화합물 라이브러리를 제안하였다.

2 장부터 4 장까지의 연구를 통해 3차원적 구조 다양성을 포함하는 저분자 화합물을 다수 확보하였고, 확보된 저분자 화합물 중에서 실제 단백질간의 상호작용을 조절할 수 있는 저분자 물질을 발굴함으로써 화합물의 유용성을 증명할 수 있었다. 따라서 본 연구에서 발굴된 피리미딘 기반의 분자다양성이 확보된 천연물 유사 저분자 물질들은 추후 더 많은 신규 생리활성 물질의 도출에 높은 잠재력을 가질 것으로 예상된다.

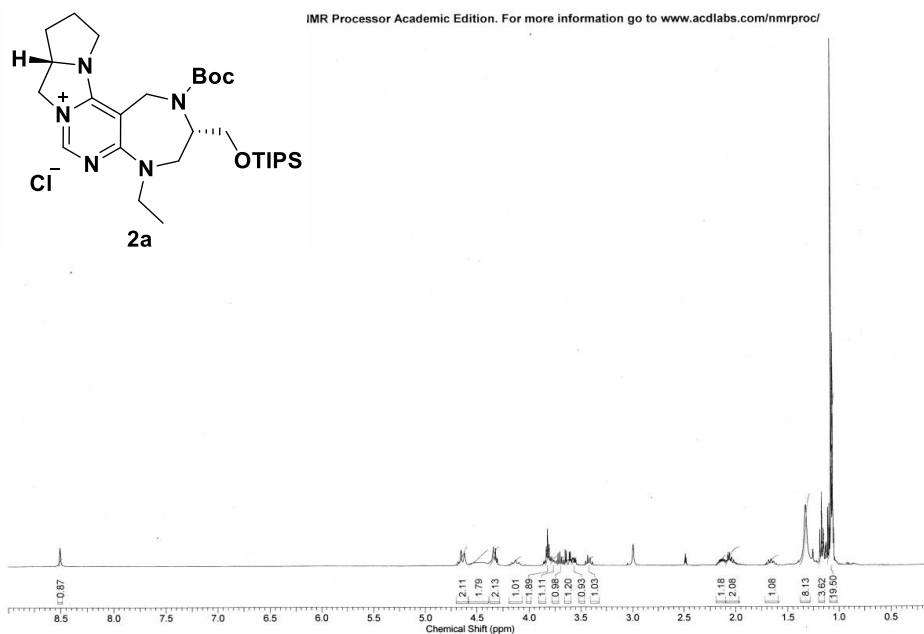
주요어 : 분자다양성, 피리미딘, 독점적 구조 기반 다양성 추구 조합화학, 금 촉매 반응, 중간고리 화합물, 거대고리 화합물, 화합물 라이브러리,

학 번 : 2013-30757

Appendix

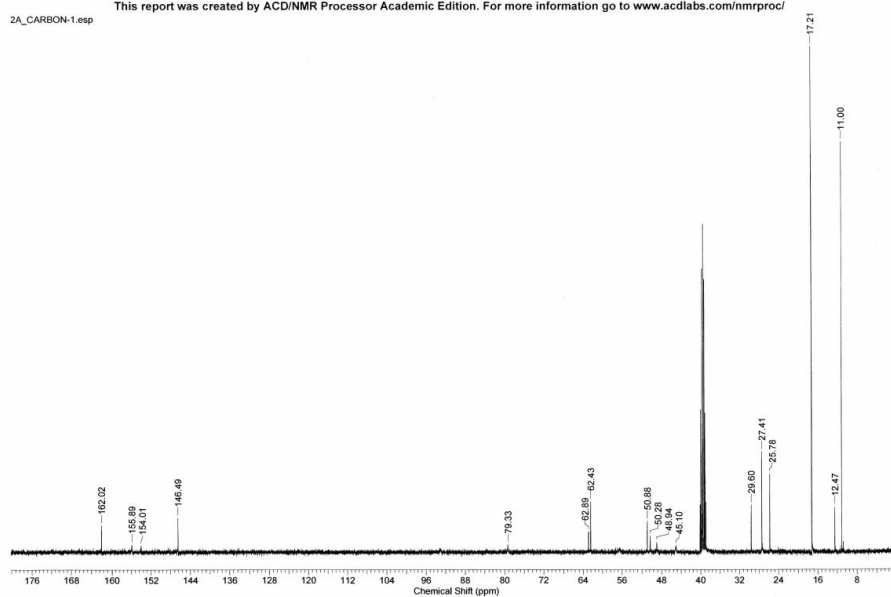
Copy of ^1H and ^{13}C NMR Spectra

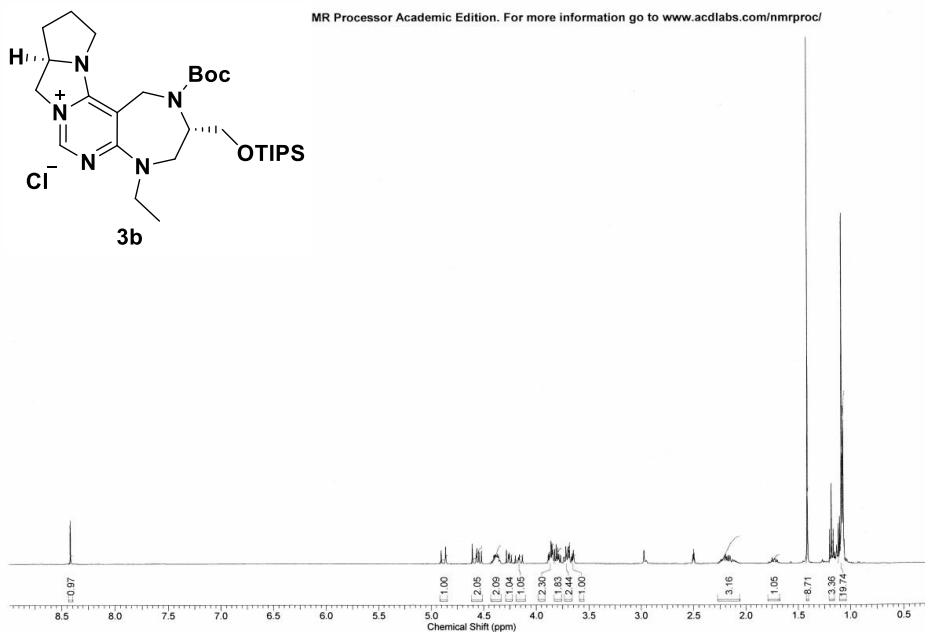
Chapter 2



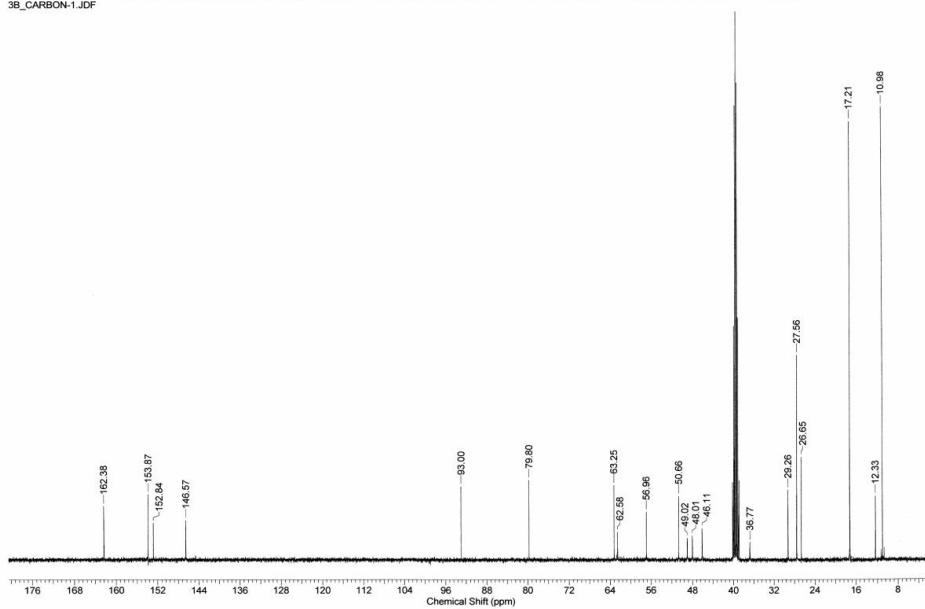
2A_CARBON-1.esp

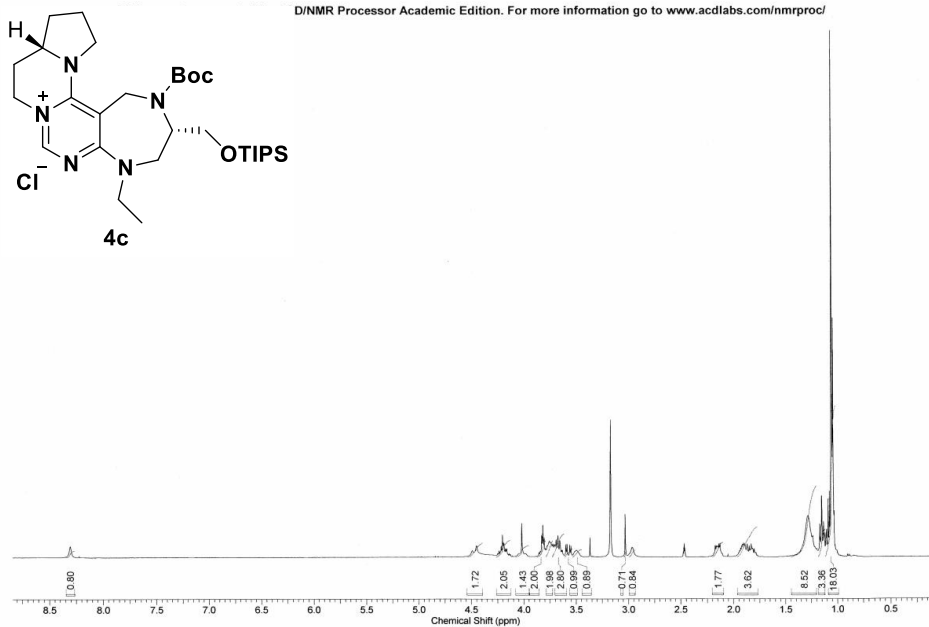
This report was created by ACD/NMR Processor Academic Edition. For more information go to www.acdlabs.com/nmrproc/



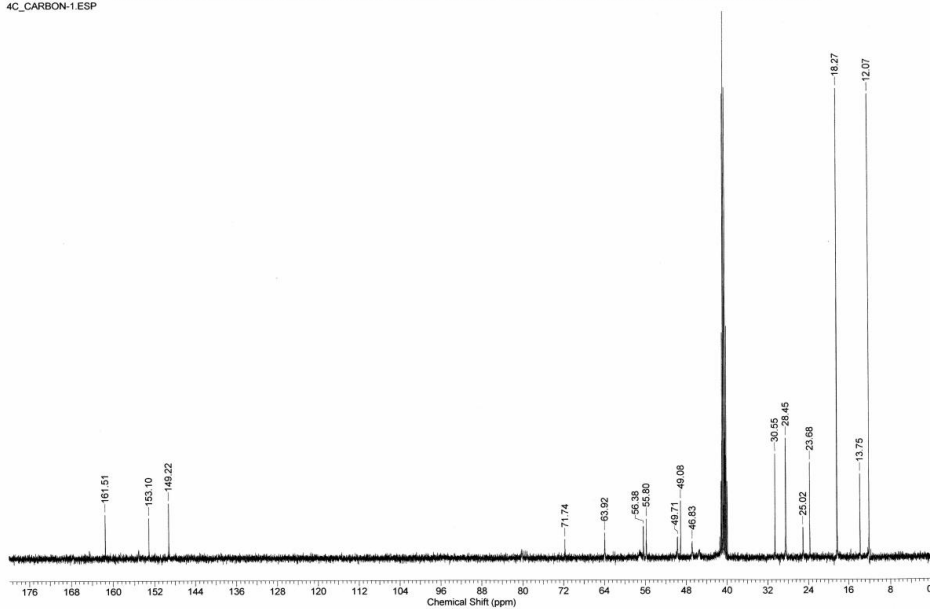


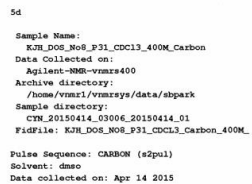
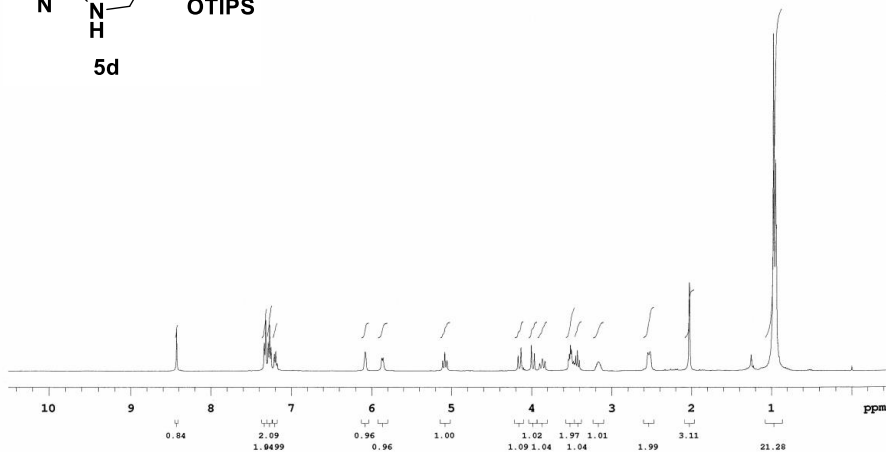
3B_CARBON-1.JDF

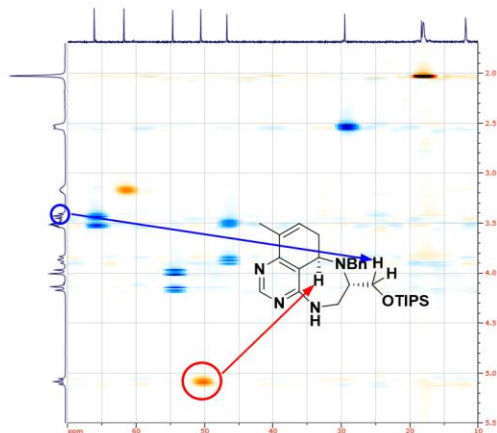
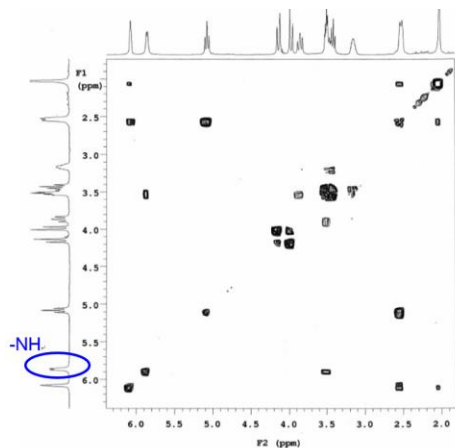




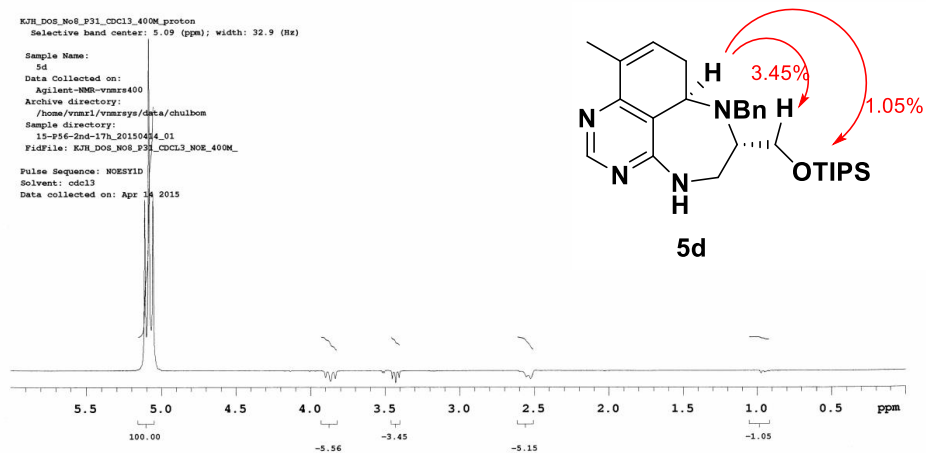
4c_CARBON-1.ESP

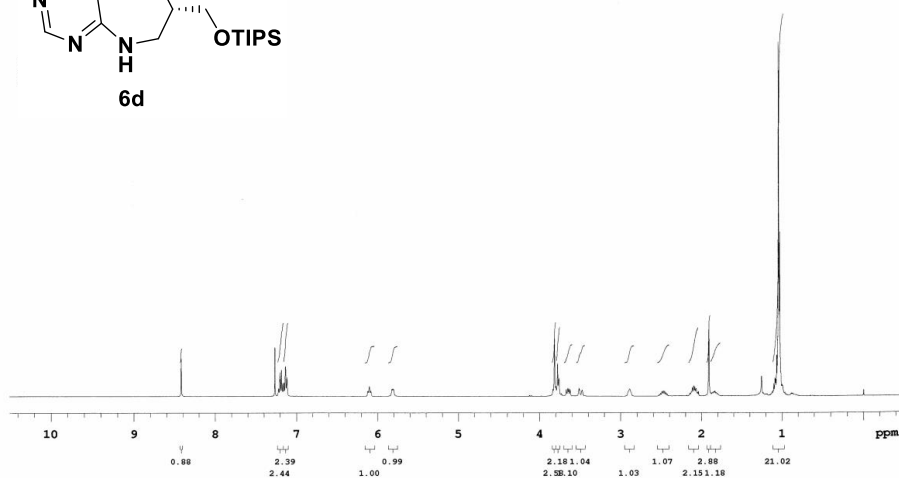
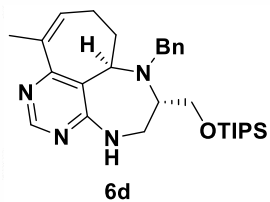






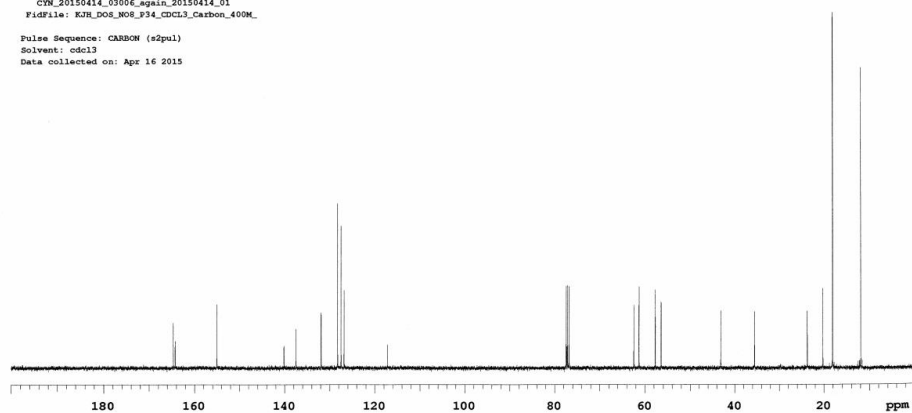
KJH_D08_No8_P31_CDCl3_400M_proton
 Selective band center: 5.09 (ppm); width: 32.9 (Hz)
 Sample Name:
 5d
 Data Collected on:
 Agilent-VNMRS-vmr400
 Archive directory:
 /home/vnmr1/vnmrsys/data/chulbon
 Sample directory:
 15-P56-2nd-17h_20150404_01
 FidFile: KJH_D08_No8_P31_CDCl3_NOR_400M
 Pulse Sequence: NOESY1D
 Solvent: cdcl3
 Data collected on: Apr 14 2015

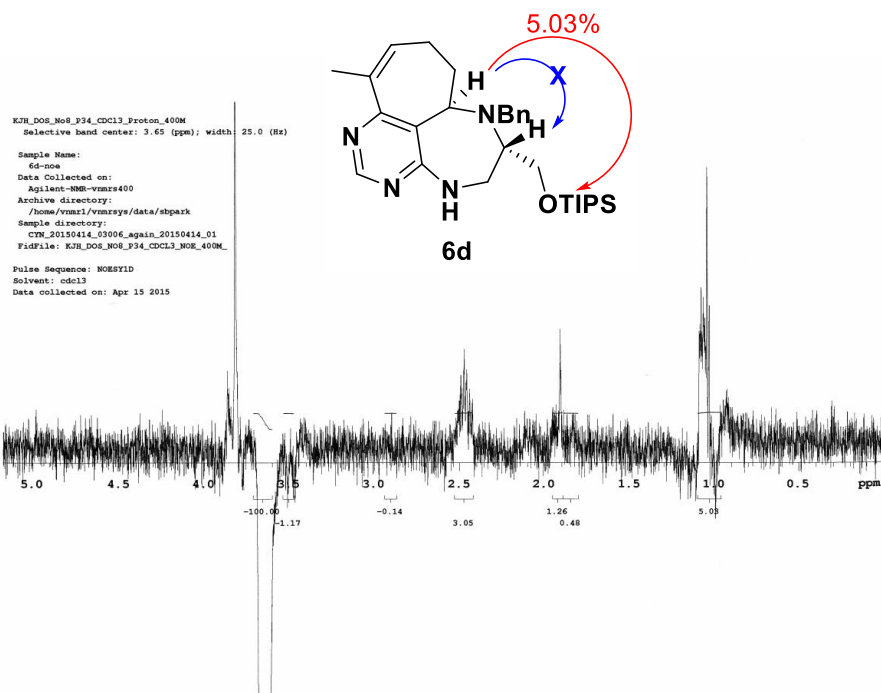
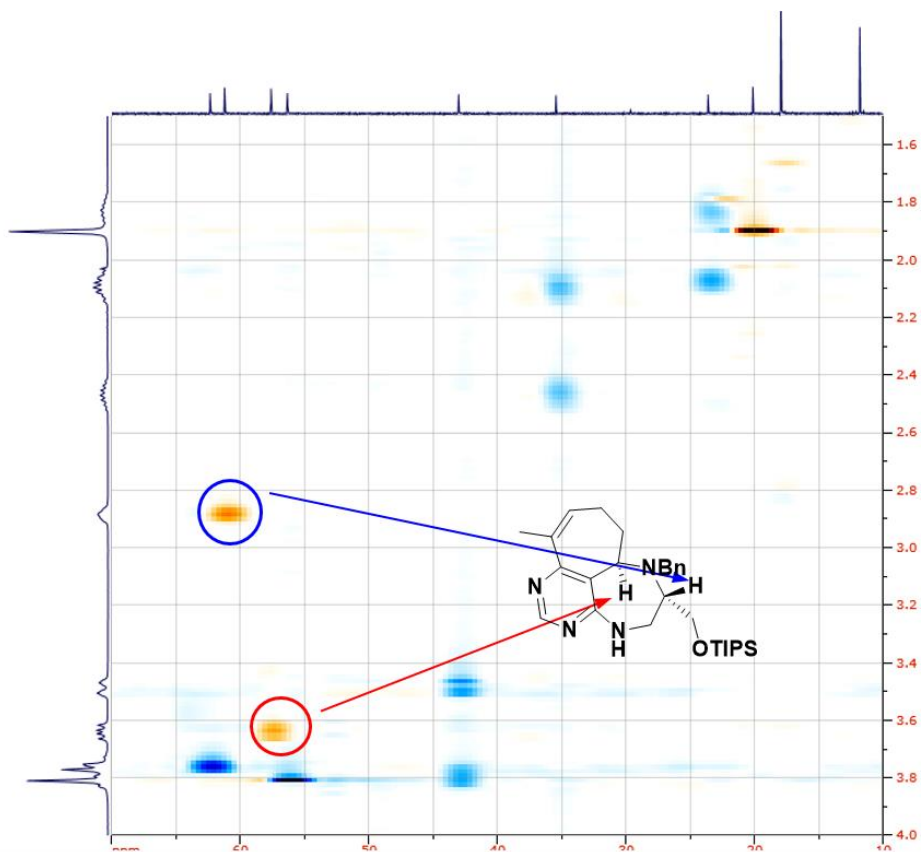


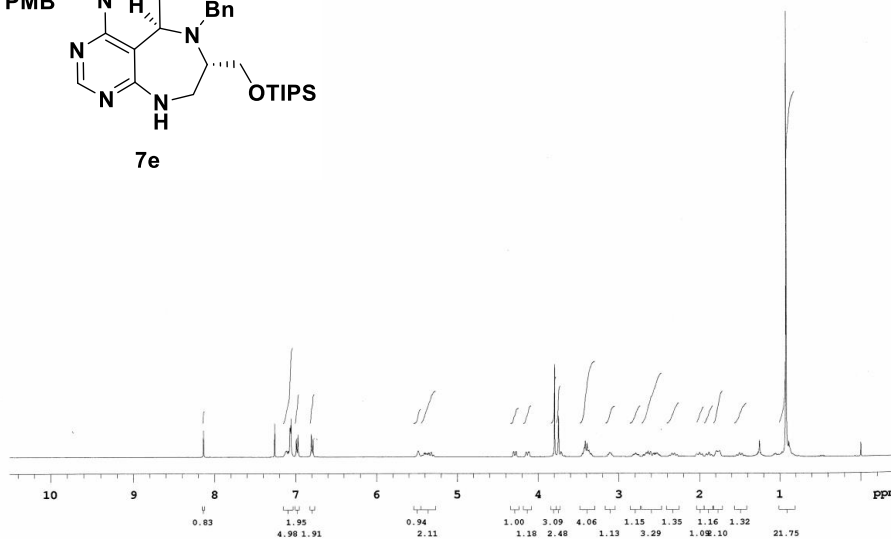
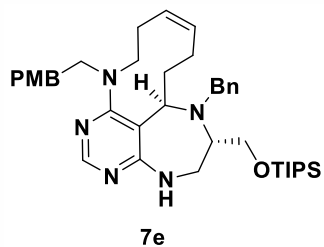


6d

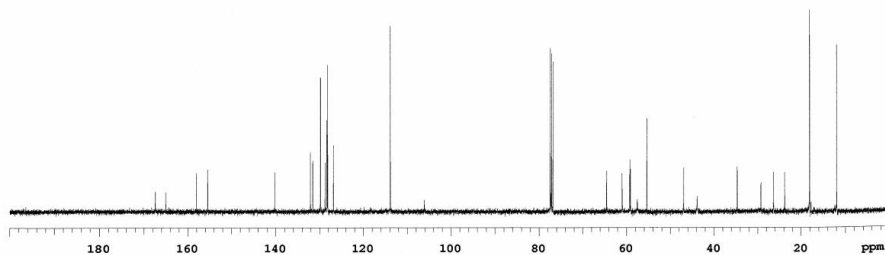
Sample Name: KJR_D08_H08_F34_CDCl3_Carbon_400M
 Data Collected on: Agilent-MMR-vnmr400
 Archive directory: /home/vnmr1/vnmrsys/data/abspark
 Sample directory: CYN_20150414_03006_again_20150414_01
 FidFile: KJR_D08_H08_F34_CDCl3_Carbon_400M_
 Pulse Sequence: CARBON (s2pul)
 Solvent: cdcl3
 Data collected on: Apr 16 2015

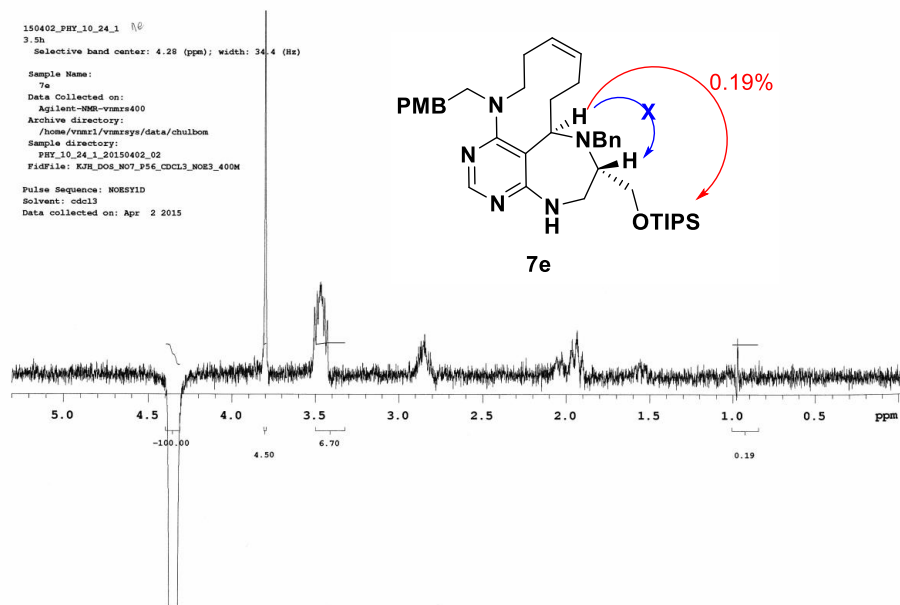
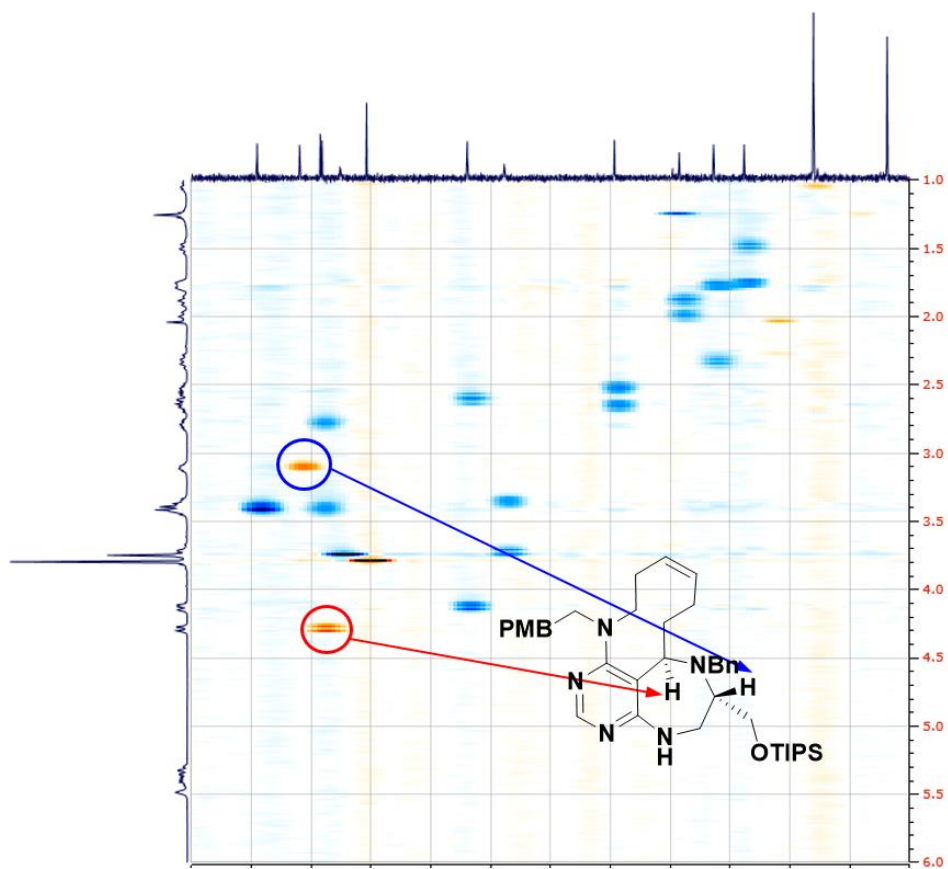


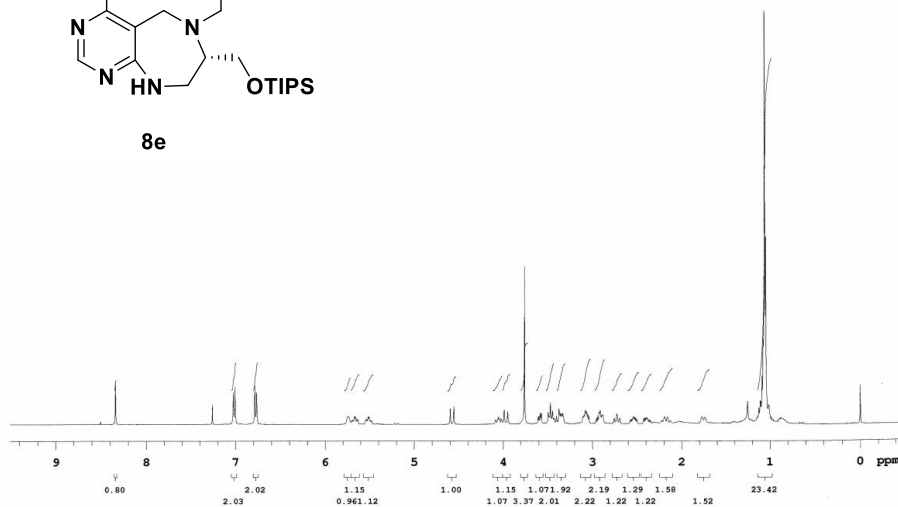
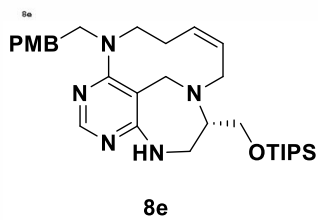




7e
 Sample Name:
 KJH_D08_M07_P56_CDCL3_carbon_400M
 Data Collected on:
 Agilent-VNM600
 Archive directory:
 /home/vnmr1/vnmrlogs/data/sbpark
 Sample directory:
 VMS_2-75_1H_Methanol_20141008_20141008_01
 FIDFile: KJH_D08_M07_P56_CDCL3_Carbon_400M
 Pulse Sequence: CARBON (s2pul)
 Solvent: cd3od
 Data collected on: Oct 9 2014



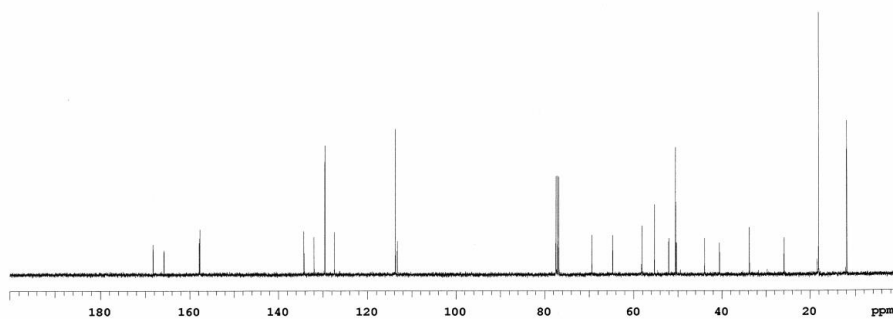


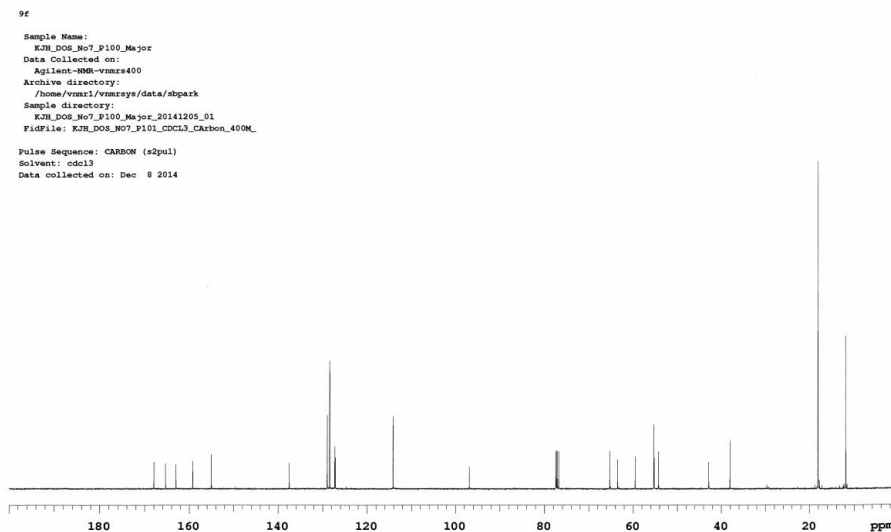
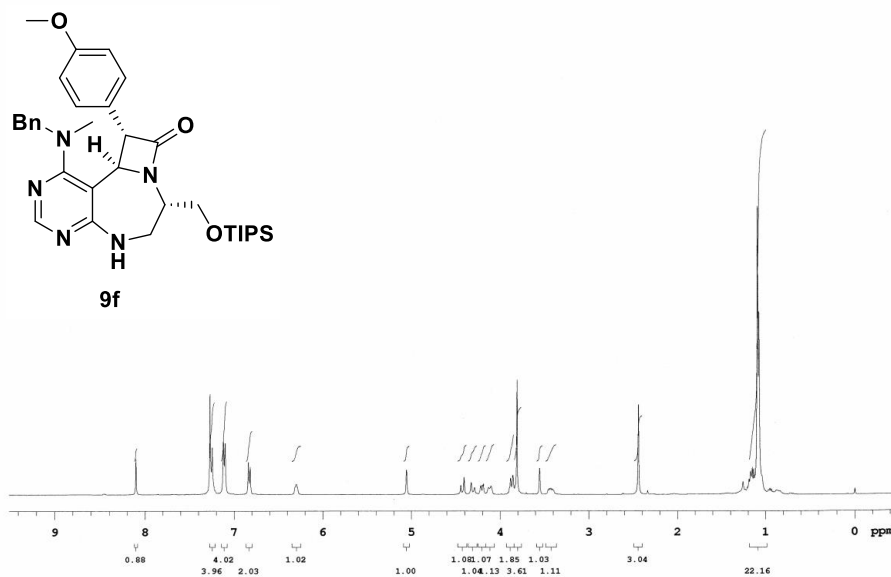


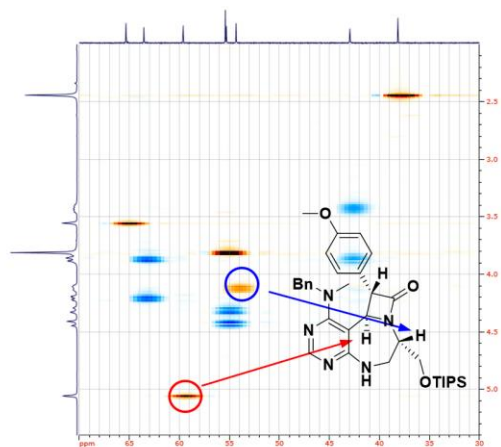
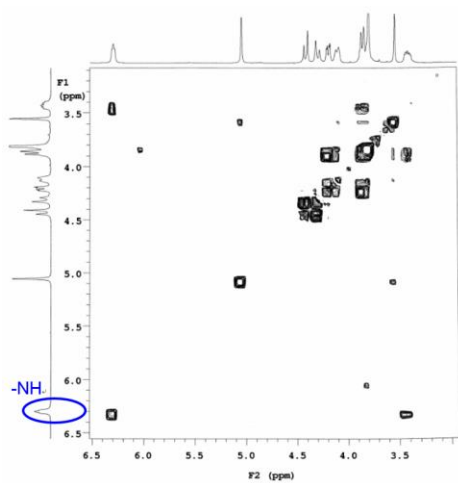
8e

Sample Name:
JAM-III-37_13C
Data Collected on:
Agilent-100-vmz400
Archive directory:
/home/vmz1/vmzsys/data/sbark
Sample directory:
JAM-III-37_13C_20140401_01
FidFile: CARBON_01

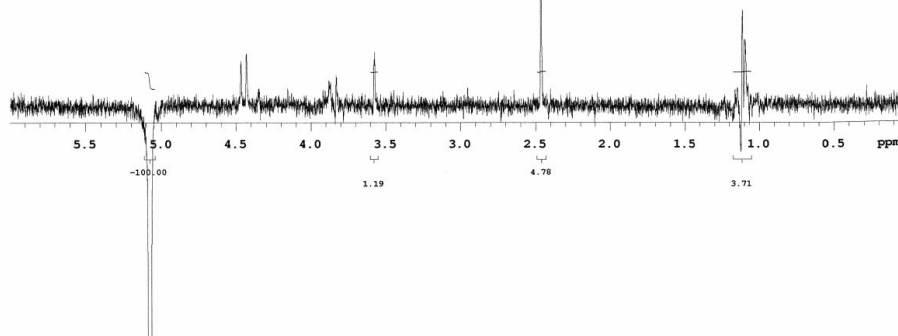
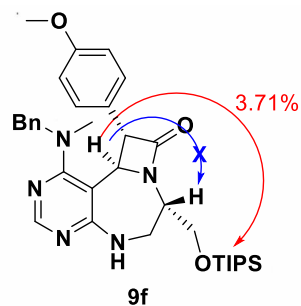
Pulse Sequence: CARBON (s2pul)
Solvent: cdcl3
Data collected on: Apr 1 2014

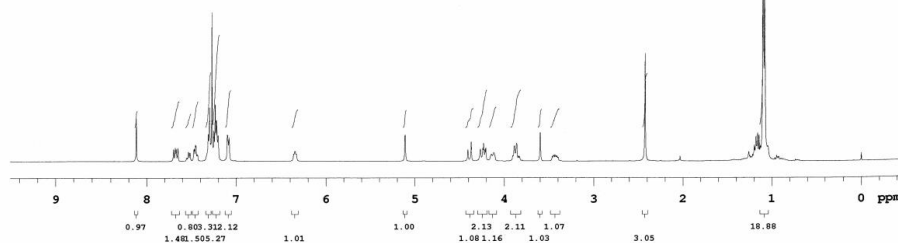
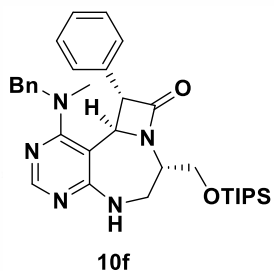






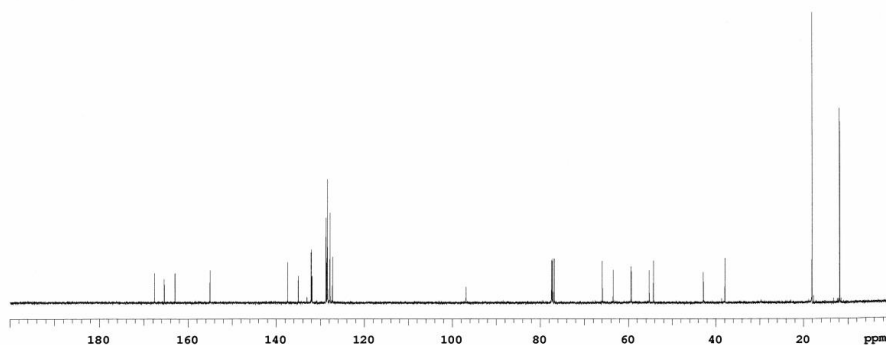
KJH_D08_No7_F101_CDCl3_proton_400M
 Selective band center: 5.06 (ppm); width: 9.8 (Hz)
 Sample Name:
 9f-noe
 Data collected on:
 Agilent-MMR-vnmr400
 Archive directory:
 /home/vmr1/vnmr400/data/chulbon
 Sample directory:
 SMU_12059_B_20141205_02
 FIDFile: KJH_D08_No7_F101_CDCl3_NOE2_400M_
 Pulse Sequence: NOESYD
 Solvent: cdcl3
 Data collected on: Dec 8 2014

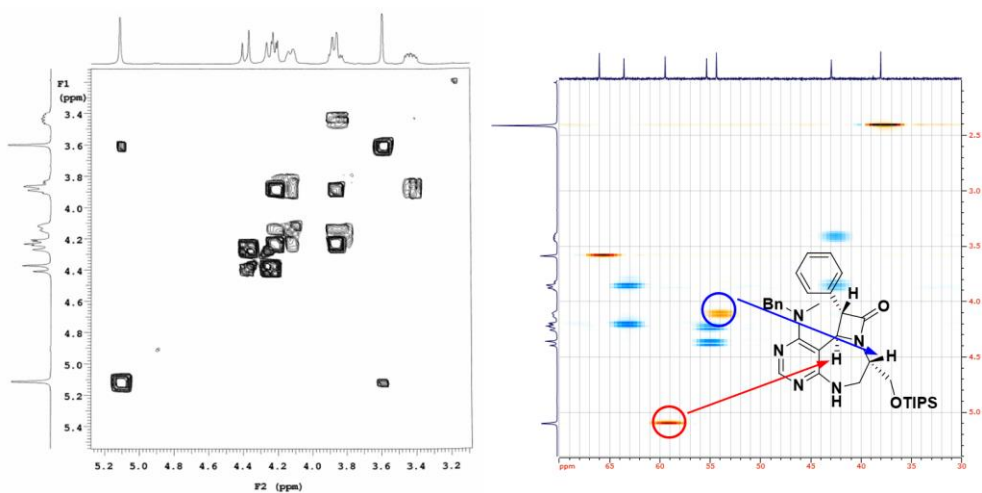




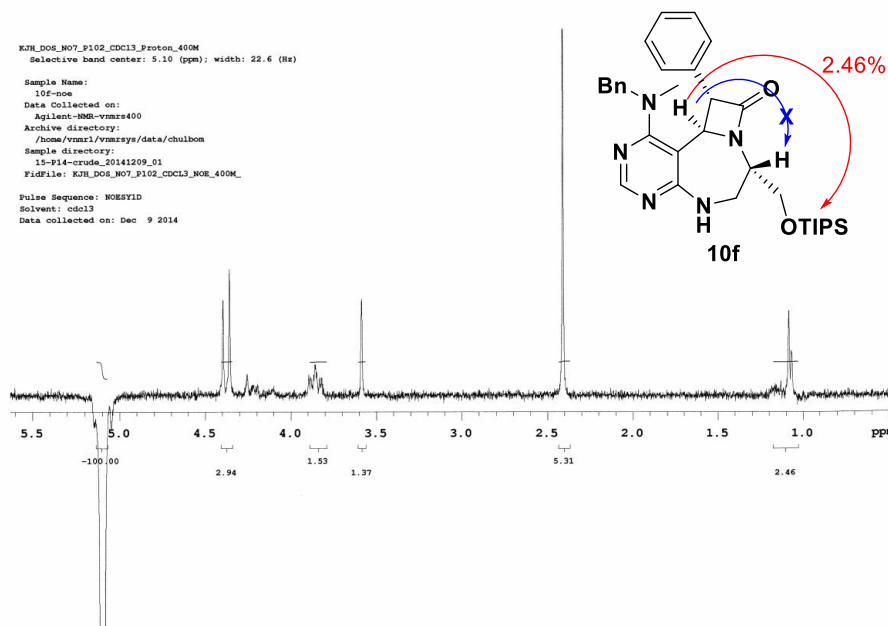
10f

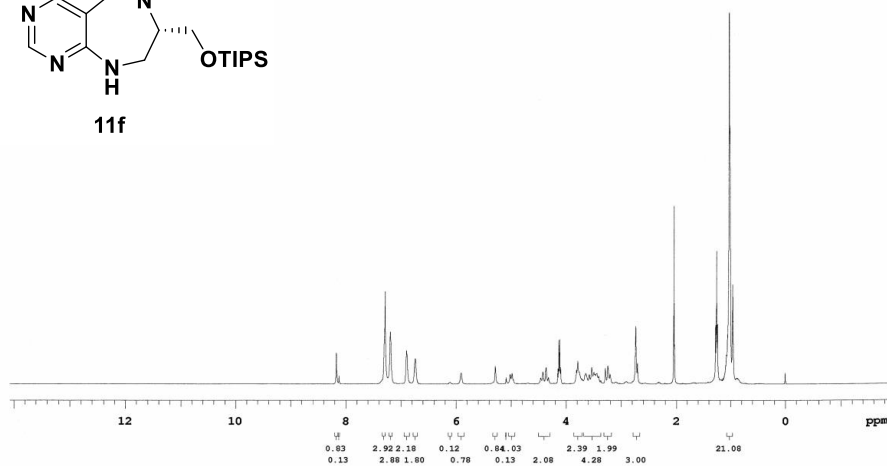
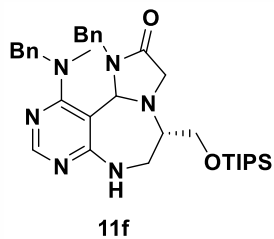
Sample Name: KRM_D08_M07_P102_CDCl3_Carbon_400M
 Data Collected on: Agilent-NMR-vnmr400
 Archive directory: /home/vnmr1/vnmrsys/data/shpark
 Sample directory: KC_bvalsp_141124_20141126_01
 File: KRM_D08_M07_P102_CDCl3_Carbon_400M_
 Pulse Sequence: CARBON (s2pul)
 Solvent: cdcl3
 Data collected on: Dec 9 2014





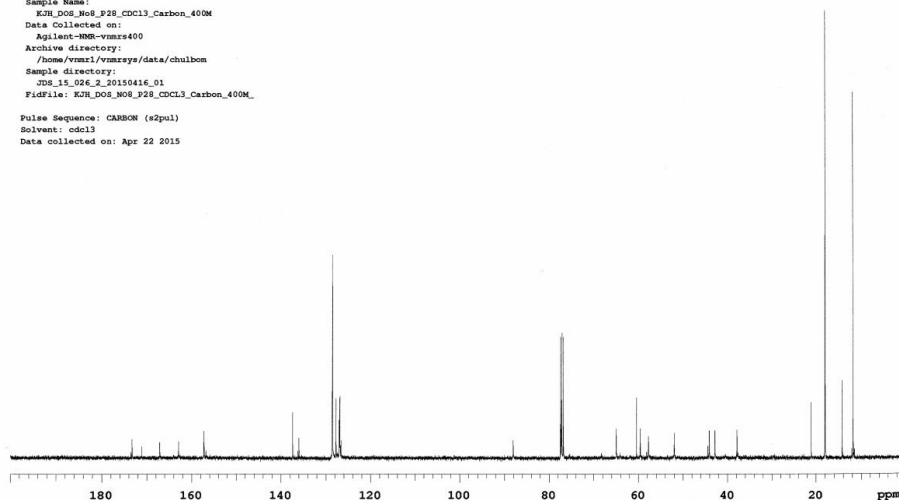
KJH_D08_N07_F102_CDCl3_Froton_400M
 Selective band center: 5.10 (ppm); width: 22.6 (Hz)
 Sample Name:
 10f-noe
 Data Collected on:
 Agilent-NMR-vnmr400
 Archive directory:
 /home/vnmr1/vnmr400/data/chulbon
 Sample directory:
 15-F14-crude_20141209_01
 FidFile: KJH_D08_N07_F102_CDCl3_NOE_400M_
 Pulse Sequence: NOESTYD
 Solvent: cdcl3
 Data collected on: Dec 9 2014

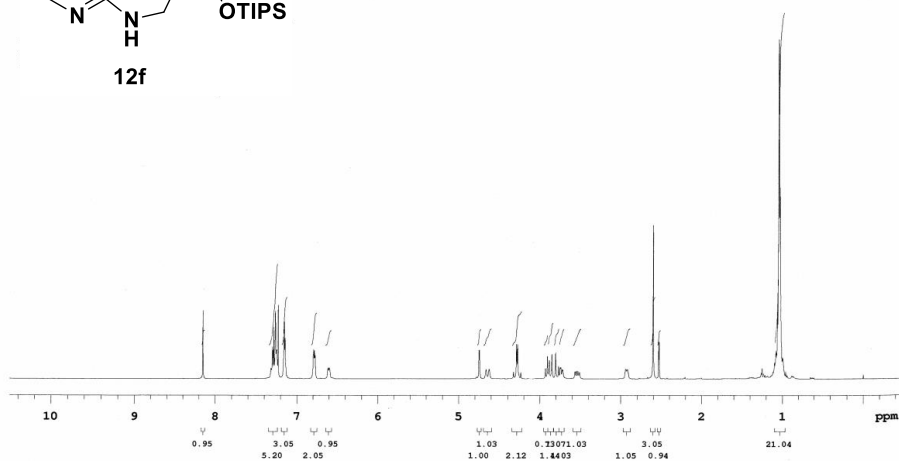
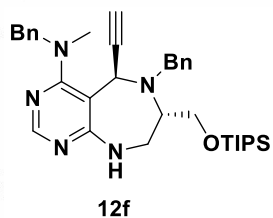




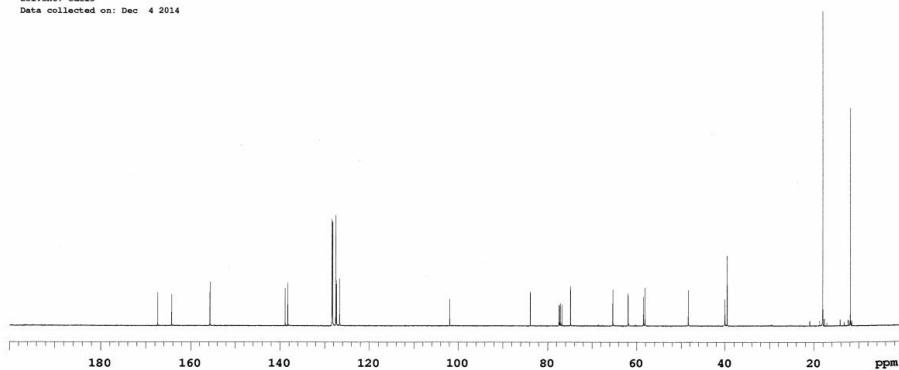
11f

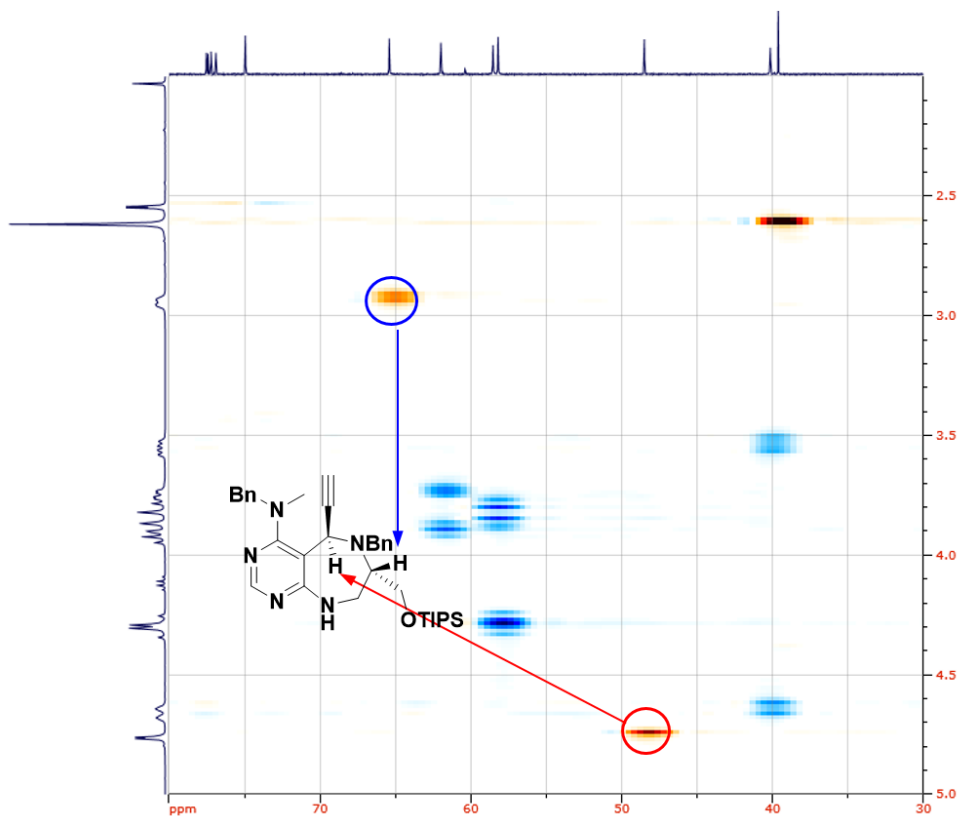
Sample Name:
KJR_D08_M08_F28_CDCL3_Carbon_400M
Data Collected on:
Agilent-VNMR-vnmrs400
Archive directory:
/home/vnmr1/vnmrsys/data/chulbon
Sample directory:
JDS_15_024_2_20150416_01
FidFile: KJR_D08_M08_F28_CDCL3_Carbon_400M_
Pulse Sequence: CARBON (s2pul)
Solvent: cdcl3
Data collected on: Apr 22 2015



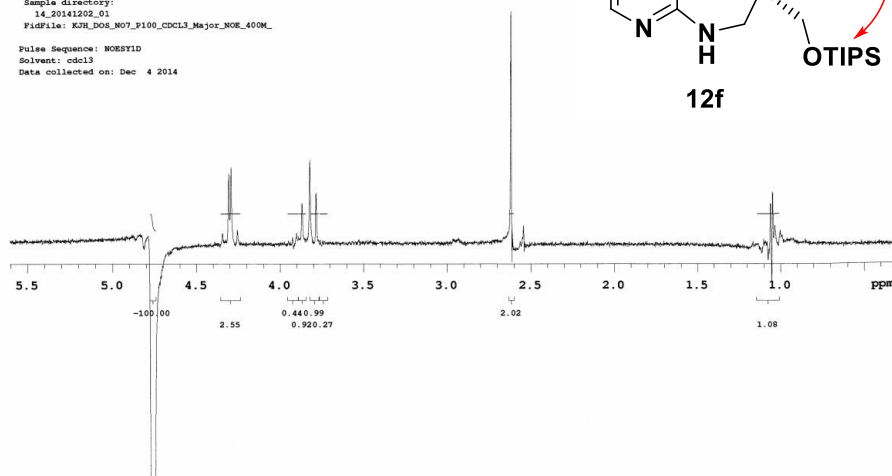
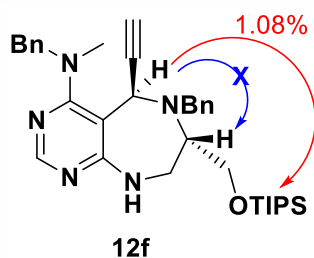


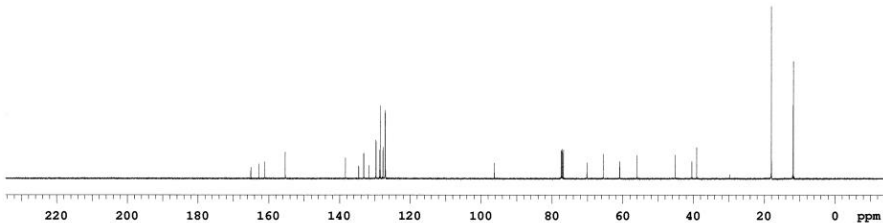
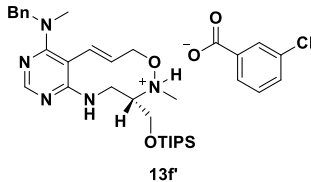
12f
 Sample Name:
 KJH2
 Data Collected on:
 Agilent-400-VRX400
 Archive directory:
 /home/vmr1/vmraysa/data/sbpark
 Sample directory:
 KJH2_20141204_01
 FidFile: KJH_DOS_N07_P100_CDCl3_Major_Carbon_400M_

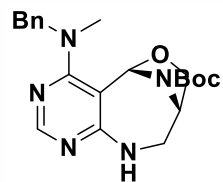




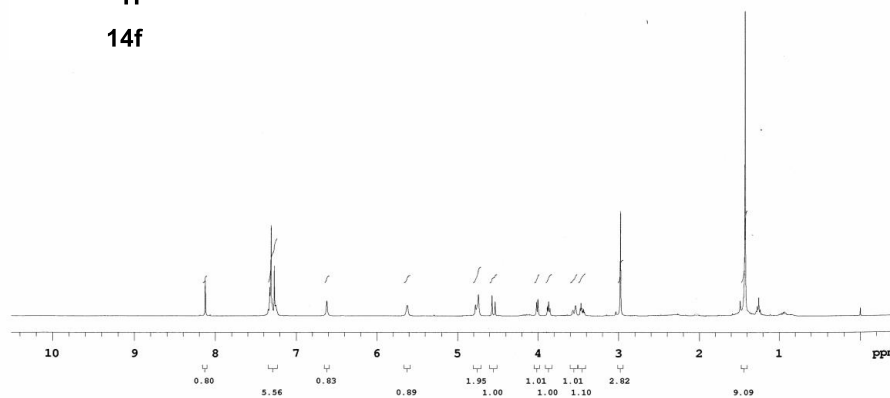
KJR_D08_M07_P100_Major_CDCl3_NOR_400M
 Selective band center: 4.77 (ppm); width: 12.7 (Hz)
 Sample Name:
 12f_nor
 Data Collected on:
 Agilent-VNMRS-VNMR400
 Archive directory:
 /home/vnmr1/vnmrsys/data/chulbon
 Sample directory:
 14_20141202_01
 FidFile: KJR_D08_M07_P100_CDCl3_Major_NOR_400M
 Pulse Sequence: NOESTYD
 Solvent: cdcl3
 Data collected on: Dec 4 2014





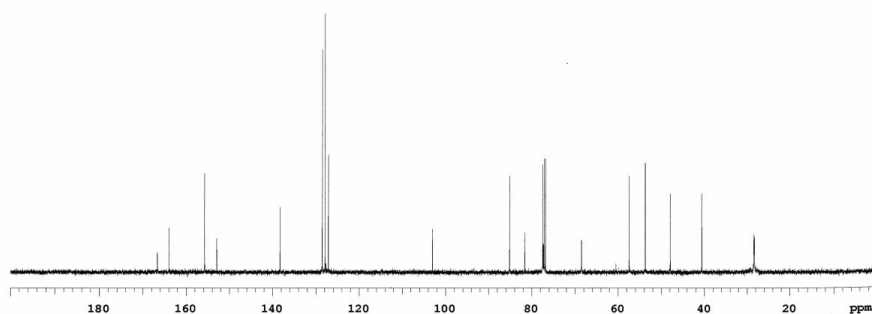


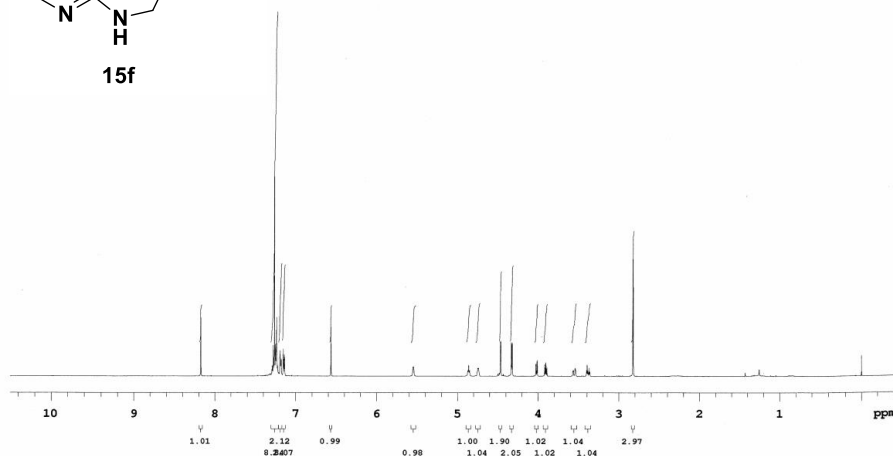
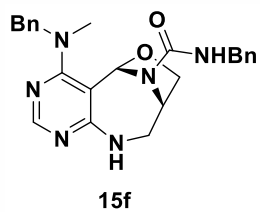
14f



13f

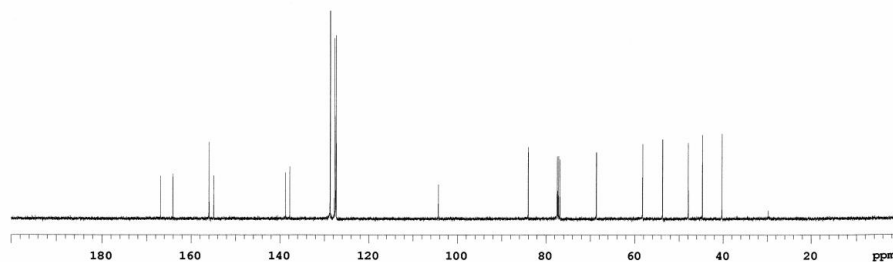
Sample Name:
13f
Data Collected on:
Agilent-MSB-vnmr400
Archive directory:
/home/vnmr1/vnmr400/data/dykhchen
Sample directory:
s1_3-65_f2_20140704_01
Fidfile: K81_005_N06_P106_Product_CDCl3_carbon_Column_400M
Pulse Sequence: CARBON (s2pul)
Solvent: cdcl3
Data collected on: Jul 5 2014

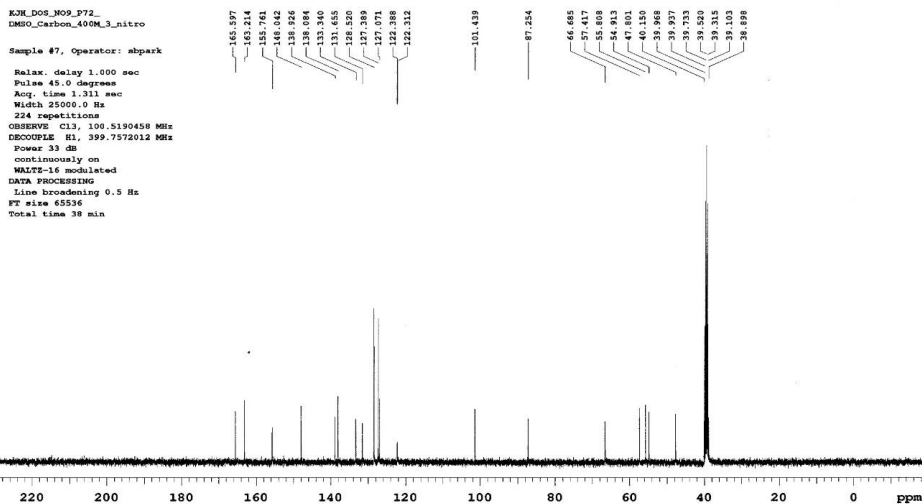
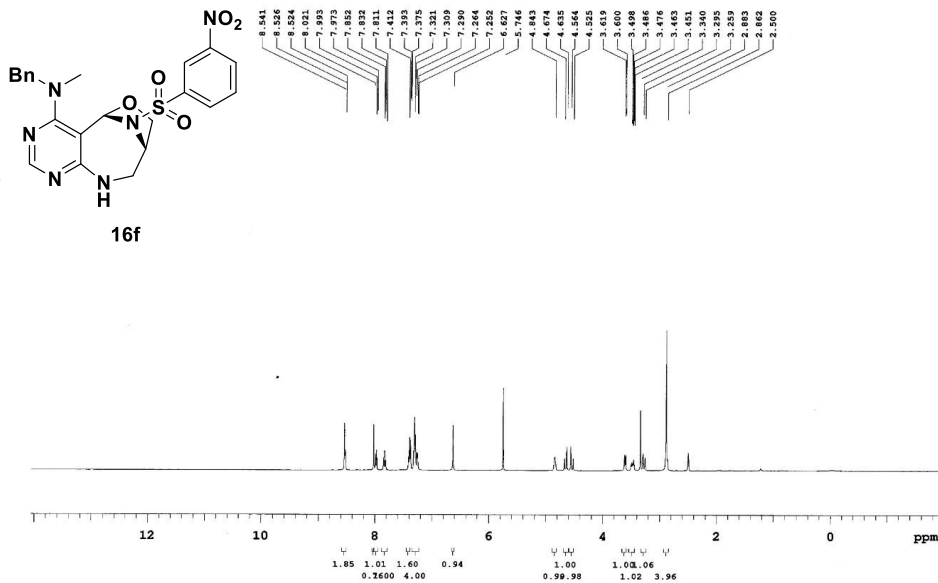


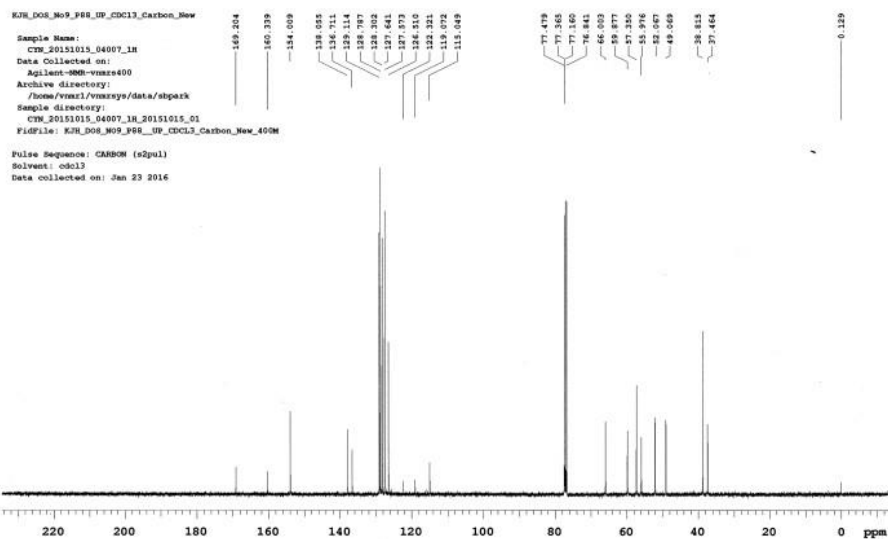
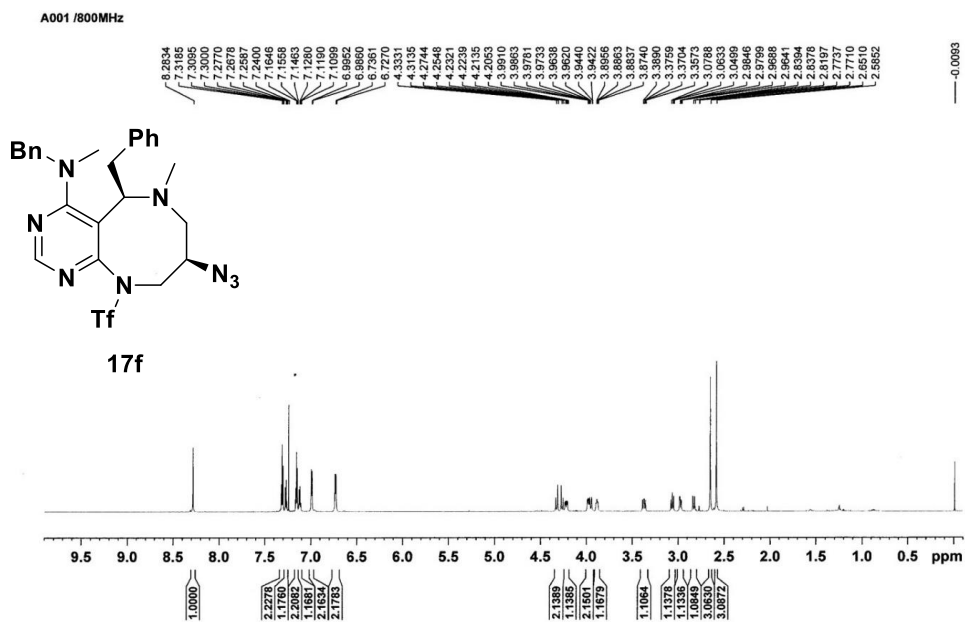


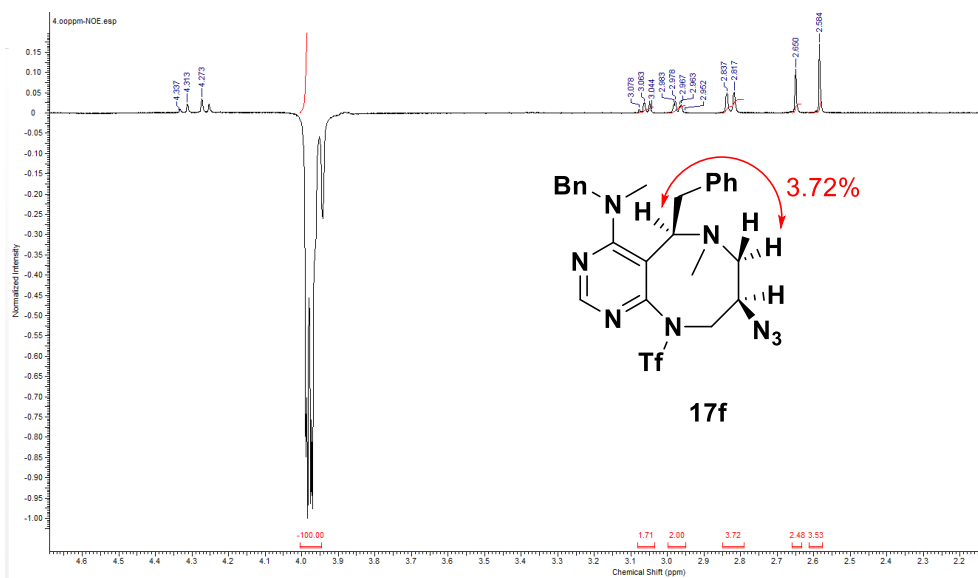
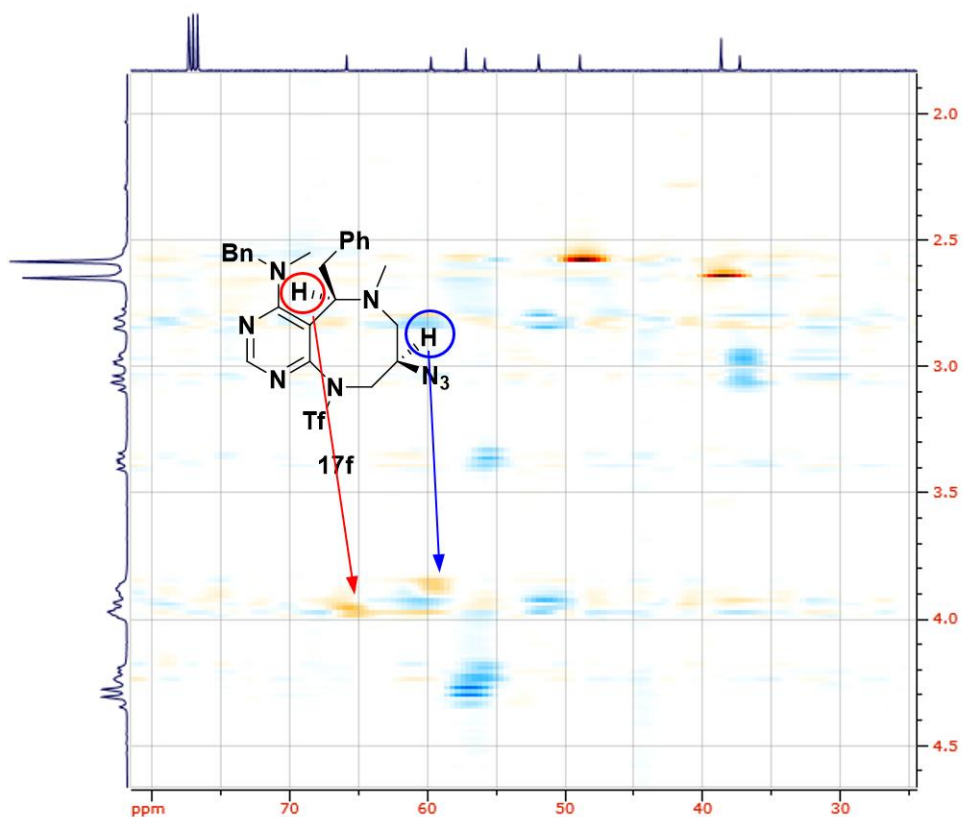
14f

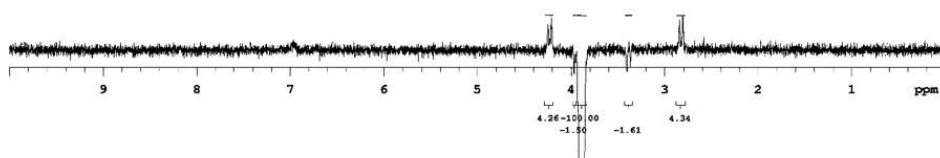
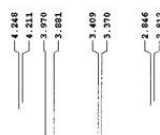
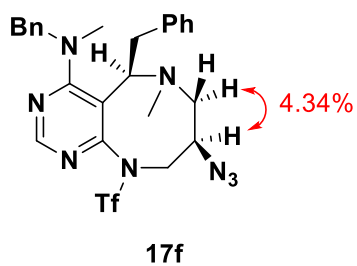
Sample Name:
14f
Data Collected on:
Agilent-NMR-vnmr400
Archive directory:
/home/vnmr1/vnmrsys/data/shpark
Sample directory:
RM1_2-41_P2_1H_Acetone_20140702_01
FidFile: RM1_D08_R06_P109_Product_CDC13_Carbon_400M
Pulse Sequence: CARBON (s2pul1)
Solvent: cdcl3
Data collected on: Jul 8 2014

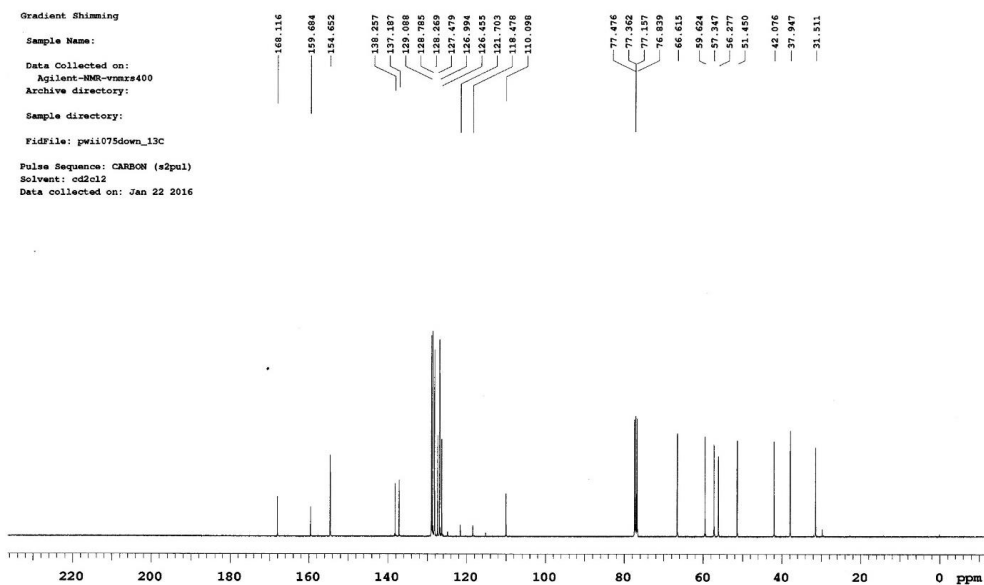
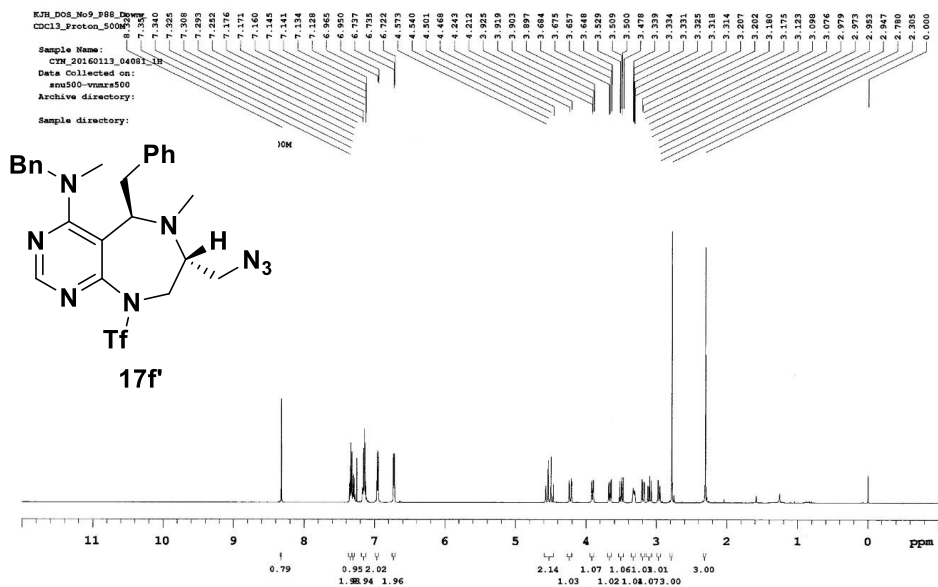


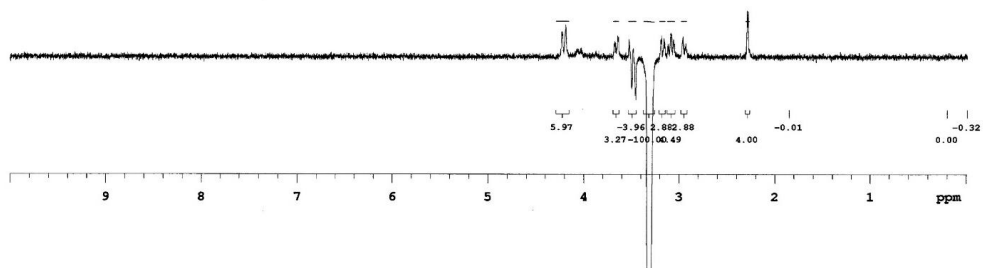
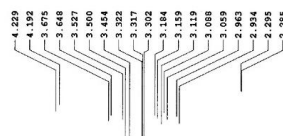
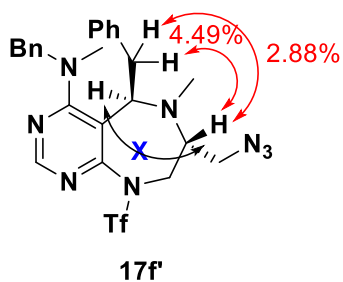
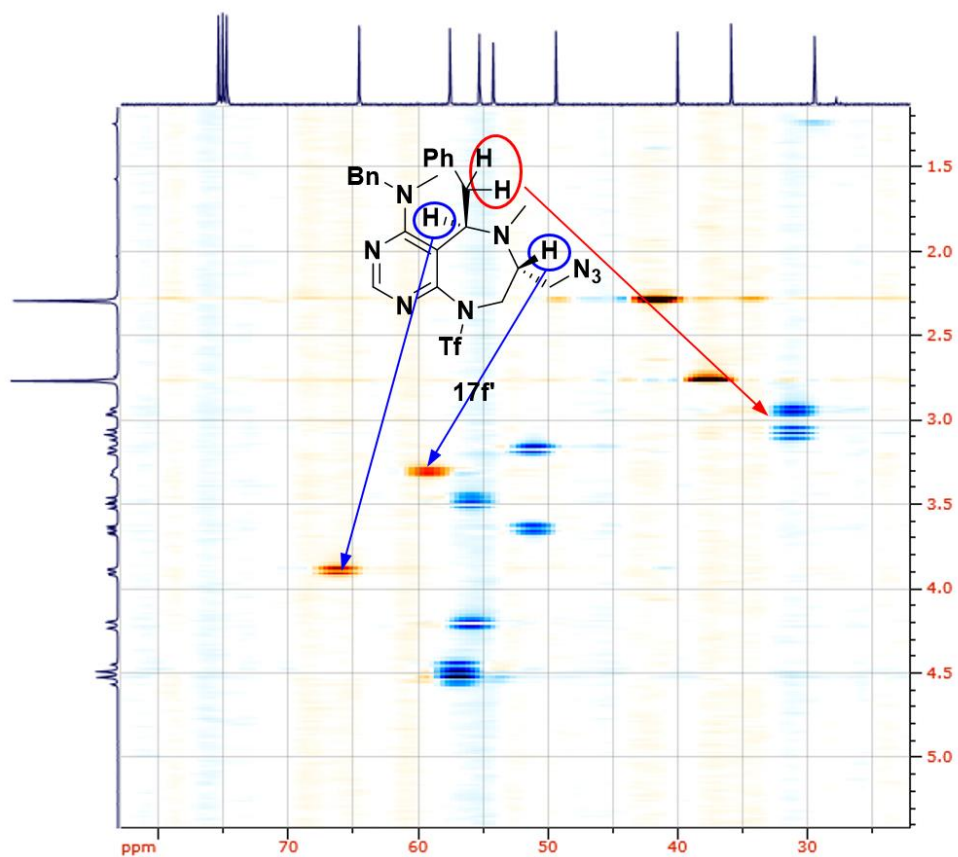


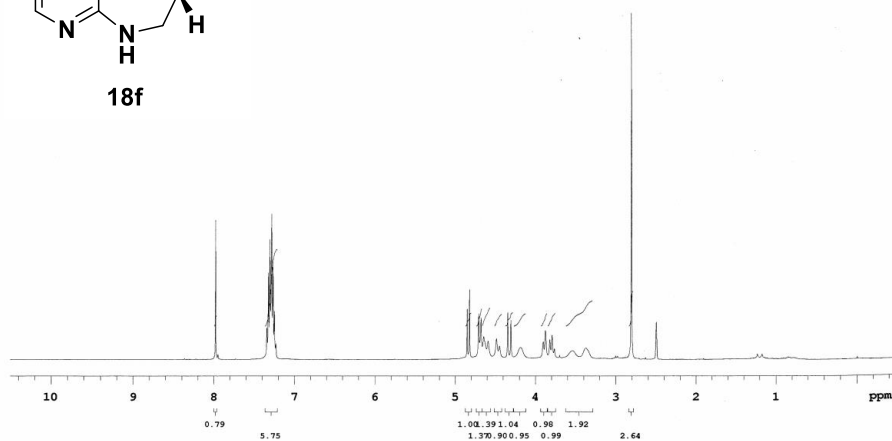
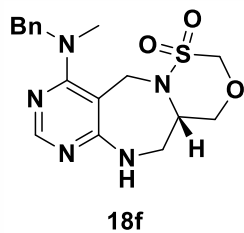




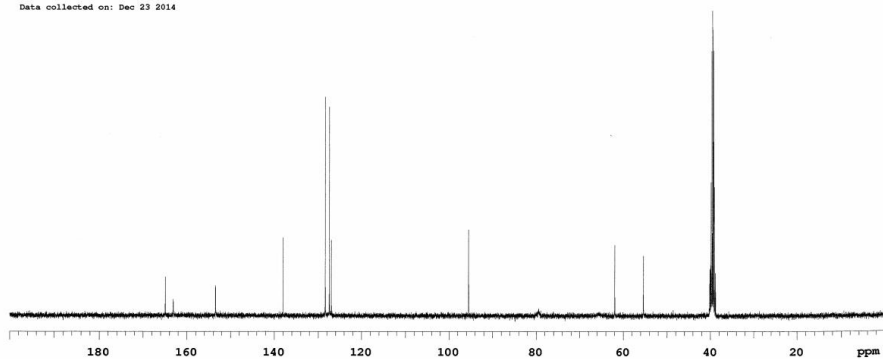


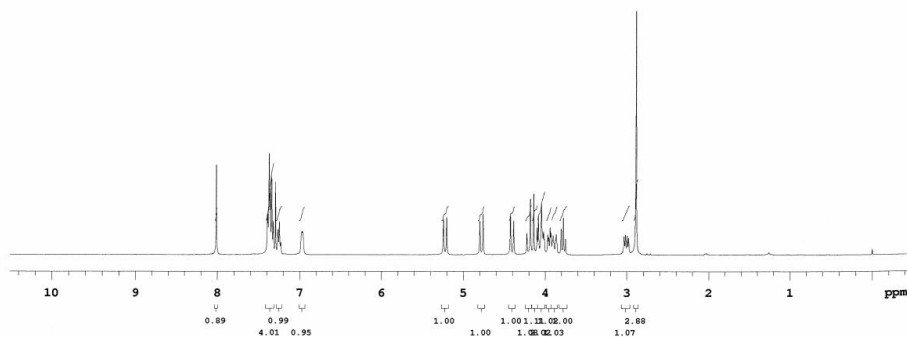
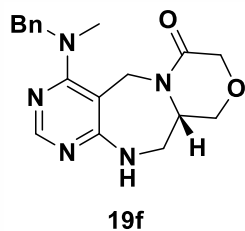




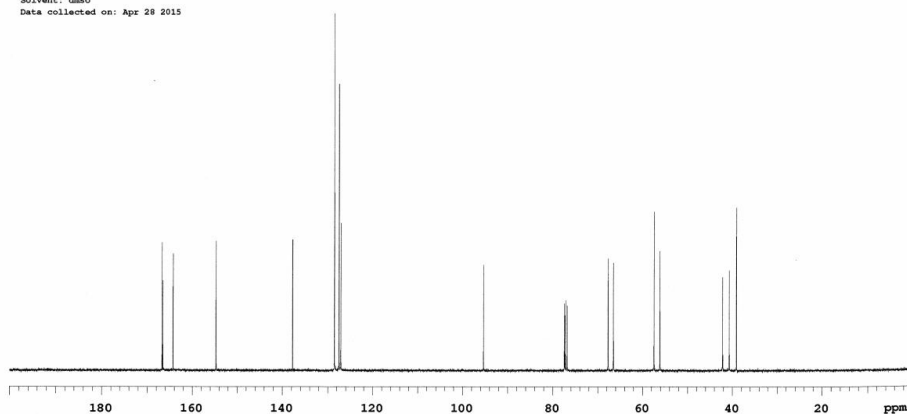


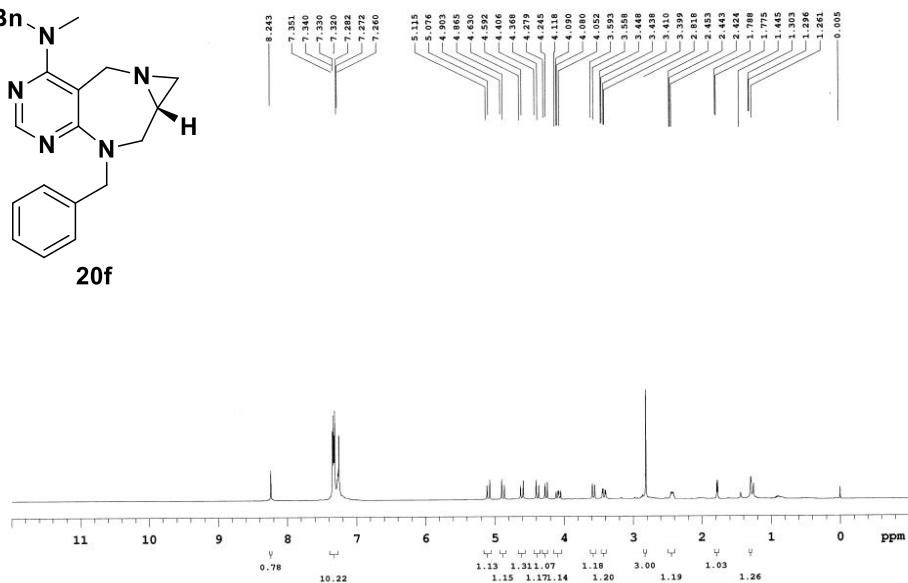
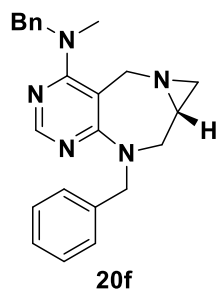
16f
 Sample Name:
 KJH_D08_M07_F107_DMSO-400M_carbon
 Data Collected on:
 Agilent-900-vnmr400
 Archive directory:
 /home/vnmr1/vnmrsgs/data/sbpark
 Sample directory:
 127_3_118_20141223_20141223_01
 FIDFile: KJH_D08_M07_F107_CDCl3_DMSO-400M_Carbon
 Pulse Sequence: CARBON (s2pul)
 Solvent: cdcl3
 Data collected on: Dec 23 2014





¹³C NMR
 Sample Name: KJH_D08_No8_P46_CDCl3_Carbon_400M
 Data Collected on: Agilent-VNMR-vnmrs400
 Archive directory: /home/vnmr1/vnmrsys/data/dhulbon
 Sample directory: 13017_b_20150427_01
 FIDFile: KJH_D08_No8_P46_CDCl3_carbon_400M_
 Pulse Sequence: CARRION (s2pul)
 Solvent: dmsc
 Data collected on: Apr 28 2015

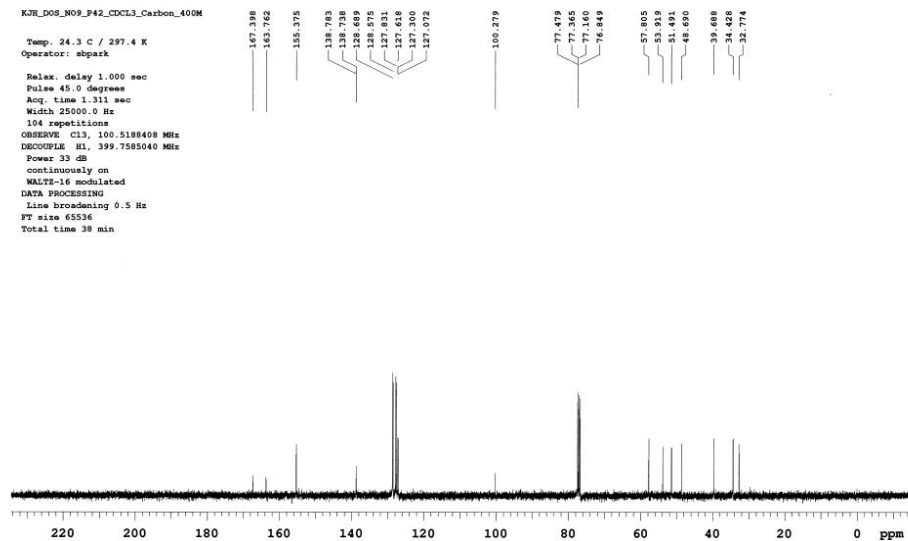


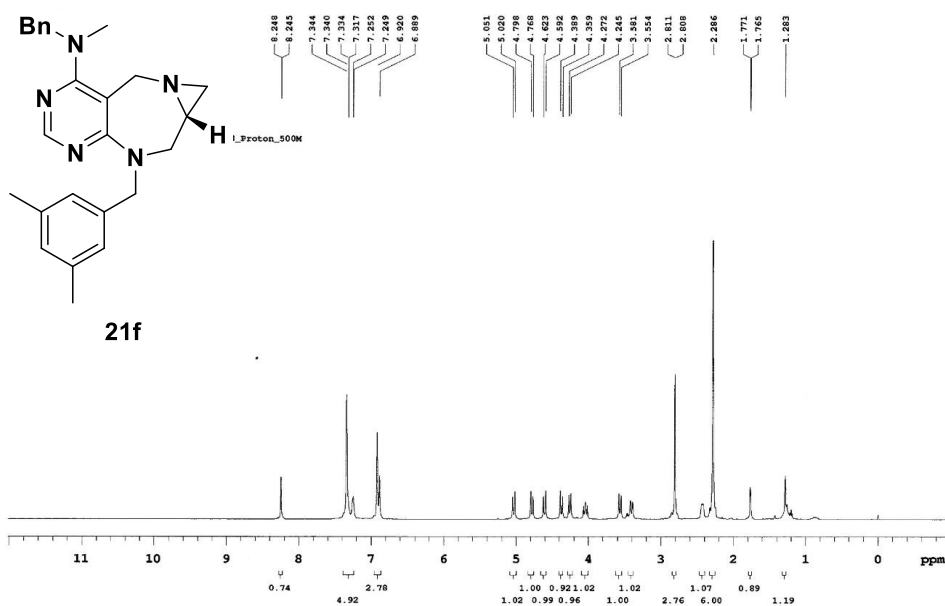


KJH_DOS_N09_F42_CDCL3_Carbon_400M

Temp. 24.3 C / 297.4 K
Operator: sbpark

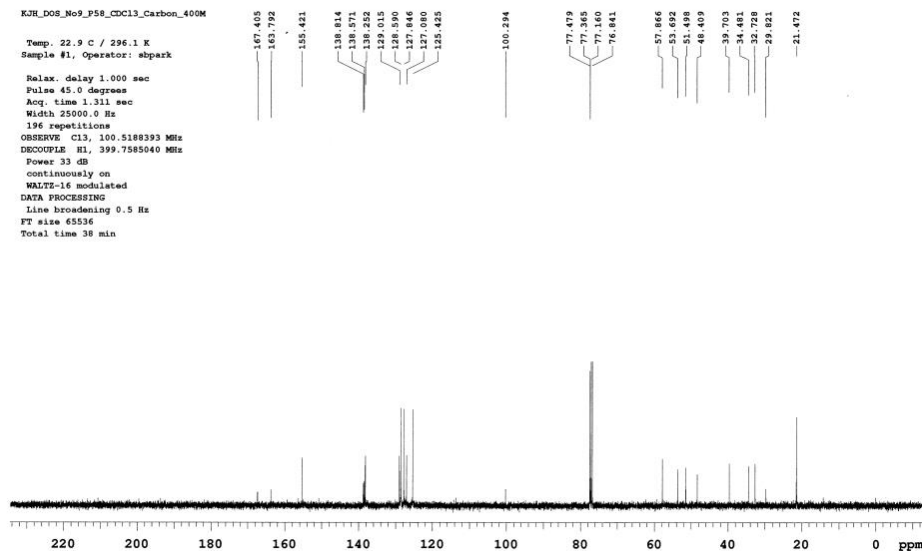
Relax. delay 1.000 sec
 Pulse 45.0 degrees
 Acq. time 1.311 sec
 Width 25000.0 Hz
 104 repetitions
 OBSERVE C13, 100.5189408 MHz
 DECOUPLE H1, 399.7585040 MHz
 Power 33 dB
 continuously on
 WALTZ-16 modulated
 DATA PROCESSING
 Line broadening 0.5 Hz
 FT size 65536
 Total time 38 min

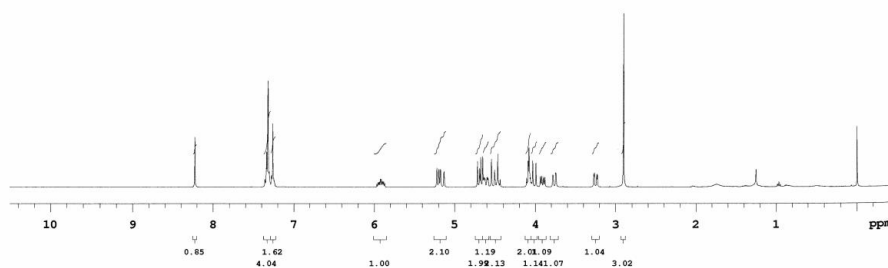
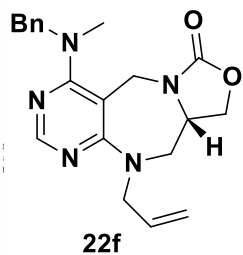




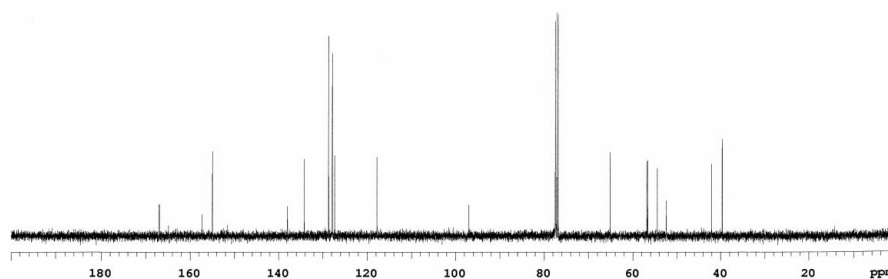
KJH_DOS_M09_P58_CDCl3_Carbon_400M

Temp. 22.9 C / 296.1 K
 Sample #1, Operator: sbpark
 Relax. delay 1.000 sec
 Pulse 45.0 degrees
 Acq. time 1.311 sec
 Width 25000.0 Hz
 194 repetitions
 OBSERVE C13, 100.5188393 MHz
 DECOUPLE H1, 399.7585040 MHz
 Power 33 dB
 continuously on
 WALTZ-16 modulated
 DATA PROCESSING
 Line broadening 0.5 Hz
 FT size 65536
 Total time 38 min

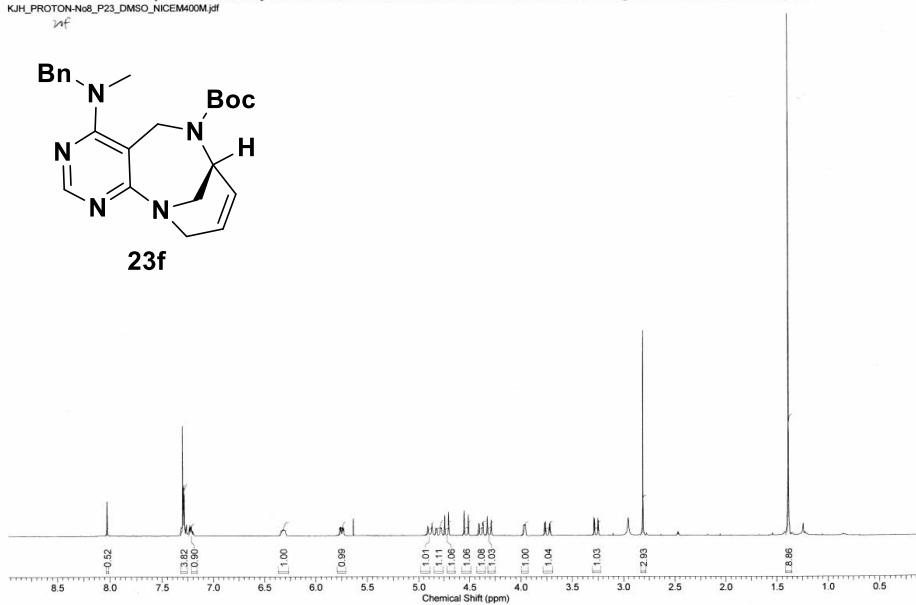
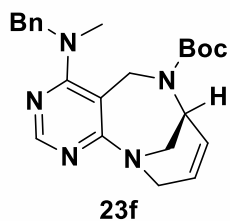




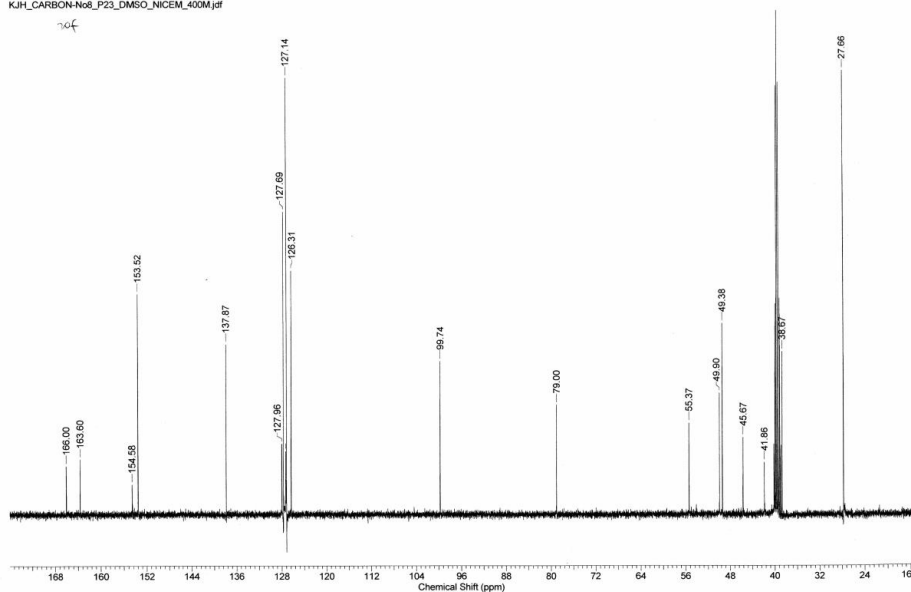
Sample Name: 19f
 Data Collected on: Agilent-NMR-vnmrs400
 Archive directory: /home/vnmr1/vnmrsys/data/sbpark
 Sample directory: JAR-V-9_re_13C_20140402_20150402_01
 FIDFile: CARBON_01
 Pulse Sequence: CARBON (s2pul)
 Solvent: cdcl3
 Data collected on: Apr 2 2015



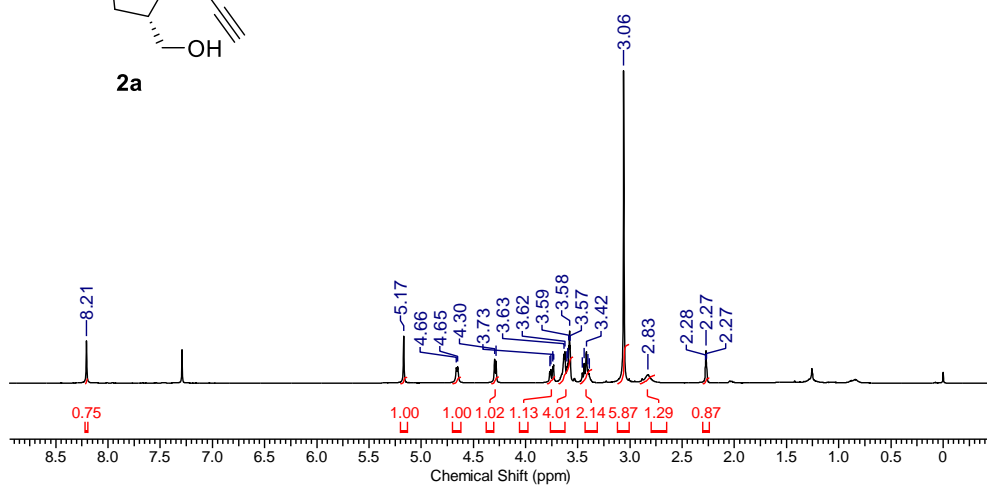
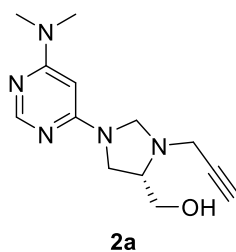
24f



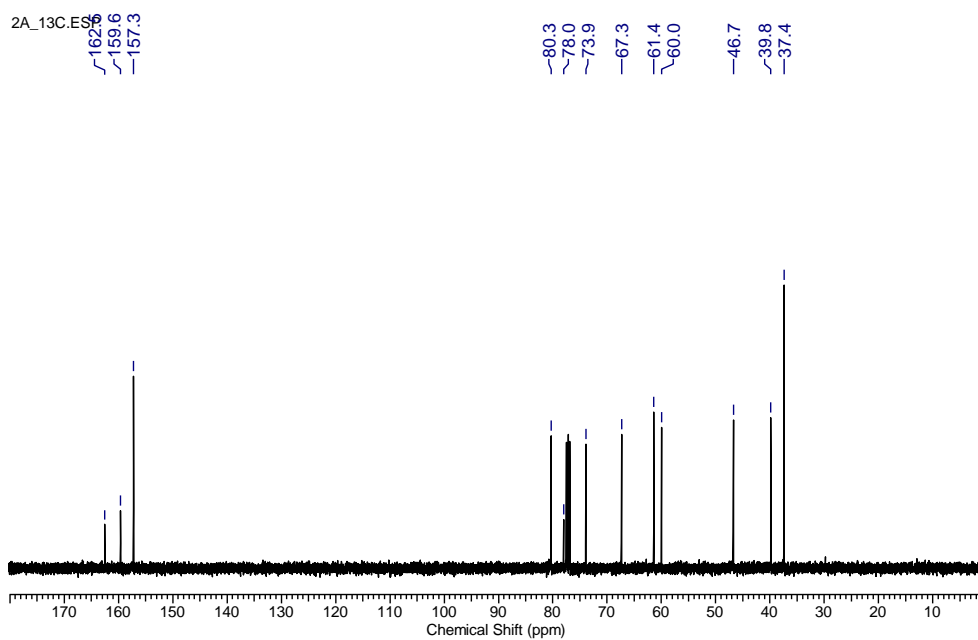
24f

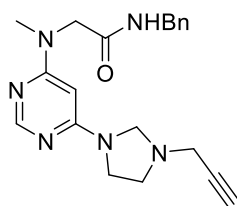


Chapter 3

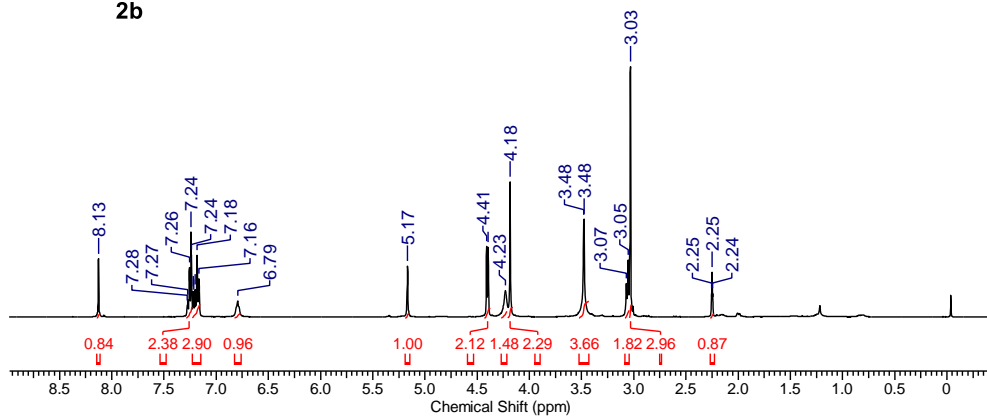


2A_13C.E59





2b

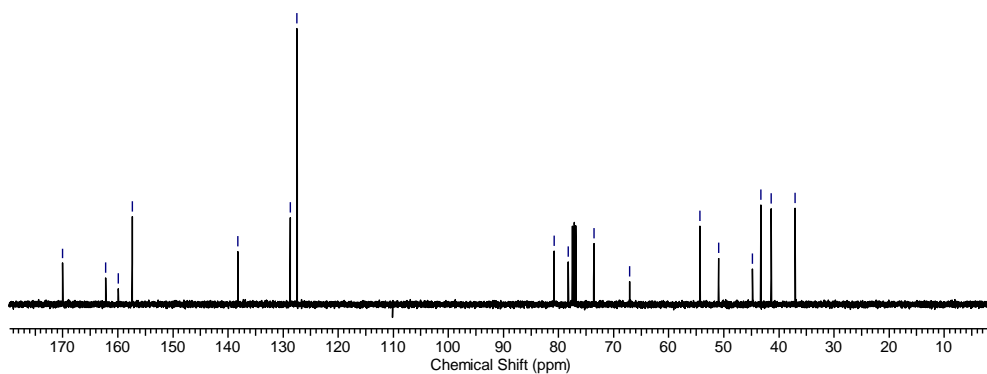


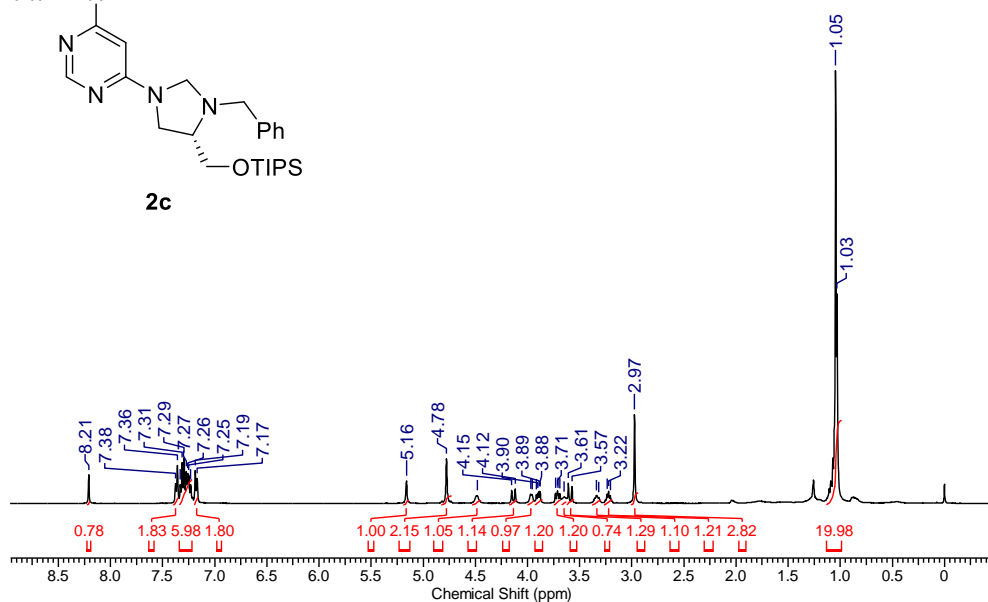
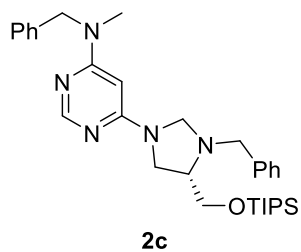
2B_130ESD
 -170.9
 -162.2
 -159.9
 -157.4

-138.2
 -128.7
 -127.5

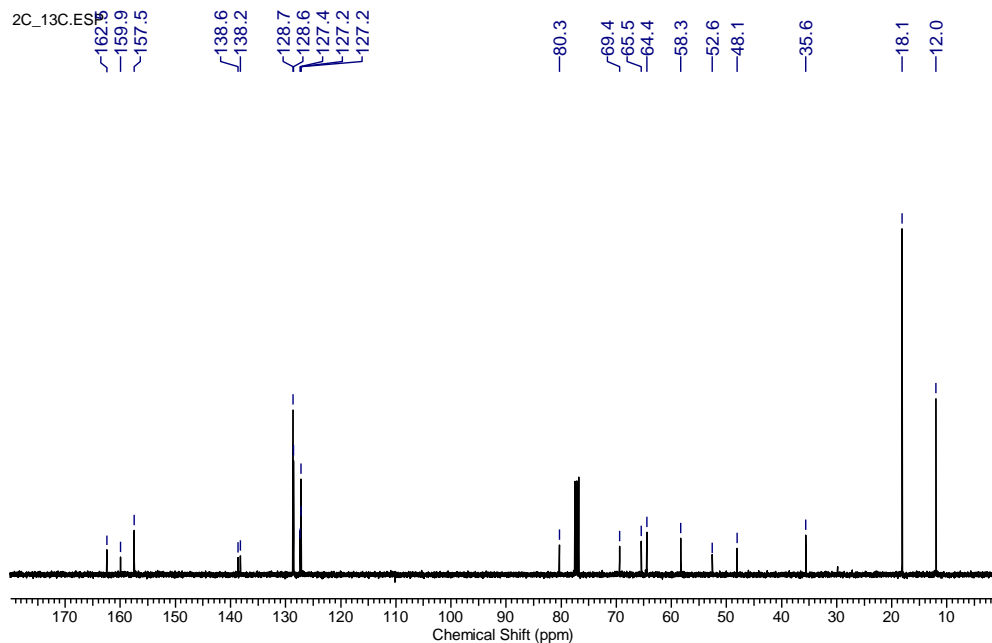
-80.8
 -78.3
 -73.6
 -67.1

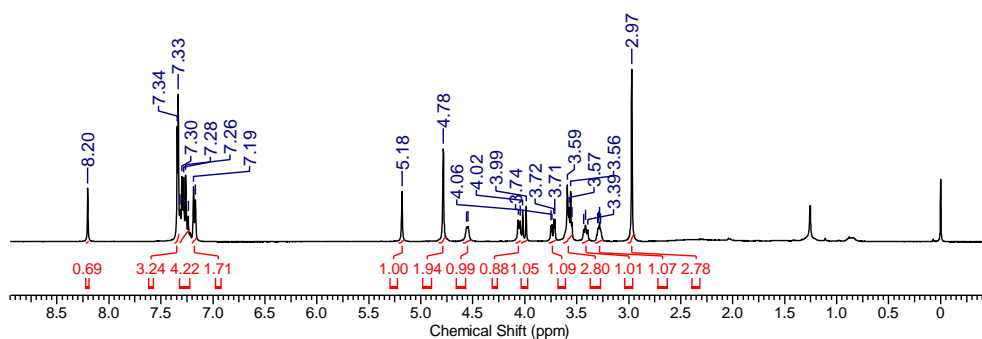
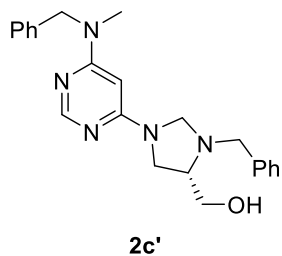
-54.3
 -50.9
 -44.8
 -43.3
 -41.4
 -37.0



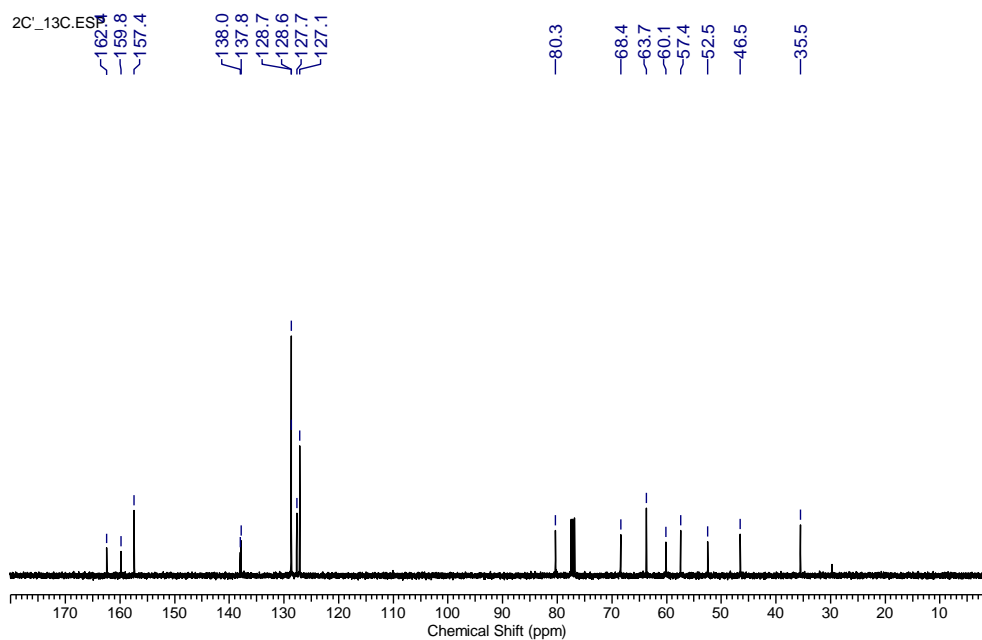


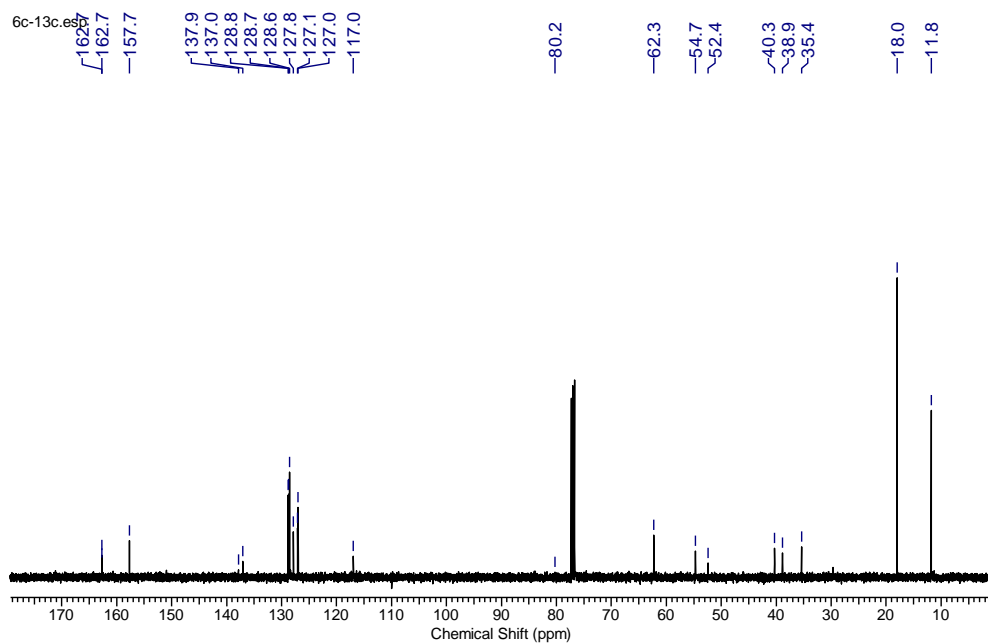
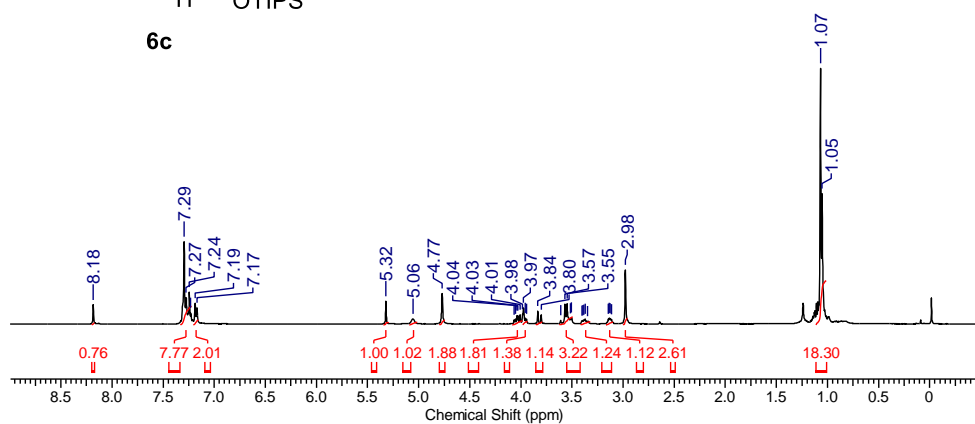
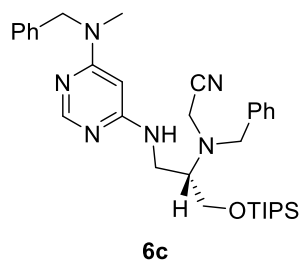
2C_13C.E5

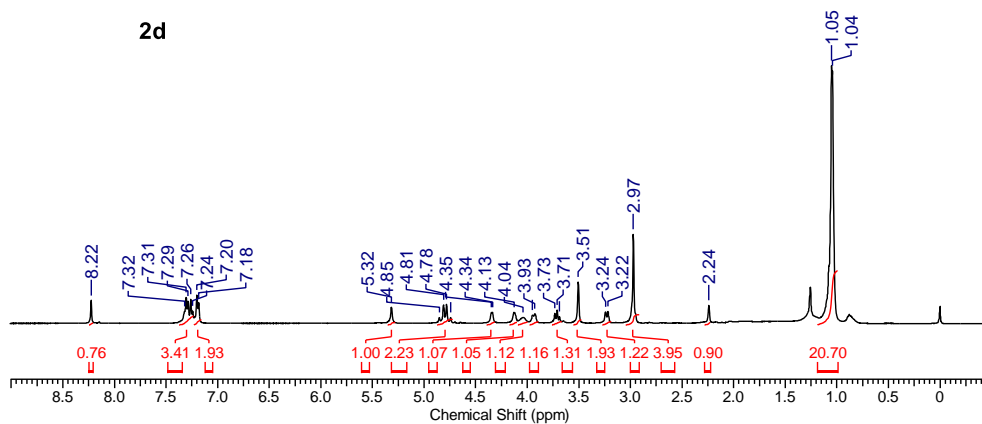
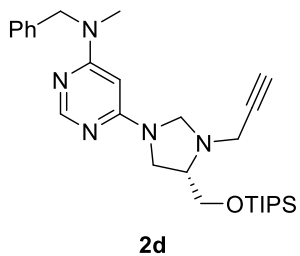




2C_13C.ES*



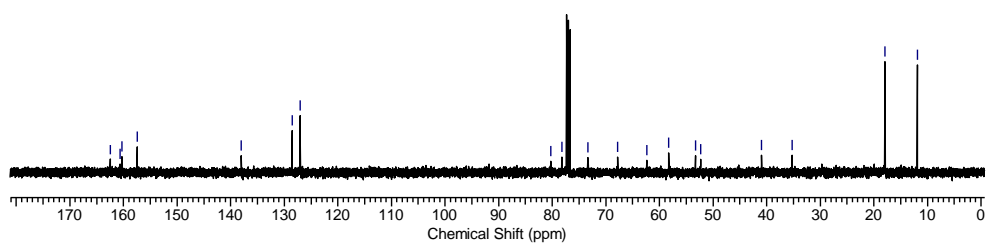


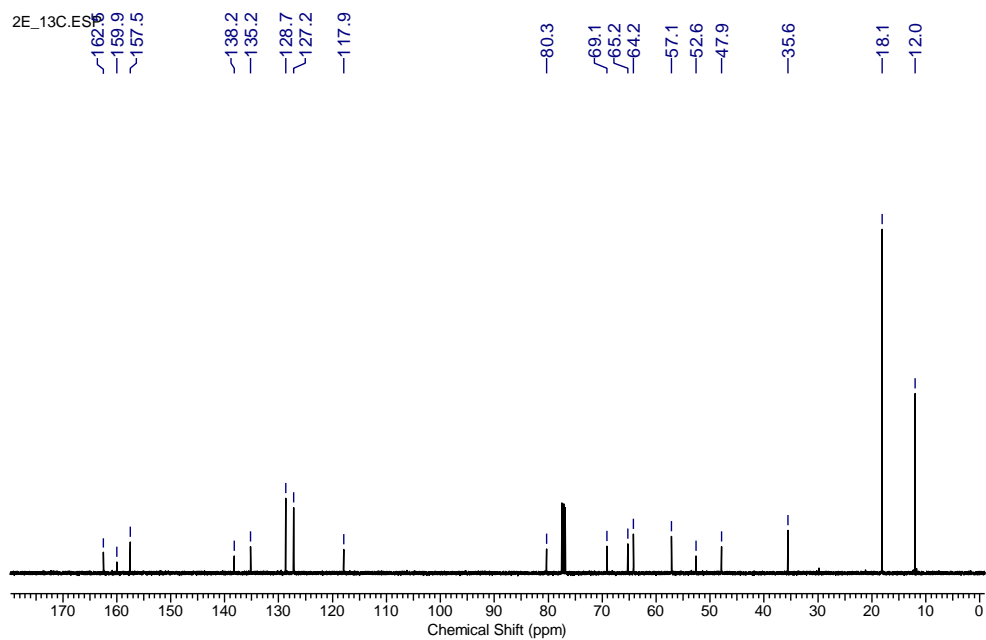
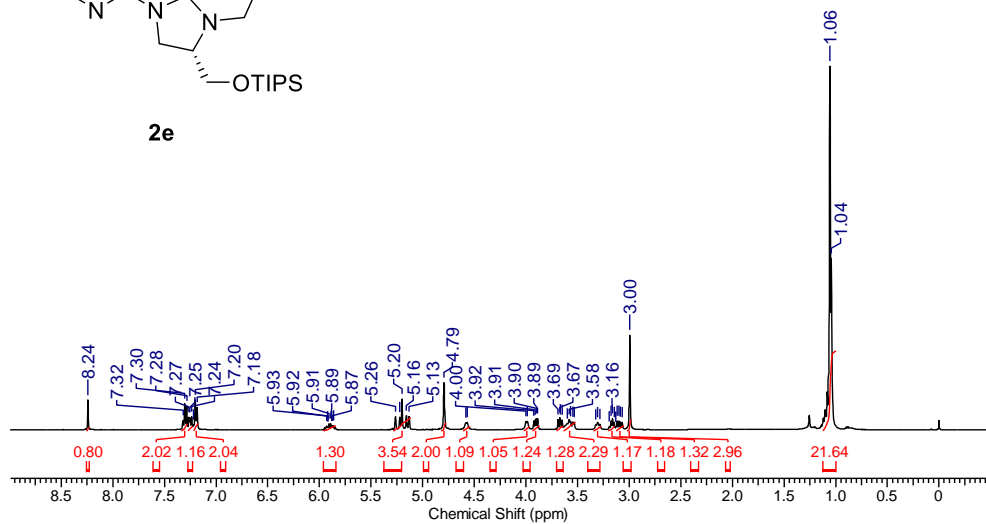
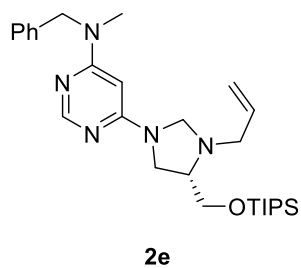


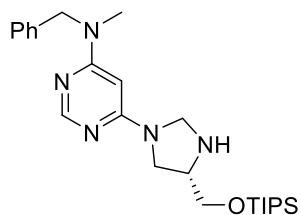
2D_13C.EP
 163.9
 160.6
 160.3
 157.5

138.0
 128.5
 127.1

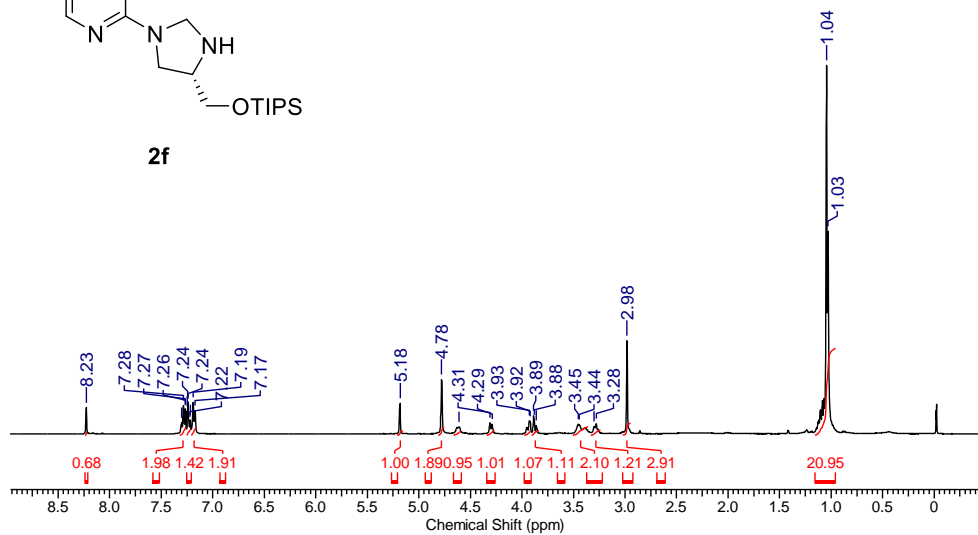
80.3
 78.2
 73.3
 67.8
 62.4
 58.2
 53.3
 52.3
 41.0
 35.3
 18.0
 11.9



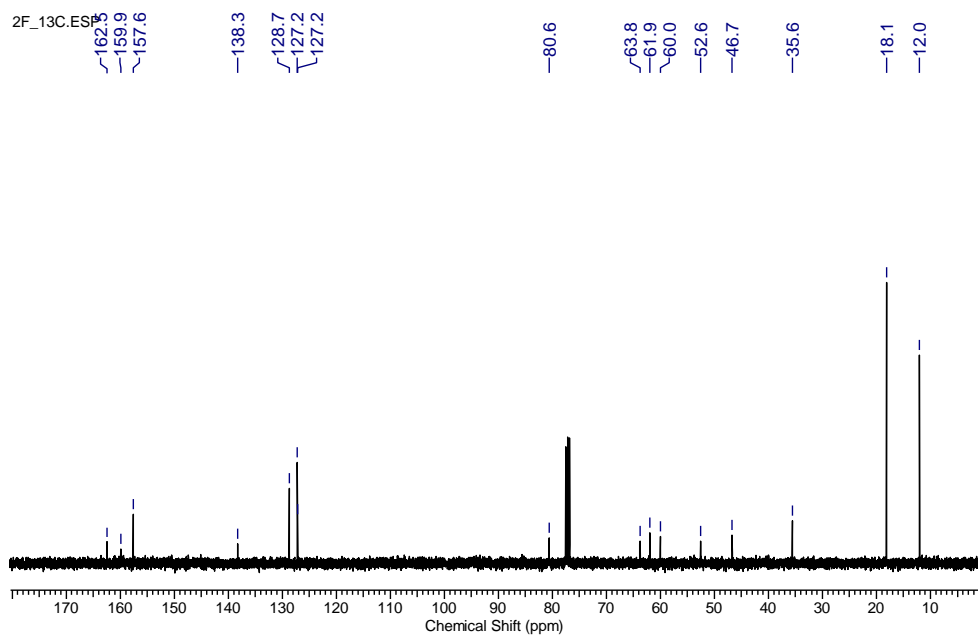


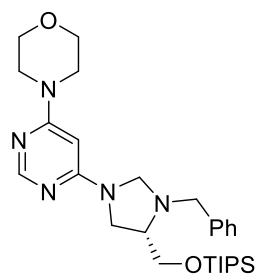


2f

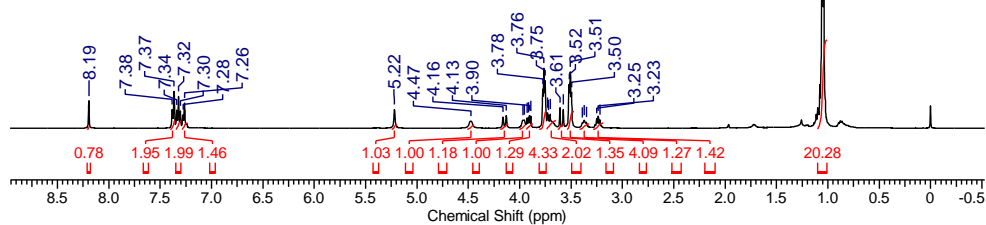


2f_13C.ESP

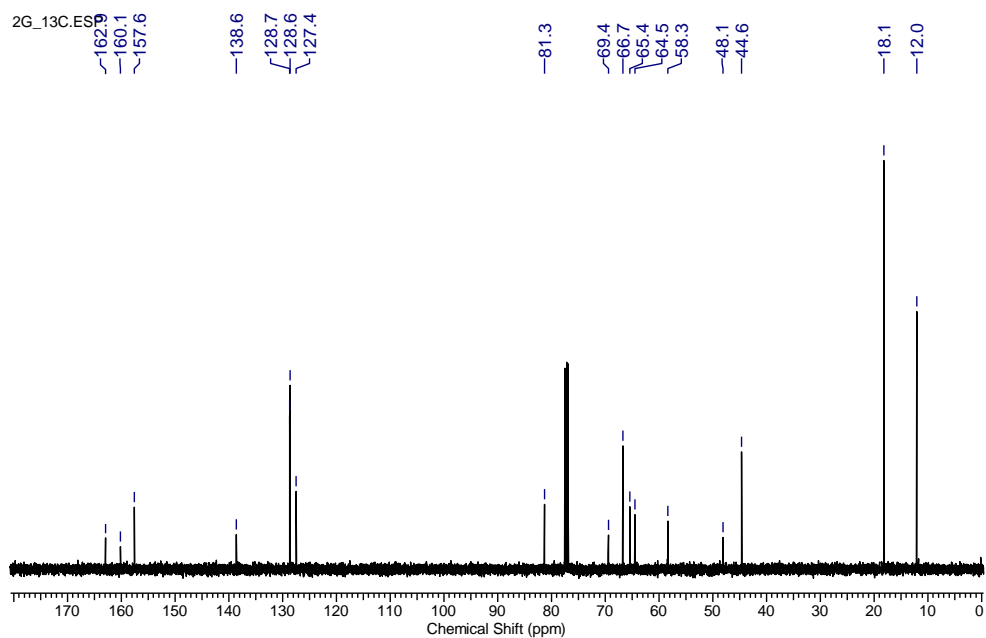


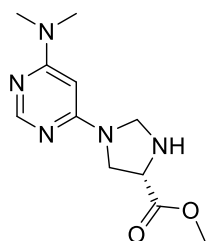


2g

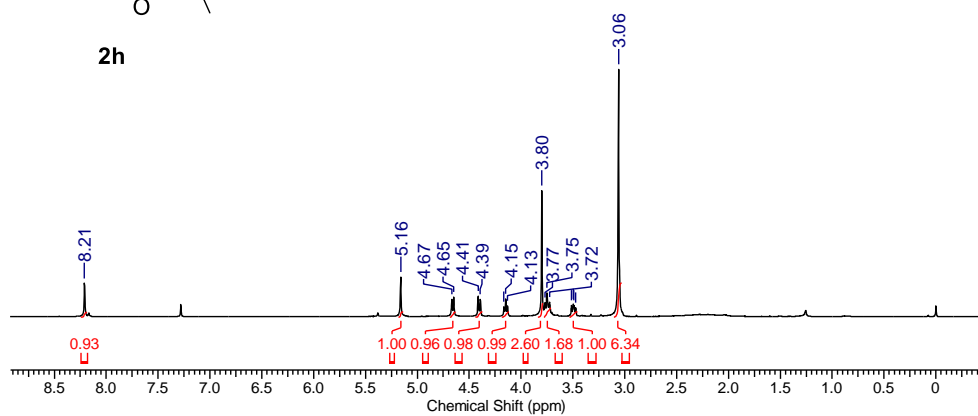


2G_13C.E5



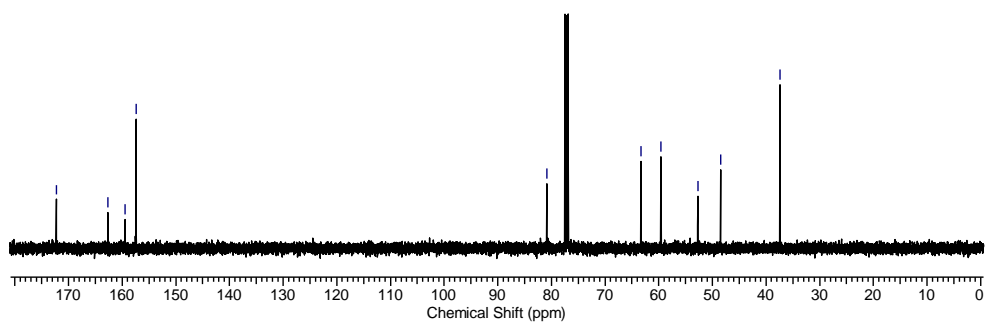


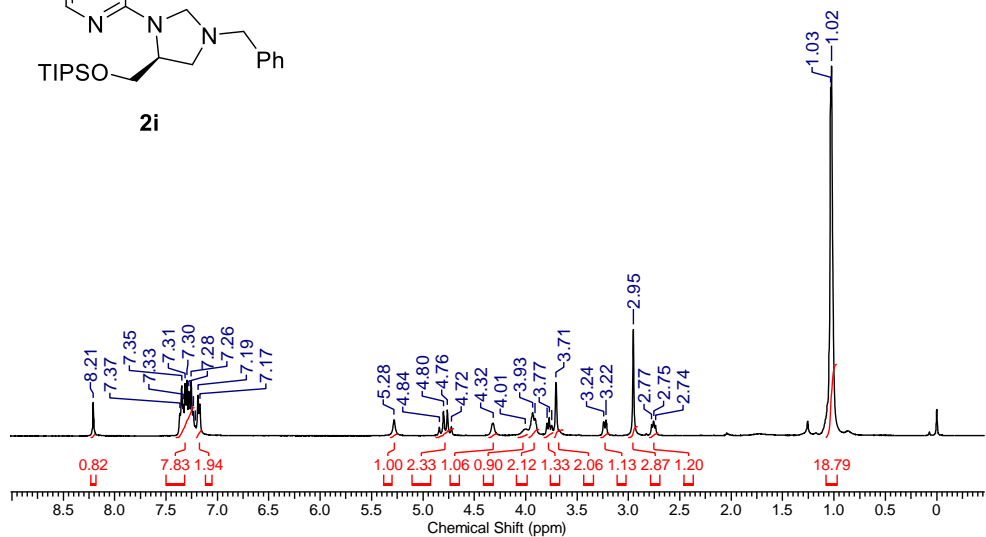
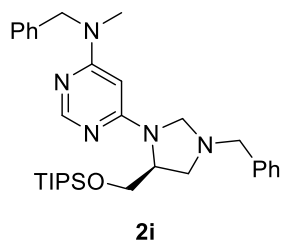
2h



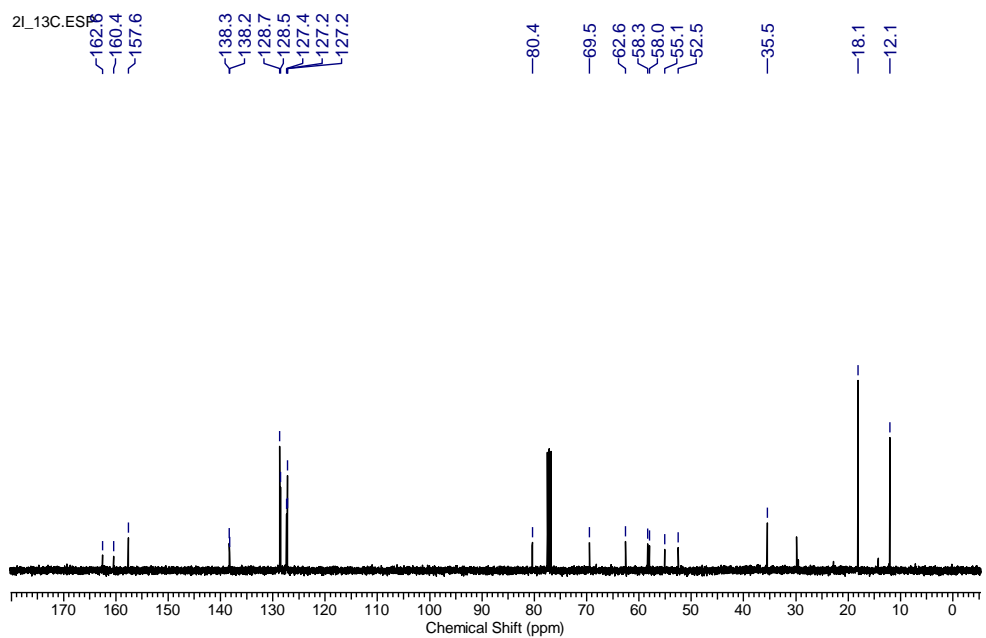
2H_13C ES
 ~172.8
 ~162.8
 ~159.5
 ~157.4

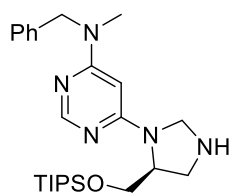
~80.9
 ~63.3
 ~59.6
 ~52.7
 ~48.5
 ~37.4



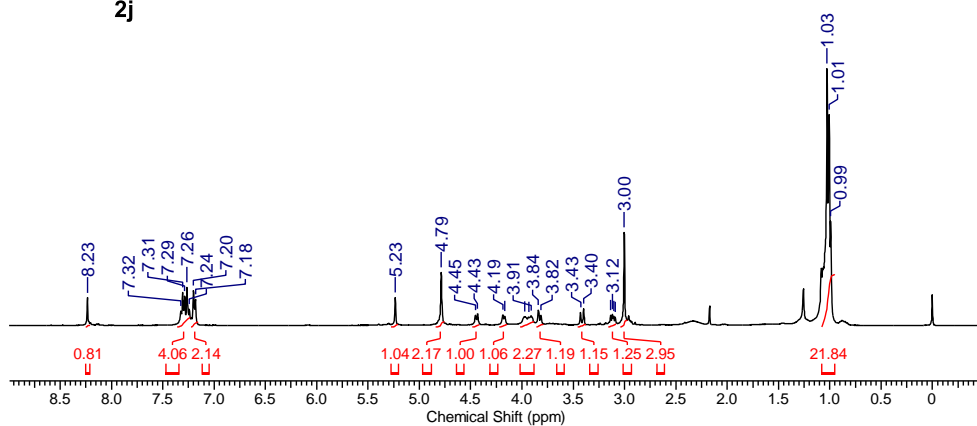


2L_13C.E5

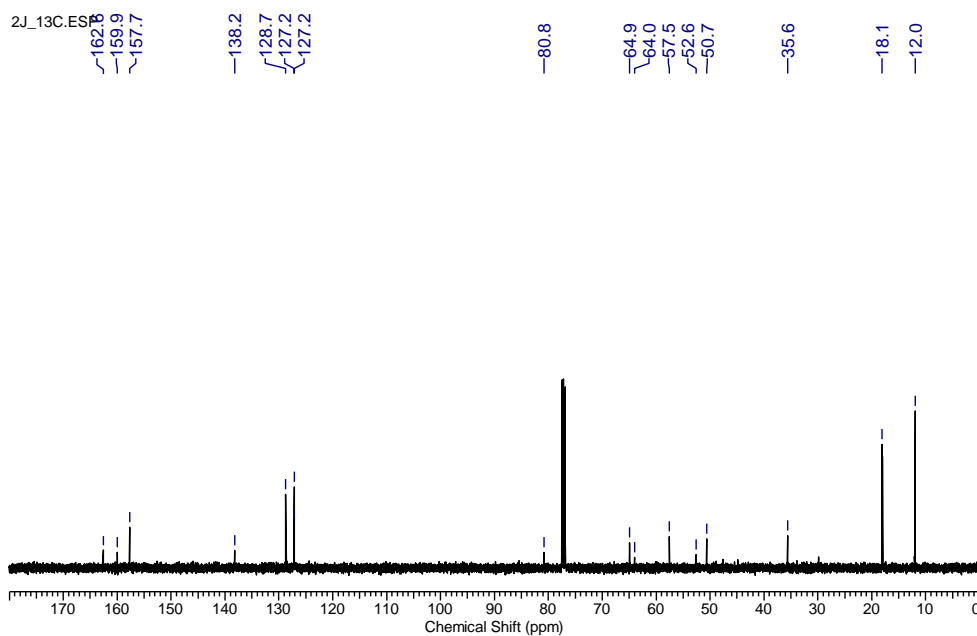


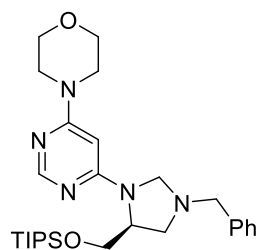


2j

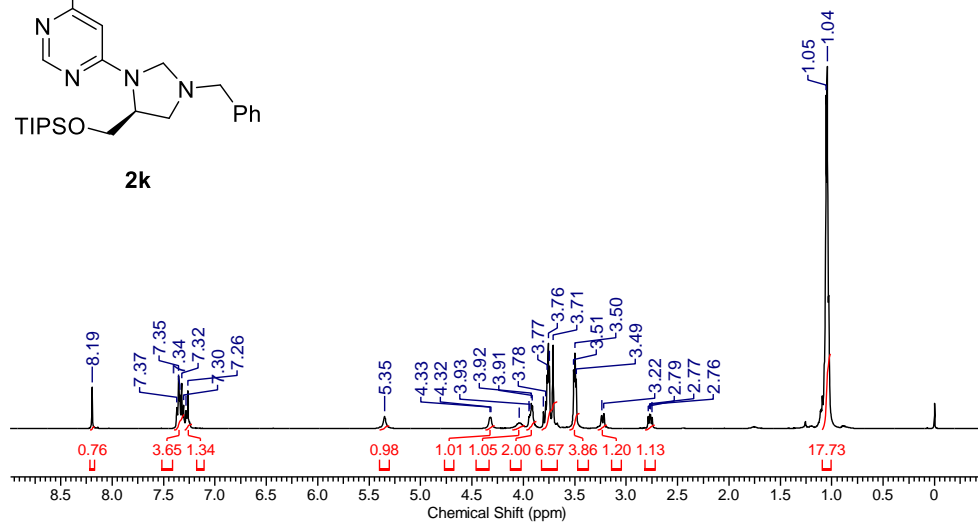


2J_13C.ESS

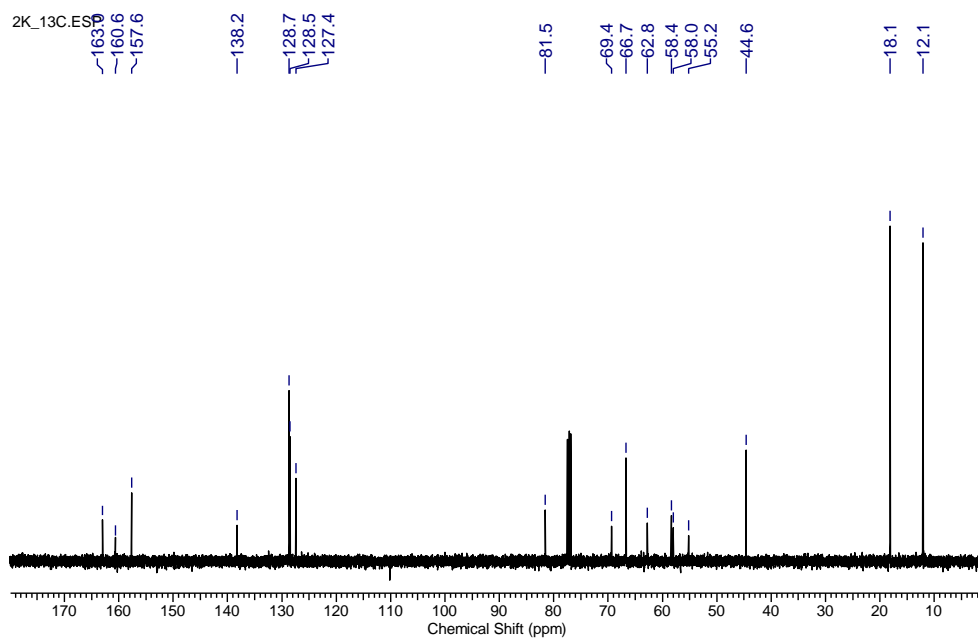


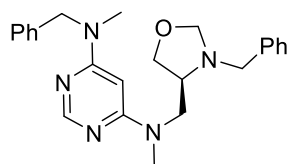


2k

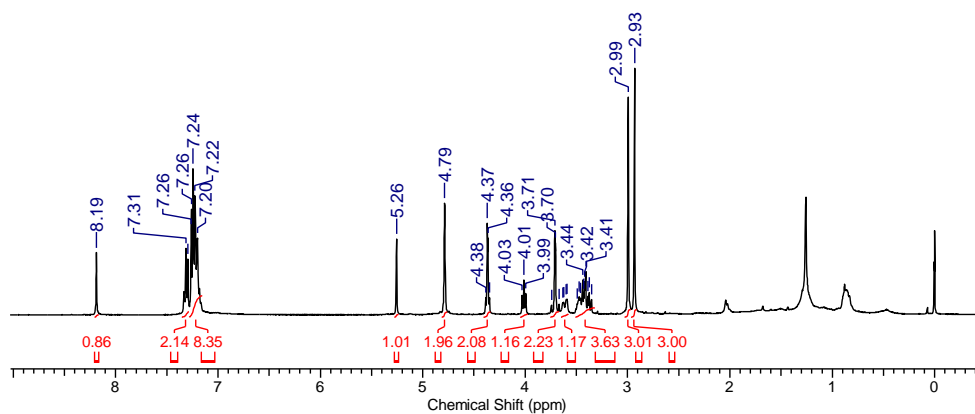


2K_13C.E50

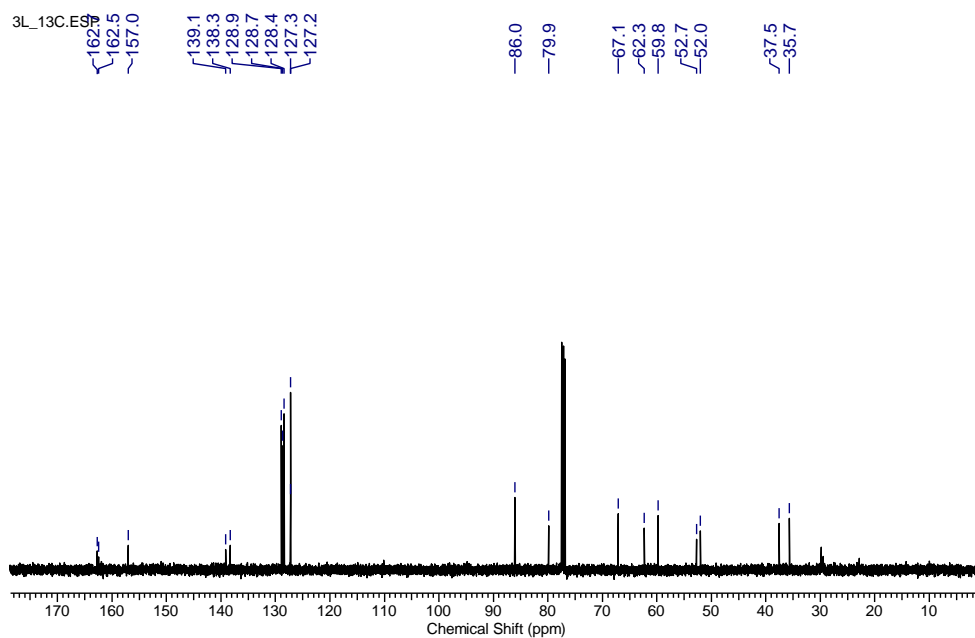


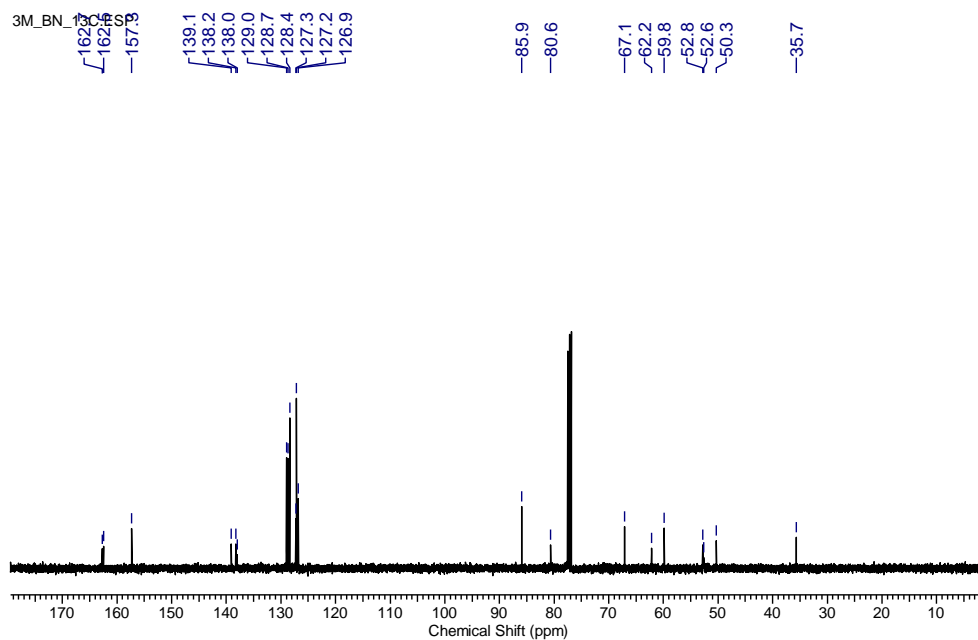
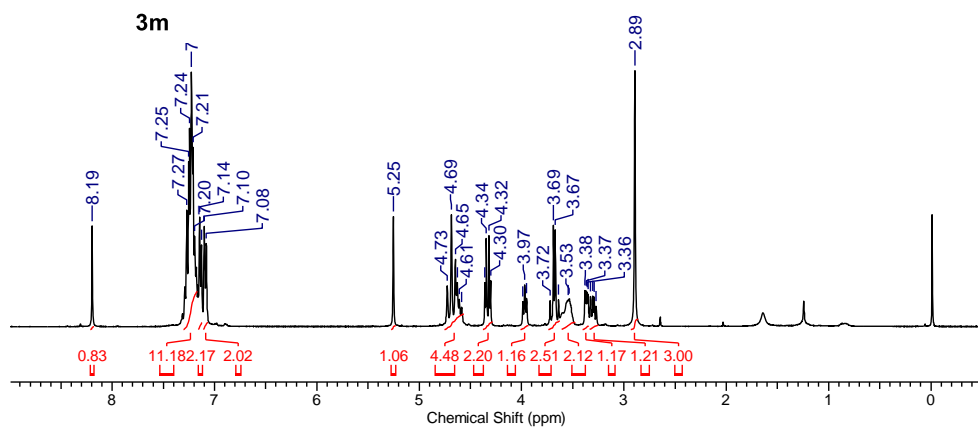
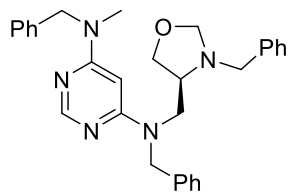


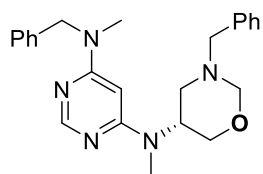
3I



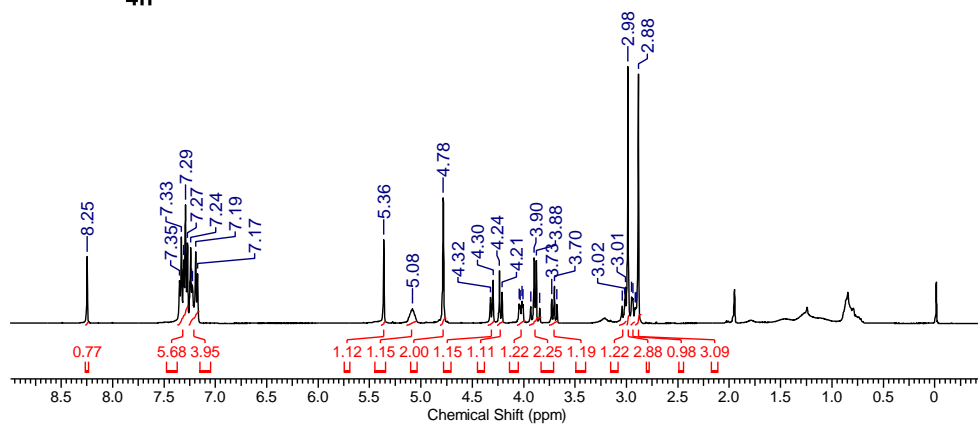
3L_13C.E9



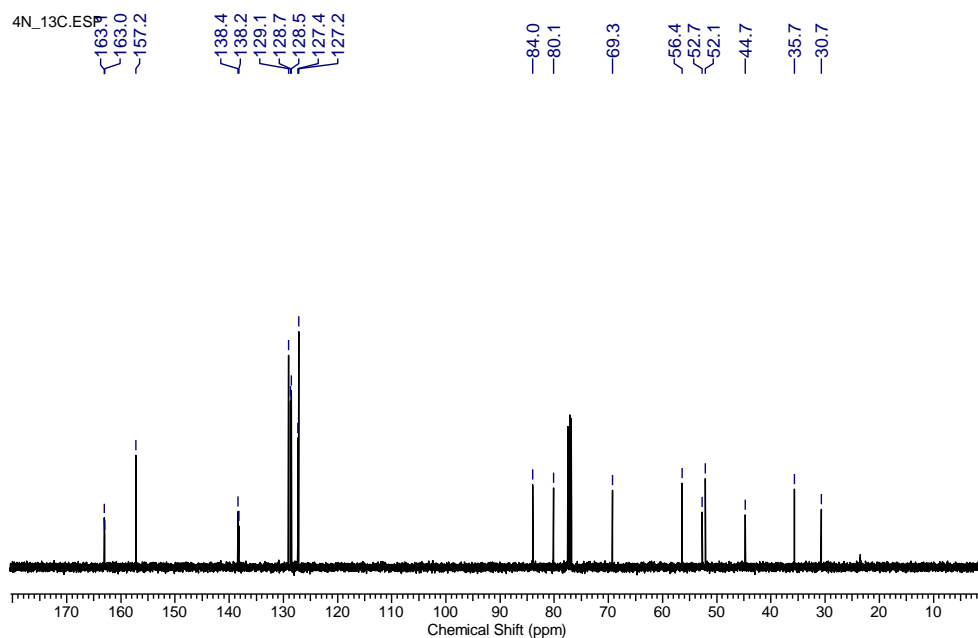


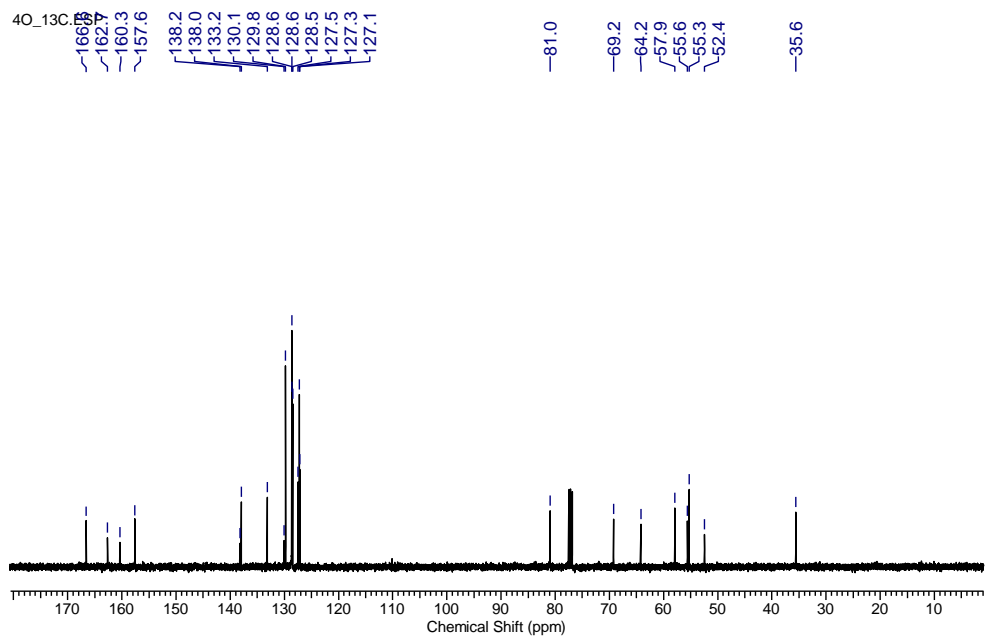
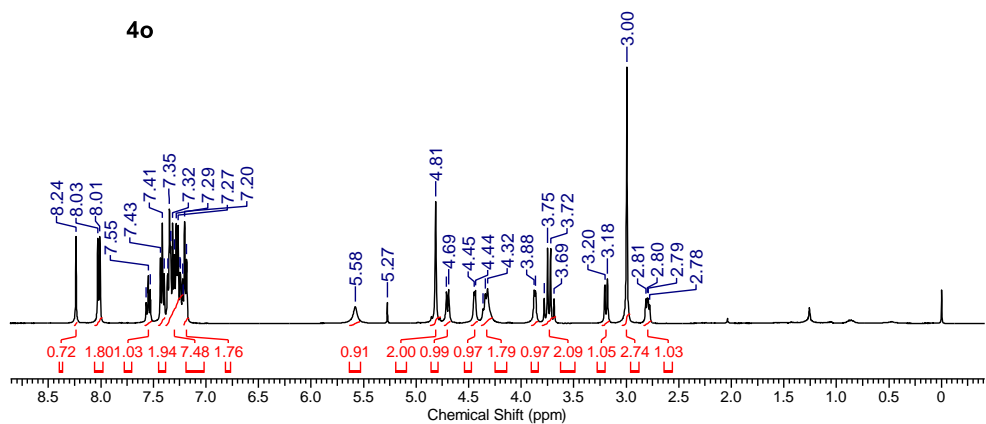
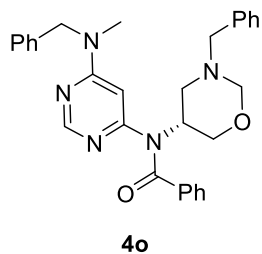


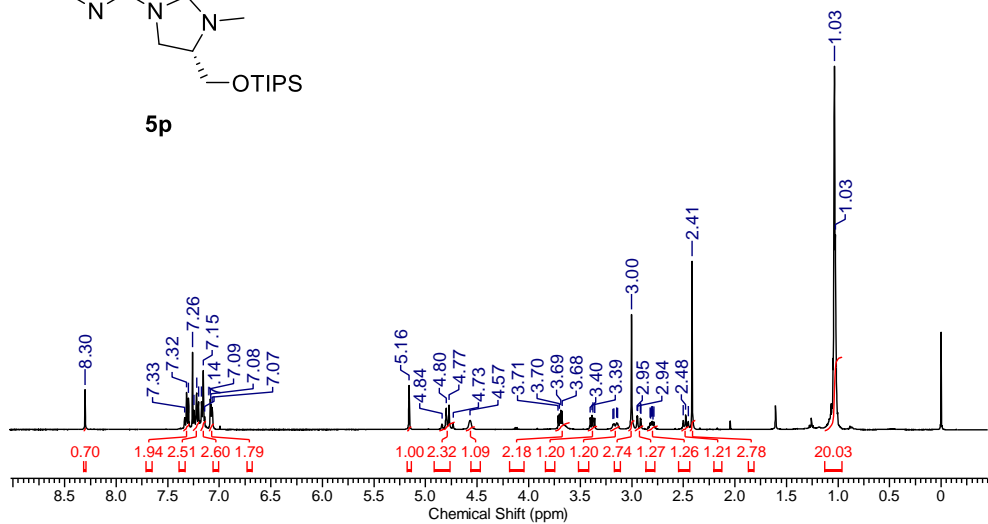
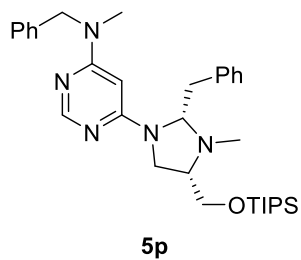
4n



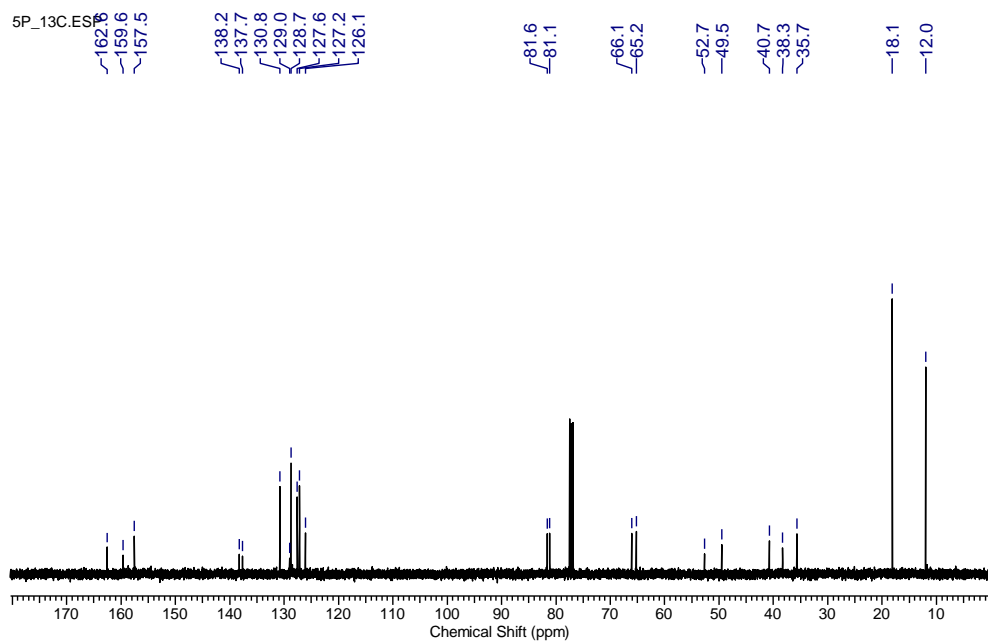
4N_13C.ESP

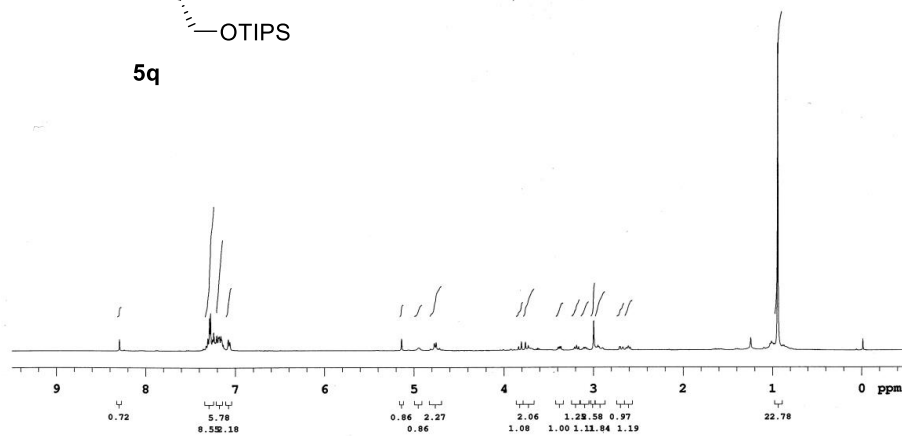
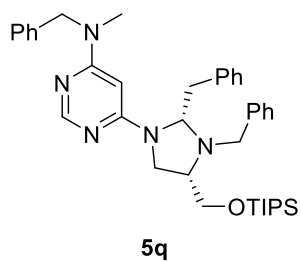






5P_13C.E566





5Q-13C.E5

